# The Palaeontology and Palaeoenvironment of the Early Cambrian Emu Bay Shale, Kangaroo Island, South Australia

**Christopher Nedin**

BSc. Hons (Adelaide 1991)

Submitted in fulfilment of the requirement
for the degree of Doctor of Philosophy

*Department of Geology and Geophysics*
*University of Adelaide*
*South Australia*

December 1995

Map reference: Kingscote 1:253,440 SI 53/16

# Abstract

Worldwide, Phanerozoic fossil Lagerstätten have provided new insights into palaeontology and evolutionary processes. One such deposit, the Emu Bay Shale from the Early Cambrian of South Australia, has received little study. The delineation of the palaeontology, palaeoenvironment, palaeoecology and subsequent taphonomy of the Emu Bay Shale and its fossil assemblage will lead to a better understanding of the processes involved in the forming the Emu Bay Shale Lagerstätte.

The Emu Bay Shale outcrops on the northern coast of Kangaroo Island as part of the Kangaroo Island Group. The fossil assemblage within the Emu Bay Shale is preserved as iron stained calcite for the most part, commonly with a core of fluorapatite. The assemblage is numerically abundant, but low in diversity. The most spectacular fossiliferous occurrence at Big Gully contains some six previously described species, the trilobites *Hsuaspis bilobata* and *Redlichia takooensis*, the phyllocarids *Isoxys communis* and *Tuzoia australis*, and the presumed annelids *Myoscolex ateles* and *Palaeoscolex antiquus*. Three other genera were identified in this study, *Anomalocaris*, *Naraoia* and *Xandrella*. Two species of *Anomalocaris* were found, *A. briggsi* sp. nov. and *A.* sp.. The anomalocaridids are the first found in the southern hemisphere. *A. briggsi* appears adapted to filter small soft bodied organisms from sediment or water and *A.* sp. appears to be a raptoral predator, possibly conspecific with a form recently described from Chengjiang in southwestern China. The presence of *Naraoia* confirms the widespread occurrence of the genus in the Early and Middle Cambrian. *Xandrella* also offers another link with the Chengjiang fauna. Previous descriptions of *Hsuaspis bilobata* are augmented by the finding of rare meraspid forms that indicate an evolutionary link with *Xystridura* from the Middle Cambrian. The previously presumed annelid *Myoscolex* is here considered to be an arthropod with a gross morphology somewhat reminiscent of the Middle Cambrian *Opabinia*. Several other forms are too poorly preserved to allow

accurate identification. No sessile forms have been identified from the assemblage and juveniles are extremely rare and restricted to *Hsuaspis bilobata.*

The stratigraphy of the 3500+ m thick Upper Kangaroo Island Group, which includes the Emu Bay Shale, suggests deposition in an active strike-slip tectonic setting. The Emu Bay Shale seems to represent a localised subsidence with temporary decrease in coarse clastic input. Sedimentological evidence suggests rapid deposition whilst geochemical evidence, especially from manganese, molybdenum and phosphate analyses, is indicative of a fluctuating low oxygen - anoxic environment.

The presence of phosphatised tissues in the Emu Bay Shale assemblage indicates the early onset of an acidic, anoxic micro-environment at or immediately below the sediment-water interface. Such conditions can result in an increased concentration of dissolved phosphate, allowing the rapid mineralisation of some soft tissues by fluorapatite. The majority of the assemblage is preserved via iron stained calcite carbonate, either around a fluorapatite 'core' or independent of fluorapatite. This indicates that either the parameters conducive to phosphate precipitation were short-lived, and the preciptation of calcite from supersaturated pore fluids was triggered by a decrease in dissolved phosphate and an increase in the ph, or such conditions did not occur, allowing only calcite precipitation from oversaturated pore-waters.

The palaeoenvironment of the Emu Bay Shale can be envisaged as one of rapid deposition into a localised suboxic to anoxic basin. The environment of soft substrate and low oxygen would be expected to discourage settlement by sessile forms and small juveniles, but permitted rapid colonisation by motile forms during periods of increased oxygenation. Such an environment would promote bottom conditions favourable for the rapid precipitation of phosphate and/or calcite. A recrystallisation event subsequent to early diagenesis has altered the primary calcite to tectonically aligned calcite fibres, whilst recrystallisation of primary phosphate obscures the original fine detail.

## Statement of Originality

I hereby certify that this thesis does not incorporate, without acknowledgement, any material which has been previously submitted for a degree or diploma in any university, and to the best of my knowledge and belief, it does not contain any written or published material by another person, except where due reference is given in the text.

**Christopher Nedin**
December, 1995

I, Christopher Nedin, give consent to this copy of my thesis, when deposited in the University Library, being available for loan and photocopying.

Signature .....

# Acknowledgements

This undertaking has benefited from input by a number of people. The technical staff of the Department of Geology and Geophysics are thanked for their help, particularly John Stanley and Sherry Proferes, but especially Rick Barrett, who spent many hours dealing with difficult photographic problems. Professor Larry Frakes and Dr. Thomas Flöttmann are thanked for their assistance with various aspects of the thesis. Dr. Tony Belperio of the Department of Mines and Energy, South Australia is thanked for helpful discussions. Dr. Des Collins of the Royal Ontario Museum is thanked for discussion on the Burgess Shale fauna and Dr. Simon Conway Morris of the University of Cambridge for discussion on aspects of Early Cambrian Palaeontology. I am grateful for the assistance given by Dr. Nevile Pledge and Mr. Ben McHenry of the South Australian Museum. Various members of staff and students in the Department of Geology and Geophysics have at one time or another given help, assistance or advice during the course of this thesis and are thanked.

Some people deserve special mention. Dr. David Gravestock of the Department of Mines and Energy, South Australia is thanked for many helpful discussions and advice, his enthusiasm for the Cambrian of South Australia was particularly infectious and his willingness to listen and impart information was particularly appreciated. I am especially indebted to Prof. Derek Briggs of the University of Bristol for valuable discussion on taphonomy and issues related to Early Cambrian palaeontology as well as his thoughts on *Myoscolex*. Phil and Hermina and Bernie and Anita are thanked for insisting that I have some sort of social life outside of university.

Finally I wish to acknowledge the help, throughout the duration of this study, of my supervisor Dr. Richard Jenkins, who suggested this project and agreed to take me on - a decision I have never regretted.

This study was assisted by grants from the Alumni Association of the University of Adelaide, the Mark Mitchell Research Foundation and the University of Adelaide Distinguished Visiting Lecturer Scheme, which supported to visit of Prof. Briggs.

Table of Contents

Page

## Chapter 4: Geochemistry of the Emu Bay Shale Lagerstätte

## Chapter 5: Taphonomy of the Big Gully Assemblage



## Chapter 6: Palaeoenvironment of the Emu Bay Shale Lagerstätte.

**List of Figures**

**List of Tables**

## List of Plates

# Chapter 1: Introduction

*"Full fathom five thy father lies;*

*Of his bones are coral made:*

*Those are pearls that were his eyes:*

*Nothing of him that doth fade,*

*But doth suffer a sea-change*

*Into something rich and strange."*

(The Tempest, I, ii: 394-399)

Fossil lagerstätten are assemblages exhibiting exceptional preservation and which contribute a disproportionate amount of palaeobiological information (Butterfield 1995). They have been of major significance in our understanding of evolutionary processes because such localities provide a brief glimpse far back, undimmed by the ravages of taphonomic processes. Processes which normally result in the decay and remove of all but the most resilient body fractions, producing fossil assemblages dominated by the easily preserved shelly component of the fauna. The preservation of soft-bodied and lightly sclerotized organisms provide much additional information about biotic diversity, ecology and evolution. This kind of exceptional preservation was thought to occur only rarely (e.g. Conway Morris 1985; Allison & Briggs 1993). However, the documentation of a number of Early Palaeozoic fossil Lagerstätten has shown that such preservation is not unique. These include the Burgess Shale, British Columbia (Whittington 1980; Collins *et al.* 1981; Conway Morris 1986), Chengjiang, southwestern China (Chen & Erdtmann 1991; Hou *et al.* 1991), Sirius Passet, northern Greenland (Conway Morris *et al.* 1987; Budd 1993), Mount Cap, Northwest Territories (Butterfield 1994), Kinzers, Pennsylvania (Resser & Howell 1938), Kaili, southern China (Zhao *et al.* 1994), Wheeler Formation (Conway Morris & Robison 1988) and the Marjum Formation, Utah (Conway Morris & Robison 1988). Other fossil Lagerstätten are discussed in Conway

Morris (1989), one such, being the Emu Bay Shale from the Early Cambrian of South Australia.

The Middle Cambrian Burgess Shale fauna from British Columbia has rightly been regarded as a premier Early Palaeozoic example of soft-bodied preservation (Whittington 1971a, b, 1980; Conway Morris 1989a, b). This has led to other Lower Palaeozoic Lagerstätten being termed 'Burgess Shale-type' if they contain fossil assemblages which include non-or lightly mineralising taxon such as are best known from the Burgess Shale (Conway Morris 1989b), and/or exhibit evidence for exceptional organic or carbonaceous preservation of non-mineralising organisms in fully marine siliciclastics (Butterfield 1995). Butterfield (1995) has suggested restricting the term 'Burgess Shale-type' to only those Lagerstätten which exhibit exceptional organic or carbonaceous preservation of non-mineralising organisms - a convention adopted here.

Deposits such as the Burgess Shale and that at Chengjiang cannot easily be reconciled with Seilacher's (1990) classification of characteristic fossil Lagerstätten in that they are not to be simply the product of obduration or stagnation, in the manner of geologically younger Lagerstätten, but preservation appears to be the result of the complex interplay of several factors (Hou *et al.* 1991). The most important factors include the lack of bioturbation and scavenging, the inhibition of degrading enzymes (e.g. Butterfield 1990) and, possibly most importantly, the inferred lower partial pressure of oxygen in the Cambrian atmosphere (e.g. Runnegar 1982; Schopf *et al.* 1983; Kasting 1986). Indeed, the partial pressure of oxygen might only have been some 50% of present atmospheric levels in the Early Cambrian (Wilde *et al.* 1990, but see Jenkins & Hasenhor 1989). There seems little doubt that this lack of dissolved oxygen plays a major role in the preservation of soft or lightly sclerotized tissues in the fossil record. The fact that macroscopic animals need oxygen to survive presents something of a conundrum, since they would appear to be precluded from areas of low dissolved oxygen levels and thus high preservational potential. In the instance of the Burgess Shale Lagerstätte, the large-scale exceptional preservation has been explained by the rapid transport of whole

communities into sub oxic-anoxic areas (e.g. Whittington 1971a; Conway Morris 1986), although the mass-transport mechanisms commonly supposed have not resulted in classical turbidites, and thinly bedded shales are commonly represented, possibly due to the homogeneity of the source. With regard to the Emu Bay Shale Lagerstätte, it is hoped that an understanding of the palaeoenvironment during deposition may provide an explanation as to the occurrence of large, centimetric, organisms in dark shales and their subsequent exceptional preservation.

The Emu Bay Shale outcrops at two localities on the north coast of Kangaroo Island (Fig. 1.1), at its type section on the western side of Emu Bay, and at Big Gully, approximately 7 km to the east. At both locations the Emu Bay Shale is underlain by the White Point Conglomerate and overlain by the Boxing Bay Formation. The lower part of the Emu Bay Shale at Emu Bay contains fossil lags predominantly composed of trilobite exuvia fragments (mostly cranidia) along with hyolithids and rare phosphatic brachiopods. This is in contrast to the situation at Big Gully, where both faunal composition and preservation are markedly different. At the Big Gully locality, the lower Emu Bay Shale contains not only the trilobites *Redlichia takooensis* and *Hsuaspis bilobata* which also occur at Emu Bay but also other elements unique to the Big Gully locality. These include the trilobite *Naraoia*, the arachnomorph *Xandarella*, the phyllocarids *Isoxys communis* and *Tuzoia australis*, as well as *Anomalocaris* and the forms *Myoscolex ateles* and *Palaeoscolex antiquus* of uncertain taxonomic placement. The preservational style is also different, with the fossils at Big Gully preserved as red-stained, fibrous calcite and/or white or buff phosphate. The nature of the preservation and a subsequent recrystallisation event has removed fine detail in the majority of instances. The fossil assemblage from the lower Emu Bay Shale at Big Gully comprises the Emu Bay Shale Lagerstätte (e.g. Conway Morris 1989b: Allison & Briggs 1993).

The Emu Bay Shale was considered late Early Cambrian in age based on the trilobites in the fauna (Daily 1956, Pocock 1964, Öpik 1975). Daily (1956) placed the Early-Middle

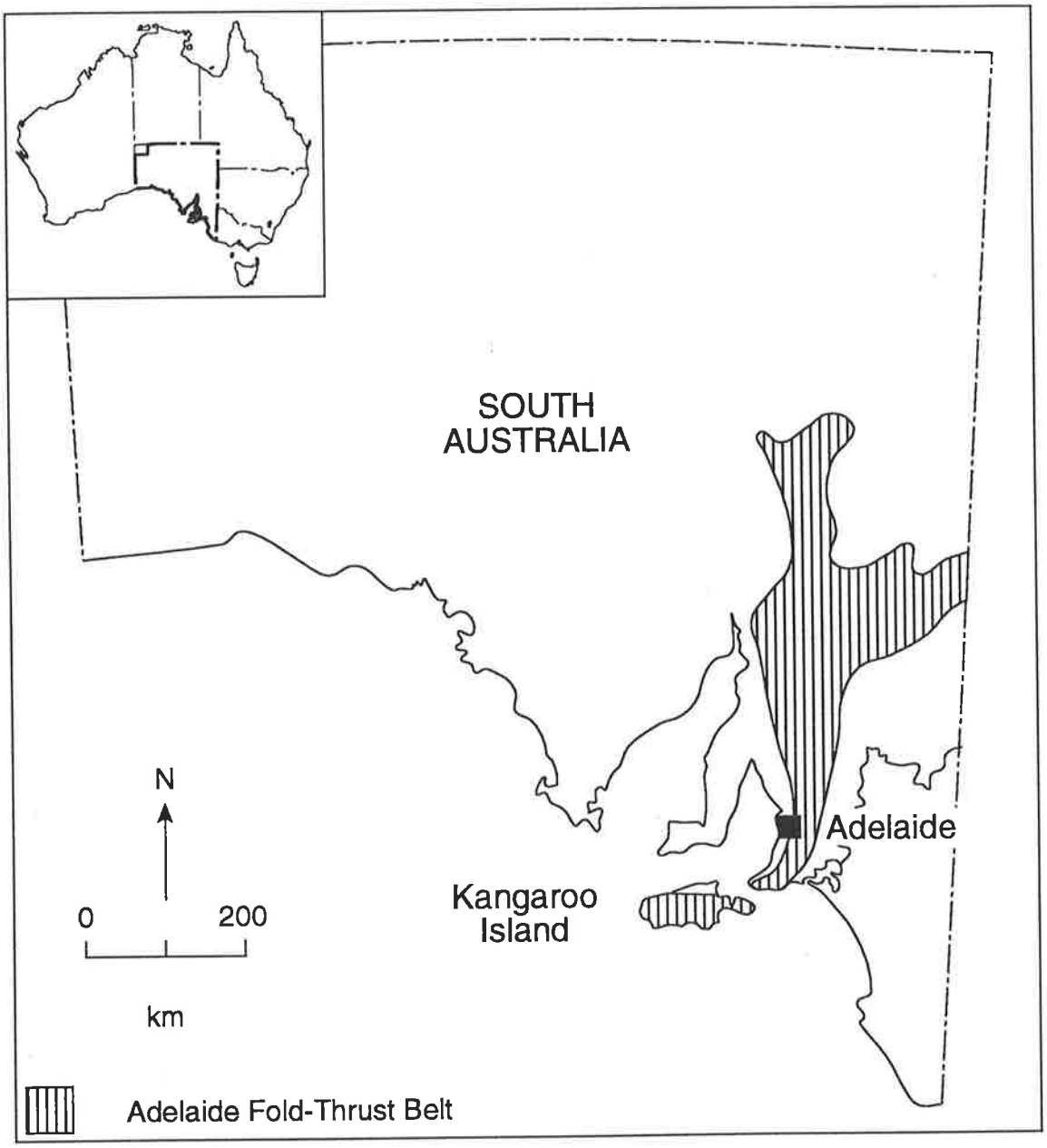


**Fig 1.1** Location map, showing arcuate southern Adelaide Fold-Thrust Belt.

Cambrian boundary within the conformably overlying Boxing Bay Formation. The proximity of the Emu Bay Shale to the Early-Middle Cambrian boundary is also suggested by the identification of Archaeocyatha of Botomian age towards the base of the lower Kangaroo Island Group and within clasts of the underlying White Point Conglomerate (D. Gravestock pers comm 1993). With reference to the Early Cambrian of Siberia, the Emu Bay Shale is apparently upper Botomian in age. Hence the Emu Bay Shale Lagerstätte appears to be older than the famous Middle Cambrian Burgess Shale Lagerstätte, but slightly younger than the more recently discovered Early Cambrian Chengjiang Lagerstätte.

Apart from an overview of the fauna given by Glaessner (1979), an unpublished honours thesis by Dinnick (1985) and a description of healed injuries from *Redlichia takooensis* (Conway Morris & Jenkins 1985), the Emu Bay Shale Lagerstätte has received little detailed study. This project was initiated in order to come to a more complete understanding of the Lagerstätte, its faunal composition and the processes involved in its formation. The formation of the Emu Bay Shale Lagerstätte, like many of the other Cambrian examples, is the result of a number of factors, probably the most important of which is depositional environment, which controls not only the original faunal composition, but also the early taphonomic processes and thus the composition of the fossil assemblage.

The study was subdivided into several parts; an overview of the regional geology; a palaeontological study of the assemblage and, since the concentration of certain elements reflect chemical, oceanographic and sedimentary controls, a geochemical analysis of the sediment and fossils within the Emu Bay Shale Lagerstätte.

Throughout this project, the 'Emu Bay Shale Lagerstätte' refers to the basal 8 metre siltstone and contained fossils, of the Emu Bay Shale at the Big Gully locality; the 'Big Gully assemblage' refers to the fossils found within the Emu Bay Shale Lagerstätte; the

'Big Gully community' refers to the community which existed at the Big Gully locality during the deposition of the lower Emu Bay Shale.

# Chapter 2: The Geology of the Kangaroo Island Group

*"A study of the Cambrian geology of South Australia by the present writer has shown that the environment of deposition on the mainland was quite different from that recorded on Kangaroo Island. On the mainland, correlation of the formations recognised can generally be carried from one area to another with relative ease but none of these formations can be linked satisfactorily with those so far recognised on Kangaroo Island."*

(Daily 1956, p 101)

## 2.1 Introduction

Kangaroo Island comprises the southwestern part of the Adelaide Fold-Thrust Belt, which has had a complex Neoproterozoic and Cambrian depositional history ( Daily *et al.* 1973, 1979; Flöttmann et al. 1994, 1995). A prism of Neoproterozoic to late Early and early Middle Cambrian sediments were deposited in an arcuate basin within continental Gondwana, and subsequently underwent compressive thrusting and folding (Jenkins 1990; Flöttmann *et al.* 1994, 1995; Flöttmann & James 1994). The greater part of this pile formed in a regime of repeated extention . Deposition of late Early and early Middle Cambrian sediments was largely controlled by the Kangarooian Movements (Daily & Milnes 1971, 1972b), originally described as the Kangaroo Island Orogeny (Daily 1956) in the area of interest. These represented a complex and persistent tectonic episode, most pronounced in the southern part of the Fold-Thrust Belt. Here, a foreland platform developed to the north of Kangaroo Island and fault controlled subsidence to the south and east formed the Kanmantoo Trough, which evidently filled rapidly with mainly turbiditic sediments derived from the west northwest. On the northeast coast of Kangaroo Island, between Point Marsden and Snelling Beach, the Cambrian sequence differs markedly from other Cambrian deposits on both Kangaroo Island and the

mainland (Daily 1956). The six formations identified in the northeast coast section were deposited in predominantly offshore marine to intertidal environments on the southern extremity of the Gawler Craton. The area was subjected to strong longshore tidal currents, as well as minor wave and occasional alluvial influences. An interplay of alluvial, intertidal and subtidal environments occurred in response to shoreline migration caused by faulting of the southern margin of the craton. Strike-slip faulting resulted in the formation of small depocentres and rapid facies variation.

## 2.2 Previous Geological Investigations

The geology of the northeast coast of Kangaroo Island was first discussed by Tate (1883), Brown (1898) and Howchin (1899, 1903). A middle-upper Palaeozoic age was tentatively assigned to the sequence based on the presence of reworked (?Cambrian) limestone boulders in conglomerates and the absence of any significant metamorphism. Attempts were made to make correlations with the Fleurieu Peninsula by Tate (1883) and Brown (1898). Howchin (1903) identified the geographical axis of the island as a continuation of the Mount Lofty Ranges and linked the "highly metamorphosic" (Howchin 1903, p. 80) zone on the south of the island with those east of the Mount Lofty Range. In the first record of a Cambrian age for these beds, Wade (1915) described probable basal Cambrian conglomerates, breccias and quartzites lying unconformably on the Precambrian schists and quartzites west of Kingscote. This is also the first record of two distinct sections outcropping along the north-central to northeast coast of Kangaroo Island, namely the metamorphosed "Precambrian schists" west of Stokes Bay and the unmetamorphosed section between Stokes Bay and Pt. Marsden. The unmetamorphosed sequence was thought to unconformably overly the metamorphosed sequence.

The first detailed geological study of the north coast of Kangaroo Island was undertaken by Madigan (1928) who examined coastal outcrops from Cape Cassini to Emu Bay. The

whole sequence from Point Marsden to Cape Cassini was named the Point Marsden Series (Fig. 2.1). Madigan also found examples of archaeocyathans within the conglomerates at Cape D'Estaing. The sequence was concluded to be of shallow marine - fluvial origin and derived from neighbouring highlands which were composed of Cambrian and Precambrian rocks and furnished the boulders of archaeocyathan limestone and other rock fragments. The Point Marsden Series was considered post-Cambrian in age. Madigan also reported trilobite tracks from a shaley sequence in Freestone Creek. A correlation was also postulated between the conglomerates of the Point Marsden Series and the Sturtian tillites from Inman Valley.

The South Australian Geological Survey commenced regional geological mapping on Kangaroo Island in 1952. However, an accident terminated the investigation after only a preliminary study of the north coast section and various inaccuracies were contained in the subsequent report of Sprigg *et al.* (1954). Four formations were defined within the "Point Marsden Group" (Fig. 2.1), which crops out from Point Marsden in the east to Snelling Beach in the west. The preliminary nature of the investigation failed to indicate any major faults or dip reversals within the sequence. Sprigg *et al.* (1954) recognised a stratigraphic succession composed of the Stokes Bay Sandstone, Emu Bay Shale, White Point Limestone and the Point Marsden Conglomerate. Sprigg (1952, 1955, p. 166) suggested "the outer edge of a narrow continental platform" as the depositional environment for the Point Marsden Group. Large slump structures within the Stokes Bay Sandstone were interpreted as suggestive of a shallow water terrace platform edge, adjacent to a steep continental slope. The conglomerates of the White Point Limestone were attributed to the outer talus slope of an eroding archaeocyathan reef, despite the low number of blocks containing archaeocyathans and the abundance of basement clasts. Fossils collected by the survey party from the Emu Bay Shale were identified by Glaessner (1952) as the trilobites *Redlichia* n. sp. and *Lusatiops* n. sp., the hyolithid *Hyolithes* sp. and the brachiopod *Acrothele*. On the basis of the trilobite associations, Sprigg (1955) suggested an uppermost Early Cambrian age for the Emu Bay Shale.

Daily's (1956) seminal work on the Cambrian of South Australia included the most comprehensive study yet done on the succession along the north coast of Kangaroo Island. The term "Point Marsden Group" was discarded in favour of the Kangaroo Island Group. Four formations were recognised in a continuous stratigraphic succession from Bald Rock (east of Emu Bay) to White Point (west of Boxing Bay) (Fig. 2.1). These comprised 33 m of an unnamed chocolate-coloured micaceous shale, conformably overlain by the White Point Conglomerate (380 m), the Emu Bay Shale (110 m) and the Boxing Bay Formation (760 m between Bald Rock and White Point plus another possible 365 m at Pt. Marsden). The conglomerates at Point Marsden were attributed to an upward extension or fault repetition of the Boxing Bay Formation and so the term "Point Marsden Conglomerate" was abandoned. The mainly carbonate-rich clasts in the lower parts of the White Point Limestone were observed to contrast with the distinctive granitic clasts at higher stratigraphic levels. Thus Daily abandoned "White Point Limestone" in favour of White Point Conglomerate. This and the lack of large numbers of clasts containing archaeocyathans, were taken to indicate erosion through a Cambrian sequence into a basement complex similar to that on Yorke Peninsula, indicating active stripping of a nearby land mass rather than talus from an archaeocyathan reef. The underlying Stokes Bay Sandstone was tentatively correlated with the Pound Sandstone in the Flinders Ranges (at that time thought to represent the basal Cambrian in South Australia). Unnamed opisthoparian trilobites found within the White Point Conglomerate were assigned to faunal assemblage 11 of Daily (1956), thus implying an upper Early Cambrian age. *Isoxys* n. sp., annelids and a crustacean found in the Emu Bay Shale were assigned to faunal assemblage 12. On the basis that faunal assemblage 12 was uppermost Early Cambrian, the Early-Middle Cambrian boundary was placed within the overlying Boxing Bay Formation. Close correlation between the Kangaroo Island Group and strata documented on the mainland remained elusive.

In 1956, Minlaton #1 was drilled on southern Yorke Peninsula by the South Australian Department of Mines and Energy, intersecting a 760 m thick sequence of Early-Middle Cambrian strata which was partially correlated with the Cambrian strata of the Kangaroo

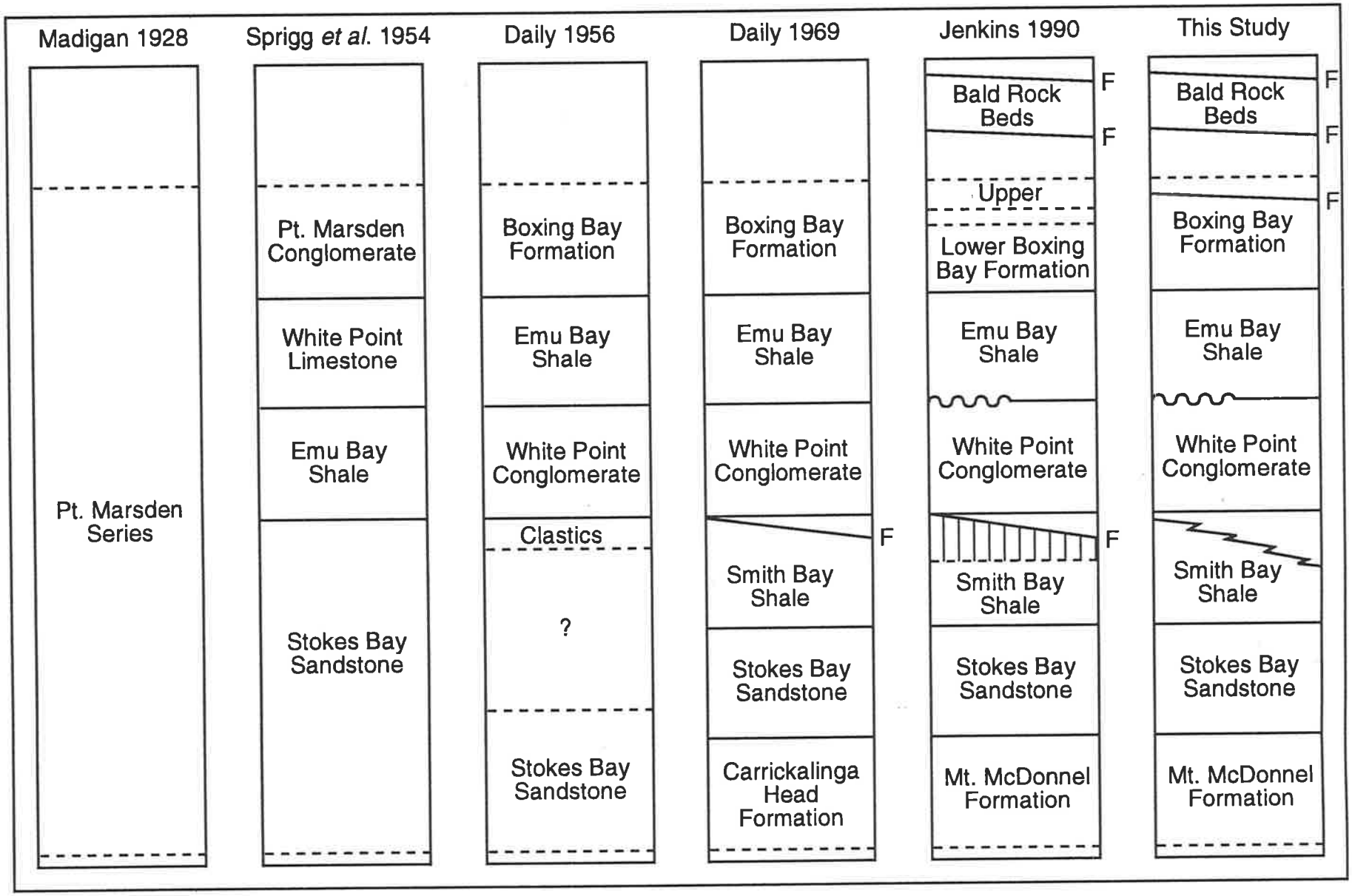


**Fig. 2.1** Successive stratigraphic nomenclature used for the sequence along the north coast of Kangaroo Island.

Island Group (Daily 1957). A 27 m thick terrestrial conglomerate unconformably overlying the Early Cambrian Parara Limestone was tentatively correlated with the marine White Point Conglomerate on lithological grounds. 110 m of red silty clastics containing gypsum and other carbonate interbeds, overlying the conglomerate in Minlaton #1, were tentatively correlated with the Emu Bay Shale and the Boxing Bay Formation (Horwitz and Daily 1958, fig. 14). The same work also revised the stratigraphy of the Kangaroo Island Group, with the recognition of the Smith Bay Shale occupying an intermediate stratigraphic position between the Stokes Bay Sandstone and the White Point Conglomerate - the unnamed chocolate-coloured shale of Daily (1956). Worm burrows and trilobite tracks were recognised from green and purple shales underlying the Smith Bay Shale, establishing a Cambrian age for what had been mapped as "Adelaidian phyllites" by Sprigg *et al.* (1954).

The palaeontology of the section was further refined with the re-classification of the trilobite *Lusatiops*, as belonging to a new genus, *Estaingia bilobata* (Pocock 1964). In subsequent studies, a new family of trilobites, the Emuellidae, was recognised from the White Point Conglomerate and the Emu Bay Shale (Pocock 1970). *Balcoracania dailyi* and *Emuella polymera* were described from Daily's faunal assemblage 11 in the upper White Point Conglomerate and *Emuella dalgarnoi* was described from Daily's faunal assemblage 12 in the lower Emu Bay Shale (Pocock 1970). With the description of *Balcoracania flindersi* from the Billy Creek Formation in the Flinders Ranges (Pocock 1970), a correlation could be made for the first time between the sequence on Kangaroo Island and the mainland. The presence of *Balcoracania* in the White Point Conglomerate and the Billy Creek Formation, which lies within a generally fossiliferous sequence, suggested a late Early Cambrian age for the White Point Conglomerate.

Further stratigraphic drilling on Yorke Peninsula occurred in 1966 and 1967. Stansbury West #1 was drilled 5 km west of Stansbury township and intersected approximately 1310 m of Cambrian strata which included almost 120 m of red-beds and minor interbedded carbonate resting unconformably on the Early Cambrian Parara Limestone

(Watts & Gausden 1966). This was correlated with the Minlaton Conglomerate and overlying red-beds in Minlaton #1.

Edithburgh #1, some 24 km southwest of Stansbury township intersected only 530 m of Cambrian strata, with a major unconformity separating the Early Cambrian Kulpara Limestone from the Middle Cambrian Dalrymple Limestone (Daily 1968). This indicated that the southern part of Yorke Peninsula was uplifted during the late Early Cambrian and (?)early Middle Cambrian, resulting in the partial erosion of the Cambrian carbonate cover. Additional evidence for this epeirogenic movement came with the drilling of Stansbury Town #1. The bore intersected a similar section to that in Stansbury West #1, except for a thicker sequence of (?)Middle Cambrian red-beds and a substantially thinner sequence of Early Cambrian carbonates (Laws & Heistler 1967). The 27 m thick basal Minlaton Formation conglomerate in Stansbury Town #1 includes mainly dolomite clasts towards the base and crystalline basement clasts towards the top. This was suggestive of progressive stripping of Early Cambrian platform cover from uplifted areas (Daily (1968). The conglomerates do not indicate local derivation, and are thus suggestive of a regional event which was correlated with the White Point Conglomerate.

Connard (1967) carried out additional mapping of the north coast of Kangaroo Island, placing beds in the Stokes and Smith Bay area stratigraphically younger than previous workers.

McKirdy (1967), in a geochemical study of the Emu Bay Shale outcropping at Big Gully, found euhedral haematite grains strongly suggestive of authigenic pyrite pseudomorphs and that authigenic calcite was ubiquitous. Haematite lenses were attributed to relic discoidal aggregates of microgranular sulfide, which formed contemporaneously with the deposition and decay of the original organic matter. A high level of elemental sulphur was noted.

The sequence of green and purple shales and siltstones underlying the Stokes Bay Sandstone near Hummocky Point on the mid north coast of Kangaroo Island was named the Mt. McDonnell Formation by Daily (1969). The sequence, considered to consist of 6 units, was also correlated with the Kanmantoo Group on the Fleurieu Peninsula, and

with the the Minlaton Conglomerate and overlying red-beds on Yorke Peninsula. A more detailed correlation was made by equating the Mt. McDonnell Formation with the basal member of the Kanmantoo Group, the Carrickalinga Head Formation (Fig. 2.1). The Kanmantoo Group was equated lithologically with the Kangaroo Island sequence, suggesting an age older than the Middle Cambrian Ramsey Limestone of Yorke Peninsula. The beginning of Kanmantoo Group sedimentation was suggested to co-inside with a rapid influx of clastics, due to the Early Cambrian Kangarooian Movement (Daily & Forbes 1969).

Erosion of the area to the west of Kangaroo Island was inferred to have been the source of sediments for the sequence along the northeast coast (Thompson 1969). However, seismic data indicate that the supposed source area is floored by a considerable thickness of Kanmantoo metasediments and associated granites (Smith & Kamerling 1969), with no evidence for a land mass in this region. The assertion that the Torrens Lineament is "truncated in the south by the Cygnet Fault" (Thompson 1969, p. 107) was not supported by the data, which indicated that the sediments continued from north-south on Fleurieu Peninsula, to east-west across Kangaroo Island and extend on to the northwest in an unbroken trend (Smith and Kamerling 1969). Daily *et al.* (1973, p. 63) interpreted this trend as representing part of a depositional trough, with the "southern section of the arc owing its shape to compression against the virtually unyielding Gawler Block".

In a more detailed geochemical study of the Emu Bay Shale, at Big Gully, McKirdy (1971) described finely laminated shales at the base of the formation at Big Gully as containing limonite pseudomorphs after pyrite, suggestive of restricted circulation and slightly reducing conditions during deposition, with relatively low organic carbon levels indicative of subsequent oxidation. Again, high levels of free sulphur were reported.

Daily (1969) formalised the Mount McDonnell Formation, underlying the Stokes Bay Sandstone on Kangaroo Island and also formalised the Carrickalinga Head Formation as being the basal unit of the Kanmantoo Group on Fleurieu Peninsula.

Detailed studies of the Kanmantoo Formation (Daily & Milnes 1971,1972a, b) resulted in the subdivision of the Carrickalinga Head Formation, on southern Fleurieu Peninsula,

into three members, the Madigan Inlet Member, the Blowhole Creek Member and the Campana Creek Member. The Carrickalinga Head Formation and the Mt. McDonnell Formation were directly correlated by Daily and Milnes (1971).

The deposition of immature shales, silts, sands and gravels within the Kanmantoo Group was attributed to the sporadic nature of the Kangarooian Movements (Daily & Milnes 1971, 1972b). A decrease in pebble size from west to east in the Inman Hill Subgroup (overlying the Carrickalinga Head Formation) and the abundance of southeast trending current indicators in the overlying Brown Hill Subgroup (Daily & Milnes 1972a) suggested uplift and erosion of a land mass to the north of Kangaroo Island in the late Early to early Middle Cambrian.

Stuart and Sanden (1972) reported an unconformity surface in Cambrian strata recognisable in seismic reflection records and extending as far east as the Eden-Burnside Fault Zone. Whilst correlating the Kangaroo Island Group with the Kanmantoo Group, Stuart and Sanden (1972, fig. 4) equated the Emu Bay Shale and the basal part of the Boxing Bay Formation with the Minlaton Conglomerate.

Daily (1977) reported the discovery of trilobite fragments on Kangaroo Island within the Mt. McDonnell Formation.

In the most comprehensive study on the stratigraphy and sedimentology of the Kangaroo Island Group yet undertaken, Moore (1979) compared the Kangaroo Island Group with the Billy Creek Formation in the Flinders Ranges, correlating the White Point Conglomerate with the laterally equivalent Warragee and Coats Hill Members of the Billy Creek Formation, utilising the common occurrence of *Balcoracania dailyi* . The correlation of the Mt. McDonnell Formation with the Carrickalinga Head Formation was maintained, with its subdivision on Kangaroo Island into the lower, Blowhole Creek Siltstone Member Equivalent and the upper, Campana Creek Member equivalent. Moore discussed the palaeoenvironment of the Kangaroo Island Group in terms of an interfingering of alluvial and tidal deposits along a shoreline migrating due to fault uplift to the north and basin subsidence to the south. The source of the alluvial fanglomerates in the White Point Conglomerate was attributed to uplifted blocks to the north.

Glaessner (1979) recognised several crustacea and annelid worms, including *Tuzoia australis*, *Myoscolex ateles* and *Palaeoscolex antiquus* from the Emu Bay Shale. Glaessner also recognised replacement of soft tissues with calcite and preservation of muscle blocks. A further unpublished study of the Upper Kangaroo Island Group by Dinnick (1985), concurred with the suggestion of a northerly source for the White Point Conglomerate sediments and the general environment of deposition as a molassic apron in front of blocks uplifted during the Kangarooian Movements. A disconformable contact between the White Point Conglomerate and the overlying Emu Bay Shale at Big Gully was also documented for the first time. With the suggestion that some Kanmantoo sediment clasts were present, Dinnick maintained the designation of the Bald Rock Beds following their recognition as possibly representing a later phase of deposition separate from rest of the Upper Kangaroo Island Group sediments by Daily *et al.* (1979). Based on observations concerning the Upper Kangaroo Island Group sediments, Dinnick postulated that the Kangaroo Island Group and the Kanmantoo Group might not be time equivalent.

In an fundamental re-appraisal of the structure of the southern Adelaide Fold-Thrust Belt, Jenkins (1990) recognised that the Mount Lofty Ranges encompassed an imbricate pattern of southeasterly dipping thrust faults, which exhibit a west to northwest vergence. The Kanmantoo sediment in the Kanmantoo Trough were considered as the flyschoid sediments of an extensional trough and the characteristic north coast sediments a molassic sequence with a foreland basin, with some sediment supply for the molassic phase from the south or southeast (Jenkins 1990), or from the east and southeast (Coney *et al.* 1990; Mancktelow 1990). Implicit in this was the suggestion that the Delamarian Orogeny occurred earlier than the previously accepted Late Cambrian - Early Ordovician time frame and that the Kanmantoo Group predated the Kangaroo Island Group (Fig. 2.1). Subsequent mapping of thrust faulting in the southern Adelaide Fold-Thrust Belt (e.g. Flöttmann & James 1994) has vindicated some of the suggestions of Jenkins (1990) and provided a more detailed tectonic framework (Flöttmann *et al.* 1994; Flöttmann *et al.* 1995) in which to place the depositional and structural history of the

southern Adelaide Fold-Thrust Belt. Recent geophysical investigations have shown that the southern margin of the Gawler Craton actually extends further south than was believed and the southern boundary is now taken as the Cygnet - Snelling Fault, which delineates the Kangaroo Island Shear Zone (Belperio & Flint 1993, Flöttmann *et al.* 1995). This southward extension of the craton allows the possibility that uplift in this area might provide a southerly source for some of the Cambrian of the north coast as suggested by Jenkins (1990).

## 2.3 Geological Setting

Neoproterozoic Adelaidean strata and suggested equivalents of the Early Cambrian mainland Normanville group occur in the core of a regional antiform at the northeastern tip of Dudley Peninsula (Daily *et al.* 1979). The Cygnet and Snelling Faults (Fig. 2.2) represent a major, early formed, structural discontinuity across the northern part of the Island (Sprigg *et al.* 1954), with late Cainozoic reactivation resulting in the uplift of the south central tableland relative to the lower, northern coastal plateau (Flöttmann *et al.* 1995).

Three distinct lithotectonic domains have recently been recognised on Kangaroo Island (Fig. 2.2), a northern structural zone encompassing the Kangaroo Island Group of Daily *et al.* (1980); a southern structural zone composed almost exclusively of psamitic and pelitic metasediments of the Kanmantoo Group; and the intervening Kangaroo Island Shear Zone (Flöttmann *et al.* 1995). This zone of intensely deformed tectonites stretches from Cape Forbin/Kangaroo Gully in the west to Point Morrison/American River and Dudley Peninsula in the east.

The southern zone displays limited inland outcrop. The sediments exhibit regional metamorphism to biotite grade and show persistent psammic/pelitic alternations. They evidently correlate with the Kanmantoo Group of Daily & Milnes (1971) and appear to

comprise sequences from the Carrickalinga Head Formation through to the Middleton Sandstone.

The Kangaroo Island Shear Zone represents a fundamental Delamerian displacement zone, separating the northern platformal sediment from the southern basinal sediments. This is a ductile, intensely mylonitized sheer zone up to several kilometres wide.

The northern zone contains the Kangaroo Island Group (Daily *et al.* 1980), which outcrops from Snelling Beach in the west to Point Marsden in the east. The zone records a northward waning of deformation and contains several reverse faults, including an imbricate fan at Cape Cassini (Flöttmann *et al.* 1995). All kinematic indicators, fibres, slickensides and mineral slip lineations, give $000^{o}$ - $010^{o}$ directed displacement vectors.

## 2.4 Geological History of the Kangaroo Island Group

The Kangaroo Island Group represents a proximal offshore to shallow water clastic sequence, maximally some 2200 m thick (Moore 1979, Belperio & Flint 1993) occurring on the northern part of Kangaroo Island. The gently deformed and weakly metamorphosed strata comprise six formations (Fig. 2.1), which , in part, directly overlies the Palaeoproterozoic basement of the Gawler Craton (Belperio and Flint 1993). The Kangaroo Island Group has been subdivided into a 'Lower' sequence comprising the Mt. McDonnell Formation, the Stokes Bay Sandstone and the 'Lower' Smith Bay Shale; and an 'Upper' sequence comprising the 'Upper' Smith Bay Shale, the White Point Conglomerate, the Emu Bay Shale and the Boxing Bay Formation (Daily *et al.* 1980) as these sequences are separated by an intervening reverse fault. However, there is no *a-priori* reason why the the 'Lower' and 'Upper' Smith Bay Shale cannot represent lateral equivalents (Fig. 2.1).

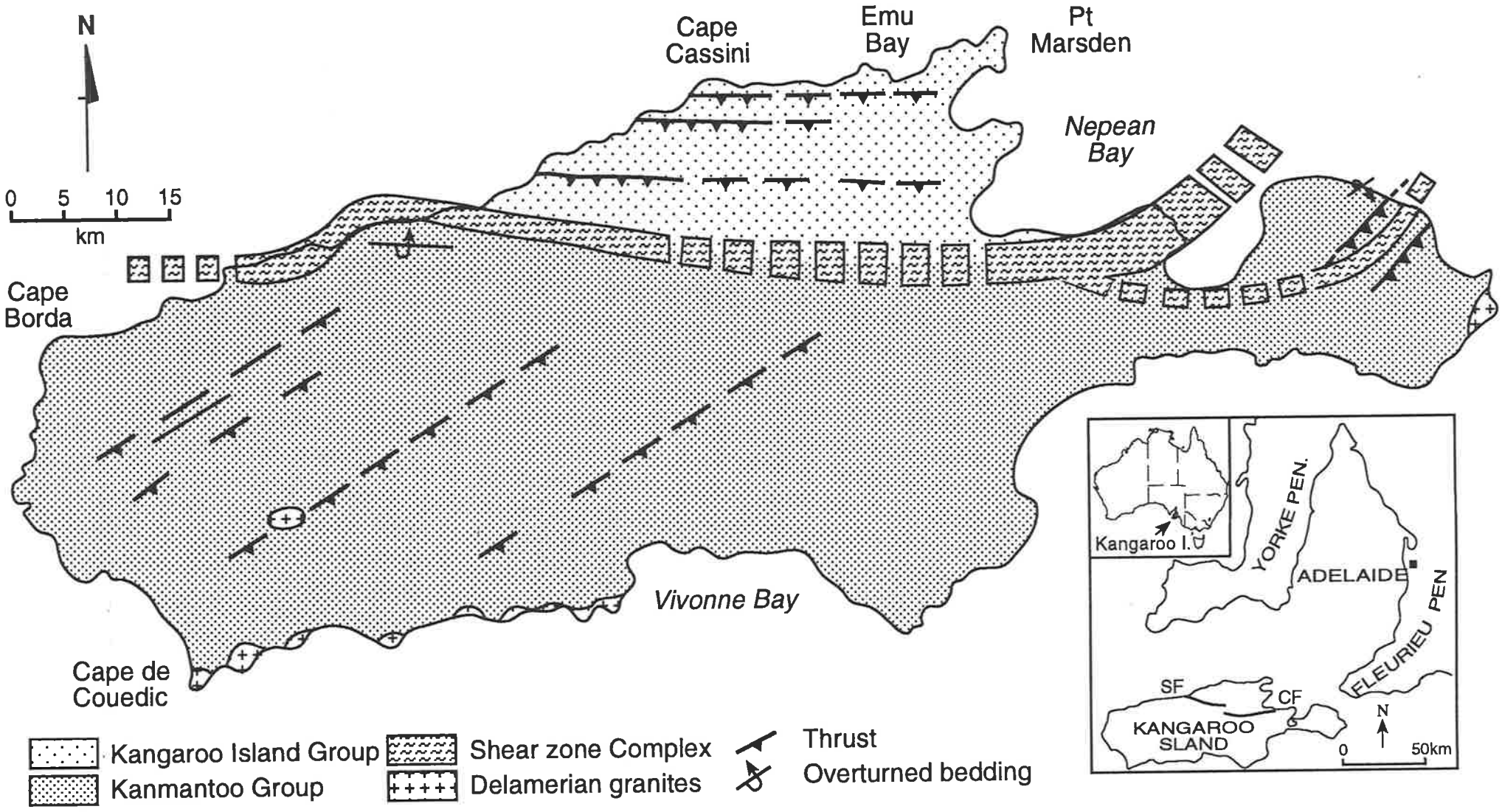


**Fig. 2.2** Tectonic scetch map of Kangaroo Island showin the three structuaral domains present. SF, Snelling Fault; CF, Cygnet Fault. After Flöttmann *et al.* 1994.

The Late Early and early Middle Cambrian Kangarooian Movements represented a complex and persistent tectonism, most pronounced in the southern portion of the Fold-Thrust Belt, with tectonic activity expressed as far away as the Officer Basin (Mt Johns Conglomerate) and the Mt. Scott Range (upper Ajax Limestone) (Gravestock 1995). Pre-Kangarooian sedimentation is represented by shallow water, platformal limestone developed to the north of Kangaroo Island, and the Lower Kangaroo Island Group on the north coast . The basal sequence of the Kangaroo Island Group was originally named the Mt. McDonnell Formation by Daily (1969), prior to being directly correlated with the Carrickalinga Head Formation (Daily & Milnes 1971). The finding of an archaeocyathan-bearing limestone high in the Upper Mt. McDonnell Formation (Gravestock 1995) suggests a potential correlation with the Forktree Limestone rather than with the the Carrickalinga Head Formation. Therefore the name Mt. McDonnell Formation is retained and the twofold subdivision erected by Moore (1979) is renamed the Lower and Upper Mt. McDonnell Formation.

The environment of deposition has been compared with modern tidal deposits (Moore 1979). However, the paucity of such characteristics as tidal channels and the presence of turbiditic sequences, at least in the lower member, appear to indicate an offshore environment. The depositional environment appears to have been initially, low energy offshore, where sandy shoals developed in response to the concentration of tidal and storm energy. Where energy was lower, flaser and linsen bedded units were deposited. The Upper Mt. McDonnell Formation represents an overall shallowing upward cycle as evidenced by the occurrence of rippled sandstones, representative of moderate-energy, shallow water, subtidal deposits. Trilobite tracks, molluscan trails and worm burrows are abundant. Rare *Redlichia* sp. fragments have been reported from a thin yellowish-brown calcareous sandstone (Daily 1969). A sparse assemblage high in the Upper Mt. McDonnell Formation is composed in part, of deep water archaeocyathans, including *Erugathocyathus aquilinus* and the problematic algae *Nuia*, with phosphatic brachiopods and trilobite fragments suggestive of a Botomian age (Gravestock 1995).

During Upper Mt. McDonnell Formation deposition, sediment supply outstripped basin subsidence producing an overall shallowing upward cycle, which culminated in the overlying Stokes Bay Sandstone.

The Stokes Bay Sandstone appears to have been deposited by strong, unidirectional west to east currents, parallel to the strandline on a shallow marine shelf (Moore 1979). The poor sorting and mineralogy of the sandstones and included clasts indicate derivation from a proximal basement source, presumably the Gawler Craton (Daily *et al.* 1979; Moore 1979) with rapid deposition following only minor sorting and abrasion. Within medium grained arkoses, contorted and convoluted layers are common (Pl. 1.1). Rare granules and pebbles of crystalline basement and poorly defined scours or shallow channels can be found (Moore 1979).

Sediments identified as the Smith Bay Shale outcrop at two localities on Kangaroo Island. At Smith Bay a 120 m thick pelitic sequence rests conformably on the underlying Stokes Bay Sandstone. The other, between Bald Rock, and Hawk Nest, has an 88 m shale sequence grading conformably into the overlying White Point Conglomerate (Pl. 1.2). At the latter locality the base of the sequence is faulted against highly silicified and contorted quartzites of uncertain but presumably Early Palaeozoic affinities (Pl. 1.3).

The Smith Bay Shale may represent an offshore to shallow subtidal environment, subject to shore parallel tides, but with only minor onshore wave activity (Moore 1979).

The coarser grained facies of the Hawk Nest sequence, together with the change in the alignment of current lineations, is indicative of a differing environment of deposition to that of the Smith Bay sequence. The two sequences, separated as they are by some 8 km, may well represent a *lateral* relationship rather than a sequential one as suggested by Daily (1976). Thus the Hawk Nest section may indicate dominantly subtidal facies with currents influenced by the nearby coastline, compared with the more intertidal mudflat environment of the Smith Bay sequence, as suggested by common arthropod tracks and

# Plate 1

**1.1** Convoluted bedding in the uppermost Stokes Bay Sandstone at Smith Bay, looking southwest. Thin, dark coloured rock above convoluted beds is the Smith Bay Shale. Outcrop at center-left of photograph 2.5 metres tall.

**1.2** Gradational contact between the Smith Bay Shale and the overlying White Point Conglomerate east of Bald Rock, in the Bald Rock to Hawk Nest section, looking south. Hammer head at base of first major sandstone bed. Hammer 30 cm.

**1.3** Faulted contact between the Smith Bay Shale (left) and quartzites of the Bald Rock Beds (left) just east of Bald Rock in the Bald Rock to Hawk Nest section, looking south. Outcrop in middle of scree slope is *in situ* Smith Bay Shale. Height of central outcrop 3 metres.

**1.4** Ripples in siltstone of the Smith Bay Shale east of Bald Rock, in the Bald Rock to Hawk nest section. Compass indicates north (up) showing palaeocurrent direction was to the west. Compass length 12 centimetres.

**1.5** Archaeocyathan limestone clasts in the White Point Conglomerate 100 m west of Big Gully, looking west. Pen is 13 centimetres.

**1.6** White Point conglomerate at Big Gully showing conglomerate grading to coarse, cross-bedded sandstone, looking west. Hammer 30 centimetres.

# PLATE 1



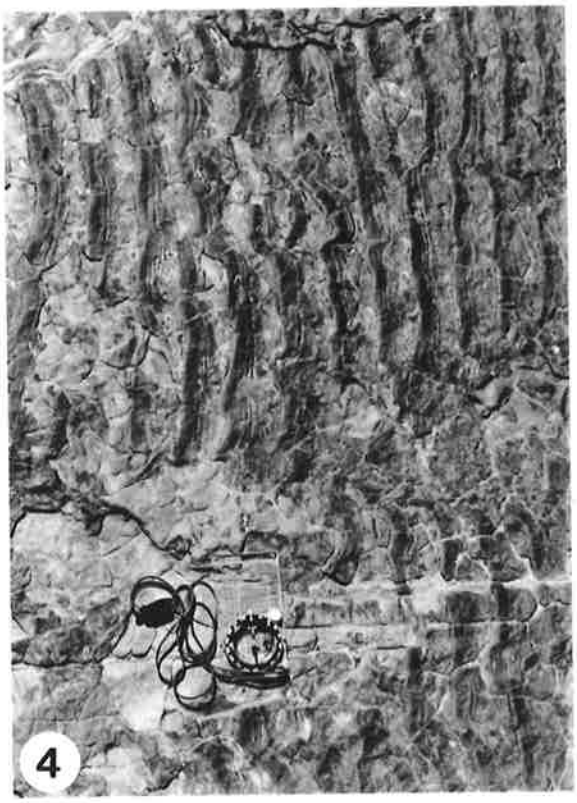




mud cracks. This depositional cycle indicates a decrease in the availability of coarse clastic sediment. This may be connected with the southward expansion of archaeocyathan reefal development in the Koolywertie Member (Zhuravlev & Gravestock 1994), which implies a reduction in sediment input to the region.

The Hawk Nest section exhibits current lineations orientated northwest to southeast, with a minor component northeast to southwest (Moore 1979). Finer grained sediments, possibly indicative of a more distal environment, exhibit dominantly westerly-directed current indicators (Pl. 1.4).

Worm burrows and arthropod tracks occur in the Smith Bay Shale, with tracks more common in the Hawk Nest sequence. *Redlichia* fragments have been recorded from a thin arenaceous limestone in the Smith Bay sequence inland along Freestone Creek (Daily 1977).

The conformable contact with the overlying White Point Conglomerate marks the upper boundary of the Lower Kangaroo Island Group and signals initiation of the Kangarooian Movements.

The White Point Conglomerate outcrops at three localities on the northeast coast of Kangaroo Island: between Bald Rock and Big Gully, in Emu Bay and in a small, fault bound outcrop on Cape d'Estaing (Fig. 2.3). At its type section, between Bald Rock and Big Gully, the White Point Conglomerate is represented by 610 metres of polymict conglomerates interbedded with occasional sandstones and rare mudstones (Pl. 1.5), the finer facies being concentrated within the basal 165 metres. Carbonate clasts dominate, with rare archaeocyathan-rich limestone clasts in the upper part of the sequence (Pl. 1.6). Gravel conglomerates exhibit trough cross-stratification and commonly grade laterally and vertically into, or are capped by, planar bedded sandstones (Pl. 2.1). Red-brown, fine to medium grained, moderately sorted arkosic sandstones dominate the lower 160 metres of the White Point Conglomerate at this locality, predominantly occurring as trough cross-stratified sandstones, occasionally with convolute soft-sediment

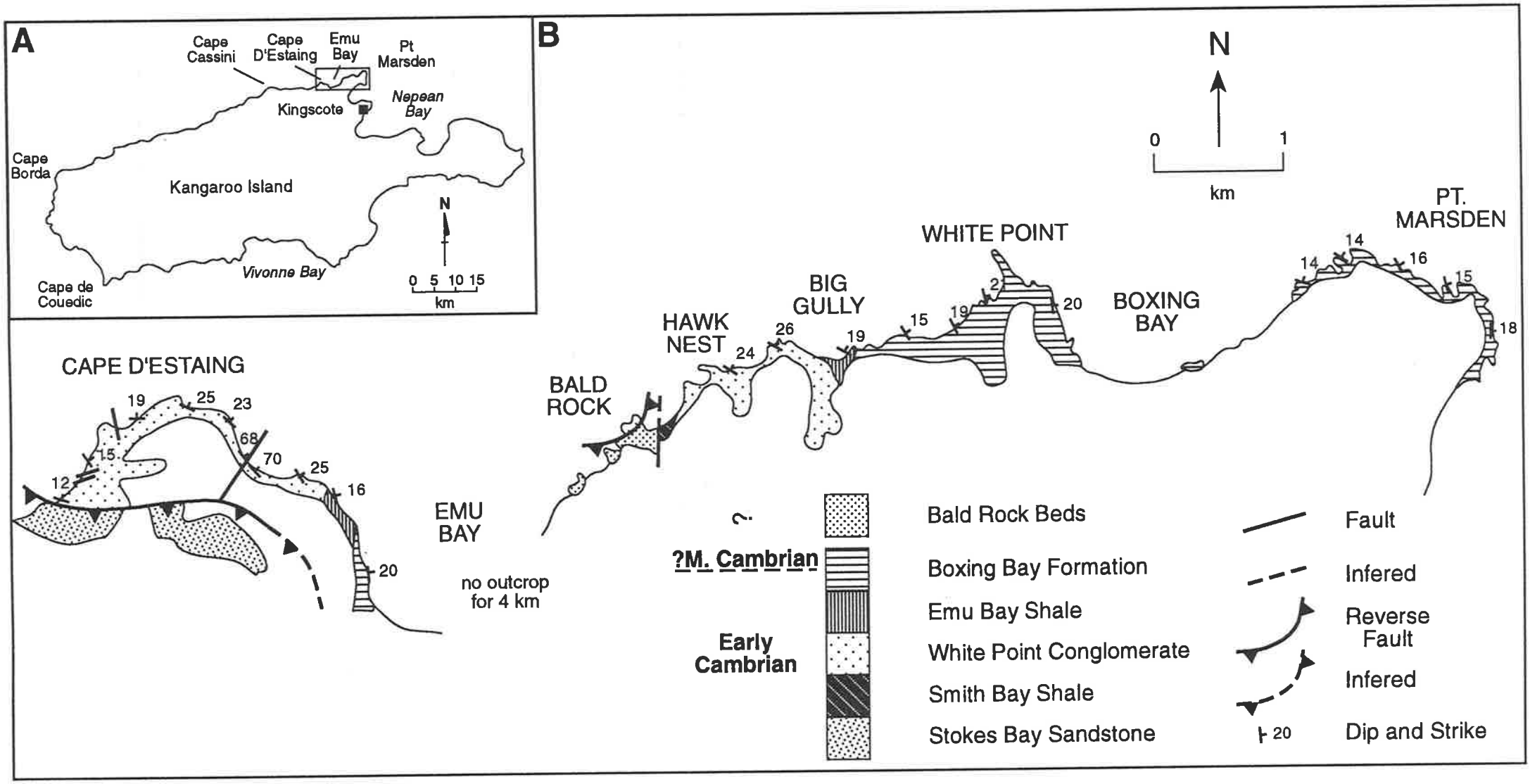


**Fig. 2.3** **A**. Map showing the location of the study area on the north coast of Kangaroo Island. **B**. Geological sketch map of the north coast between Cape D'Estaing and Pt. Marsden. Outcrop is confined to the coastal strip. Emu Bay has been omitted due to lack of outcrop.

# Plate 2

**2.1** Fining upward cycle in the White Point Conglomerate at Big Gully from matrix supported conglomerate (bottom) through cross-bedded grits to flat bedded sandstones with occasional grit pods, looking west. Hammer is 30 cm.

**2.2** Grit bands within the White Point Conglomerate at Emu Bay, looking north west. Pen is 13 cm long.

**2.3** Conglomerate at the contact between the White Point Conglomerate and the overlying Emu Bay Shale at Emu Bay, looking north west. Hammer is 30 cm.

**2.4** Conglomerate with micritic limestone clasts at Cape d'Estaing, looking south. Hammer is 30 cm long.

**2.5** Extensively burrowed limestone bed in White Point Conglomerate at Emu Bay. This unit also occurs at Cape d'Estaing and at Big Gully and is here considered correlative, looking northwest. Pen is 14 cm long.

**2.6** Distinctive conglomerates in the Bald Rock Beds filling fissures in the underlying beds. Clasts, well rounded and polished, predominantly of metasediments and metamorphics, looking west. Hammer is 30 cm long.

# PLATE 2


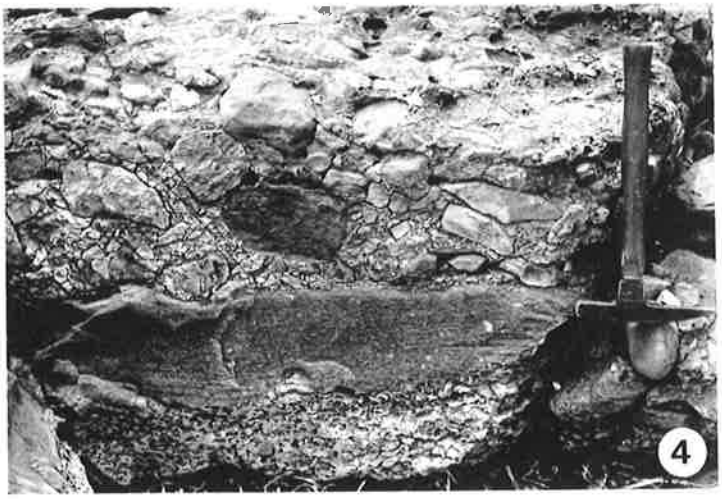



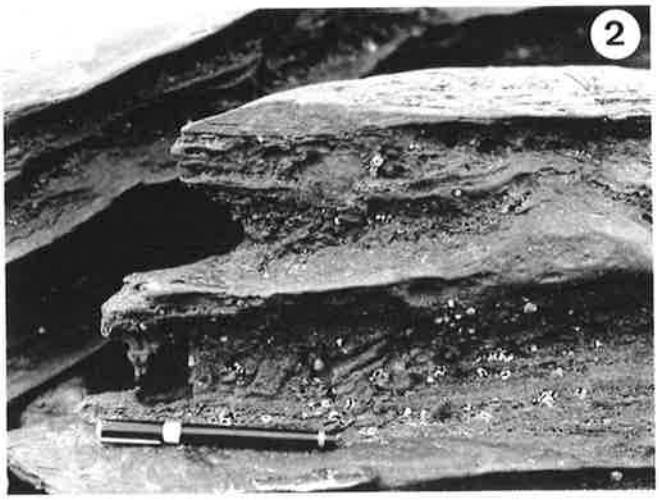



deformation. Red-brown to red sandstones, siltstones and mudstones exhibiting mud cracks and arthropod trails are confined almost exclusively to the this basal sequence.

At Emu Bay, the outcropping White Point Conglomerate has been ascribed to the upper part of the formation (Daily *et al.* 1979). Here, conglomerates are rarely developed. The lower part is dominated by fine grained facies whilst the upper part is composed mainly of sandstones and occasional siltstones. Planar stratified and trough cross-stratified, micaceous, arkosic and quartzose sandstones may grade up into grit beds containing rare, isolated basement clasts (Pl. 2.2). A conglomeratic development within the sequence consists of horizontally bedded conglomerates with development of sandy interbeds. Another conglomerate occurs at the contact with the overlying Emu Bay Shale (Pl. 2.3). The lower part of the sequence at Emu Bay is faulted against another part of the White Point Conglomerate at Cape d'Estaing (Dinnick 1985).

At Cape d'Estaing well developed conglomerates occur high in the formation and more fine grained facies below. The conglomerate facies are dominated by horizontally bedded conglomerates with sandy interbeds (Dinnick 1985). Clasts consist of micritic limestones (Pl. 2.4) and occasional archaeocyathan limestones.
Laminated or cross-stratified red-brown, arkosic sandstones, are also present.

The predominance of horizontally bedded conglomerates in the lower part of the White Point Conglomerate at the Bald Rock to Big Gully section (Daily *et al.* 1980), combined with the sub-angular clast shape, large clast size and interbedding of debris flow deposits with stream flow deposits, point to this being a proximal alluvial fanglomerate sequence (Rust 1975; Daily *et al.* 1980). The large percentage of clast supported conglomerates suggests that debris flows are a major component in the sequence (Dinnick 1985). The conglomerates may well represent a large, coalescing alluvial fan cone forming between the uplifted area and the sea (Daily *et al.* 1980) (Fig. 2.4). Clasts of archaeocyathan limestone, along with granitic and gneissic basement clasts begin to become increasingly

common up section (Dinnick 1985), probably reflecting continued unroofing of the source area.

Fine gravel conglomerates indicate a northeasterly and subordinate westerly palaeoflow direction. Palaeocurrent direction indicators in the coarse conglomerates have provided evidence for conflicting ideas on palaeoslope direction during deposition (e.g. Daily *et al.* 1979; Jenkins 1990). The presence of conglomerate lenses which thin to the north seem indicative of a southerly source. However, no exposed parts of such a source area exists today, although the transtensional tectonic regime which is envisaged to have been active during this time may well have provided uplift to the south. The conglomerates exhibiting these characteristics seem confined to the upper White Point Conglomerate which may indicate a period of basin reversal and/or migration. These deposits probably underwent reworking by wave and tidal currents with the subordinate westerly flow possibly indicative of longshore drift.

Both coarsening upward and fining upward cycles occur within the conglomeratic sequences within the White Point Conglomerate (Daily *et al.* 1980). Coarsening upward cycles in the Devonian Hornelen Basin of the Nordfjord region of Western Norway have been interpreted as representing continuous fan progradation due to lowering of the basin floor and uplift of the basin margin, related to fault movements (Steel & Gloppen 1980). This, with lateral migration, can result in stacked, coarsening upward cycles. Fining upward cycles (Pl. 2.1) represent periods of quiescence, which occasionally resulted in marine incursions over the fans.

The bulk of the sandstone and mudstone facies are probably unrelated to the conglomerates as they appear mineralogically distinct (Dinnick 1985). These facies probably represent marine conditions with sediment supplied from a more distal, basement source. Weak north-south flow indicators probably represent off shore ebb and flood tidal flow (Dinnick 1985). The fine grained facies containing arthropod tracks, mud cracks and east-west bipolar current indicators, possibly represent low intertidal to subtidal, or even lagoonal sedimentation.

**Fig. 2.4** Reconstruction of palaeogeography at the end of lower White Point Conglomerate deposition. Note differential movement along synthetic listric faults results in greater deposition in the area that is now Hawk Nest to Big Gully. Stratigraphic columns of lower White Point Conglomerate measured at Cape D'Estaing and Hawk Nest - Big Gully to scale, for comparison.

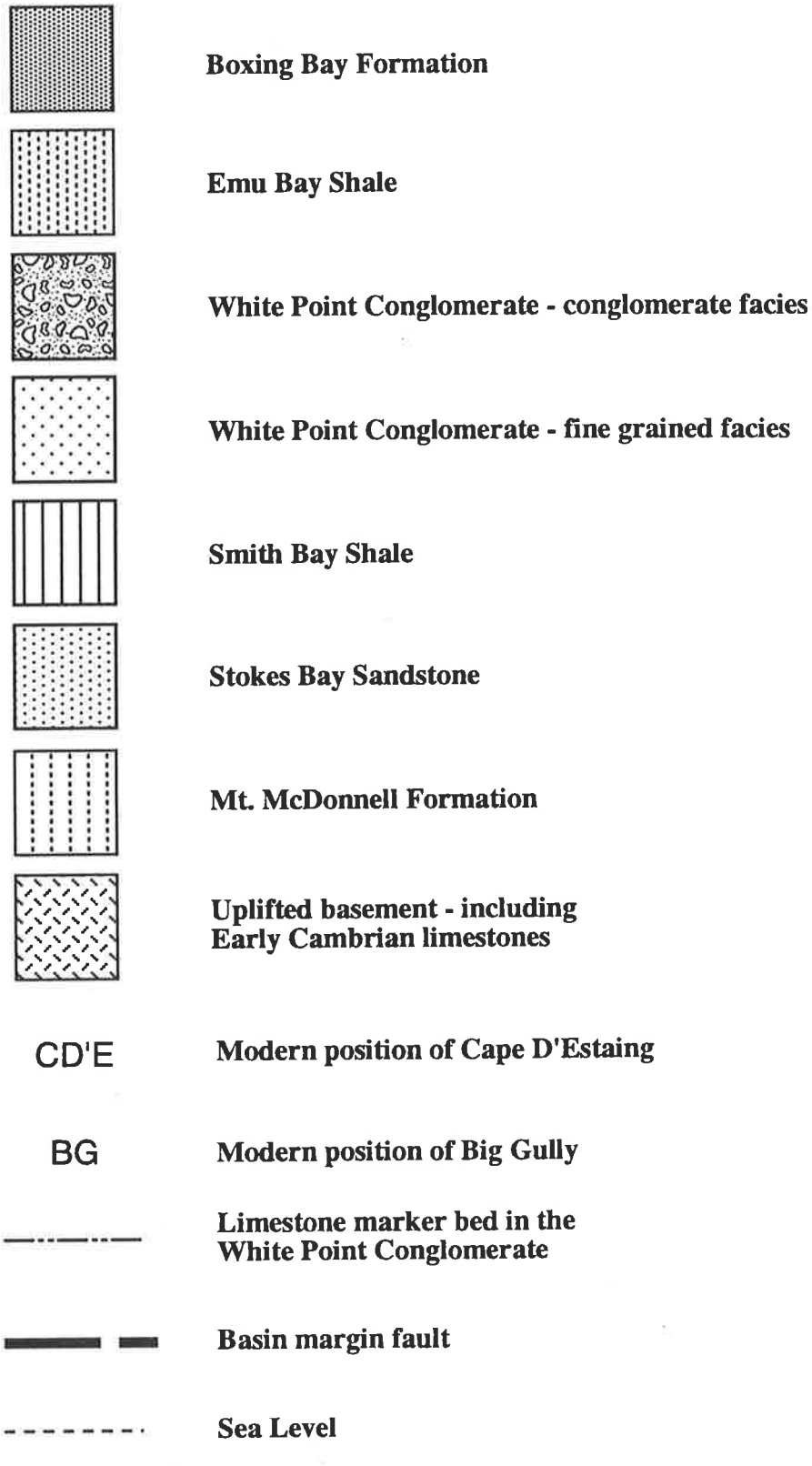

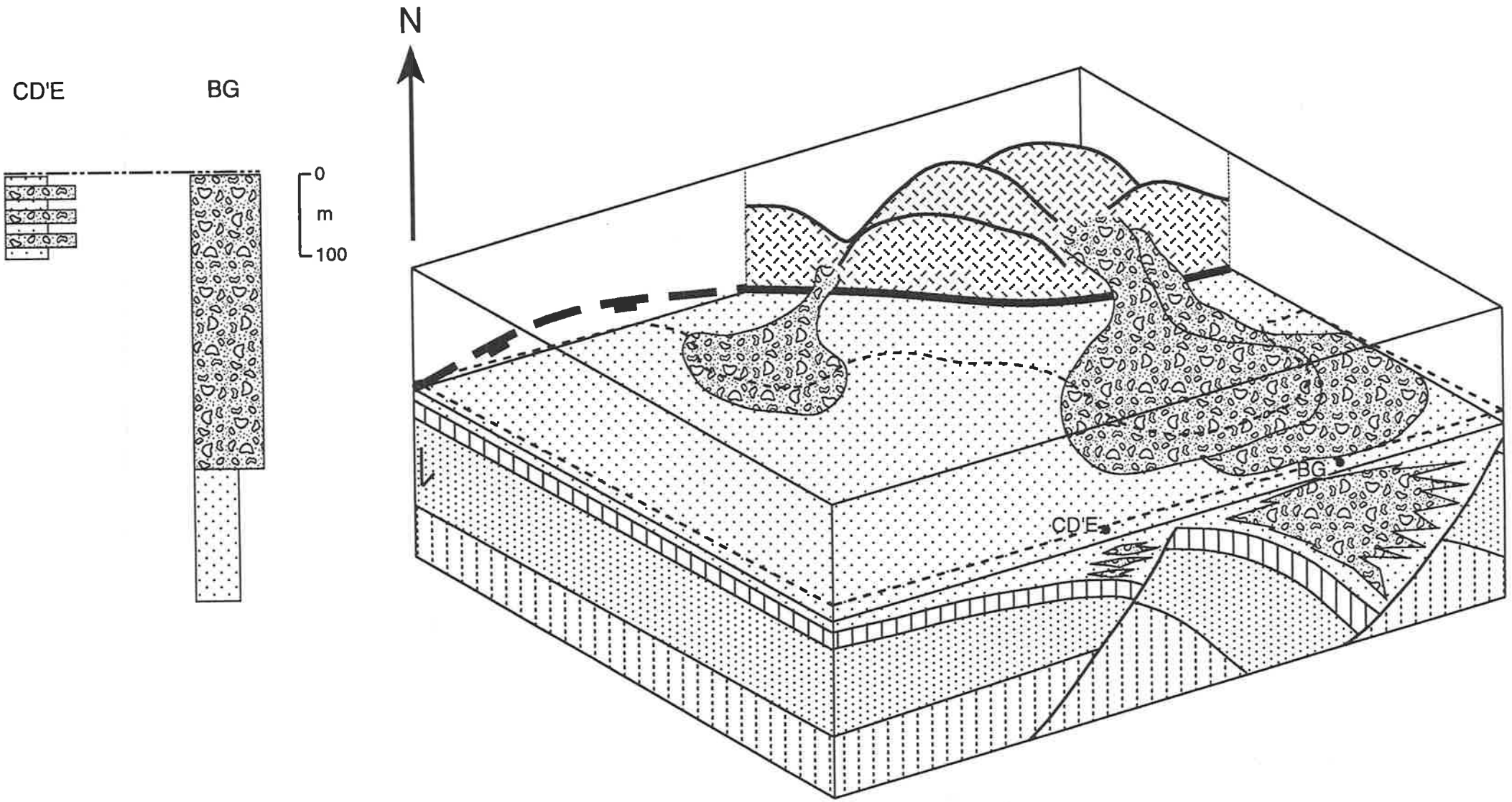
CD'E
BG
0
m
100
N
BG
CD'E

The separate occurrences of the White Point Conglomerate in the Emu Bay-Cape d'Estaing area and at Big Gully-Bald Rock can also be divided informally into lower and upper sequences separated by a grey, mottled, argillaceous, micritic limestone bed (Pl. 2.5) which appears to be a significant stratigraphic marker within the White Point Conglomerate (Moore 1979, Daily *et al.* 1979). The lithological and palaeontological continuity of this bed and the immediately surrounding mudstones, supports its consideration as a contemporaneous marker bed. Thus the deposition of the White Point Conglomerate can thus be discussed in terms of pre- (lower) and post-limestone (upper) deposition.

It is apparent when comparing the lower White Point Conglomerate sequences that a remarkable disparity in the thickness occurs (e.g. Moore 1979) (Fig. 2.4). At the Bald Rock-Big Gully, the lower sequence below the limestone is some 575 metres thick (Daily *et al.* 1980) and is composed of 160 metres of sandstones with minor siltstones, overlain by 415 metres of massive conglomerates. By contrast, the lower section at Emu Bay-Cape d'Estaing reaches at thickness of only about 100 metres and is composed of sandstones with interbedded conglomerates at Cape d'Estaing and siltstones with occasional sandstones at Emu Bay. Since the limestone appears in such disparate levels in the sequences, the question as to the correlation of this bed needs to be addressed. It is possible that in the Emu Bay and Cape d'Estaing sequences limestone deposition occurred early in the depositional history of the White Point Conglomerate. If this were so, then the limestone in the Big Gully-Bald Rock section represents a second, later, limestone deposit. No second limestone bed is present in the Emu Bay sequence despite the fact that this appears to represent continuous, shallow marine deposition. There is no apparent evidence for emergence or erosion to account for the absence of a limestone bed near the top of the sequence. This, coupled with the similarity of body fossils in close association with the limestone bed indicates its likely regional contemporaneity.

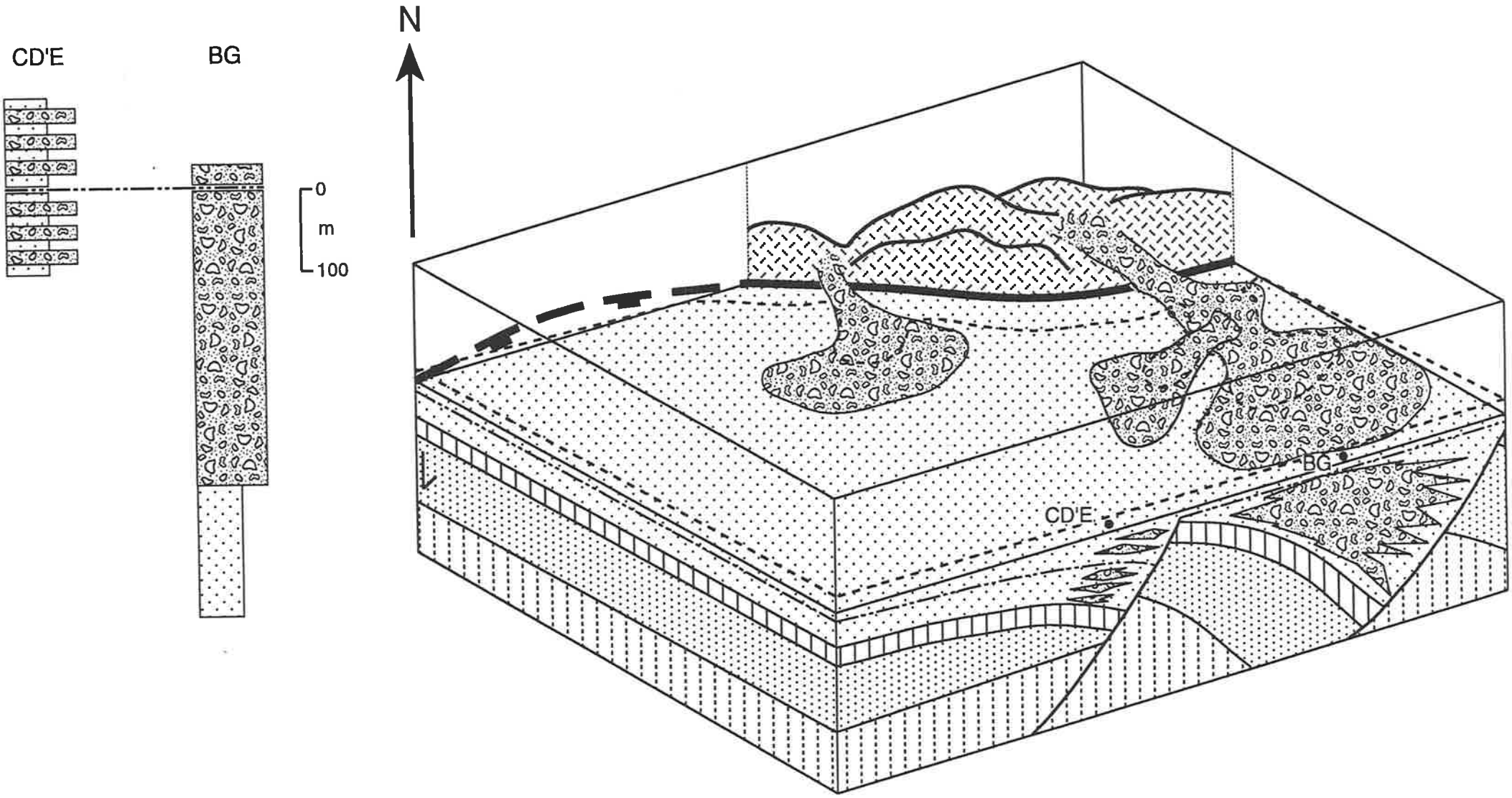


**Fig. 2.5** Reconstruction of palaeogeography at the end of upper White Point Conglomerate deposition. Note differential movement along synthetic listric faults results in greater deposition in the area that is now Cape D'Estaing as the result of basin migration to the west. Stratigraphic columns of White Point Conglomerate measured at Cape D'Estaing and Hawk Nest - Big Gully to scale, for comparison. See Fig. 2.4 for key to symbols.

Dramatic lateral variations in thickness are common in areas influenced by transtensional strike-slip faulting as a result of localised crustal extension, with adjacent uplift providing coarse clastic sediments, leading to the occurrence of abrupt lateral facies changes (Reading 1980; Christie-Blick & Biddle 1985). Commonly, small laterally restricted, deep basins are formed (Reading 1980). Such coarse clastic filled basins have been described from known strike-slip zones in California and New Zealand (Summerhayes 1969; Moore 1979). The lower White Point Conglomerate at the Big Gully-Bald Rock locality may represent the rapid infilling of a localised depocentre caused by transtensional strike-slip faulting by sediment from locally emergent area (Fig. 2.4). The basal 160 metres of sands and muds probably represent initial deposition in a more distal environment before being overridden by prograding alluvial fans. Continued faulting allowed a thick sequence of proximal alluvial fan conglomerates to develop. Rare arthropod tracks in the fine facies suggest that the alluvial fans were deposited close to the shoreline and were periodically submerged at times when sediment supply was insufficient to keep up with subsidence.

At Cape d'Estaing, the lower sequence is composed of interbedded conglomerates, sandstones and siltstones. The conglomerates are not as massively developed as at the type locality. The sequence appears indicative of a mid to distal alluvial fan sequence, or a fine-gravel to medium-gravel midfan sequence of the kind figured by Collinson (1986, fig. 3.16). Marine and fluvial reworking appear to have occurred at various times during deposition. Dramatic facies variation occurs, both laterally and vertically, grading from conglomerates into sands and muds within a few metres. Distal braid-bar facies produce gravel bars and megaripple bars, the margins of which may be subsequently reworked by streams and tide. This complex array of influences often produces a seemingly conflicting set of palaeocurrent information. Such conflicting indicators were pointed out by Jenkins (1990) who suggested that some of these could be explained by a southerly source rather than a northerly source favoured by Daily *et al.* (1980). Whilst a southerly source cannot be ruled out - indeed a similar scenario of source direction reversal was suggested within the Carboniferous Hopewell group conglomerates of

southern New Brunswick (Plint & van de Pool 1984) - the mixing of braid bar facies with marine influences may be an explanation for the apparent northward palaeocurrents.

The lower White Point Conglomerate at the Emu Bay section is composed mainly of siltstones and fine sandstones, with only one major sand body and one conglomerate. Thus the sequence probably represents a distal, marine environment, possibly an offshore-lower shoreface - rarely foreshore transition, with a profile similar to that Clifton (1981) described from the Miocene of California .

Widespread deposition of the distinctive limestone bed indicates a period of tectonic quiescence and probable sea level highstand. The thickness of the limestone possibly follows the topography of the basin, with the thickest development being in the Emu Bay sequence, probably due to the fact that more continuous marine deposition is recorded there. The bed thins towards the east and west, possibly due to the shallower water at these locations due to the buildup of fluvial fan sequences. At both western localities, the limestone is underlain by fossiliferous mudstones containing the trilobite *Balcoracania dailyi*. However, near Big Gully, the limestone rests on sandstones and conglomerates indicative of alluvial fan deposition suggesting probable emergence prior to limestone development. Here, fossiliferous mudstones overly the limestone, indicating a retention of marine conditions.

The upper White Point Conglomerate also exhibits a marked difference in thickness between the two main localities, though not as pronounced as for the lower White Point Conglomerate (Fig. 2.5). At the Big Gully-Bald Rock section the upper sequence comprises some 25 metres of ripple laminated and flaser bedded sandstone, interbedded mudstones, occasional granule beds and one trough cross bedded conglomerate at the top of the sequence. The main development of mudstone above the limestone bed contains the trilobite *Balcoracania dailyi* (Daily *et al.* 1979). The development of the upper sequence appears to represent continuing marine deposition but with only limited

sediment accommodation due to a cessation of subsidence. The granule beds possibly mark periods of emergence and erosion. The upper part of the sequence, below the topmost conglomerate, is composed of sandstone - siltstone interbeds, indicating a fluctuating sediment supply. The topmost, discontinuous conglomerate, grades laterally over a few metres into coarse, cross-stratified sandstones and possibly reflects a renewed episode of tectonism.

The upper White Point Conglomerate at the Emu Bay-Cape d'Estaing section consists of a much thicker sequence. At Cape d'Estaing, the upper sequence is best developed on the Cape itself, where approximately 110 metres of sandstones, conglomerates and occasional mudstones occur. A similar thickness of strata overlies the limestone bed at Emu Bay, with the sequence mainly comprising trough cross-stratified and planar bedded sandstones with occasional mudstone development. The Cape d'Estaing - Emu Bay sequence probably represents a mid-fan to distal fan environment in a situation where the main depocentre have migrated westward from the type locality. Such basin migrations are a common element of strike-slip basins (Christie-Blick & Biddle 1985) and have been recognised from sedimentation in the Dead Sea Rift (Manspeizer 1985) and in the Ridge Basin of California (Nilson & McLaughlin 1985).

The difference in thickness of the two sequences and the differing thickness of White Point Conglomerate below the Emu Bay Shale and above the marker limestone, has been cited by Gravestock (1995) as evidence that the two outcrops may not correlate. However, the appearance of similar body fossils at a similar level in the two sequences, and the abrupt change from conglomeratic deposition to a deeper water environment, marks a fundamental change in basin palaeoenvironment. The differing thickness of sediment above the limestone marker bed can be explained as the result of localised tectonism and basin migration in a strike-slip régime, especially since the contact between the White Point conglomerate and Emu Bay Shale at Big Gully is erosional (e.g. Dinnick 1985) and not conformable as at Emu Bay.

Most previous workers have placed the source of the sediments in the White Point Conglomerate in the region of the Investigator Straight High. However, there is no evidence of a substantial "Investigator Strait Range" as envisaged by Dinnick (1985). Also, since the main constituent of the conglomerates appears to be Early Cambrian limestones (Gravestock 1995), an extensive range to the north of the current shoreline would seem to be ruled out. Some limestone clasts seem identical with Early Cambrian limestones on Yorke Peninsula (Gravestock 1995). Thus it is more likely that localised uplift of Early Cambrian marine limestones a few kilometres north of the current coastline of Kangaroo Island as a consequence of transtensional faulting, would have provided sediment to fill the narrow basins.

Pocock (1967, 1970) described several species of trilobites from the White Point Conglomerate sections at Cape d'Estaing and Emu Bay. *Balcoracania dailyi* was recorded from red-brown mudstones immediately below the limestone bed in the White Point Conglomerate within the Cape d'Estaing section and also from red-brown mudstones from a thin layer within the (?)equivalent limestone bed in the Emu Bay section. Also recorded was *Emuella polymera* from a thin bed below the occurrence of *B. dailyi* within the Cape d'Estaing section. Pocock (1970) noted rare *Hyolithes* and "a species of *Estaingia* " in association with *B. dailyi* in the Emu Bay section of the White Point Conglomerate. Daily *et al.* (1979) located *B. dailyi* in grey-green siltstones and shales associated with a limestone bed in the section between Bald Rock and Big Gully. Although the presence of *Hsuaspis bilobata* in the White Point Conglomerate was noted by Moore (1979) and Daily *et al.* (1979), this appears erroneous. In both instances this placement is referenced to "Pocock 1964, 1967". In neither reference is *H. bilobata* recognised from the White Point Conglomerate. Pocock (1970) recorded a species of *Hsuaspis* [*Estaingia*] on the eastern side of Cape d'Estaing, in the Emu Bay section of Pocock (1964), in a zone, approximately 30 ft. thick, near the top of the White Point Conglomerate, whilst beds of the overlying the Emu Bay Shale contained *Hsuaspis*

[*Estaingia*] *bilobata* Pocock and a species of *Redlichia.* Clearly Pocock differentiated between *Hsuaspis* [*Estaingia*] *bilobata* and a "species of *Estaingia*". No other evidence for the presence of *Hsuaspis* within the White Point Conglomerate can be found and no samples are documented. It may well be that be that in the first mention of the presence of *Hsuaspis* [*Estaingia*] *bilobata* within the White Point Conglomerate, by Daily (1977), a mistake was made in attributing *Hsuaspis* [*Estaingia*] *bilobata* to the White Point *Conglomerate* rather than to Pocock's (1964) White Point *section* (which included the Emu Bay Shale).

The main manifestation of the Kangarooian Movements in the southern part of the Adelaide Fold-Thrust Belt, was the fault-controlled uplift of the Gawler Block on Yorke Peninsula and especially in the Investigator Strait area, and the formation of the Kanmantoo Trough via fault controlled collapse of the sea floor to the south and southeast, according to Moore (1979). Early transtensional movements may have been taken up primarily along the Kangaroo Island Shear Zone , which is probably a "fundamental" fault (*sensu* de Sitter 1964) at the southern edge of the craton. This zone now marks the boundary between the platformal sediment to the north and the Kanmantoo Trough sediments to the south. Subsequent erosion of thin Early Cambrian cover and the underlying metasediment and metamorphic basement, provided sediment for the platformal sequence along the north coast of Kangaroo Island. However, Jenkins (1990) suggested an alternative scenario, with the Kanmantoo Group sediments representing an early flyschoid phase, followed by the "Upper" Kangaroo Island Group representing a molassic apron within the foreland basin affected by an advancing thrust front from the south during the Delamerian Orogeny.

There seems little doubt that the deposition of the White Point Conglomerate marks a major tectonic event in the region. Regional transtensional movements which accompanied deposition along the southern margin of the Gawler Craton, or the Latitudinal Basin Domain (Flöttmann & James 1994), equates with the opening up of the Kanmantoo Trough along the southeast margin of the craton, or the Longitudinal Basin

Domain (Flöttmann & James 1994). These authors describe the Kanmantoo Trough as a wrench related tear-basin, forming along an intracratonic tear fault between the Antarctic and Australian continents.

The transition from the White Point Conglomerate to the overlying Emu Bay Shale, varying from conformable in Emu Bay to disconformable at Big Gully, represents a change to deeper water sedimentation. The presence of laterally discontinuous unconformities is another characteristic of strike-slip basins (Reading 1980; Christie-Blick & Biddle 1985).

The Emu Bay Shale outcrops at two locations on the north coast of Kangaroo Island. At the type section in Emu bay, east of Cape d'Estaing, the Emu Bay Shale is some 42 m thick. At the other locality, Big Gully, some 8 kms to the east, the sequence is considerable thicker (86 m; Pl. 3.1, 3.2). The Emu Bay Shale can be informally subdivided into lower and upper parts on lithological and palaeontological grounds. In the type section at Emu Bay, the lower part conformably overlies the White Point Conglomerate and is composed of 16 metres of grey-green and brown, flat laminated to wavy bedded, slightly calcareous mudstones and shales. Occasional calcareous nodules are developed. Bioturbation is pervasive in parts and fossils are common. The transition to the upper part of the sequence is marked by a 1.5 metre thick ripple bedded, red-brown, arkosic sandstone, which has an erosive base. The remainder of the upper sequence is dominated by brown, flat laminated mudstones and siltstones with occasional flaser bedding. Bioturbation is pervasive in parts and arthropod tracks are common, but body fossils are apparently absent from the upper sequence.

The contact between the White Point Conglomerate and the lower Emu Bay Shale at the Big Gully locality is represented by an undulose erosive surface, above which is an up to 80 cm thick interformational conglomerate, which comprises clasts of the underlying

# Plate 3

**3.1** View of the Big Gully locality, looking east. White Point Conglomerate in foreground, Emu Bay Shale in middle distance comprising light coloured rocks in cliff, grading to dark coloured rocks below contact with the massive Boxing Bay Formation. Two gullies in the cliff mark the position of two steep, normal faults, downthrow side to the left (north).

**3.2** Lower Emu Bay Shale on wave-cut platform at Big Gully, looking north.

**3.3** Unconformity and basal conglomerate between the White Point Conglomerate and the overlying Emu Bay Shale at Big Gully, looking east. Base of pen is on the topmost White Point Conglomerate sandstone. Overlying conglomerate contains clasts of micritic limestone, quartzite, rare basement clasts and 'books' of siltstone, sometimes deformed. Pen is 13 centimetres.

**3.4** Soft sediment slumping in the lower Emu Bay Shale on the wave cut platform at Big Gully, looking north. Hammer 30 centimetres.

**3.5** Emu Bay Shale in cliff section at Big Gully, looking south. Contact with underlying White Point Conglomerate downfaulted to near beach level at left of photograph (site of **3.3**) and occurs again just above the tree line in centre of cliff. Site of Emu Bay Shale Lagestätte is dark basal 8 metres above tree line to first major sandstone body and is marked by the major talus slope leading down between the trees.

**3.6** Top 2 metres of Emu Bay Shale Lagerstätte in cliff section at Big Gully, looking east. Major sandstone body marking base of upper Emu Bay Shale at top of photograph, 80 cms of fine green and red sandstones lie beneath, followed by 1.2 metres of shale. Note highly cleaved and faulted nature of the Emu Bay Shale and thin 2 cm thick sand bed just above hammer handle, displaced downwards to the left (north). Hammer 30 centimetres

# PLATE 3






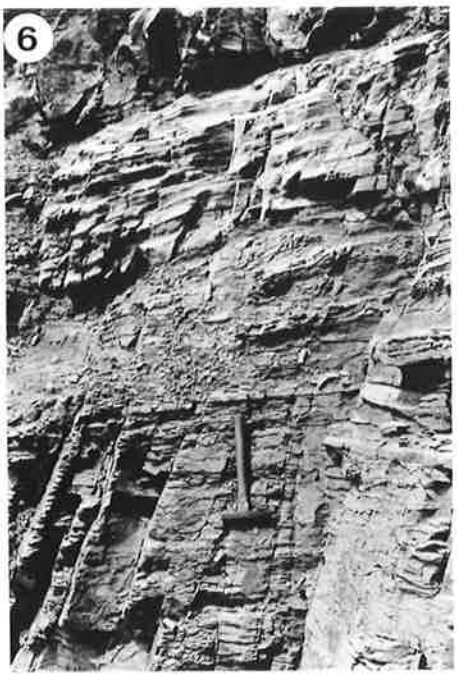

sandstone, a dark grey siltstone, uncommon micrite pebbles and rare quartz and basement pebbles, in a red, ferruginous, medium grained arenaceous matrix (Pl. 3.3).
The lower Emu Bay Shale at Big Gully (Pl. 3.4) comprises some 8 metres of dark grey and brown poorly sorted, laminated to rarely wavy-bedded or thin bedded, commonly micaceous, slightly calcareous siltstones intercalated with thin, red-brown, fine grained, moderately well sorted, arkosic, flat-based and finely ripple-topped sandstones. Deformation features indicative of soft sediment slumping also occur (Pl. 3.5).
The basal 2 metres of the section is composed of dark grey to black, thinly laminated siltstones which weather to a grey-green colour. Above this, the section rapidly grades to dark grey to brown siltstones which weather to a red-brown colour (Pl. 3.5).
Fossils are common in the lower part of the Emu Bay Shale (for a more detailed description of the stratigraphy of this section see Appendix 1). The top of the lower sequence is marked by a 1 metre thick grey, fine grained, well sorted, slightly calcareous sandstone, massive at the base, but grading through flat laminated to be rippled at the top. The contact with the underlying beds is undulose and lies above an 80 cm thick sequence of red-brown and green, laminated, interbedded siltstones and red-brown, very fine grained, calcareous sandstones (Pl. 3.6). These beds show slight deformation and long amplitude microrippled tops.
The upper Emu Bay Shale consists of red-brown mudstones and sandy siltstones, interbedded with massive red-brown fine to occasionally medium grained trough cross-stratified, rippled and planar bedded sandstones (Pl. 3.5). The upper member contains several fining upward and coarsening upward cycles. Some cycles are capped with thin, poorly sorted gravel and pebble conglomerate lenses containing small, well rounded clasts. The thickest of these exhibits a highly undulose channelised and loaded base (Dinnick 1985). Planar-laminated, flaser, linsen and ripple bedding occurs, with starved ripples and desiccation cracks present towards the top of the sequence.

The abrupt termination of coarse sediment supply preceding the start of deposition appears coupled with a relative sea level rise, possibly caused by the down faulting,

resulting in a relocation of the palaeoshoreline to the north (Fig. 2.6). This may have altered the configuration of the basin, shifting dominantly westward flowing currents further to the south and resulting in weak easterly currents prevailing along the northern margin. A separate, localised, tectonic movement affected the Big Gully area only. The resultant basal conglomerate contains clasts of weakly lithified siltstone. The presence of such shale clasts, often exhibiting deformation (Plate 3.3), suggests a hiatus of a long enough duration to allow the deposition and compaction of the shale before its incorporation into the conglomerate. Thus the conglomerate probably represents a slide-slump deposit formed as a result of downfaulting.

The lower Emu Bay Shale appears to have been deposited in a low energy environment, below wave base. Fine interlaminated sands possibly represent storm deposits. This is comparable to the low energy/outer shelf environment of the lower part of Member 1 of the late Neoproterozoic Ekkerøy Formation of North Norway (Johnson 1975), where offshore muds were periodically draped by thin, distal storm sand layers, settling out of suspension clouds during decreasing turbulence. The dominance of streaked muds and flaser bedding is similar to the storm dominated, mud-rich offshore platform environment documented from the Lower Carboniferous of County Cork, southern Ireland (de Raaf *et al.* 1977).

The lower member grades into the upper member which resembles interbedded low energy silts and fine to medium grained storm-surge to current swept sands of the moderate-energy storm-dominated shelf to high-energy current-dominated shelf zone of the upper part of Member 1 of the Ekkerøy Formation of North Norway (Johnson 1975). A similar facies has been described from the Silurian Kilbride Formation of Galway, Ireland (Doyle 1994), also exhibiting distal storm deposited sands interbedded with finer, offshore sediments. Shoaling of the Big Gully setting is indicated by the change from flat laminated to cross bedded sandstones. The dominance of asymmetrical current ripples indicate a tidal current dominated environment for the upper Emu Bay Shale (Daily *et al.* 1980).

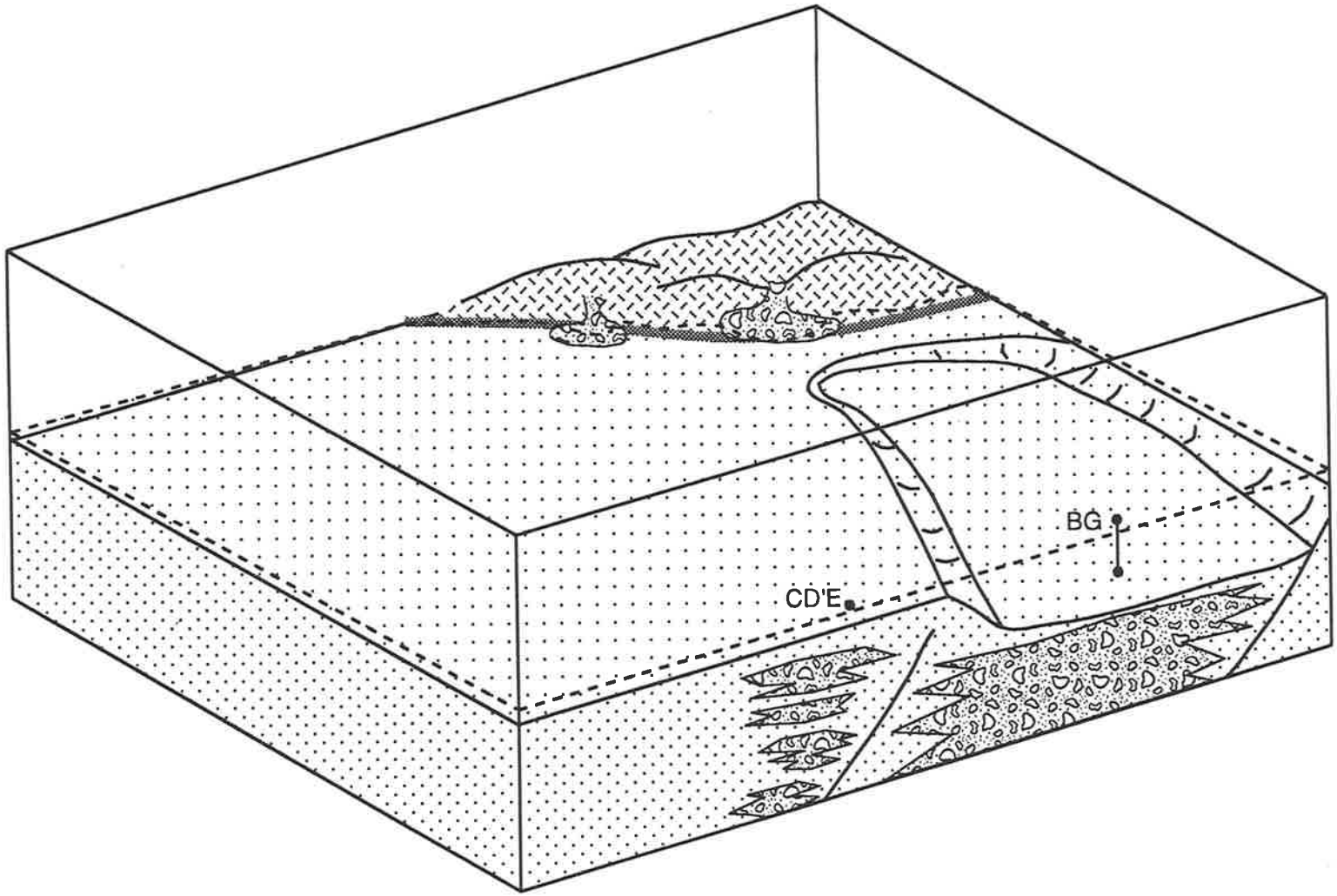


**Fig. 2.6** Reconstruction of palaeogeography at the start of Emu Bay Shale deposition. See Fig. 2.4 for key to symbols.

Weak westerly currents resulted in poor circulation and reduced dissolved oxygen availability. Within the now relatively deep basin, the oxic/anoxic boundary was positioned at the sediment -water interface and periodically within the water column, resulting in the exceptional preservation of organisms. The position of the oxic/anoxic boundary was probably controlled by the sluggish circulation in this part of the basin. Fine grained sedimentation continued, incorporating occasional thin, storm sands until an increase in sand content towards the top of the lower member at Big Gully signaled the influence of more course clastic sedimentation and a general shallowing upward cycle, with the progradation of shallow water sands (Fig. 2.7). At Emu Bay, a shallow subtidal mudflat environment is envisioned, resulting in a predominantly siltstone facies similar to that described from the lower part of Member 1 of the Ekkerøy Formation of North Norway (Johnson 1975). A renewed episode of backfaulting and erosion resulted in an influx of coarser grained sediment recorded by the overlying Boxing Bay Formation.

The lower Emu Bay Shale is richly fossiliferous, containing the most diverse fossil assemblage to be found in the Kangaroo Island Group. The kinds of fossil which occur and the mode of preservation, however, differ between the two localities.
At Emu Bay, Pocock (1964) documented the trilobites *Hsuaspis* [*Estaingia*] *bilobata*, *Emuella dalgarnoi* and *Redlichia* sp., the hyolithid, *Hyolithes*, and a possible brachiopod from the lower member. The assemblage consists largely of isolated cranidia and free cheeks and disarticulated thoracic segments, preserved via replacement of the exoskeleton with a thin layer of calcite (Pocock 1964). Dinnick (1985) confirmed the presence of an as yet unidentified brachiopod, and Jell (1990) identified *Redlichia* sp. as *Redlichia takooensis*. Rare worm burrows occur but arthropod tracks are confined to the upper member, where they become common.

Within the lower member at Big Gully, the fossil assemblage is somewhat different. The trilobites *Hsuaspis bilobata* and *Redlichia takooensis*, occur with the phyllocarids

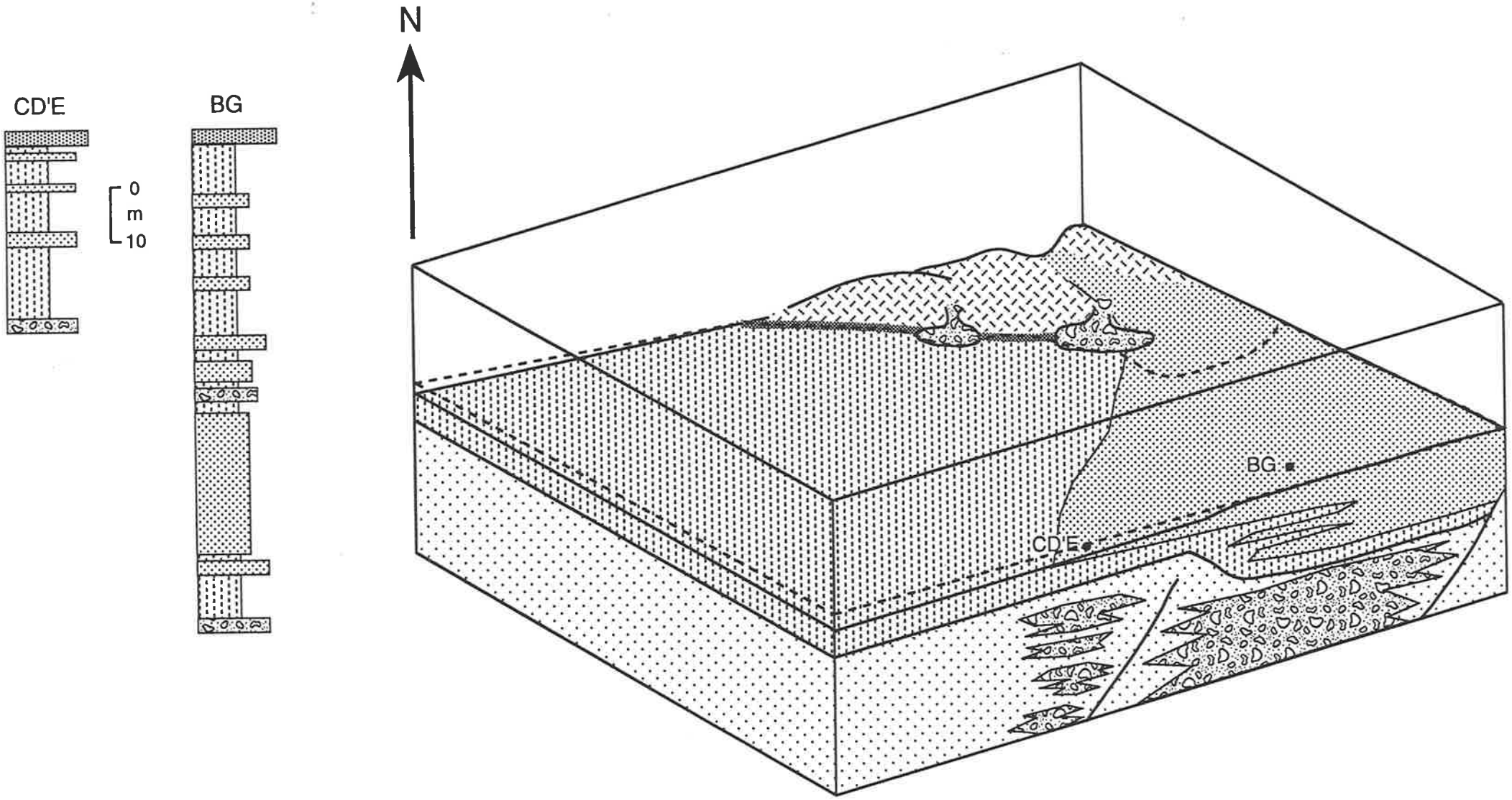


**Fig. 2.7** Reconstruction of palaeogeography at the end of Emu Bay Shale deposition. Stratigraphic columns of the Emu Bay Shale from Cape d'Estaing - Emu Bay and Big Gully to scale, for comparison. See Fig. 2.4 for key to symbols.

*Isoxys communis* and *Tuzoia australis*, the presumed annelid *Palaeoscolex antiquus* and the possible arthropod *Myoscolex ateles*. Other forms are also present. *Anomalocaris* was reported from the lower Emu Bay Shale at Big Gully by Nedin (1992) and McHenry & Yates (1993). Nedin (1994, 1995) discussed the first meraspid trilobites to be found in the deposit. Significantly, neither hyolithids nor brachiopods are present. Preservation differs from that at Emu Bay. Here, the fossils are preserved via replacement by iron stained calcite, commonly exhibiting uniformly long, obliquely orientated crystals, which commonly reach millimetric lengths. In some forms a central layer of fluroapatite occurs, surrounded by calcite. Both preservational styles indicate that secondary recrystallisation has taken place. Arthropod trails are absent from the lower Emu Bay Shale, but occur commonly in the upper section.

Daily (1956) designated the 515+ metres of strata which conformably overlie the Emu Bay Shale at Big Gully (Pl. 3.1), as the Boxing Bay Formation. A basal 46 metre sequence occurs west of the Emu Bay Jetty. The top of the Boxing Bay Formation is not exposed and so its true thickness is unknown.

The fine-grained facies of the Boxing Bay Formation exhibit many characteristics common to tidal deposits. These include the association of mud cracks and trace fossils and the interbedding of ripple-bedded and laminated marine sandstones and coarse siltstones with varying proportions of mudstones. The mud cracks indicate periodic, possibly tide-related emergence, and desiccation. Fining upward and coarsening upward cycles possibly indicate cycling between subtidal - lower intertidal facies and lower-upper subtidal facies (Dinnick 1985). The sandstone facies exhibits shore parallel palaeoflow, dominantly to the west. Such asymmetrical dominance has been ascribed to asymmetric tidal flow (e.g. Klein 1970). Rare hummocky cross-stratification indicates the influence of storms. Storm surges could have also transported isolated pebbles and pods of pebbles found in association with the hummocky cross-stratification (Dinnick 1985).

The conglomerate facies differs from the corresponding facies in the White Point Conglomerate in being composed of many cross-stratified intervals, having smaller, more rounded clasts and having a much higher proportion of basement clasts. The conglomerates commonly fill shallow channels and such trough cross-stratified channel fill conglomerates have been described from ancient distal fan to proximal braid plains (e.g. Miall 1970; Røe & Steel 1985). Maximum progradation is marked by the occurrence of debris flow conglomerates. Drowning of the distal fan environment resulted in the re-establishment of the shallow subtidal to occasionally low intertidal environment.

A minor, but enigmatic component of the sequence on the north coast of Kangaroo Island is represented by the Bald Rock Beds, defined by Dinnick (1985) as a fault bounded sequence of medium grained to pebbly sandstones, minor siltstones and conglomerates of ?Cambro-?Ordovician age, outcropping between the eastern side of Emu Bay and Bald Rock in fining upward cycles similar to the braided river facies of the Upper Cannes de Rouche Formation of eastern Quebec (Rust 1978). The pebble facies were considered to be unlike conglomerates recorded from the underlying sequences due to their lithological nature and the high degree of rounding and polishing of the clasts (Pl. 2.6). This distinction was noted by Daily *et al.* (1980), who tentatively correlated them with the Middle Cambrian Yurunga Formation of Yorke Peninsula. If the clasts within the Bald Rock Beds are metamorphosed Kanmantoo metasediment as suggested by Jenkins (1990), and as seems likely, then the Bald Rock Beds are of a younger early Palaeozoic age. The fault trending inland from Bald Rock, which represents the contact between the Bald Rock Beds and the Smith Bay Shale, may represent a major reverse fault which may well have originally been a synthetic listric normal fault generated through extension.

Since the top of the Boxing Bay Formation is not exposed, it is difficult to tell when deposition ceased. Evidence from Yorke Peninsula indicates that deposition continued,

under the influence of the Kangarooian Movements, into the early Middle Cambrian (Daily *et al.* 1980, Gravestock 1995).

The close of sedimentation appears to overlap another major tectonic event, this time much more pervasive and extensive, the Delamerian Orogeny. This orogeny is interpreted as indicating extensive compressional tectonics which affected the whole of the Adelaide Fold-Trust Belt. During the early phase of the orogeny, deeply buried sediments in the Kanmantoo Trough were exposed to increasing heat. Syntectonic granites which intruded this sedimentary pile at a depth of between 5-10 km, give Rb-Sr ages of between 511±3 and 496 ±6 Ma (Milnes *et al.* 1977), which may represent the peak of metamorphism or subsequent cooling ages. The younger ages were thought to confine the orogeny to the Late Cambrian and Ordovician. However, subsequent work has indicated that the Middle to Late Cambrian boundary may possibly be as young as 500 million years ago (Perkins and Walshe 1993). Thus locally, the Delamerian Orogeny appears to begin in the Middle Cambrian, as suggested by Jenkins (1990). Compression reactivated and reversed Kangarooian faults to produce a leading imbricate fan in overstepping Kanmantoo Group sediments characterised by zones of phyllites with bedding parallel foliation (Jenkins 1990). These movements possibly reversed movement along synthetic listric normal faults resulting in basin inversion and overthrusting such as suggested by Flöttmann *et al.* (1995).
Northerly displacement in the platformal Northern Structural Zone on Kangaroo Island appears to reflect partitioning between the northwest directed shortening in the southern zone, transpressional convergence along the Kangaroo Island Shear Zone and dip-slip displacement in the northern zone (Flöttmann *et al.* 1995). The section along the north coast of Kangaroo Island was affected, by renewed movements along the anastomosing fault set formed by the Kangarooian Movements, during the Delamerian Orogeny.

Nothing is known of the geological history of Kangaroo Island after the Delamerian Orogeny until the Early Permian. During this time, some 10 km of sediments were

removed by erosion, exposing the Encounter Bay Granites and surrounding Kanmantoo metasediments (Daily *et al.* 1979). A thick sequence of ?Early Permian fluvio-glacial sediments, the Cape Jervis Beds, were deposited in ice-scoured depressions around Kingscote, reaching a thickness of 318 m in some areas (Ludbrook 1967), with obscure leaf fossils reported from deposits in the Kingscote area (Sprigg *et al.* 1954).
Ice flows eroded out depressions up to 300 m below present sea level (Daily *et al.* 1980), especially immediately south of the north east coast of Kangaroo Island. The depressions were inundated by the rising sea as the ice retreated, with agglutinated foraminifera represented in the Permian section (Ludbrook 1967). Renewed uplift later excluded the sea.

Local Mid Jurassic volcanics of limited extent may signal the Gondwana break up. Subsequent episodes of Tertiary laterization and limited marine transgressions depositing fossiliferous limestones are recorded. It appears that the whole island was uplifted, initially as a single block, by Pleistocene faulting (Daily *et al.* 1980).

## 2.5 Correlation

### 2.5.1 Regional Correlation

Daily and Milnes (1971) correlated the basal member of the Kangaroo Island Group, the Mt. McDonnell Formation, with the Carrickalinga Head Formation on Fleurieu Peninsula on lithological grounds only. However, recent finds of offshore archaeocyathans, including *Erugatocyathus aquilinus* (Gravestock) along with phosphatic brachiopods and the problematic Alga *Nuia*, indicate a position within Upper Faunal Assemblage II or Faunal Assemblage III of Gravestock (1984) (D. I. Gravestock 1994, pers. comm.). Gravestock (1984) and Debrenne & Gravestock (1990) described *Mennericyathus dissitus* (Kruse), *Erismacoscinus uratanensis* (Gravestock) and

*Kaltatocyathus* cf. *gregarius* (Gravestock) from the upper Sellick Hill Formation and Fork Tree Limestone on Fleurieu Peninsula and from the Ajax Limestone in the Mt. Scott Range, Flinders Ranges, in Gravestock's (1984) Faunal Assemblage II. Debrenne & Gravestock (1990) also described *Robertocyathus* and *?Inacyathella* from the upper Sellick Hill Formation. This occurrence was used by Zhuravlev & Gravestock (1994) to correlate the Sellick Hill Formation with the newly erected *Jugalicyathus tardus* Assemblage Zone, the Upper Faunal Assemblage II of Gravestock (1984) and Faunal Assemblage 2 of Daily (1956). However, the top of this zone, correlated with the Atdabanian - Botomian boundary by Zhuravlev & Gravestock (1994), is somewhat uncertain, since *Robertocyathus* and *?Inacyathella* have been found associated with typical mid Botomian genera in the Oraparinna Shale and Moorowie Formation (Lafuste *et al.* 1991). Thus the *Jugalicyathus tardus* Assemblage Zone may well extend into the Botomian and is suggested here that the zone be possibly considered to include the Fork Tree Limestone (Fig. 2.8)

Jell (1990) recorded *Abadiella huoi* from low in the Parara Limestone on Yorke Peninsula, low in the Wilkawillina Limestone near Wirrealpa and in the basal Ajax Limestone of the Mt. Scott Range, Flinders Ranges. These occurrences correspond to Daily's (1956) Faunal Assemblage 3 and, in part, with Gravestock's (1984) Upper Faunal Assemblage II, in which *Abadiella huoi* and *Elicicola calva* also occur. Bengtson *et al.* (1990) erected the *Abadiella huoi* Zone, which encompassed the upper part of Daily's (1956) Faunal Assemblage 2, his Faunal Assemblage 3, and Gravestock's (1984) Upper Faunal Assemblage II. Thus the upper part of the Mount McDonnell Formation may be correlated with the Sellick Hill Formation and Fork Tree Limestone on Fleurieu Peninsula, the basal Parara Limestone and underlying Kulpara Formation on Yorke Peninsula and the basal Parara Limestone and Wilkawillina, Wirrapowie and lower Ajax Limestones in the Flinders Ranges (Fig. 2.8).

The *Syringocnema favus* beds is an informal name given to a widespread assemblage of archaeocyaths occurring in bioherms and reef complexes (Zhuravlev & Gravestock

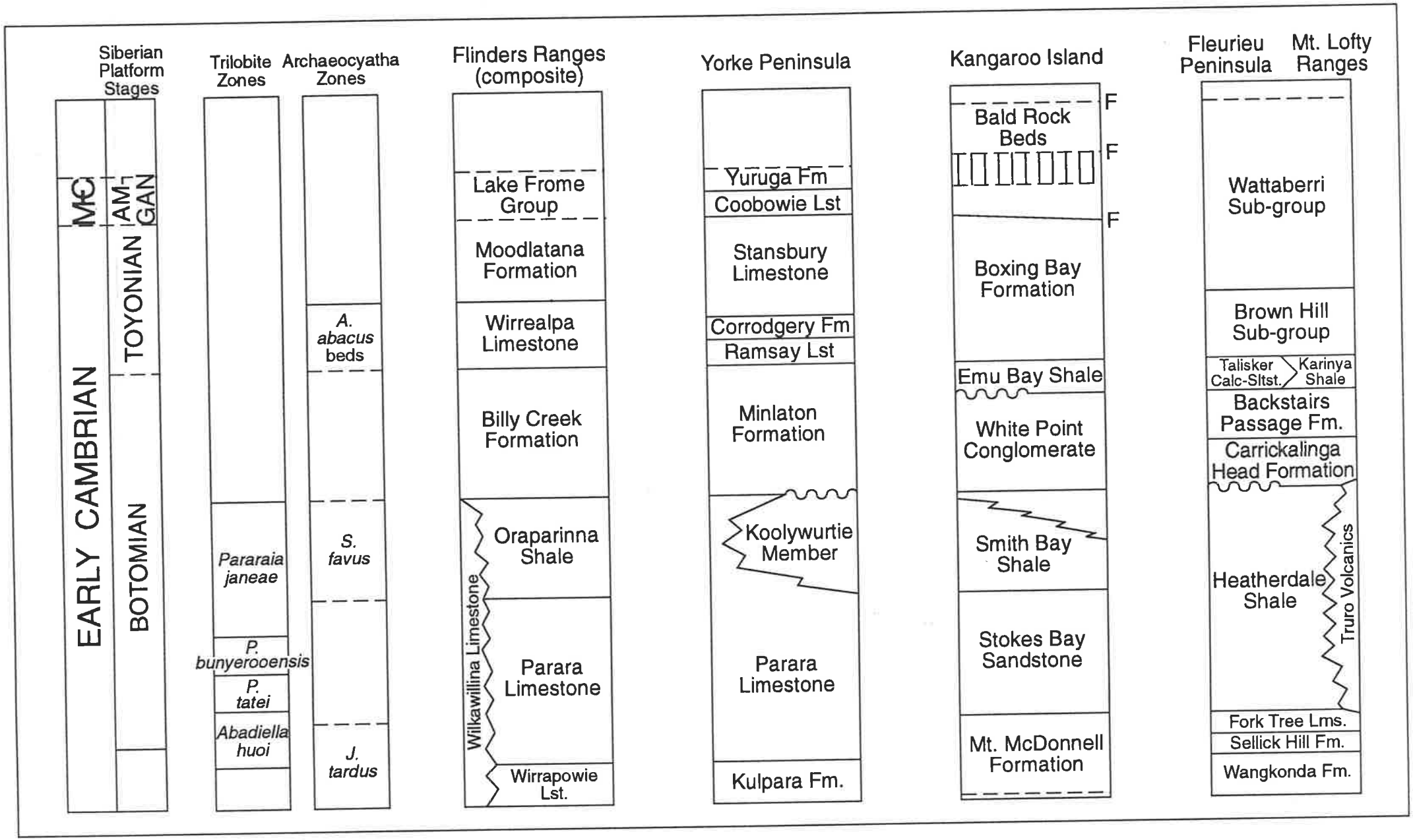


**Fig. 2.8** Early Cambrian stratigraphy and correlation of key regons of South Australia. Trilobite zones of Jell (*in* Bengtson *et al.* 1990) and archaeocyathan zones of Zhuravlev & Gravestock (1994)

1994). Archaeocyatha from these beds are widely distributed in the Flinders Ranges, where they occur in strata coeval with the Oraparinna Shale (Zhuravlev & Gravestock 1994). This encompasses Daily's (1956) Faunal Assemblage 9 and lies within the *Pararaia janeae* Zone of Bengtson *et al.* (1990). Commonly occurring species include, *Syringocnema favis*, *Graphoscyphia graphica*, *Pycnoidocyathus vicinisepta*, *Kruseicnema gracilis* and *Acanthinocyathus aptertus*. These species are also found in the Koolywurtie Member of the Parara Limestone on Yorke Peninsula, and in Fauna 2 of Kruse (1982) from the Cymbric Vale Formation, Mt. Wright, New South Wales. Since archaeocyaths from Assemblage ?V of Gravestock (1984) also correlate with the fauna present in the Koolywurtie Member (Zhuravlev & Gravestock 1994), the top of the informal *Syringocnema favus* beds may well extend to the contact between the Ajax Limestone and the overlying Billy Creek Formation at Mt Scott Range. This correlates with the base of the Billy Creek Formation in the central Flinders Ranges and the base of the Minlaton Formation on Yorke Peninsula ( Zhuravlev & Gravestock 1994). Conocoryphid trilobite remains were reported from the upper part of the Heatherdale Shale by Jago *et al.* (1984). Jenkins & Hasenhohr (1989) formally identified the trilobite as *Ivshinellus briandailyi*. Jell *et al.* (1992) described *Atops rupertensis* from the upper Parara Limestone or Lower Oraparinna Shale of Bunnyeroo Creek, Flinders Ranges and placed *Ivshinellus briandailyi* in *Atops*. While the forms do represent different species (Jenkins and Hasenhohr 1989), they clearly belong in the same genus. Given the small number of specimens used to erect the genus and the plasticity of defining characteristics in Early Cambrian trilobites (G. D. Edgecombe 1994, pers. comm.), the placement in *Atops* is supported here. The two species imply a link between the upper Parara Limestone in the Flinders Ranges and the Heatherdale Shale on Fleurieu Peninsula, a correlation suggested by Daily (1976) on stratigraphic grounds. However, the apparent absence of eodiscid trilobites in association with *Atops briandailyi* or elsewhere within the Heatherdale Shale is puzzling. Indeed it has been suggested that the absence of eodiscid forms implies an older age for the Heatherdale Shale (Cooper *et al.* 1992; R. J. F. Jenkins pers. comm. 1994). Other late Early

Cambrian trilobite occurrences in the southern part of the Adelaide Fold-Thrust Belt such as the White Point Conglomerate and the Emu Bay Shale also lack eodiscids. Thus the lack of eodiscid trilobites of itself cannot be used to imply an older age.
Zircons from a volcanic tuff within the Heatherdale shale, in close proximity to *Atops briandailyi*, are given an age of 526 ±4 Ma by ion microprobe U-Pb zircon analyses (Cooper *et al.* 1992). However, this age is under review and its recalculated numerical value may be marginally younger (R. J. F. Jenkins pers. comm. 1995).

The conglomeratic Minlaton Formation on Yorke Peninsula, conformable above the Parara Limestone, contains conglomerates suggested to have formed as a result of uplift during the Kangarooian movements (Daily 1976). Clasts resembling the Kulpara Formation and Parara Limestone occur in the conglomerates, suggested a correlation between a 20 m dolomitic limestone in the Minlaton Formation and the Milendella Limestone Member of the Carrickalinga Head Formation and a marker limestone in the White Point Conglomerate (Gravestock 1995). *Balcoracannia* occurs in siltstones associated with this limestone in the White Point Conglomerate on Kangaroo Island and also occurs close to, or at, the top of the Warrangee member and its eastern equivalent, the Coats hill Member, of the Billy Creek Formation in the central Flinders Ranges (Moore 1979). A new species of *Balcoracannia* also occurs in nodules from the lower Oraparinna Shale (R. J. F. Jenkins pers. comm. 1994). The presence of these fossils was used as the basis for a correlation between the Billy Creek Formation and the White Point Conglomerate (Daily 1969; Daily *et al.* 1979; Moore 1979; Gravestock 1995), a link which may now be extended to include the Oraparinna Shale. Bengtson *et al.* (1990, p. 12, figs. 7.1, 7.6) noted the occurrence of *H. bilobata* in the Oraparinna Shale, and *H. bilobata* with *Redlichia takooensis* in the White Point Conglomerate and Emu Bay Shale. However, there is no evidence for the presence of *H. bilobata* in the White Point Conglomerate (see section 2.4). Also, the only reference to *Redlichia* in the White Point Conglomerate is to "occasional scraps of *Redlichia*" (Pocock 1967, p. 3).

3). No formal diagnosis is given and so this placement of *R. takooensis*, though possible, is not supported.

*Balcoracannia flindersi*, *H. bilobata* and *R. takooensis*, are considered diagnostic for the *Pararaia janeae* Zone (Bengtson *et al.* 1990). The presence of *Balcoracania* within the Oraparinna Shale provides another possible index taxon. Gravestock (1995) described conglomerate clasts from the White Point Conglomerate as being identical to the Koolywurtie Member on Yorke Peninsula. Thus the shallowing-upward basal White Point Conglomerate may occupy part of the time of the apparent diastem between the Oraparinna Shale and the overlying Billy Creek Formation. This disconformity evidently represents a major phase of tectonic activity and resulted in an increase in clastic input, linked to the Kangarooian Movements of Daily & Forbes (1969). It is possible that minor limestone development at all three localities represents occasional, localised reduction in clastic input coincident with a maximum flooding surface.

The Emu Bay Shale contains a mostly endemic fauna with the exception of *H. bilobata*, which also occurs low in the Oraparinna Shale, within the *P. janeae* Zone (Bengtson *et al.* 1990). The stratigraphically higher occurrence of *H. bilobata* in the Emu Bay Shale (suggested by its occurrence above *Balcoracannia*) may equate with the occurrence of *H. bilobata* in the upper Cymbric Vale Formation in New South Wales (Öpik 1975b), overlying Fauna 2 of Kruse (1982), a fauna which has been correlated with the *P. janeae* Zone and the *Syringocnema favus* Zone (Zhuravlev & Gravestock 1994). Although Jell (1990) and Jenkins (1990) queried the placement of the New South Wales form in *H. bilobata*, the larger size, shorter preglabellar field and advanced genal spines can be explained in terms of evolutionary development (see section 3.4.1.3) within a separate population. *H. bilobata* from the Emu Bay Shale appear to be, on average, larger than those from the Oraparinna Shale, whilst the forms from the Cymbric Vale Formation are larger again. This may be linked to the evolutionary development of *H. bilobata*, leading to *Xystridura* (Nedin 1994).

In the Flinders Ranges the Wirrealpa Limestone conformably overlies the Billy Creek

Formation. With the recognition of Daily's (1956) Faunal Assemblage 10 in the Wirrealpa Limestone and the Ramsay Limestone on Yorke Peninsula (Daily 1956, 1976) and a suite of small shelly fossils common to both formations, it was concluded that the Ramsay Limestone was the stratigraphic equivalent of the lower part of the Wirrealpa Limestone (Brock & Cooper 1993). Both Brock and Cooper (1993) and Gravestock (1995) correlate the Wirrealpa Limestone with the Coobowie - Ramsay Limestone section on Yorke Peninsula. Due to its stratigraphic position, the Boxing Bay Formation on Kangaroo Island evidently correlates with the Wirrealpa Limestone and Moodlatana Formation in the Flinders Ranges. It further correlates with the Coobowie - Ramsay Limestone 'group' on Yorke Peninsula (Gravestock 1995).

Recent (unpublished) work on core recovered from the Port Julia 1A well on Yorke Peninsula, has enabled the Early - Middle Cambrian boundary in this area to be delineated for the first time (D. I. Gravestock pers. comm. 1995). The presence of *Pagetia* sp. in the lower part of the Coobowie Limestone shows this to be basal Middle Cambrian in age (G. Ushatinskaya *in lit.*), placing the Early - Middle Cambrian boundary at the base of the Coobowie Limestone. The overlying Yuruga Formation represents the youngest Early Cambrian sediments on Yorke Peninsula (Gravestock 1995). Sediments are of intertidal - alluvial origin and are disconformably overlain by Permian sediments in Stansbury Town - 1 borehole (Daily 1976). The erosive top of the formation possibly represents the onset of Delamerian compressional tectonics and thus may correlate with the upper part of the Boxing Bay Formation on Kangaroo Island.

Correlation of the Bald Rock Beds on Kangaroo Island remains tentative. The presence of inferred Kanmantoo metasediment clasts in conglomerates within the formation and a southerly sediment source indicated by palaeocurrent data suggest a possible younger Palaeozoic age (Dinnick 1985, Daily *et al.* 1979). Given its stratigraphic position, the Bald Rock Beds may well post-date the upper Lake Frome Group in the Flinders Ranges and the upper Kanmantoo Group sediments on Fleurieu Peninsula, possibly being equivalent to the Grindstone Range Sandstone as suggested by Jenkins (1990).

An alternative view is that the Bald Rock Beds are Permian in age (D. I. Gravestock 1994, pers. comm.). However, the marked lithification of the sediments, together with a pervasive fracture pattern typical of underlying Cambrian rocks indicates that the Bald Rock Beds have undergone the same major tectonic history as other Cambrian sediments and thus do not post-date the Middle to Late Cambrian Delamerian Orogeny.

### 2.5.2 International Correlation

Little new information pertinent to refining international correlations has been found in this study and so the correlations suggested by Bengtson *et al.* (1990) and Zhuravlev & Gravestock (1994) are used here. Zhuravlev & Gravestock (1994) suggested that their *J. tardus* Archaeocyathan Zone spans the Atdabanian - Botomian boundary due to the presence of *Robertocyathus*, and ?*Inacyathella*. This is supported by the presence of the uppermost Atdabanian form *Microdictyon* in the uppermost Kulpara Limestone and in a condensed section low in the overlying Parara Limestone (Bengtson *et al.* 1990; Cooper *et al.* 1992; Zhuravlev & Gravestock 1994). It thus appears that the *A. huoi* trilobite zone of Bengtson *et al.* (1990) is not wholly within the Atdabanian, but also spans the Atdabanian - Botomian boundary (Zhuravlev & Gravestock 1994).

Bengtson *et al.* (1990) correlated their *P. janeae* Zone with the late Botomian of Siberia using *Paleofossus*, *Serrodiscus* and *Atops*. The eodiscid trilobites *Serrodiscus gravestocki* and *Hebediscina yuqingensis* are associated with *Atops rupertensis* in the Oraparinna Shale (Jell *et al.* 1992). These occurrences, along with the presence of *Pararaia janeae*, *Hsuaspis bilobata* and *Paleofossus*? imply a late Botomian age for the Oraparinna Shale (Bengtson *et al.* 1990, Jell *et al.* 1992). Bengtson *et al.* (1990) suggested tentative correlation was also made with the early Tsanglangpu Stage of China using *R. takooensis*, *Hsuaspis* and *Hebediscina*, but expressed caution due to the lack of published range charts. Brasier (1992, p. 586, fig. 1) correlated the Canglangpu [Tsanglangpu] Stage with the mid and upper Botomian of Siberia.

Correlation with Avalonia is more difficult since there are few common genera. Using small shelly fossils and trilobites, Landing *et al.* (1989) correlated the lower *Protolenus* Zone with the mid to upper Brigus Formation of Newfoundland and the Botomian of Siberia. Thus the lower *Protolenus* Zone may be correlated in part with the *P. janeae* Zone of South Australia and the overlying White Point Conglomerate and Emu Bay Shale may possibly correlate with the upper Botomian of Siberia and the upper Tsanglangpu Stage of China.

Other phyla in the Emu Bay Shale appear to have both long time ranges and wide geographic ranges. Palaeoscolecidan worms range from the Lower Cambrian to the Upper Silurian (Müller & Hinz-Schallreuter 1994). The phyllocarids, *Isoxys* and *Tuzoia* occur in the Early Cambrian of China and the Middle Cambrian in North America, as does *Anomalocaris* (Conway Morris 1989b). *Anomalocaris* sp. is possibly conspecific with a form from the Chengjiang formation of China (Nedin 1994, 1995). However, given the apparent longevity of some groups, the co-occurrence appears of little correlative value.

The Wirrealpa Limestone has been correlated with the Toyonian of the Siberian platform based on varied skeletal fossils ( Kruse 1991; Brock & Cooper 1993). The identification of *Redlichia guizhouensis* from the Wirrealpa Limestone near the Wirrealpa Mine (Bengtson *et al* 1990) allows correlation with the Lungwangmiao Stage of China (Zhang & Jell 1987), and also suggests a Toyonian age (Brock & Cooper 1993).

# Chapter 3: Palaeontology of the Big Gully Assemblage

*"Nothing of him that doth fade,*

*But doth suffer a sea change*

*into something rich and strange."*

## 3.1 Introduction

The preservation of soft-bodied or poorly mineralised faunas in fossil Lagerstätten (*sensu* Seilacher *et al.* 1985), represents an unparalleled view into the past, allowing the 'fleshing out' of the far more commonly preserved skeletons of extinct groups as well as providing anatomical information from organisms which would never have survived the normal taphonomic processes.

While the Burgess Shale Lagerstätte from British Columbia is considered the premier example of soft-body preservation, the lack of other Lagerstätten of similar age posed a query as to whether the fauna within the Lagerstätte was representative of Cambrian faunas generally and whether the fauna and its depositional environment was unique (e.g. Gould 1989), or indeed whether the majority of the taxa in the Burgess Shale fauna was representative of any known group, Cambrian or younger (Gould 1989; Foote *et al.* 1992; but see Briggs & Fortey 1989; Briggs *et al.* 1992 for an opposing view). Also the composition and evolution of similar soft-bodied faunas earlier than the Middle Cambrian remained virtually unknown.

Recently, assemblages of Burgess Shale-type biotas have been found in Cambrian rocks elsewhere in the world (see Conway Morris 1989b, Allison & Briggs 1993; Butterfield 1995). Burgess Shale-type fossil occurrences are thus, not unique, but appear representative of more widely distributed faunas (e.g. Robison 1991). The Chengjiang fauna represents the earliest known of the Burgess Shale-type Lagerstätten, being upper

Atdabanian in age (Qian & Bengtson 1989; Bengtson *et al.* 1990). The presence of a diverse arthropod assemblage within the Chengjiang fauna supports the view that the basic radiation of the coelomates, or the Cambrian Explosion, was essentially complete by the Atdabanian.

At Big Gully, outcrops have been affected by extensional faulting, resulting in the strata being downthrown to the north (seaward) (Pl. 3.1). The assemblage occurs in a 8 metre thick siltstone which outcrops both in the cliff (Pl. 3.5) and again, on a wave-cut platform to the north (Pl. 3.2). The basal siltstone unit outcropping in the cliff has been highly shattered due to its proximity to an almost vertical fault plane, making collecting difficult. The outcrop on the wave-cut platform shows less shattering. Its low dip (average 19º towards the north east), has resulted in an exposure with an apparent thickness of some 24 metres (compared with a true vertical thickness of 8 metres in the cliff section). This allows a detailed study of beds along strike and thus the majority of counts and collections were made from the wave-cut platform.

The rock is difficult to split along bedding planes, and is traversed by closely spaced vertical or oblique joints/fractures/cracks. As with Burgess Shale specimens, fossils from the Emu Bay Shale at Big Gully adhere to both sides of the split rock, giving part and counterpart. Part and counterpart have been kept together where possible (some material shattered or some specimens may have first been overlooked). However, when a split following a bedding plane reveals part of a specimen, it often proves impossible to open the same plane on the other side of the vertical fracture that cuts through the fossil. Counts and collections were undertaken along strike on the wave-cut platform. Total area included at each level was approximately equal and thus the counts provide a good comparison of relative occurrences between levels.

The lower 2 metres was partially obscured by boulders (Pl. 3.2), but proved to be poorly fossiliferous. Above this level, fossil occurrences increased, becoming most numerous between 5 and 7 metres above the base. Above 7.25 metres the section became sandy and non-fossiliferous (Pl. 3.6).

Since the Emu Bay Shale Lagerstätte is restricted to the Big Gully locality (Fig. 1.1), the term 'Big Gully assemblage' will be used in reference to this Lagerstätte fossil assemblage - the latter term is used instead of 'fauna' because, unlike the Burgess Shale and Chengjiang faunas, the fossils found at Big Gully do not appear representative of the community which existed at the time of deposition). The Emu Bay Shale appears to be uppermost Botomian in age (see section 2.5). Hence the Big Gully assemblage is only slightly younger than the Chengjiang fauna. Given the well documented similarity between Chinese and Australian Early Palaeozoic fossils (e.g. Bengtson *et al.* 1990), some similarity between elements of the Chengjiang fauna and the Big Gully assemblage may be expected.

## 3.2 Faunal Composition of the Big Gully Assemblage

In a detailed analysis of the community structure of the Phyllopod Bed from the Middle Cambrian Burgess Shale, Conway Morris (1986) found that arthropods dominated the assemblage, both in numbers of genera and individuals (Table 3.1), with polychaetes and brachiopods also present. However, those organisms which were alive at the time of burial and which possessed hard parts sufficient to survive normal taphonomic processes (excluding sponges) comprised only some 2-12% of the fauna (Conway Morris 1986). The dramatic loss of information during normal taphonomic processes is clearly shown by the fact that, given a community structure similar to that in the Burgess Shale, in which trilobites constituted some 0.005% of individuals alive at the time of deposition, they are estimated to constitute approximately 23% of the surviving fossils after normal

taphonomic processes. This figure does not include trilobite exuvia which would also make a significant contribution to the fossil record of the community due to their high preservation potential.

# Plate 4

**4.1** *Redlichia takooensis* (private collection). Showing general style of preservation as iron-stained calcite. Note also large size of trilobite. (x0.3)

**4.2** *Hsuaspis bilobata* (AUGD1046-726). Intact moult. (x2.5)

**4.3** *Naraoia* (AUGD1046-575). Intact specimen, note impression of antennae on the anterior shield. (x3)

**4.4** *Xandarella* (AUGD1046-320). Note iron concretion around posterior of specimen, possibly after pyrite and yellow, limonitic stain. (x1.6)

**4.5** *Isoxys communis* (AUGD1046-710). Left lateral view, note large stalked eyes. (x1.6)

**4.6** *Tuzoia australis* (AUGD1046-315). Disarticulated valves, note typical reticulate pattern on valves. (x1)

# PLATE 4


1


2


3


4


5


6

**Table 3.1** Number of species referable to various selected groups from the Chengjiang, Burgess Shale and Emu Bay Shale assemblages along with percentages of total species. [1] based on Hou *et al.* (1991).

| | Chengjiang[1] (%) | Burgess Shale[1] (%) | Emu Bay Shale (%) |
|---|---|---|---|
| Arthropods | 34 (46) | 63 (42.4) | 9 (90) |
| (Trilobites) | 4 (5) | 19 (12.5) | 3 (30) |
| Sponges | >20 (>36) | 36 (24) | - |
| Annelids | 3 (4) | 14 (10) | 1(?) (10) |
| Brachiopods | 4 (5) | 7 (5) | - |
| Hyolithids | - | 1 (0.5) | - |
| (Total Species) | (73) | (152) | (10) |

The Early Cambrian Chengjiang fauna is similar to the Burgess Shale fauna (Table 3.1) with fossils of arthropods dominating. Indeed Hou *et al.* (1991) documented 18 genera which appear to be present in both faunas, including *Anomalocaris*, *Isoxys*, *Naraoia*, *Eldonia* and *Chancelloria*. It was suggested that *Anomalocaris canadensis* may represent the first specific link between the two localities, but, Nedin (1994, 1995) has queried the identification of *A. canadensis* from the Chengjiang fauna (see also section 3.4.6.1).

The Big Gully assemblage has for some time, been regarded as an important Early Cambrian fossil Lagerstätte (Conway Morris 1986, 1989b; Allison & Briggs 1993). However, it is clearly different in a number of ways compared with the Burgess Shale and Chengjiang faunas.

The most conspicuous difference is in the diversity of the assemblage (Table 3.2). Only ten species have been identified during this study. Three genera previously unrecorded from this locality have been recognised, adding to those described by Glaessner (1979); all are arthropods. Also, *Myoscolex ateles* Glaessner is here re-described as an arthropod (see section 3.4.6.2). This low diversity and preponderance of arthropods is suggestive of other the Cambrian shelly faunas and is similar to the composition of the Burgess Shale fauna if normal taphonomic conditions had applied during early

# Plate 5

**5.1** *Anomalocaris briggsi* sp. nov. (AUGD1046-630). Holotype. Intact appendage. (x0.62)

**5.2** *Anomalocaris* sp. (AUGD1046-346). Intact appendage, note large spines on first segment. Curved nature of appendage and presence of iron oxide auggests that this represents an intact appendage and not a moult. *Myoscolex ateles* also occurs. (x0.5)

**5.3** *Myoscolex ateles* (AUGD1046-385). colour represent differing preservational styles. Grey area are fluorapatite, red-white areas are coarse calcium carbonate fibres. Grey areas represent phosphatised muscle tissue. (x0.9)

**5.4** *Myoscolex ateles* (AUGD1046-646). Preservation of head area showing two globose eyes and a proboscis-like organ running backwards. (x2)

**5.5** *Myoscolex ateles* (AUGD1046-611). Preservation of heas area showing one globose eye, the lower area is a small *Hsuaspis bilobata.* (x2.5)

**5.6** *Myoscolex ateles* (P21020). Close-up showing red, fibrous calcium carbonate over grey fluroapatite, representing phosphatised muscle tissue. Note nature of fluorapatite, suggestive of muscle fibres. (x3)

# PLATE 5






**Table 3.2** Total numbers of individuals and percentage of total assemblage counted in this study from the Emu Bay Shale at Big Gully.

| | Individuals | Percentage |
|---|---|---|
| *Hsuaspis* | 870 | 31.1 |
| *Redlichia* | 750 | 26.8 |
| *Naraoia* | 3 | - |
| *Xandarella* | 1 | - |
| *Isoxys* | 375 | 13.5 |
| *Tuzoia* | 300 | 10.9 |
| *Anomalocaris* | 25 | 0.9 |
| *Myoscolex* | 434 | 15.5 |
| *Palaeoscolex* | 40 | 1.4 |

diagenesis (e.g. Conway Morris 1986). Several lines of evidence suggest that the low diversity, arthropod-dominated Big Gully assemblage, may not simply be the result of taphonomic filtering.

Another unusual aspect of the Big Gully assemblage is the lack of sessile organisms, with or without hard parts. Sessile and slow moving epifaunal organisms such as brachiopods and molluscs are a small but persistent part of the Burgess Shale and Chengjiang faunas (Table 3.1), but are absent from the Big Gully assemblage. Brachiopods and hyolithids are present in the Emu Bay Shale at Emu Bay and in other Early Cambrian deposits. Their absence from the Big Gully assemblage therefore is suggestive of an environmental filter, since their hard parts would be expected to survive the normal taphonomic processes.

The presence of *Hsuaspis bilobata* meraspids indicates that in certain circumstances there appears to be no taphonomic barrier to the preservation of juvenile forms. Therefore, their rarity (only 12 *H. bilobata* meraspis individuals and no *Redlichia* juveniles, have been found) is again indicative of an environmental filter (note: the small size of the individuals is not a factor in their rarity, since although small, they are easily recognisable on rock surfaces due to the presence of elongate, curved spines).

Thus it appears as though the environment of deposition at Big Gully was significantly different to that occurring at the implied contemporaneous deposit in Emu Bay, some 8 kms to the west.

The large size of some elements of the assemblage has been note previously (e.g. Jell 1990). *Redlichia takooensis* appears to grow up to 25 cm in length, and *Isoxys communis* is much larger than similar forms found in the Burgess Shale (D. H. Collins pers. comm. 1993). The large size of *Redlichia* may be explained as a response to low oxygen levels, since larger individuals generally have a lower weight specific oxygen consumption (Bayne 1971). *Hsuaspis bilobata* by contrast, is not represented by individuals of an unusual size. This may be because *Hsuaspis* was not adapted for low oxygen levels. Similarly the large size of *Isoxys* may be due to an adaptation to low oxygen levels, or be due to reduced competition in low oxygen environments (e.g. Peterson & Andre 1980).

While it appears that most of the animals were alive, or at least intact, when buried, the preservation of soft parts is very rare. The exceptions appear to be *Myoscolex*, where the crude (due to recrystallisation) preservation of muscle tissue has apparently occurred, and very rare examples of the soft-bodied forms *Naraoia* and *Xandarella*. Thus, while there appears to have been a taphonomic bias towards those organisms with more robust skeletal elements, the assemblage appears to lack forms which are common in shelly Cambrian deposits, suggesting some control by taphonomic and environmental filters.

## 3.3 Big Gully Assemblage: Arthropods

### 3.3.1 Trilobites

3.3.1.1 *Redlichia takooensis*(Pls. 4.1, 6)

*Redlichia takooensis* represents the second most abundant element in the Big Gully assemblage, comprising some 26.8% of total individuals. *R. takooensis* also provides the largest complete specimens in the assemblage with some trilobites reaching 25 cm in length. Claims of trilobites up to 30 cm long (Daily *et al.* 1979) appear inaccurate (R. Jenkins pers. comm.). Complete moults evidently comprise the majority of specimens. There is no correlation between size and level within the Lagerstätte.

A characteristic of *Redlichia* is the long medial spine on the 11th thoracic segment (Pl. 6.1). However *R. takooensis* appears to differ from most other species in having a second medial spine on the 6th thoracic segment and, in larger forms, bases of spines, medially on each axial lobe (Pl. 6.2). While a specimen of *R.* (*Pteroredlichia*) *murakamii* figured by Zhang & Jell (1987, pl. 10, fig. 5) appears to possess a long medial spine on the 6th thoracic segment, the occurrence of medial spines on each thoracic segment appears to be distinctive in *R. takooensis* from the Big Gully locality. This trait appears to be confined to the larger individuals, indicating a possible ontogenetic reason for their apparent absence in the type specimen.

The hypostome of *R. takooensis* is commonly seen impressed into the glabella from below and thus has not previously been described in detail. However the presence of a disarticulated hypostome (Pl. 6.3) shows that it is similar to that occurring in *R. nobilis* (Zhang & Jell 1987, pl. 7 fig. 8) except that the anterior wings appear better defined and placed more laterally in *R. takooensis*, a situation similar to that figured for *R. chinensis* (Kobayashi & Kato 1951, pl..5, fig. 6). The tips of these anterior wings appear to have lain immediately under the axial furrow at the antero-lateral edge of the glabella (Whittington 1988). The type description of *Redlichia* states that the hypostome was fused to the rostral plate. This was supported by Öpik (1958) and by Jell (1990). However, Whittington (1988) suggested that a hypostomal suture may be present, citing Öpik's (1958, pl. 5, fig. 1, pl. 6, figs. 4 & 5) photographs, which showed hypostoma both linked together with the rostral plate, and isolated. A comparison may be made with

# Plate 6

**6.1** *Redlichia takooensis* (AUGD1046-630). Exuvia showing elongate thoracic spine on 11th segment. Free cheeks, posterior 4 segments of the thorax and pygidium missing. Disarticulated hypostome visible to left of cranidium. (x2.5)

**6.2** *Redlichia takooensis* (AUGD1046-319). Exuvia with detached cephalon, showing spine bases on the axis of each thoracic segment, note enlarged spine base on 11th segment. (x0.5)

**6.3** *Redlichia takooensis* (AUGD1046-630). Enlarged view of **6.1**, showing hypostome. (x2.4)

**6.4** *Redlichia takooensis* (AUGD1046-246). Specimen exhibiting the 'saltation' mode of exuviation. (x0.9)

**6.5** *Redlichia takooensis* (AUGD1046-349). Specimen exhibiting exuviation via the disarticulation of the thorax and the inversion of the left hand free cheek. (x1.5)

**6.6** *Redlichia takooensis* (AUGD1046-359). Specimen showing extreme exuviation via the disarticulation of the thorax. Free cheeks and doublure, with hypostome attached is twisted underneath the thorax. (x1.3)

# PLATE 6

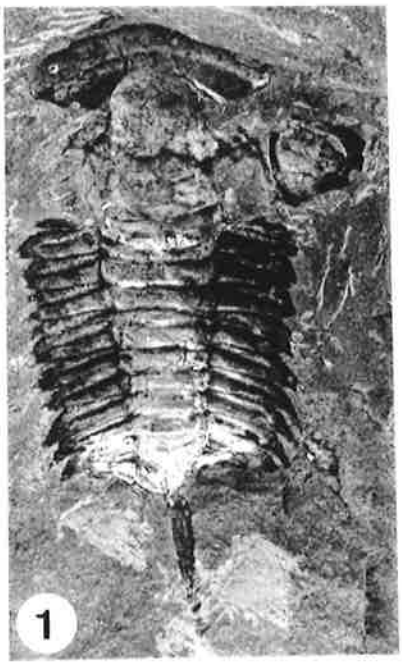




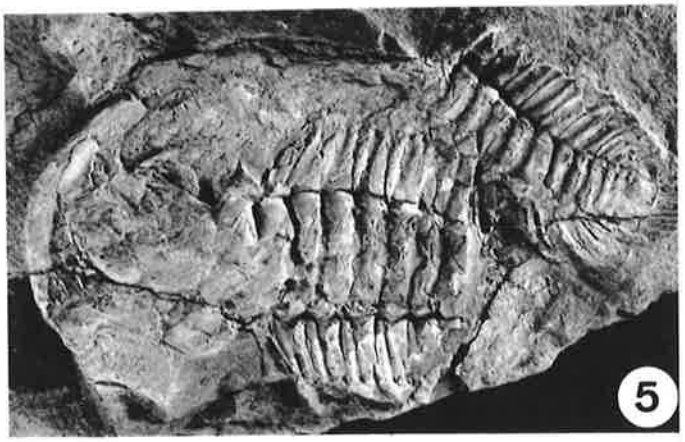


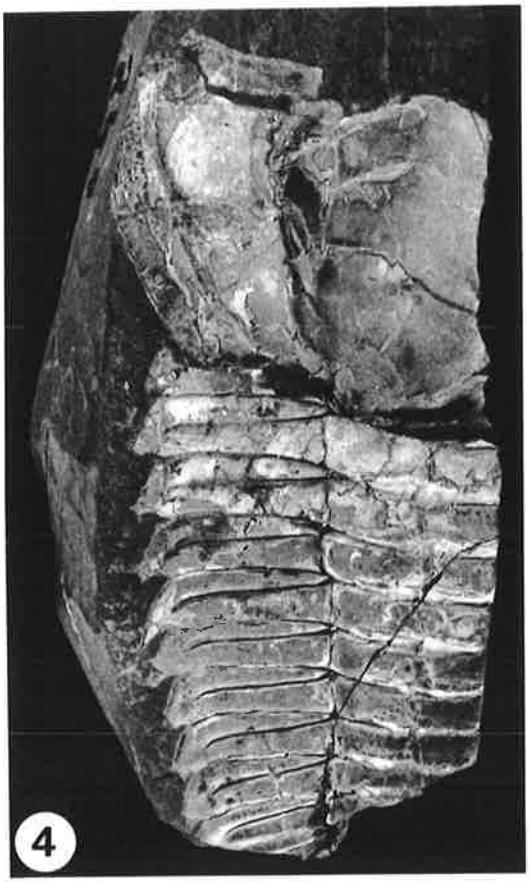


*Paradoxides*, where the hypostome is considered fused with the rostral plate due to the fact that they are never found separately and terrace lines run continuously across the boundary between them (Whittington 1988). The presence of the disarticulated hypostome figured here and similar specimens figured elsewhere (e.g. Zhang *et al.* 1980, pl. 20, fig. 5) lend further support to the possibility that some species of the Early Cambrian trilobite *Redlichia* may have possessed a hypostomal suture. Indeed, Fortey (1990) suggests that fusion of the hypostome and the rostral plate may well be an advanced character, derived from an original sutured condition.

Exuviation, or the active phase of ecdysis involving the withdrawing of an individual from its old skeleton, can occur with or without the inversion of proecdysial skeletal elements (McNamara 1986c). Trilobites with backwardly directed spines, such as *Redlichia*, would have been forced to emerge anteriorly during moulting. This process was made possible by the sutures being marginal or traversing the eye lobe. One of the most common methods of moulting was described by Richter (1937) as the 'Salterian' mode, whereby the animal emerged after the exoskeleton had split along the hypostomal suture and along the back of the cephalon and inversion of the cephalon. This resulted in the exuviated thorax coming to rest over the inverted and backwards facing cephalon. This mode of exuviation can also be observed in *R. takooensis* (Pl. 6.4) which indicates that on some occasions the facial sutures in *R. takooensis* apparently failed to spilt. It also suggests that, at least on rare occasions, *R. takooensis* may have possessed a functional hypostomal suture.

McNamara (1986c) documented three forms of exuviation involving inversion of skeletal elements in *Redlichia*, whereby partial enrollment of the trilobite resulted in the separation and inversion of some elements of the proecdysial skeleton. Of the three forms of exuviation discussed, only one, the lateral inversion of the free cheek has been observed in specimens of *R. takooensis* (Pl. 6.5). The production of inverted free cheeks was explained as being caused by a vigourous upward thrust after the initial separation of the free cheeks. This may have caused a low pressure area to develop and

the inward movement of water led to rotation of the free cheeks (McNamara & Rudkin 1984). Whittington (1990) suggested an alternative method for *Paradoxides*, whereby the trilobite arches its body and pushed the anterior border of the cephalon into the sediment, producing pressure on the facial sutures, forcing them open. The newly moulted animal could then emerge anteriorly, forcing the free cheeks up over the 90° to substrate position, allowing the old thorax to fall over the inverted free cheeks. However, if the free cheeks became disarticulated from the rest of the trilobite while they were in the 90° position, they could well fall forwards and lie in essentially the normal, if inverted, position. Once the newly moulted trilobite had exited the old exoskeleton, the exuvia would collapse in line with the inverted free cheeks.

While the exact moulting technique is unknown, it is apparent from trilobites in the Big Gully assemblage that the majority may have encountered little trouble in moulting, since most show only slight disarticulation of one free cheek and a slight misalignment between the thorax and cephalon. This is either indicative of a successful moult or the slight crushing of complete individuals with diagenetic compaction.

As has already been shown, the failure of the facial sutures to split has resulted in the 'salterian' mode of exuviation. However, other specimens show different problems. Perhaps the most extreme example of problematic exuviation is represented in the specimen shown in Pl. 6.6. Here the free cheeks appear to be still attached to the rostral plate and hypostome, but are inverted and twisted. Also the right free cheek has been pressed into the sediment. The strong flexing motion which would be needed to bury and twist the free cheek appears to have disarticulated the thorax at three points; behind the cephalon, between thoracic segments 4 and 5 and either side of thoracic segment 11. The disarticulation and subsequent dislocation of segment 11 is understandable given that it bore an elongated medial spine which extended beyond the pygidium. A vigorous flexing motion such as that described by McNamara (1986c), may have resulted in this spine penetrating the sediment and thus acting as a brace, placing extra pressure on segment 11. During flexure, the point of maximum pressure exerted on the thorax is around segment 5 which lies at the maximum curvature. Thus the exuvial configuration

can be explained by the vigorous flexure of the trilobite during moulting and the pressing into the sediment of the anterior of the cephalon. The facial sutures split while the cephalon was in the 90° position, but the thorax also split due to the severity of the flexing motion. Egress of the newly moulted trilobite may have inverted and twisted the free cheeks.

A similar pattern of exuviation is exhibited in Pl. 6.5. However, in this example, although the thorax is disarticulated, the cephalon is not pressed into the sediment and only the left free cheek is inverted. The thorax is again disarticulated behind segment 11, due to the presence of the elongated medial spine, and also behind segment 6. The disarticulation behind segment 6 may be explained by the focus of flexural pressure at or around that point. Segments 1 to 5 bear a notch on the posterior margin of the pleura which might act to 'lock' the first 6 segments together into a more rigid unit. This may result in the focusing of pressure in the weaker joint between segments 6 and 7, although this joint appears to have held in the previous example.

3.3.1.2 *Hsuaspis bilobata*(Pls. 4.2, 7)

*Hsuaspis bilobata* is the most numerically abundant species in the Big Gully assemblage, comprising some 31.1% of individuals counted (Table 3.2). *H. bilobata* was first described as *Estangia bilobata* by Pocock (1964) and was placed tentatively within the Paradoxididae. However, Öpik (1975a, b) suggested a closer relationship with *Xystridura* Whitehouse and placed *Estaingia bilobata* within the Xystriduridae. Jell (1990) considered *Estaingia* a junior synonym of *Hsuaspis* from the Early Cambrian of China and placed the renamed *Hsuaspis bilobata* within the Ichangiidae. *H. bilobata* is also described from the Cymbric Vale Formation in western New South Wales (Öpik 1975b), an identification challenged by Jenkins (1990) and Jell (1990) on the grounds of its shorter preglabellar field and advanced genal spines. *H. bilobata* has since been found in the Oraparinna Shale of the Flinders Ranges (Jell 1990, Jell *et al.* 1992), along with *Hsuaspis occipitospina* Jell (Jell 1990). *Hsuaspis* is common in the late Early

Cambrian Tsanglangpu Stage (upper Botomian) of China (Zhang & Jell 1987). Whitehouse (1936) placed *Xystridura* in a separate subfamily of the Paradoxididae, the Xystriduridinae, due to the strongly developed pygidial features and lack of reflexed glabellar furrows, and the distance from the glabella to the facial suture. Öpik (1975b) suggested a lineage from *Hsuaspis* to *Xystridura*, and placed *Hsuaspis* in the Xystriduridae. Jell (1990) accepted the possibility of a lineage between *Hsuaspis* and *Xystridura*, but challenged the grouping of the Xystriduridae and the Paradoxididae, suggesting that the resemblance between the two was the result of contemporaneous homeomorphy. Thus Jell suggested that the Paradoxididae and the Xystriduridae should be considered end members of separate lineages within the Ellipsocephaloidea, along with at least the Ichangiidae, the Protolenidae and the Ellipsocephalidae. Recently the taxonomic position of *Xystridura* has been thrown into some confusion with its placement in the Centropleuridae (Lin & Jago 1993) and in the Paradoxididae (Babcock 1994). With regard to the Centropleuridae, this placement is surprising because this family is distinguished by the 3S being directed diagonally backward, the anterior end of the palpebral lobes being in front of the widest part of the glabella, the anterior sections of the facial sutures being at right angles to the glabella or running obliquely backwards paralleling the lateral portions of the anterior border, and a thorax of 14 or more segments. Neither *Xystridura* or *Hsuaspis* exhibit these distinguishing characteristics and so maintenance of *Xystridura* within the Xystriduridae seems more appropriate. The discovery of a small number of individuals representing the meraspid stage of *H. bilobata* from the Emu Bay Shale at Big Gully allows the ontogenetic growth of this species to be documented for the first time. An understanding of the ontogeny of *H. bilobata* can be used as a basis for a comparison between *H. bilobata* and *Xystridura* and as a possible test of the suggested lineage between them.

### 3.3.1.2 Ontogeny of Hsuaspis

The meraspid stage begins at degree 0 with the appearance of the first transverse joint in

the exoskeleton, separating the cephalon from the transitory pygidium (Whittington 1957). Thoracic segments become fully formed at the anterior end of the transitory pygidium and are released into the thorax. Each meraspid degree or stage is represented by the addition of another thoracic segment, although addition of more than one segment per moult may occur (Whittington 1957), and is numbered according to the total number of thoracic segments present. The meraspid of *Hsuaspis* appears to be represented by 4 stages, meraspis degree 1? (Pl. 7.1), degree 7 (Pl. 7.2), degree 10 (Pl. 7.3) and degree 12 (Pl. 7.4). The holaspid stage begins when the last segment (segment 13) is added to the thorax. With growth there are other changes in morphology, some gradual, some rapid.

Measurements of the increase in size of the cranidium (Fig. 3.1) shows that the meraspids fall on the trend shown by holaspid instars of *Hsuaspis bilobata* from the Emu Bay Shale. This correlation is also mirrored in measurements of increasing glabella size (Fig. 3.2). Thus it appears that the meraspid instars found in the Big Gully assemblage do indeed represent juvenile *Hsuaspis*. Measurements form discrete clusters, thought to represent moult stages, or instars, in the growth cycle of the trilobite (e.g. Whittington 1957).

The specimen in Pl. 7.1 appears to be of a meraspid form, degree 1. The thorax and attached transitory pygidium are overlain for at least 75% of their combined length by the cephalon. Thus this specimen is probably a moult, whereby the exoskeleton has split along the posterior margin of the cephalon and the facial sutures. After emergence, the cephalic exuvium has fallen back onto the thorax and pygidium, obscuring some morphological relationships. The cranidium of meraspis degree 1 has a width of about 1.66 its cranidial length (cranidial width is taken as the widest point on the cranidium, which in *Hsuaspis* and *Xystridura* corresponds to "J - the palpebral cranidial width" measurement of Shaw 1957, p. 200, fig. 7b; Appendix 3). During development the cranidium narrows so that by the meraspis degree 12 stage the width is 1.30. During growth in the holaspid stage, this narrowing continues albeit more slowly so that holaspids with a cranidial length of 10 mm have widths of about 1.1-1.12 (Fig. 3.3).

# Plate 7

**7.1** *Hsuaspis bilobata* (AUGD1046-700). Meraspis 1. Note elongate pleural spine on first thoracic segment. (x30)

**7.2** *Hsuaspis bilobata* (AUGD1046-701). Meraspis 7. Note pleural spines on the first and second thoracic segments. (x28)

**7.3** *Hsuaspis bilobata* (AUGD1046-543). Mersapis 10. Note single pleural spine on the second thoracic segment and advanced genal spines. (x14.5)

**7.4** *Hsuaspis bilobata* (AUGD1046-547). Meraspis 12. Note much reduced pleural spine on second thoracic segment and enlarged preglabellar field. (x16)

**7.5** *Xystridura* (AUGD3-231). From Templetone River, Queensland. Note enlarged frontal lobe of glabellar and lack of preglabellar field. (x2)

**7.6** *Hsuaspis bilobata* (AUGD1046-370). Holaspid form. Note reduced preglabellar field compared with meraspid 12. A large *Palaeoscolex* lies above the specimen. (x1.8)

# PLATE 7



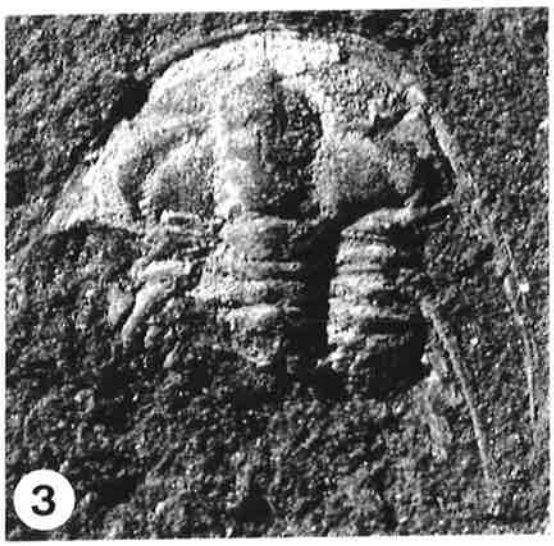



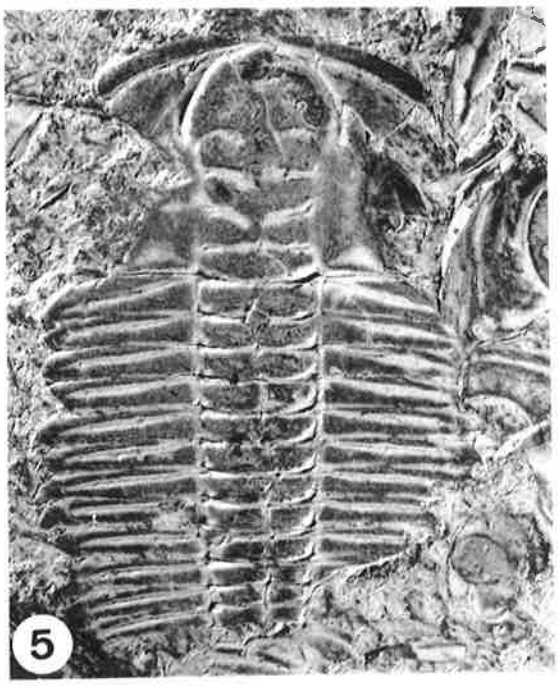


However, measurements taken from cranidia identified as *Hsuaspis bilobata* from the late Early Cambrian Cymbric Vale Formation of New South Wales by Öpik (1975b) shows an apparent reversal of this trend. Although the smaller cranidia from the Cymbric Vale Formation do plot with those from the Emu Bay Shale, the largest cranidium (CPC 13152 - Öpik 1975b, pl. 1, fig. 1), with a length of 16 mm, appears to exhibit a trend towards increasing cranidial width as a percentage of cranidial length, with a value of 1.21 compared with an average value for cranidia 10 mm in length of 1.10. Thus it appears that with extended growth, the trend of slowly decreasing cranidial width is reversed.

The anterior facial sutures diverge at 95°, curving slightly anteriorly in meraspis degree 1. During development the sutures become more anteriorly divergent, reaching 115-117° in meraspis degree 12 and >120° in the holaspid. This has occurred because the junction of the facial suture with the eye lobe migrates inwards, relative to the axial furrow, during meraspid growth. In meraspis degree 1 the distance between the junction and the axial lobe is 0.35 the cranidial length. This decreases through 0.23 in small holaspids to < 0.20 in large holaspids. This migration is probably at least partially due to the increase in the width of the glabella during meraspid growth.

In meraspid 1, the eye lobe extends almost tangentially away from the posterior of 3L, until the point where the anterior facial suture and the eye lobe meet. Posterior to this, the eye lobe curves gently back. The posterior tip does not reach the posterior furrow of the cranidium. During meraspid growth the length of the tangential part of the eye lobe decreases as the junction of the anterior facial suture and the eye lobe migrates towards the axial furrow. The eye lobe becomes more convex as a result and the distal part of the eye lobe becomes recurved towards the glabella. Thus the distance between the posterior tip of the eye lobe and the axial furrow, relative to cranidial length, decreases from 0.45 in merapsis 1 to 0.30 in meraspis degree 12 (Fig. 3.4). The trend towards decreasing distance between the eye lobe and the axial furrow terminates abruptly at the onset of the holaspid stage (equivalent to a cranidial length of 2.5 - 3.0 mm) and subsequently this distance remains static at about 0.25 relative to cranidial length. Along with migration of

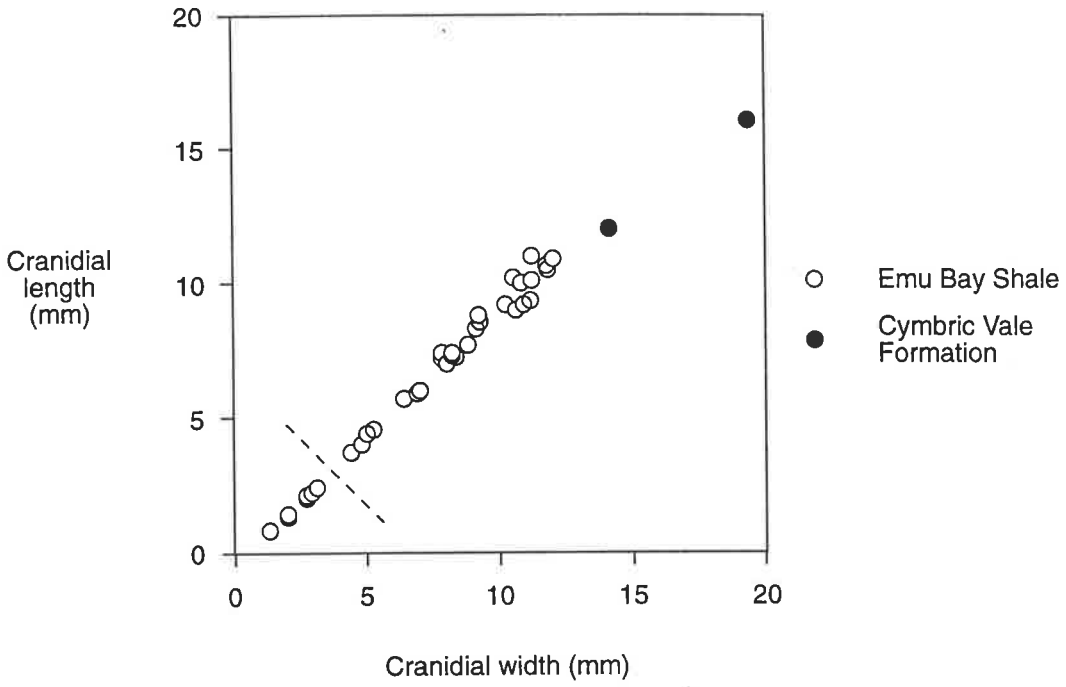


**Fig. 3.1** Measurements of cranidial length against cranidial width for *Hsuaspis bilobata* from the Emu Bay Shale and Cymbric Vale Formation. Dotted line marks the boundary between the meraspid and holaspid stage.

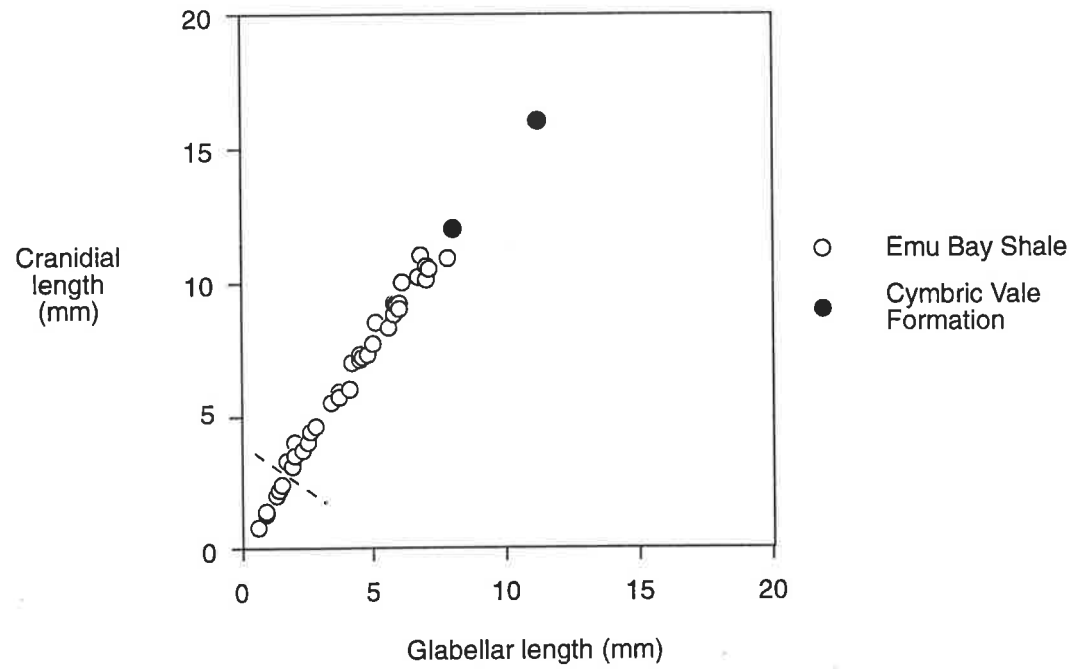


**Fig. 3.2** Measurements of cranidial length against glabellar length for *Hsuaspis bilobata* from the Emu Bay Shale and Cymbric Vale Formation. Dotted line marks the boundary between the meraspid and holaspid stage.

the posterior portion of the eye ridge, the width of the palpebral lobe also increased with growth, resulting in a reduction in area of the fixed cheek. The posterior tip of the eye lobe reaches the posterior furrow of the cranidium by Meraspid 7.

Ontogenetic changes of the glabella includes the retraction of the glabella from the anterior border to produce a preglabellar field. This is most marked in the meraspid period, where the preglabellar field rapidly increases from 0.05 of the cranidial length in meraspis degree 1 to 0.14 in meraspis degree 12 (Fig. 3.5). This retraction continued into the holaspid period for a short while, with a maximum preglabellar field of 0.15 the cranidium length being reached by instars with cranidia 3.5 mm long. After this, protraction of the glabella occurs and 3L extends back, slowly, towards the anterior border. This protraction results in the gradual decrease of the preglabella field, which although slow, appears to have continued throughout the life of the organism. The ontogenetic retraction and protraction of 3L can be seen in Fig. 3.6, whereby, after an initially large 3L in meraspis degree 1, at 0.18 of the cranidial length, this decreases to 0.14 by the early holaspid stage with a cranidial length of 3.5 mm, and then increases steadily to be approx. 0.22-0.24 in holaspids with cranidia of 10 mm.

There is a gradual trend in the width of 3L with growth, although not as marked as that of length. The width increases from 0.36 of cranidial length in meraspis degree 1 to about 0.38 at the onset of the holaspid period. However, this trend continues with increasing size, whereby instars of 10 mm cranidial length attain a 3L width of some 0.425-0.45 of cranidial length. The glabella changes from being almost parallel sided in early meraspids to clavate in holaspids. During meraspid growth, the glabellar furrows reach the axial furrow. However, in the holaspid period, 1S moves into the glabella and contact with the axial furrows is lost. This is probably due to the protrusion and expansion of 3L.

Metafixagenal spines are absent, but this could be a preservational artifact in meraspis degree 1, due to the overlapping position of the cephalon, since they may be aligned parallel to and directly above the pleural spines of the first thoracic segment. However,

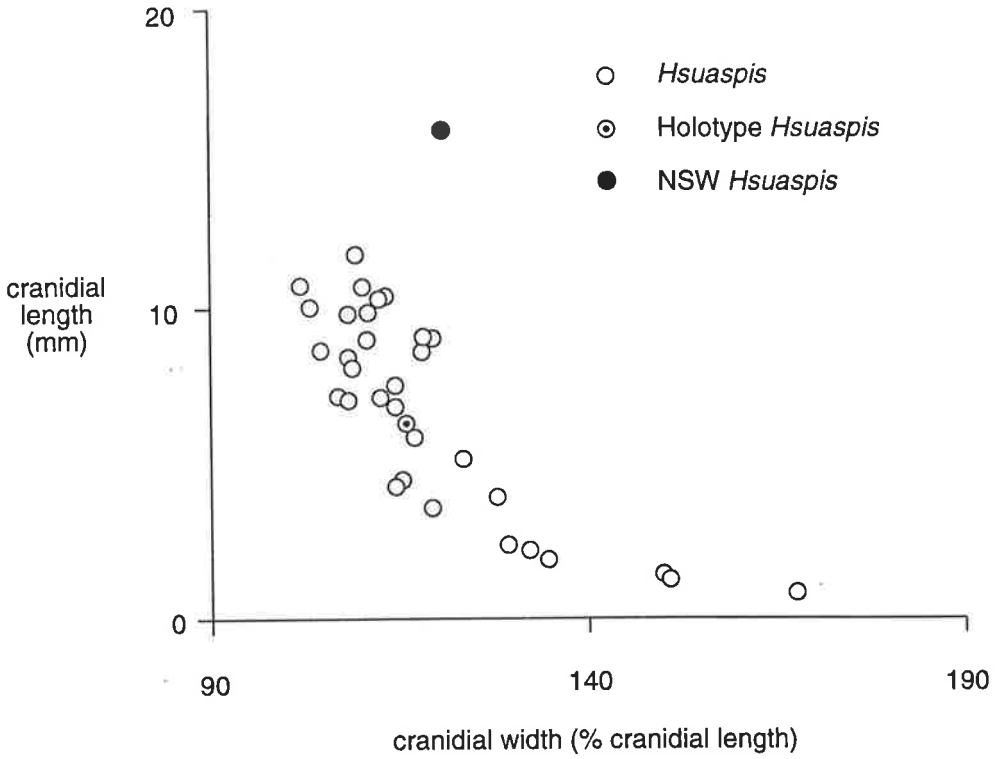


**Fig. 3.3** Plot of cranidial length against cranidial width for *H. bilobata* showing the difference in growth pattern between meraspid and holaspid stages.

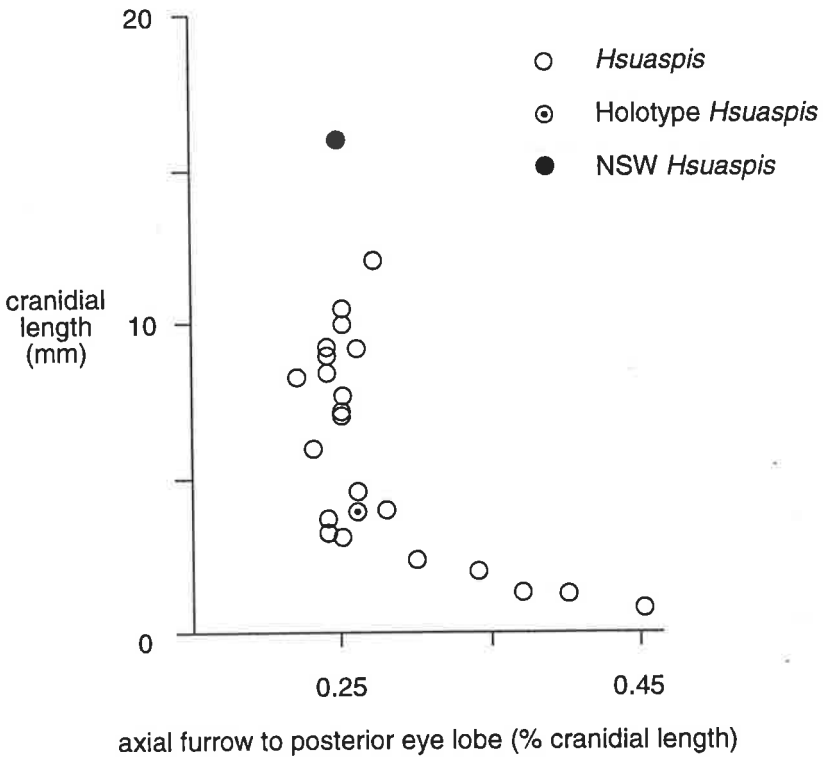


**Fig. 3.4** Plot of cranidial length against axial furrow to posterior furrow distance as a percentage of cranidial length for *H. bilobata* showing the difference in growth pattern between mesaspid and holaspid stages.

there is no evidence of metagenal spines in subsequent meraspids. Long, slim genal spines are present in meraspis degree 1 and continue to meraspis degree 12, although there is a reduction in the length of the spine in relation to cranidium length from around 1.7 in meraspis degree 1 to 0.9 in meraspis degree 12. The holaspid has genal spines which are short, at 0.5 cranidial length, and possess a broad base.

Well developed pleural spines allow the identification of at least one thoracic segment in meraspis degree 1. A ridge on the fixigena overlying the contact between the first segment and the second indicates that they were separate and thus the segment is a true thoracic segment. The second segment bears a much smaller set of pleural spines (0.5 length cephalon) and no indication of a partition between it and the transitory pygidium can be seen. Therefore this segment has not yet been shed from the transitory pygidium. A poorly preserved, very short pair of pleural spines on the transitory pygidium, immediately medial of the second pair, indicates that a third segment is in the process of forming behind the anteriormost segment. The meraspid thorax possesses elongate pleural spines on the first and second segments initially. The meraspis degree 7 specimen (Pl. 7.2) possesses long pleural spines on the first and second segments of the thorax. During the transition between meraspis degree 7 and meraspis degree 8, the pleural spines on the first segment are lost and subsequent meraspid instars possess only one pair of long pleural spines, on the second thoracic segment (Pl. 7.3). During the meraspid period, the length of the spines relative to the cranidium decreases from around 2.2 in meraspis degree 1 to 1.0 in meraspis degree 12. Long pleural spines are absent in the holaspid. The presence of elongate pleural spines on the first two thoracic segments of early meraspids is a common characteristic amongst the Paradoxidacea (Whittington 1957).

The trend of elongate spines on the cephalon and thorax is almost certainly related and is probably linked to protection and buoyancy. Planktonic protaspid forms are often elaborately spinose (e.g. Whittington 1957). This may well be to enhance their buoyancy by increasing the relative Stokes Radius and thus slow the rate of passive sinking (e.g. Vogel 1983). However, as the size of the organism increases, this practice

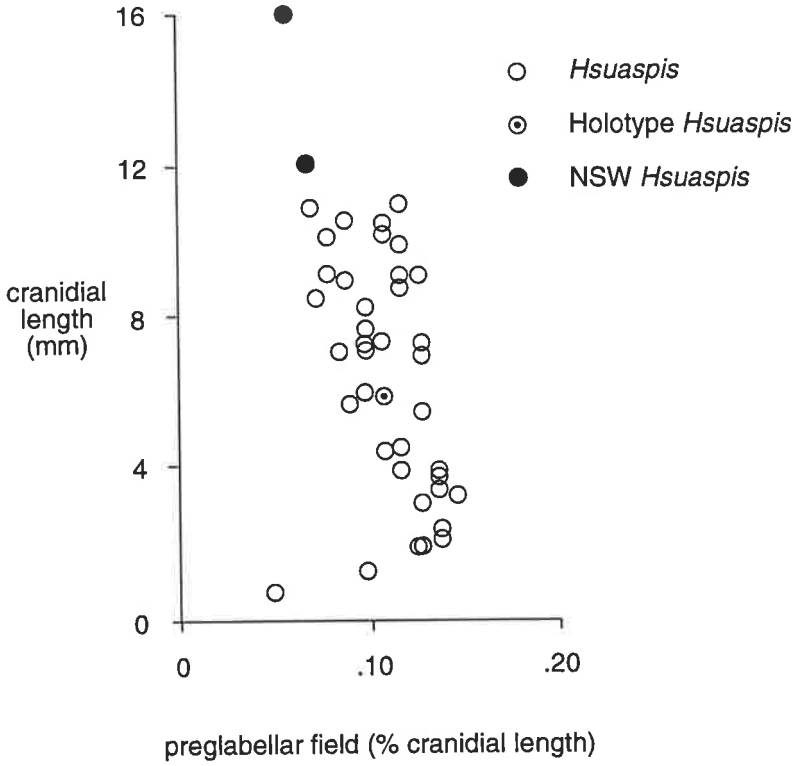


**Fig. 3.5** Plot of cranidial length against preglabella field as a percentage of cranidial length for *H. bilobata* showing the difference in growth pattern between mesaspid and holaspid stages.

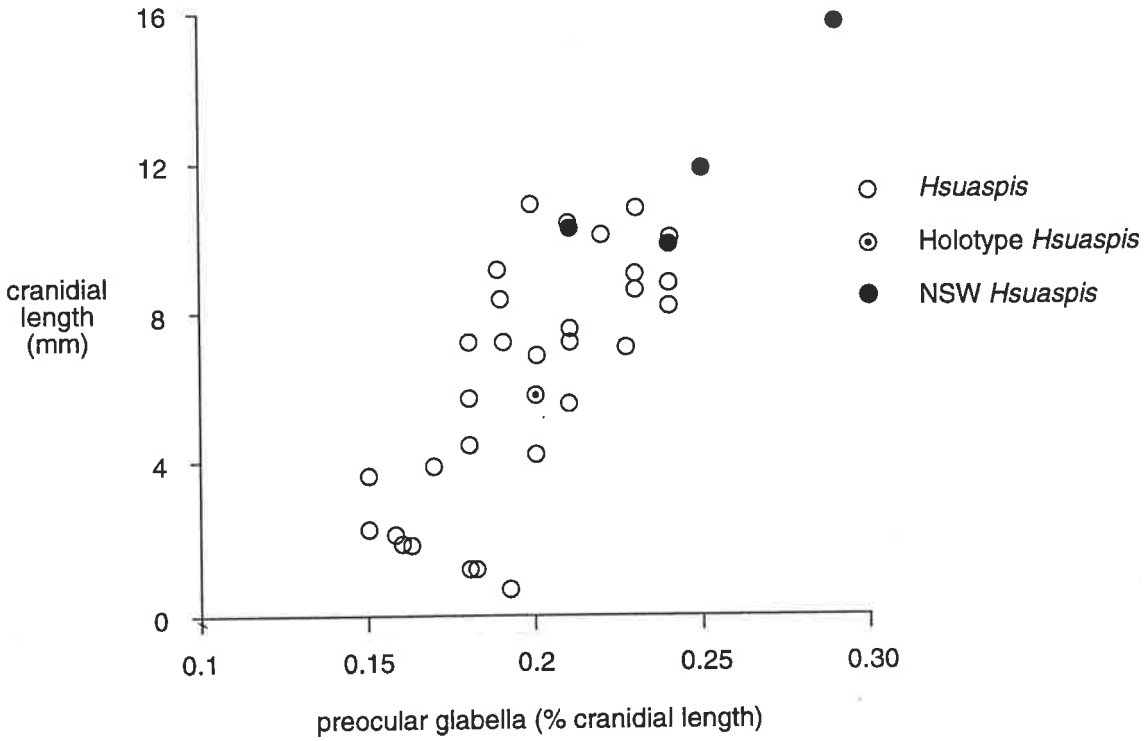


**Fig. 3.6** Plot of cranidial length against preocular glabella as a percentage of cranidial length for *H. bilobata* showing the difference in growth pattern between mesaspid and holaspid stages.

becomes ineffective. In *H. bilobata*, the meraspid stage, with its retention of long genal and pleural spine in one plane only (exsagittal), appears likely to have been benthonic. The spines then may well have served a dual function of protection and buoyancy on soft substrates. The size and shape of the meraspids is indicative of a low energy, rather than a moderate or high energy environment. Thus the increase in surface area offered by the spines would have provided extra buoyancy on soft, fine grained substrates found in low energy environments. With increasing body size, the need for extra buoyancy would diminish. Since predation is likely to have been a continuous problem, the sequential diminution of the spines indicates that protection may have been a secondary function.

The holasapid condition of 13 thoracic segments was reached at a cranidial length of approximately 2.5 mm. After this size was attained morphological development slowed dramatically (Figs. 3.4, 3.5) as is usual in the growth of trilobites (Whittington 1957). The thorax in the early holaspid period tapers posteriorly so that the posterior width is 0.5 the anterior width. The widest point on the axis also moves posteriorly until it is widest across segment 5.

Pygidia are poorly preserved and no trends were discernible.

A reconstruction of the ontogeny of *Hsuaspis bilobata* can be seen in Fig 3.7.

3.3.1.3 Evolutionary Relationship Between *Hsuaspis* and *Xystridura*.

The change through time in the appearance or rate of development of ancestral characters is known as heterochrony (Alberch *et al.* 1979). This process comprises two basic phenomena; paedomorphosis and peramorphosis (McNamara 1982, 1986a, b). Paedomorphosis can be defined as the retention of ancestral juvenile characters in a descendant adult (e.g. McNamara 1986a). Thus paedomorphic forms pass through fewer morphological stages during their ontogeny than their ancestors. This retention of juvenile characters can be achieved in three ways:

Neoteny - a reduced rate of morphological development during the juvenile phase

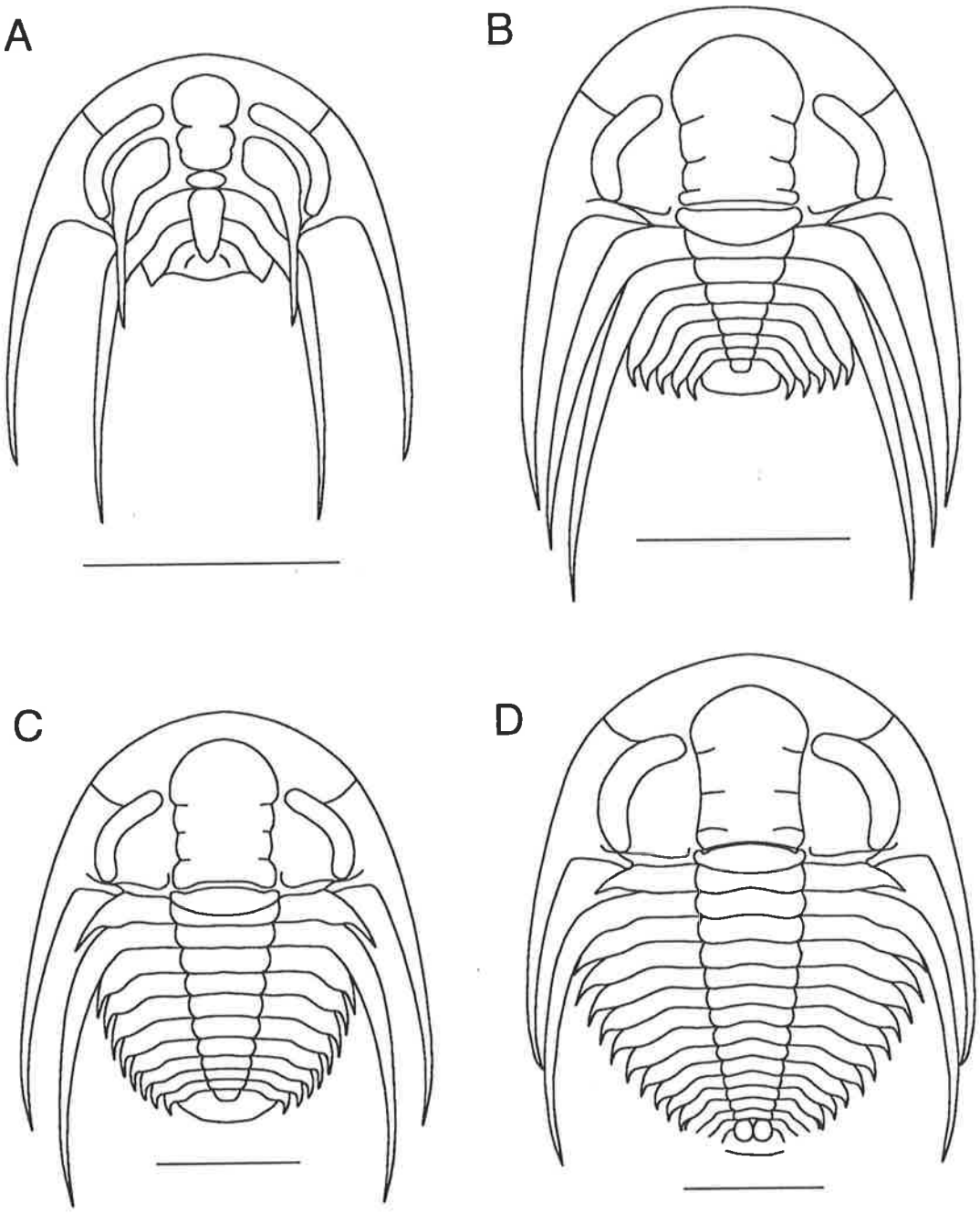


**Fig. 3.7** Reconstruction of the ontogeny of *Hsuaspis bilobata*. **A**. meraspid degree 1, 1046-700. **B**. meraspid degree 7, 1046-701. **C**. meraspid degree 10, 1046-543. **D**. meraspid degree 12, 1046-547. Scale bar = 1 mm.

which results in a morphologically retarded adult.

Progenesis - onset of maturity occurs at an earlier stage of development in the descendant. The resultant adult retains ancestral juvenile characters, but is smaller than ancestral adults due to the shorter time spent in the juvenile rapid growth phase.

Post-displacement - a change in timing of the onset of certain structures. One or more structures will commence development at a later stage with respect to other parts of the organism, resulting in the structure being smaller than in the ancestor.

On the other hand, peramorphosis is the occurrence of ancestral adult morphology in the descendent juvenile stage of development. Peramorphosis involves three processes:

Acceleration - an increase in the rate of morphological development during ontogeny. If the onset of maturity is also accelerated, then the descendant will be smaller than the ancestor, if the onset of maturity is not affected then the descendant will be of a similar size to the descendant.

Hypermorphosis - an extension of ancestral ontogeny, or delayed maturation, resulting in an extension of the juvenile growing period. The extension of late ontogenetic development results in morphological characters different from the ancestral adult and the longer growth period produces a larger descendant.

Pre-displacement - while the rate of development and growth may be the same as the ancestor, development of any number of structures is initiated at an earlier stage, producing a morphologically more advanced adult.

Öpik (1975a) greatly expanded on the early work of Etheridge (1897), Chapman (1929) and Whitehouse (1939) on *Xystridura*, and described two genera, *Xystridura*, (Pl. 7.5) with 15 new species and the monospecific *Galahetes*. Öpik (1975b) also commented on a possible link between *Hsuaspis* and *Xystridura*. If Öpik's suggestion is correct, a view supported by Jell (1990), it would potentially allow correlation between *Hsuaspis* and *Xystridura* bearing strata and thus be an invaluable aid to the understanding of rock relationships in the late Early to early Middle Cambrian of Australia.

In a detailed study on heterochrony amongst xystridurid trilobites (McNamara 1981,

1986b), several key morphological indicators in the ontogeny of *Xystridura* were used to monitor the changes between *Xystridura* and *Galahetes*. These included: the cranidial width as a percentage of cranidial length; the length of the preglabellar field as a percentage of cranidial length; and the width from the axial furrow the the posterior of the eye lobe as a percentage of cranidial width. Precocious maturation, or progenesis, was delineated as the mechanism for the evolution of *Galahetes fulcrosus* from *Xystridura templetonensis*. In this case sequential progenesis (McNamara 1983), whereby the rate of moulting, and not the number of moults, increases, resulting in less time being spent in the rapid growth phase, and consequently a smaller adult which retained the ancestral number of thoracic segments.

Growth in trilobites can occur only after moulting, and is therefore discontinuous. In such situations, resulting body size does not correspond accurately with time or "external" age. However, body size is a measure of the organisms "internal" age and is potentially more useful (e.g. Blackstone & Yund 1989), since most ontogenetic events are size-specific rather than age-specific (McKinney & McNamara 1991).
In the ontogeny of *H. bilobata*, the width of the cranidium relative to cranidial length decreases from about 1.66 in meraspis degree 1 to 1.30 in meraspis degree 12 (Fig. 3.3). In the holaspid period, this rate of decline is slowed so that in specimens with cranidia of 10 mm in length, the relative size is 1.10-1.12. The large cranidium from New South Wales appears to indicate a reversal in this trait and appears indicative of a trend away from *H. bilobata* towards larger individuals with a broader cranidium. Analysis of the relative cranidial widths of *X. templetonensis* (Fig. 3.8), in comparison, shows that the juvenile growth stages have exaggerated morphological development compared with *H. bilobata* of similar cranidial length. For example, early *X. templetonensis* meraspids have a relative cranidial width of 1.80 compared with 1.66 for *H. bilobata* meraspids of similar cranidial length. The initial larger relative cranidial widths in early *X. templetonensis* may be due to a longer period of time spent in the protaspid stage, allowing a broader protaspid cranidium to persist into the early meraspid

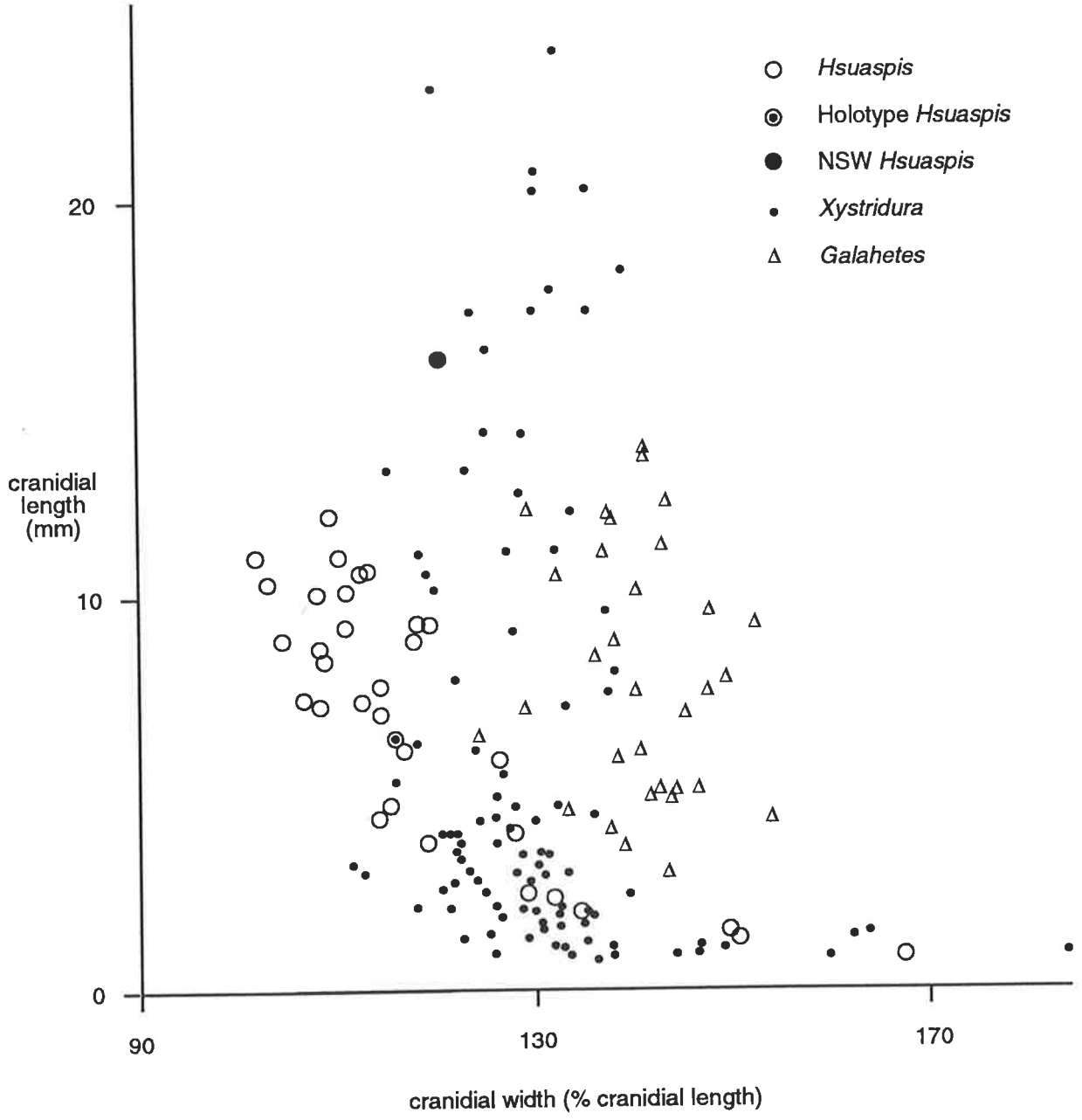


**Fig. 3.8** Plot of cranidial length against cranidial width as a percentage of cranidial length for *Hsuaspis*, *Galahetes* and *Xystridura*. (Data on *Galahetes* and *Xystridura* from McNamara 1981, reproduced with permission of the Australiasian Association of Palaeontologists).

period. Relative reduction in cranidial width is more rapid in *X. templetonensis* than in *H. bilobata*. The point at which the rapid relative reduction of cranidium width changes to a much slower rate occurs in *X. templetonensis* individuals of approximately 4 mm cranidial length, whereas this change occurs in *H. bilobata* individuals of approximately 2.5 mm cranidial length. This suggests that the onset of maturation in *X. templetonensis* has been slowed and, if a simple heterochronic connection exists between *H. bilobata* and *X. templetonensis*, then the gradual relative decrease in cranidial width, with growth, seen in *H. bilobata*, would also be seen and exaggerated in *X. templetonensis*. This does not happen. Cranidial width relative to cranidial length remains static in holaspids of *X. templetonensis*, at about 1.25 instead of decreasing as in *H. bilobata*, and with growth, the relative width actually increases slightly to be 1.35 in individuals of cranidial length 20 mm (Fig. 3.8). The change in cranidial width in relation to cranidial length seen between *X. templetonensis* and *Galahetes fulcrosus* has been explained as progenesis (McNamara 1981, 1986b), whereby *G. fulcrosus* instars mature rapidly. Thus the trend to relative cranidial width reduction is halted by the early onset of the holaspid growth pattern. This change appears to occur at a relative cranidial width of about 1.45, compared with 1.25 for *X. templetonensis*, producing holaspid instars with a much wider relative cranidium. The relative width of the cranidium then remains static (as in the early holaspids of *X. templetonensis*). Although other contemporary species, *X. milesi* and *X. carteri* have slightly smaller cranidial widths, a trait they share with the earliest form, *X. negrina* (McNamara 1981). Thus *Xystridura* meraspid instars begin with a much wider cranidium than *H. bilobata*. By the end of the meraspid stage, their cranidial width has reduced by a amount equal to or greater than that occurring in *H. bilobata*, possibly due to a greater length of time spent in this growth stage. In the holaspid stage of *Xystridura*, there is very little further decrease and, in fact, there is some increase in cranidial width in large individuals. However, a decrease in cranidial width continues in *H. bilobata* holaspids. Measurements on *H. bilobata*(?) cranidia from New South Wales show a reversal of the trend (Fig. 3.3), suggesting that at larger sizes than those present in the Emu Bay Shale, the cranidial width may increase with

increasing size.

The anterior facial sutures diverge at about 100° in *Xystridura* meraspids of less than 1 mm cranidial length, reaching some 150° in instars of 4 mm cranidial length (McNamara 1981). In *H. bilobata*, small instars have anterior facial sutures which diverge at approximately 95°, but by an instar cranidial length of 4 mm, the angle of divergence is only 120°. The change in the angle of divergence for both genera appears to be the result of the inward migration of the junction of the anterior facial suture and the eye lobe. The larger angle of divergence in *Xystridura* is possibly the result of a longer period of time spent in this growth stage.

In small meraspids of *Xystridura*, the eye lobes extend almost tangentially from the posterior of 3L to the junction with the anterior facial suture, before curving gently back and becoming increasingly recurved towards the posterior (McNamara 1981). With growth, the length of the tangential portion of the eye lobe (the portion between the axial furrow and the junction with the anterior facial suture) decreases, apparently due to the migration inwards of the junction of the eye lobe and the anterior facial suture. The posterior tip of the eye lobe becomes increasingly recurved, with the distance between it and the axial furrow decreasing from 0.59 of cranidial length in instars of 1 mm cranidial length, to 0.32 in instars of 2 mm cranidial length (McNamara 1981). This reduction continues until in instars of 4 mm cranidial length the distance is only 0.20 of cranidial length. After this, in holaspid growth, the distance remains static with a slight increase in distance with growth (Fig. 3.9). The posterior tip of the eye lobe reaches the posterior furrow of the cranidium in instars of 1 mm cranidial length.

Such an ontogenetic pattern can be seen in *H. bilobata*, where in instars of 1 mm cranidial length the distance between the posterior tip of the eye lobe and the axial furrow is 0.49 cranidial length and is reduced to 0.28-0.25 cranidial length in instars of 2 mm cranidial length (Fig. 3.9). The distance then remains static at approximately 0.25 cranidial length during holaspid growth. The overall ontogeny of the eye lobe in *H. bilobata* is repeated almost exactly by *X. templetonensis*, except that the growth pattern

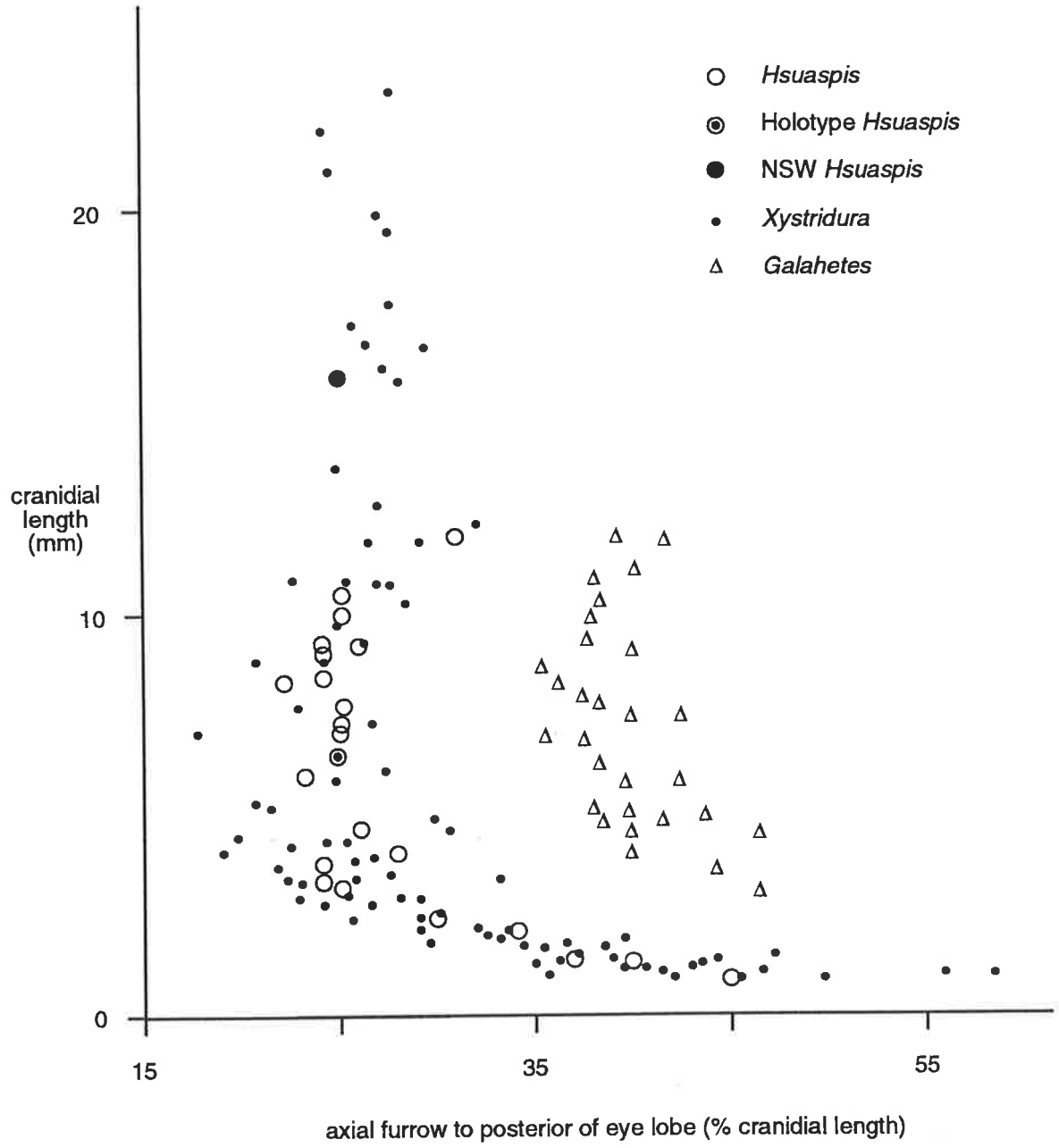


**Fig. 3.9** Plot of cranidial length against distance from axial furrow to posterior of eye lobe as a percentage of cranidial length for *Hsuaspis*, *Galahetes* and *Xystridura*. (Data on *Galahetes* and *Xystridura* from McNamara 1981, reproduced with permission of the Australiasian Association of Palaeontologists).

of *Xystridura* does not mirror that of *H. bilobata*, as expected if a simple heterochronic relationship is present. The wholesale shift exhibited by the plot of *G. fulcrosus* (Fig. 3.9) can be explained by precocious maturation which inhibited the trend occurring in the meraspid period (McNamara 1981). This resulted in the onset of the holaspid growth pattern while the eye lobe to axial furrow distance was still quite large. Thus the juvenile characteristic of a large eye lobe to axial furrow distance is retained in the descendent adult.

To understand why the trends of relative cranidial width and relative distance from the posterior of the eye lobe to the axial furrow in *X. templetonensis* do not conform to that expected by simple heterochronic development from *H. bilobata*, it is necessary to look at other morphological developments on the cranidium and observe their effects in order to ascertain whether these changes may have influenced these trends. The other major morphological character which may have effected cranidial width and eye lobe development, is the development of the glabella.

The most obvious and striking characteristic exhibited by the ontogeny of *X. templetonensis* is the retraction and subsequent protraction of 3L. This morphological development resulted in the increase and then loss of the preglabella field as 3L approached and finally contacted the anterior border of the cranidium (Fig. 3.10). In *H. bilobata* the length of the preglabellar field increases rapidly during meraspid growth, from 0.05 relative to cranidial length in meraspis 1, to 0.14 in meraspis 12 (Fig. 3.5), due to the retraction of 3L. The retraction of 3L then stops abruptly at the beginning of the holaspid period, in cranidia of about 2.5 mm. The holaspid period marks a change in development, resulting in the slow protraction of 3L. This appears to continue throughout the lifetime of the individual, resulting in very large forms having a correspondingly shorter preglabellar field (e.g. Pl. 7.6), a holaspid with a cranidial length of 10.6 mm and a preglabellar field of 0.09 cranidial length).

This meraspid growth pattern also occurs and is exaggerated in *X. templetonensis* (Fig. 3.10). Here, from a preglabellar field of <0.05 cranidial length in meraspids of >1 mm

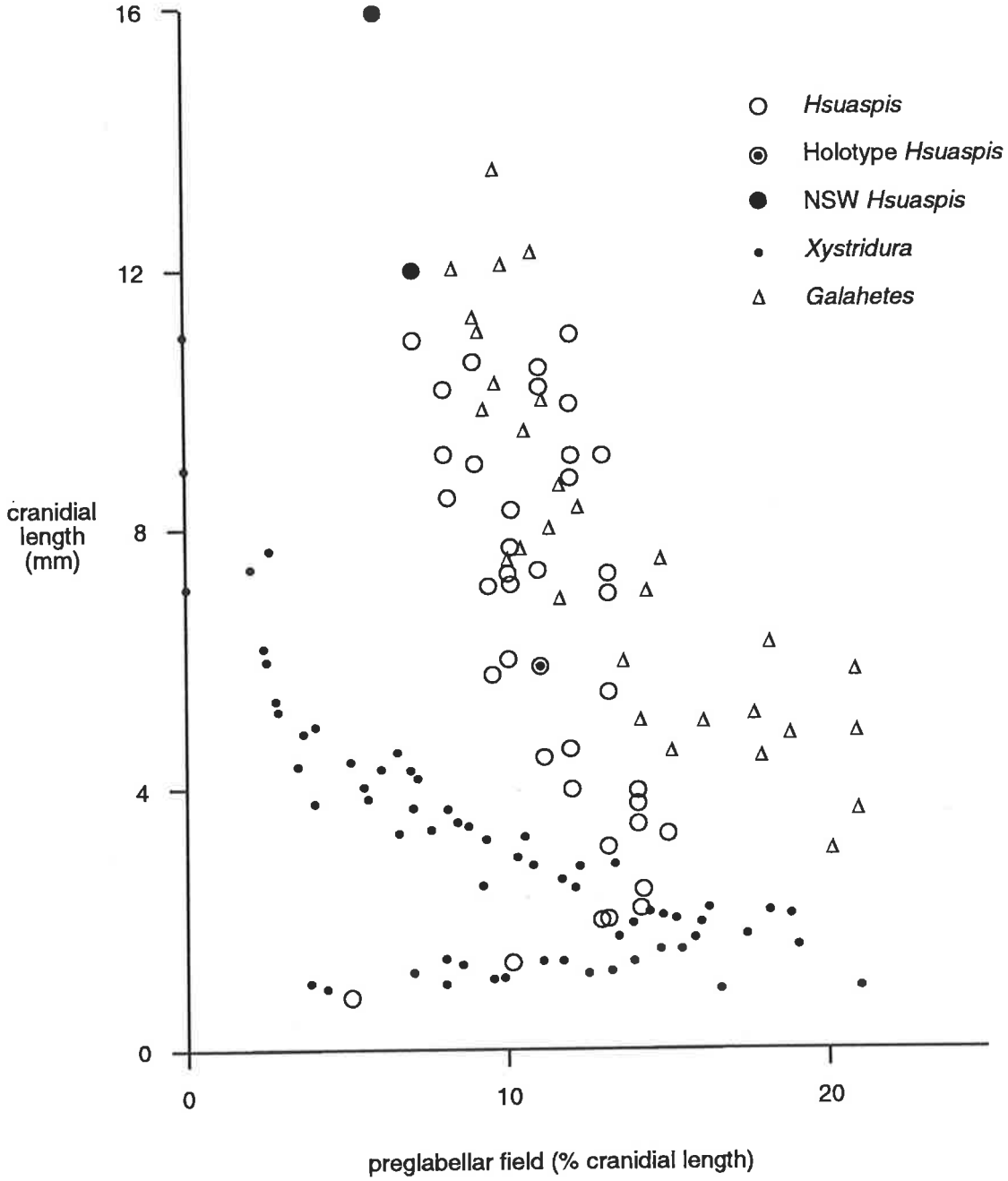


**Fig. 3.10** Plot of preglabellar field as a percentage of cranidial length for *Hsuaspis*, *Galahetes* and *Xystridura*. (Data on *Galahetes* and *Xystridura* from McNamara 1981, reproduced with permission of the Australiasian Association of Palaeontologists).

cranidial length, the preglabellar field increases due to glabellar retraction, to 0.20 cranidial length in instars of 2 mm cranidial length. Subsequently, glabellar protraction begins. Since this occurs within the meraspid growth stage, the protraction of the glabellar is accentuated, resulting in a much smaller preglabellar field of approximately 0.05 cranidial length by the onset of holaspid growth.

Thus, the late meraspid stage of *X. templetonensis* includes a phase of rapid glabellar protraction. The holaspid growth pattern is identical to *H. bilobata* and represents a much more gradual rate of glabella protraction. As an extended protraction phase occurs in the late meraspid stage, the holaspid growth period begins with the anterior lobe very close to the anterior border of the cranidium. This results, even at the slow rate of protraction exhibited in holaspid growth, in the eventual loss of the preglabellar field at a cranidial length of 8 mm. With the onset of the holaspid period delayed until individuals attained a cranidial length of approximately 5 mm in *X. templetonensis* (compared with 2.5 mm in *H. bilobata*), the beginning of the protraction trend appears to have been incorporated into the faster growing meraspid period, resulting in the exaggerated development of 3L. The delayed offset of the meraspid growth pattern is indicative of hypermorphosis (McKinney & McNamara 1991).

The extent of glabellar protraction can be seen in the measurements of 3L. In meraspids of > 1 mm cranidial length, the relative size of the glabella is the same in *H. bilobata* and *Xystridura*, both in length (approximately 0.18 cranidial length) and width (approximately 0.37 cranidial width). However, while the length of 3L decreases in *H. bilobata* until at an instar size of 3.5 mm cranidial length, 3L is only 0.14 cranidial length; in *Xystridura* the length of 3L is 0.55 cranidial length in instars of 4 mm cranidial length. In the largest instars measured from the Emu Bay Shale the length of 3L reached a maximum size of 0.20 cranidial length. The rapid increase in the size of 3L in *Xystridura* is due to the delayed offset of the late meraspid growth pattern, resulting in rapid protrusion of the glabella. A similar situation is highlighted in measurements of the width of the anterior lobe. In *H. bilobata*, the width increases very slowly from approximately 0.37 cranidial length in the smallest instars to 0.38 by the start of the

holaspid stage, reaching a maximum 0.42 cranidial length in the largest instars from the Emu Bay Shale. *Xystridura* however, shows a rapid increase in 3L width to 0.55 cranidial length by instars of 4 mm cranidial length. Again this increase is due to the delayed offset of the meraspid growth pattern, resulting in a greater length of time spent in the rapid-growth meraspid state and a consequently larger expansion of the gabella. During holaspid growth this trend continued, if very slowly until instars of 20 mm cranidial length have anterior lobes of approximately 0.60 cranidial length (McNamara 1981).

The differences in ontogenetic development between *H. bilobata* and *X. templetonensis* with regard to the cranidial width and the distance between the posterior eye lobe and the axial furrow, can now be explained in terms of the protraction and expansion of 3L. The increase in the size of the glabella, although mainly of 3L, has also slightly increased the overall width of the glabella. This appears to have translated into a slight increase in the overall width of the cranidium relative to *H. bilobata*. The result is that, unlike *H. bilobata*, the width of the cranidium in *X. templetonensis* does not decrease with holaspid growth, but shows a slight increase (Fig. 3.8). Similarly, the distance from the posterior of the eye lobe to the axial furrow in *X. templetonensis* also exhibits this slight increase in size with growth, unlike *H. bilobata* (Fig. 3.9). Thus the re-orientation of these morphological trends are due to the accommodation of a larger glabella within the cranidium.

Protrusion of the glabella is not uncommon in Cambrian trilobites. McNamara (1986b) documented peramorphic expansion of the glabella in the Redlichiidae, in the Olenellidae and in *Irvingella*. The process probably led to the increase in size and/or complexity of the stomach and may have allowed access to previously restricted niches. This may have resulted in niche and resource partitioning between ancestor and descendant, allowing rapid colonisation of previously underutilised microenvironments.

Another trait of *H. bilobata* which can be compared with *Xystridura* is the presence and

ontogeny of spines.

Metafixigenal spines are absent in the meraspid period of *Hsuaspis*. However, they are known in a *Xystridura* meraspis degree 0 (Öpik 1975a text fig. 5). Also, a *Xystridura templetonensis* cranidium of length 3.2 mm, possibly meraspis degree 10 - 12, figured by Öpik (1975a, table 1, no. 8; pl. 20, fig. 10) possess metafixigenal spines. So it would seem that they are retained by the developing *Xystridura* meraspid.

The ontogeny of genal spines in *Xystridura* appears little understood except that this spine shortens during the early life of the animal (McNamara 1981) and the holaspid form possesses short, stout, broad based genal spines as in *H. bilobata*. However, more is known of the ontogeny of pleural spines in the meraspid stage of both forms.

In *H. bilobata*, elongate pleural spines occur on the first and second segment of the meraspid up to meraspis 7. Meraspis 8 appears to loose the pleural spines on the first thoracic segment and subsequent meraspids retain the pleural spines on the second thoracic segment, although the spines become reduced with each succeeding stage, until in the holaspid, the pleural spines are no bigger than those on other thoracic segments. Öpik (1975a, p 21, pl 20, fig. 4) recorded an inferred meraspis degree 2 (CPC 10360) in which both thoracic segments bore long pleural spines. A meraspis degree 7 of *Xystridura saintsmithi* figured by Whitehouse (1939, pl. 21, fig. 16) indicates that xystridurid meraspids had lost the elongate pleural spines on the first thoracic segment by this stage of development, in comparison to *Hsuaspis*, which at the same meraspid stage (Pl. 7.2) still retained both sets of thoracic pleural spines. Since the *Xystridura* meraspid is much bigger than the *Hsuaspis* meraspid of equivalent degree (2.3 mm cranidial length compared with 1.3 mm), the loss of pleural spines may be allied to size, since most ontogenetic events are size specific (Werner & Gillium 1984, McKinney & McNamara 1991).

The form from the Cymbric Vale Formation does appear referable to *H. bilobata*. Although only four individuals were measured, the cranidial measurements of the smaller individuals were indistinguishable from specimens of *H. bilobata* from the Emu Bay Shale. The differences noted by Jenkins (1990) and Jell (1990) can be explained as

being the result of an extension of late ontogenetic growth patterns. It may be that this form represents the beginning of a change from holotypical *H. bilobata* towards *Xystridura*. The forms from the Cymbric Vale Formation suggest that this transition was underway by the late Early Cambrian, continued during the eustatic sea level fall marking the Early-Middle Cambrian boundary (e.g. Hallam 1984), and was completed by the end of the marine transgression which initiated Middle Cambrian deposition. *Xystridura* is common in the early Middle Cambrian of New South Wales, Queensland and the Northern Territory (Öpik 1975a), however *H. bilobata* is absent. The environment conducive to *H. bilobata* and presumable *Xystridura*, soon disappeared from southern South Australia, with the advent of a long lasting episode of moderate to high energy, shallow water, siliciclastic sedimentation (Moore 1979). Daily (1963) identified *Xystridura* from the early Middle Cambrian Kalladeina Formation, in the Warburton Basin, South Australian, which unconformably overlies the late Lower Cambrian Mooracoochie Volcanics (Gatehouse 1983, 1986). The latter are probable lateral equivalents of the late Lower Cambrian Mount Wright Volcanics in northwestern New South Wales (Gatehouse 1983). The Mount Wright Volcanics underlie the Cymbric Vale Formation, from which *H. bilobata* has been reported (Öpik 1975b).

During the ontogeny of *X. templetonensis*, the onset of maturity has been delayed relative to *H. bilobata*, allowing for the an increased period of time in the meraspid rapid growth stage. This has resulted in a general size increase relative to *H. bilobata*. This delay has also allowed certain ancestral holaspid morphological characteristics to become developed within the descendant meraspid period, thus exaggerating them and resulting in morphological differences between the ancestral and descendant adults. *X. templetonensis* may therefore have evolved from *H. bilobata* via the peramorphic process of hypermorphosis.

The identification of *H. bilobata* by Öpik (1975b) challenged by Jenkins (1990) and Jell (1990) may be based on forms showing the first stages of the developmental changes between *H. bilobata* and *Xystridura*. However, the changes are by and large still

confined to trends delineated by *H. bilobata* and thus represents an extension of allometric growth. At this time it is impossible to tell whether the Cymbric Vale forms represent the onset of hypermorphosis, and thus a new species, or merely large individuals of *H. bilobata*. Therefore, Öpik's identification is retained.

3.3.1.3 *Naraoia*(Pls.4.3, 8)

*Naraoia* (Pl. 4.3) was first described from the Burgess Shale by Walcott (1912) and has since been documented from the late Early and Middle Cambrian of North America (Whittington 1977; Collins *et al.* 1983; Robison 1984; Collins 1987; Conway Morris & Robison 1988), and from the Lower Cambrian Chiungchussu Formation from Yunnan, China (Zhang & Hou 1985). Thus *Naraoia* has the greatest known stratigraphic range of any Cambrian trilobite genus (Conway Morris 1989b). The finding of the genus in Australia confirms its widespread geographic range. Its apparent rarity is probably an artifact of possessing a poorly- or unmineralised exoskeleton.

In a comprehensive review, Whittington (1977) reaffirmed Walcott's placement of *Naraoia* within the Trilobita, despite the occurrence of some unusual characters, including the presence of only two uncalcified tagmata divided by a single transverse articulation. Approximately 20-25% of the specimens used in that review possessed short postero-lateral spines on the anterior shield, a characteristic suggested as evidence of dimorphism. These spines were also found on some specimens from the possibly late Early(?) Cambrian Gibson Jack Formation in Idaho (Robison 1984). The three specimens from the Big Gully assemblage do not appear to possess these spines.

*Naraoia* sp. 1 (Pl. 8.1-2) appears compacted dorso-ventrally, with the horizontal plane of the body parallel to bedding. The occurrence of the ?hypostome and ?antennae indentations on the anterior shield indicate that this is the ventral aspect, compared with the smooth area of the anterior shield in the counterpart, which must represent a view of the dorsal surface. The specimen is therefore, in life orientation. It appears that the point of attachment for the ?antennae coincides with the antero-lateral margin of the

# Plate 8

**8.1** *Naraoia* sp. 1 (AUGD1046-622). Specimen poorly preserved as carbonate film. deformation of anterior shield suggests external covering was extremely thin. Trace of antennae on anterior shield. Inprint of appendages on posterior shield. Doublure apparent. (x4.5)

**8.2** Composite camera lucida drawing of AUGD1046-622, from part and fragmentary counterpart. Antennae apparently emerge from the anterio-lateral margin of the hypostome

**8.3** *Naraoia* sp. 2 (AUGD1046-575), preserved as a carbonate film. Deformation of anterior and posterior shields suggests that the external covering was extremely thin. Trace of anterior shield appendages present. Large doublure apparent. (x3.8)

**8.4** Composite camera lucida drawing of AUGD1046-575

# PLATE 8

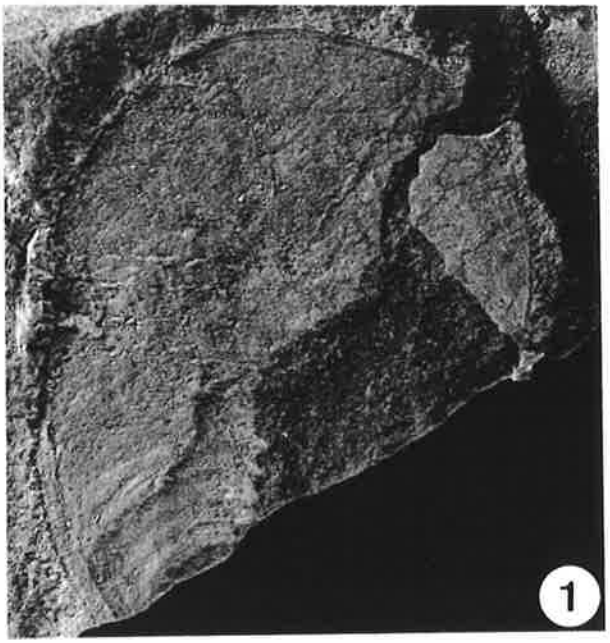


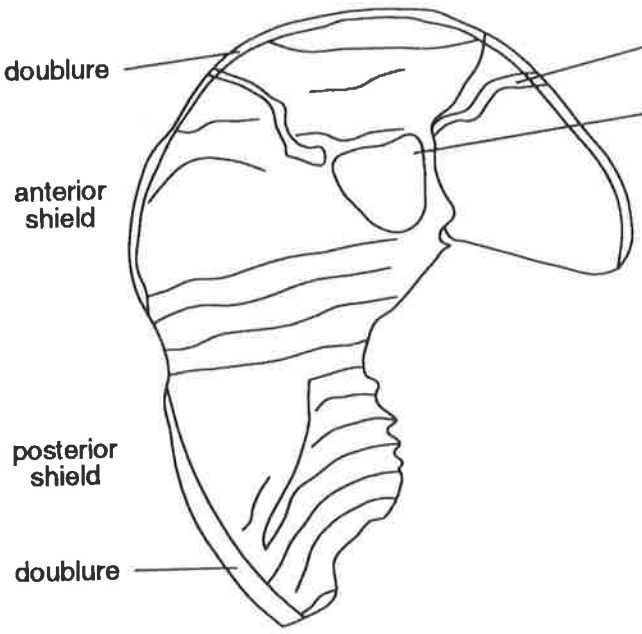


2

5 mm

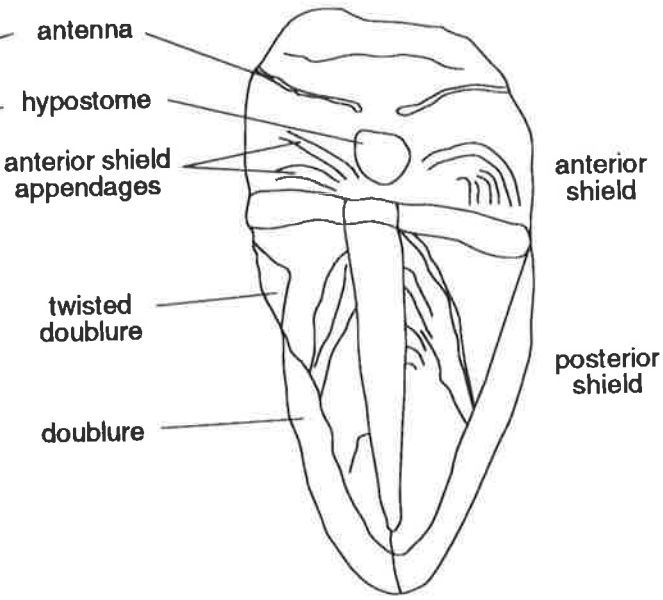


4

5 mm

?hypostome, unlike the situation in *N. compacta*, in which the attachment points were described as being both anterior and exsagittal of the hypostome (Whittington 1977, fig. 96). The total number of appendages in this specimen is unknown, but a total of between 17 -19 biramous appendages posterior of the antennae has been reported in specimens from elsewhere (Whittington 1977, Robison 1984) and so a similar number does not seem unreasonable for this specimen. The presence of oblique or curving furrows on the lateral part of the posterior shield was taken by Whittington (1977) to represent the compression of appendages against the shield and not a primary trait. The presence of similarly curved furrows on part of the lateral part of the posterior shield may represent the imprint of some appendages. Thus the specimen appears to represent the whole organism and not a moult. The decay of the soft tissues may well have provided a suitable micro-environment to enhance preservation in this instance (see section 5.3.2) Measurements are difficult due to the poor preservation, but, those which were possible, indicate a close similarity between *Naraoia* Sp. 1 and other species, but highlight the differences between *Naraoia* Sp. 2 and all other forms (Table 3.3). *Naraoia* sp. 2 (Pl. 8.3-4) exhibits a strikingly broad doublure on the posterior shield. Also the axial region appears much more convex and narrower, at approximately one quarter of the width of the posterior shield at its widest point. The ratios given in Table 3.3 for this specimen

**Table 3.3**. Measurements of *Naraoia* from Idaho, Utah and the Emu Bay Shale. Idaho and Utah measurements from Robison (1984). (Measurements in millimetres, estimated measurements due to incomplete specimens in parentheses)

| Measurement | Idaho | Utah | Sp. 1 | Sp. 2 |
|---|---|---|---|---|
| Full Length | 19.3 | 26.5 | (19.5) | 18.5 |
| Ant. Shield Length | 9.5 | (13) | (8.5) | 6 |
| Ant. Shield Width | 11.3 | 16.6 | 13.5 | 9.5 |
| Post. Shield Length | 11.1 | (15) | (12.5) | 12.5 |
| Post. Shield Width | 10.8 | 14.3 | 12 | 9.5 |
| Ant. len./total length | 0.49 | 0.49 | 0.43 | 0.32 |
| Post. len/total length | 0.58 | 0.57 | 0.64 | 0.68 |
| total width/total length | 0.59 | 0.63 | 0.69 | 0.51 |

appear significantly different to those from the others to warrant it's separation from *Naraoia* sp.1, into a separate species.

### 3.3.2 Arachnomorphs

3.3.2.1 *Xandarella* sp.(Pls. 4.4, 9)

*Xandarella* has been described from the Chengjiang fauna of southern China (Hou *et al.* 1991) and this represents the first occurrence of the genus in Australia. Only one specimen was recovered, and it is poorly preserved, making detailed description difficult. Eyes are dorso-lateral as in *X. spectaculum*, and not on the lateral margin of the cephalon as in some species (G. D. Edgecombe, pers. comm. 1994). (?)Antennae possibly present (Pl. 9), diverging widely after originating just antero-laterally from small (?)hypostome. Apart from the possible presence of eyes, the cephalon appears smooth, even lacking the sutures present in *X. spectaculum*, although this might be a preservational artifact. Three possible cephalic appendages are preserved, but total number unknown; five were reported in *X. spectaculum*. Hou *et al.* (1991) noted an isolated, small axial shield between the cephalon and the 'thorax', but poor preservation precluded identification of this plate in *X.* sp. The 'thorax' consists of seven apparently unfused, imbricate tergites. The lateral margin of each is recurved posteriorly and ends in a broad-based spine. The third tergite is apparently the widest exsagittally and the 'thorax' tapers posteriorly from it, unlike *X. spectaculum* in which the 'thorax' tapers from the first segment. Three 'abdominal' tergites are preserved, but the posterior on the specimen is too poorly preserved to tell the exact number (four in *X. spectaculum*) or whether a telson is present as in *X. spectaculum*. The number of appendage pairs per 'abdominal' tergite is difficult to resolve, but the first tergite appears to have two pairs, assuming an apparent subdivision of the axial area is significant and the second tergite appears to have three appendage pairs. This increase in the number of appendage pairs has also been noted in *X. spectaculum*, and is a characteristic of the genera The number

# Plate 9

**9.1** *Xandarella* sp. (AUGD1046-320). Poorly preserved as an iron oxide encrusted carbonate film. (x2)

**9.2** Camera lucida drawing of specimen AUGD1046-320, composed from part and fragmentary counterpart. (Note. apparent thoracic appendages are too poorly preserved to be identified.)

# PLATE 9


1

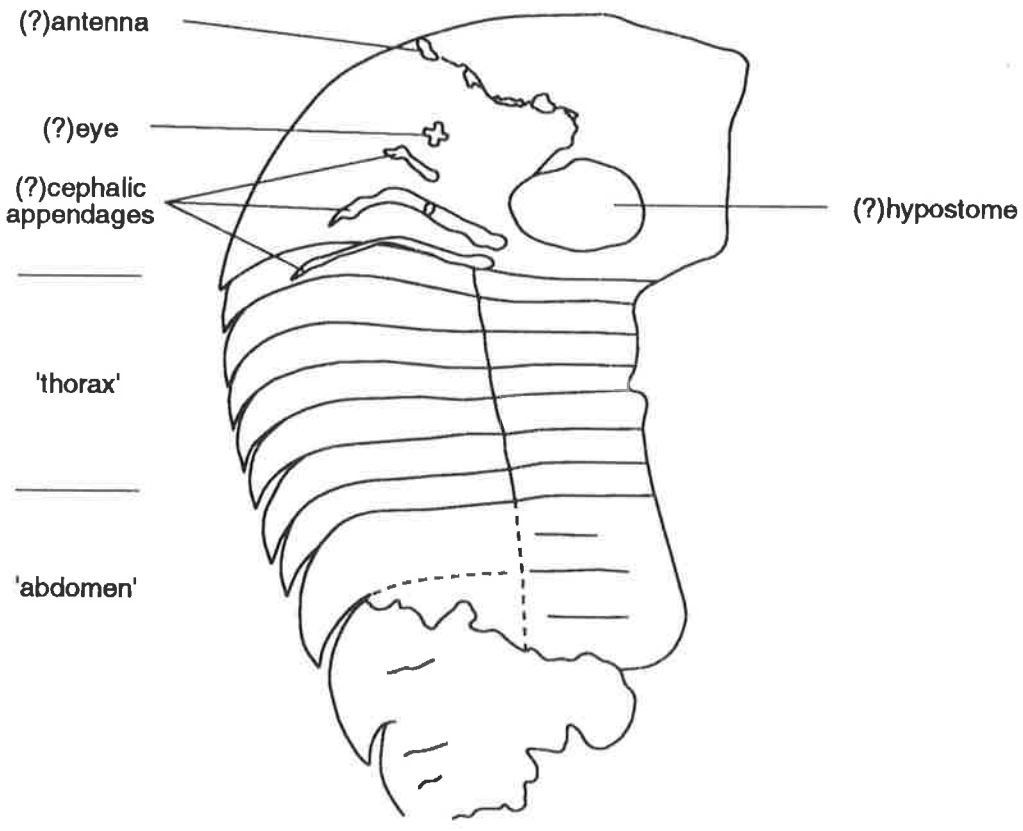
(?)antenna
(?)eye
(?)cephalic appendages
(?)hypostome
'thorax'
'abdomen'

2

5 mm

of 'abdominal' pairs in subsequent tergites cannot be resolved.

It is apparent that *X.* sp. possessed a very poorly mineralised exoskeleton, composed of free, imbricate tergites.

The maximum length to maximum width ratio of 1.2 for *X.* sp. indicates that its overall shape (Fig. 3.11) appears more equant than *X. spectaculum*, which has a maximum length to maximum width ratio of 1.6. The maximum length to maximum width ratio of the cephalon of *X.* sp., at 0.35, indicates that the cephalon is wider than that of *X. spectaculum*, which has a ratio of 0.54.

Hou *et al.* (1991) compared the thorax and abdomen of *Xandarella* with the Early Cambrian form *Kodymirus* and the Silurian xiphosurid *Pseudoniscus* respectively, although the fusion of the telson to the segment in front is a character of *Xandarella* apparently not shared with the xiphosurids. Xiphosaurids also lack antennae.

### 3.3.2 Phyllocarids

#### 3.3.2.1 *Isoxys communis*(Pls. 4.5, 10.1-2)

Rolfe (1969), Briggs (1976) and Glaessner (1979) suggested that *Isoxys* be placed in the Tuzoiidae. Robison & Richards (1981, p. 6) described the order, class and familial classification of *Isoxys* as "uncertain". Bengtson (1990, p. 325) noted the class, order and family assignations as "unassigned", an assignation utilised here.

The presence of eyes in *I. communis* (Pl. 10.1) is the first recorded occurrence. They appear large, globate and stalked, protruding between 2 - 5 mm from the antero-ventral margin. Their presence allows the true orientation of the organism to be known for the first time. In his description of *I. communis*, Glaessner (1979, fig. 1) orientated the organism with the anterior of the organism represented by the straight ventral margin. This appears to have been an error and the orientation of *I. communis* is here reversed so that the strongly convex ventral margin represents the anterior of the organism. This is the orientation used by Hou & Bergström (1991, pl. 2, fig. 4). Interestingly Glaessner

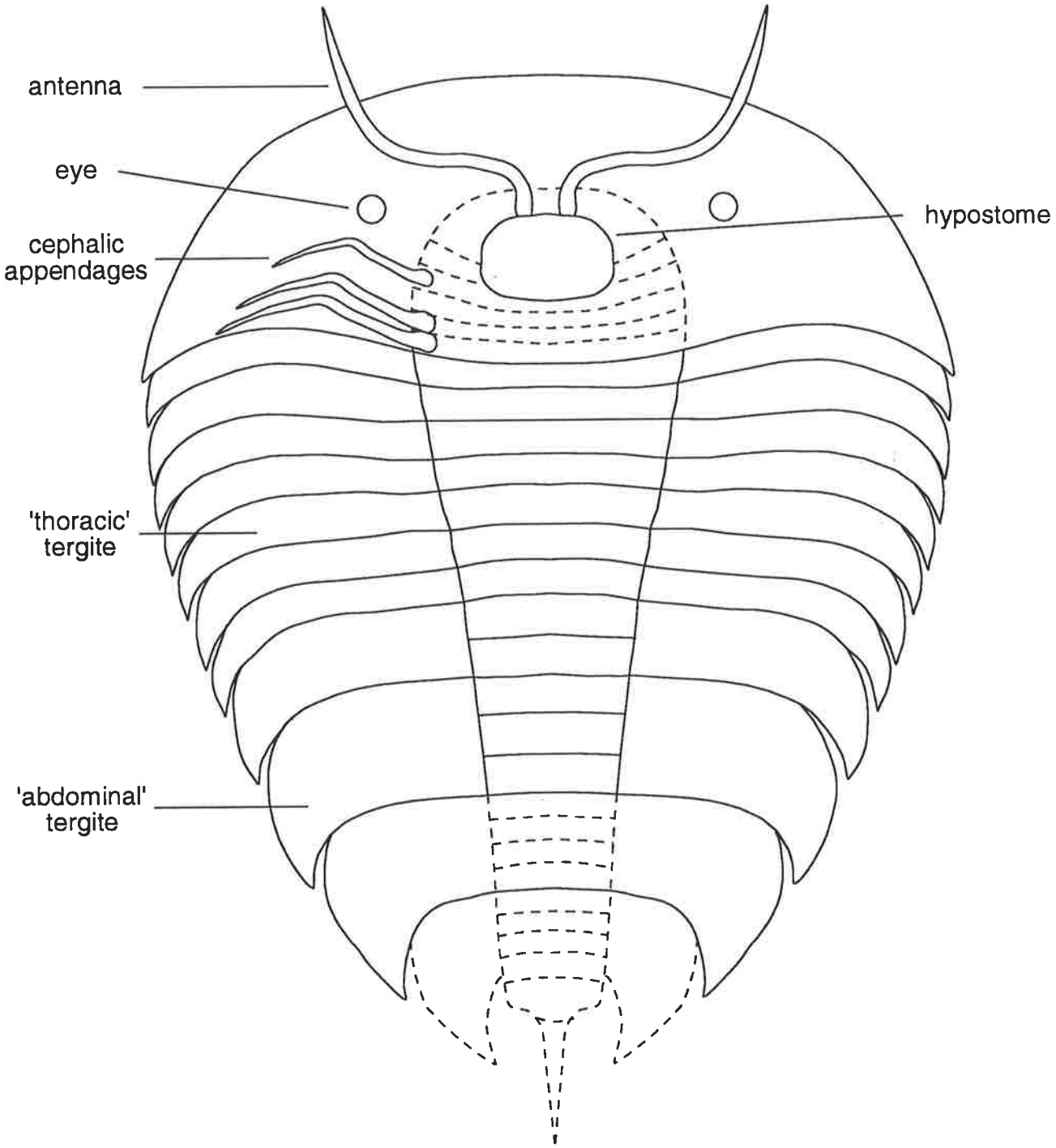


**Fig. 3.11** Reconstruction of the ventral veiw of *Xandarella* sp. using specimen 1046-320 from the Emu Bay Shale Lagerstätte. Dotted lines indicate tentative reconstruction based on *X. spectaculum* from the Chengjiang fauna of China

# Plate 10

**10.1** *Isoxys communis* (AUGD1046-710). Left lateral view with stalked eyes. A larger specimen lies diagonally underneath. (x2)

**10.2** *Isoxys communis* (AUGD1046-331). Right lateral view with possible stalked eyes. (x1.15)

**10.3** *Tuzoia australis* (AUGD1046-315). Disarticulated valves showing characteristic reticulate ornamentation. (x1.3)

**10.4** *Tuzoia australis* (AUGD1046-281). Dorsal view along hinge line, with both valves open. Note prominant ridge on valves 2/3 below the hinge. Characteristic reticulate ornamentation apparent. (x1.6)

**10.5** Coprolite (AUGD1046-613). Composed of *Redlichia takooensis* fragments, identifiable from their ornamentation and size. Large genal spine at right of coprolite. Note dark stain below particulate mass, possibly representing the fluid portion of the original fecal mass. (x0.65)

# PLATE 10

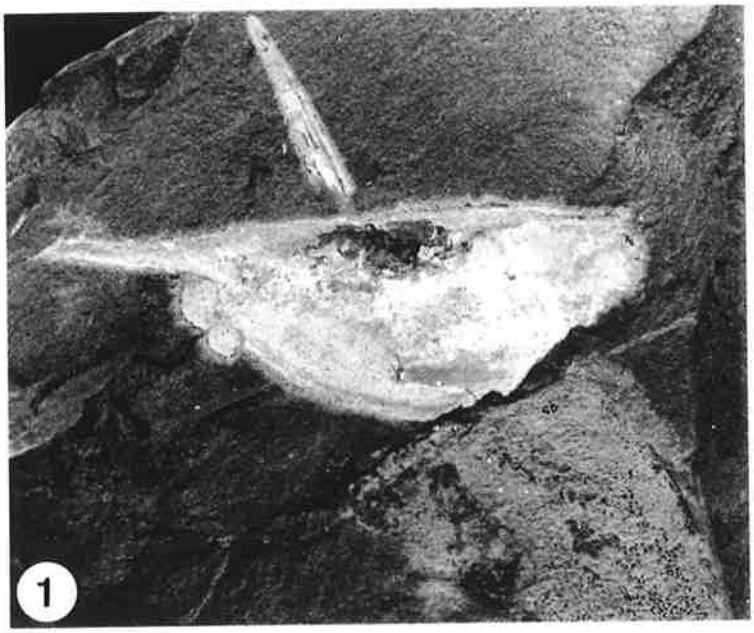




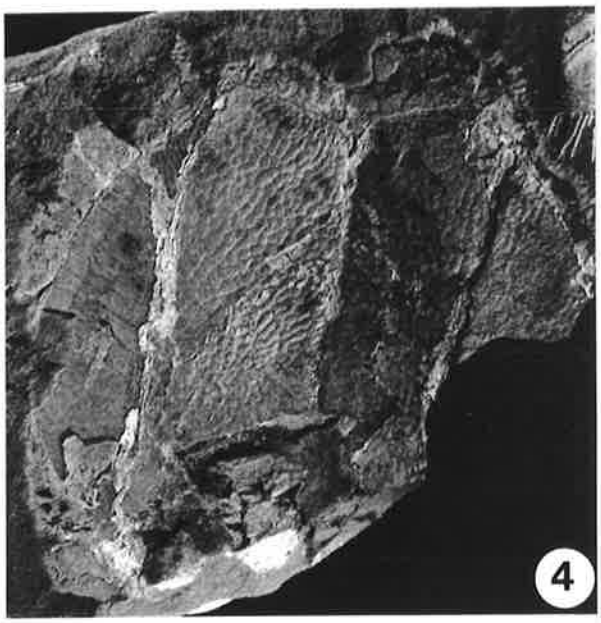


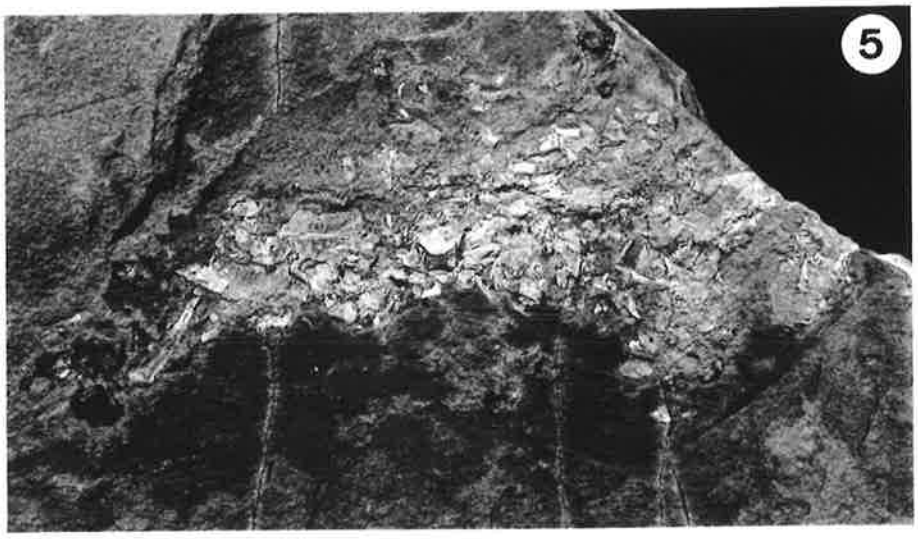

(1979, p. 23) noted that "several specimens show rounded areas of shell protruding from the posterior margin below the spine." These appear to have been poorly preserved eyes.

Specimens of *I. communis* appear to be unusually large (Pl. 10.2), much larger than those found in the Burgess Shale (D. H. Collins pers. comm 1993) and some four times the size of *I. longissimus* (Glaessner 1979).

The surface of the shell appears smooth (Pl. 4.5), and although replacement by calcite and recrystallisation has not preserved fine detail, there is little evidence of surface ornamentation.

3.3.3.2 *Tuzoia australis*; (Pls. 4.6, 10.3-4)

*Tuzoia* differs from most other large bivalved genera in possessing a conspicuous surface reticulation and having marginal spines.

A lateral ridge is found on most species of *Tuzoia* (Pl. 10.4) This ridge has been described as a preservational artifact (Briggs 1976, Glaessner 1979), or as a primary aspect (Rolfe 1969). Robison and Richards (1981) concluded that the ridge was primarily based on the difference in the reticulation on the ridge and the lack of evidence for differential deformation. In most species the ridge, where present, is positioned centrally. However in *T. australis* the ridge appears to be positioned slightly ventral of this position. Glaessner (1979) considered *T. australis* most similar to *T. manchuriensis* Resser & Endo from the Lower Cambrian of south China (P'an 1957) and the Middle Cambrian of northeastern China (Endo & Resser 1937).

### 3.3.4 Classification Uncertain

3.3.4.1 *Anomalocaris*

Anomalocaridids are a group of fossil animals which include *Anomalocaris* found in the

Burgess Shale and other Cambrian deposits in North America (e,g, Briggs & Mount 1982; Briggs & Robison 1984; Whittington & Briggs 1985), in the Lower Cambrian of Poland (Dzik & Lendzion 1988) in southern China (Hou & Bergström 1991) and in southern Australia (Nedin 1992). First found as isolated fragments attributed to a number of different groups, including crustaceans, jellyfish and holothurians, these fragments were later combined to form one of the largest Cambrian organisms known (Briggs 1979). Due to their large size and unusual combination of characters, the affinities of anomalocaridids remains unresolved. Briggs and Robison (1984) suggested a separate phylum for *Anomalocaris*, Chen et al. (1994) suggested affinities within the Arthropoda, Bergström (1986) and Dzik And Lendzion (1988) suggested that *Anomalocaris* represented a separate trend of arthropodization, and Hou *et al.* (1995) suggested an affinity with the aschelminths. Material from the Emu Bay Shale provides no new insights into this problem. The appendages, first thought to be the trunk of a crustacean (Whiteaves 1892), are usually found in isolation. The appendages of *A. briggsi* (Pls. 5.1, 11, 13; Fig. 3.12) are paired and indistinguishable from each other, as with other anomalocaridid species. Each appendage consists of 14 segments, tapering distally (Pl. 11), similar to the spinose forms *A. canadensis* (Fig. 3.13A) and *A.* cf. *pennsylvanica.* (Fig. 3.13B). Segment 1 bore two broad, dagger-like ventral blades, similar to *A.* cf. *pennsylvanica.* As with *A. canadensis* and *A.* cf. *pennsylvanica*, segments 2 to 13 each bore a pair of ventral spines. However, *A. briggsi* has a spine length to segment height ratio of >1, a characteristic shared with the blade-bearing forms *A. nathorsti* (Fig. 3.13C) and *Cassubia infercambriensis* (Fig. 3.13D). This is in contrast to the spinose forms *A. canadensis* and *A.* cf. *pennsylvanica* which have a ratio of ≤1. Each pair of ventral spines bore a pair of auxiliary spines similar to *A. canadensis* and *A.* cf. *pennsylvanica.* Each pair of ventral spines also bore a series of spinules possibly similar to *A. nathorsti*, but much more elongate (Pl. 13.1-2).

*A. briggsi* shares characteristics with both the spinose forms *A. canadensis* and *A.* cf. *pennsylvanica* and the blade bearing forms *A. nathorsti* and *C. infercambriensis* and appears to be intermediate between them.

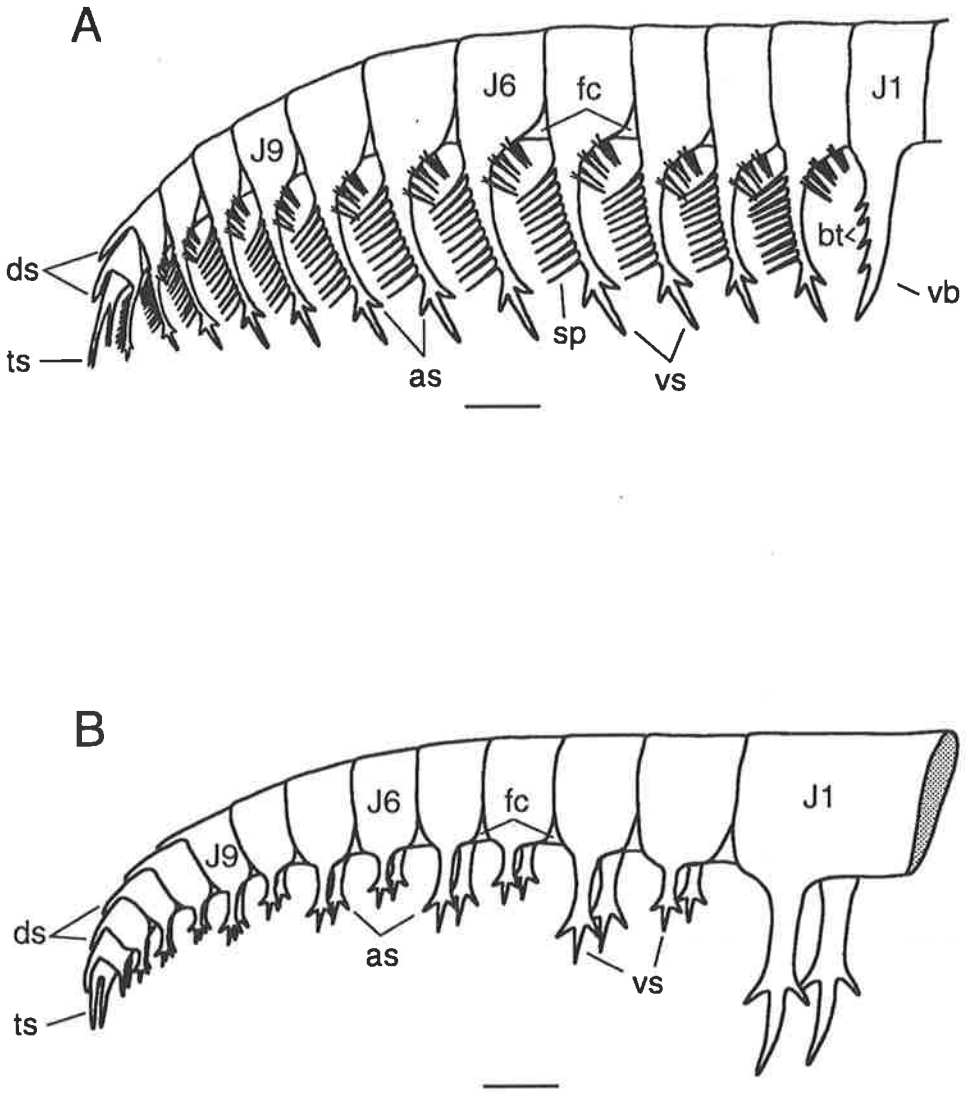


**Fig. 3.12** Reconstruction of anomalocaridids found in the Emu Bay Shale Lagerstätte. **A**. *Anomalocaris briggsi*. Note, for clarity only one ventral spine per segment is shown. **B**. *Anomalocaris* sp. Terminology based on Whittington and Briggs (1985). as, auxiliary spines; bt, blade teeth; d, dorsal spine; fc, flexible cuticle or arthrodial membrane; j, segment, numbered distally from assumed attachment with the body; sp, spinules; ts, terminal spine; vb, ventral blade; vs, ventral spine. Scale bar = 1 cm.

# Plate 11

**11.1** *Anomalocaris briggsi* (AUGD1046-630). Holotype. Entire appendage showing ventral spines and spinules. Note large spine on first segment bent backwards. (x0.9)

**11.2** Camera lucida drawing of AUGD1046-630. vs2, second ventral spine on segment. For key to other abbreviations see Fig. 3.12.

# PLATE 11

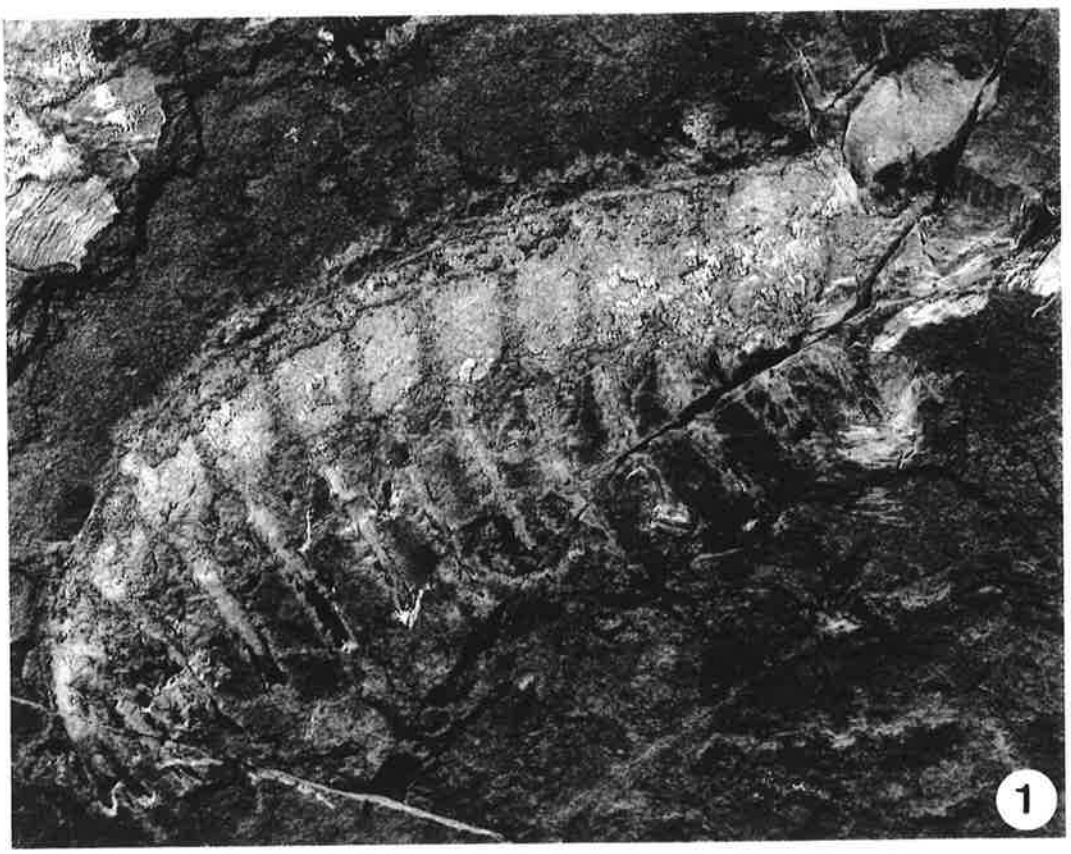

1

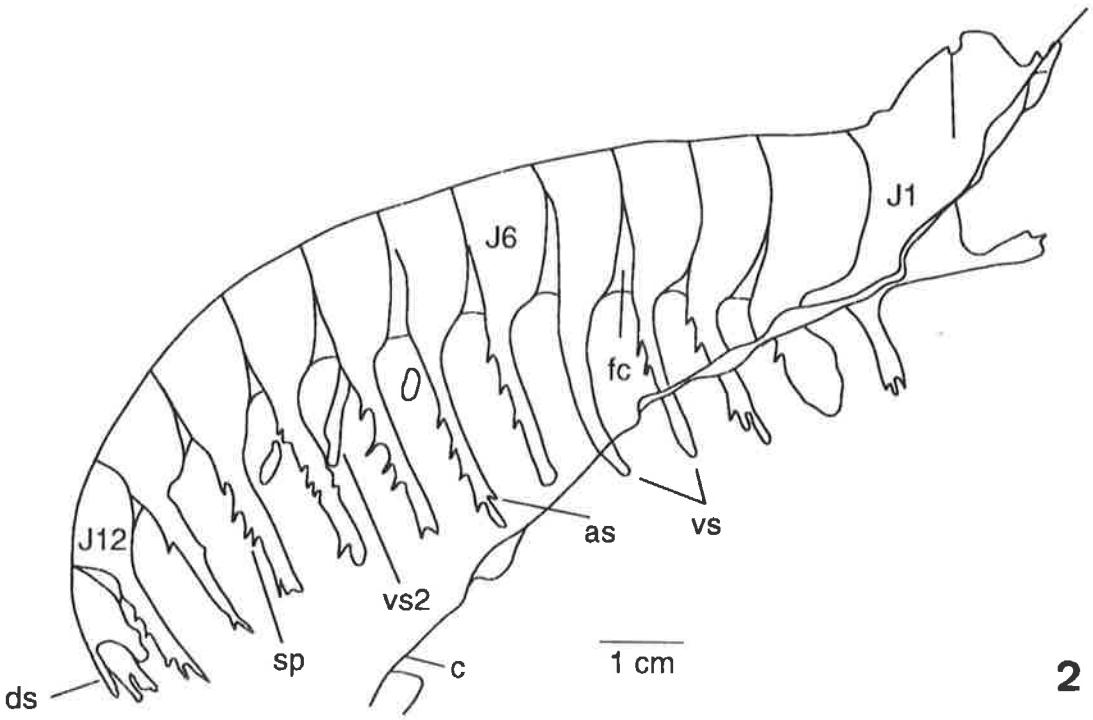


2

*Anomalocaris* sp. (Pls. 5.2; 12) bears a striking resemblance to *A. canadensis* and indeed the form found in the Chengjiang Lagerstätte was classified as such (Hou & Bergström 1991). However, *A. canadensis* does not possess an enlarged ventral spine on the first segment. Also, while the size of the ventral spines alternate in length on successive segments in both species, the longer spines are on the even segments in *A. canadensis* (Briggs 1979), while they are on the odd segments in *Anomalocaris* sp. The similar construction of the appendage in both species may well be due to convergence toward a similar niche rather than a direct relationship. This is supported by the fact that both the Asian species described here, plus another anomalocaridid from Chengjiang (Chen, *et al.* 1994) possess an enlarged ventral spine or blade on the first segment, structures apparently lacking in the North American species.

With the exception of the ventral blades, the appendages on *A. briggsi* appear too fragile to have been used in active raptorial hunting, as suggested by McHenry & Yates (1993), such as that envisaged for *A. canadensis* and *A.* cf. *pennsylvanica* by Briggs (1979) and possibly *Anomalocaris* sp. Instead they may have been used to probe for and trap, shallowly buried or surface dwelling, small invertebrates, and essentially formed the configuration of a net or basket. *A. briggsi* differs from the other members of the group in having the largest segments towards the middle of the appendage. Flexure of the limb around this segment, segment 6, may then have forced larger prey backwards on the dagger-like blades on segment 1, which were used to pierce or rupture the prey before ingestion. Such medial flexure would retain the two proximal ventral blades in an orientation conducive to rupturing prey. However, it is also possible that the appendages were adapted to catch smaller, more motile prey, the net-like form of the appendage acting more effectively to stop the lateral escape of such organisms. The blades might represent the proximal termination of the feeding apparatus, rather than an active tool for predation and may have thus been structurally constrained to accommodate the curled appendage (D.E.G. Briggs pers. comm. 1994). A fortuitous juxtaposition of the two appendages in one specimen (Pl. 13.4) shows distortion of the segments of one

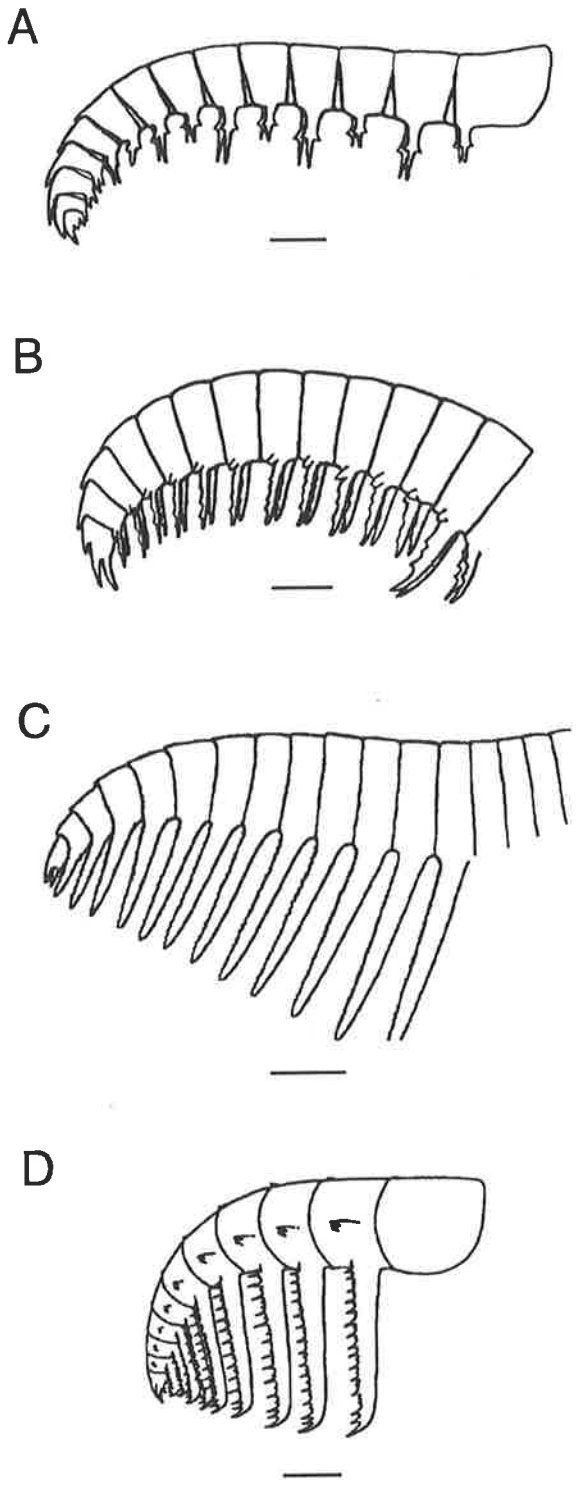


**Fig. 3.13** Appendages of known anomalocaridids. **A**. *A. canadensis* Whiteaves 1892. **B**. *A.* cf. *pennsylvanica* Resser 1929. **C**. *A. nathorsti* Walcott 1911. **D**. *Cassubia infercambriensis* Lendsion 1975. Reprinted from *The oldest arthropods of the East European platform* by Dzik and Lendzion, Lethaia, 1988, vol. 21, pp 29-38, by permission of Scandinavian University Press. Scale bar = 1 cm.

# Plate 12

**12.1** *Anomalocaris* sp. (AUGD1046-600). Tightly coiled, disarticulated appendages. Note large ventral spine on the first segment. Small *Palaeoscolex* fragment below appendage. (x2.3)

**12.2** Camera lucida of specimen AUGD1046-600, showing one (presumed left appendage) appendage and the large ventral spine on the first segment of the second appendage. as, auxillary spine; ds, dorsal spine; J, segment number; P, *Palaeoscolex*; 1rs, large ventral spine on first segment of inferred right appendage; 1s large ventral spine on the first segment of inferred left appendage; uas, auxilary spine on second ventral spine on first segment of inferred right appendage.

# PLATE 12


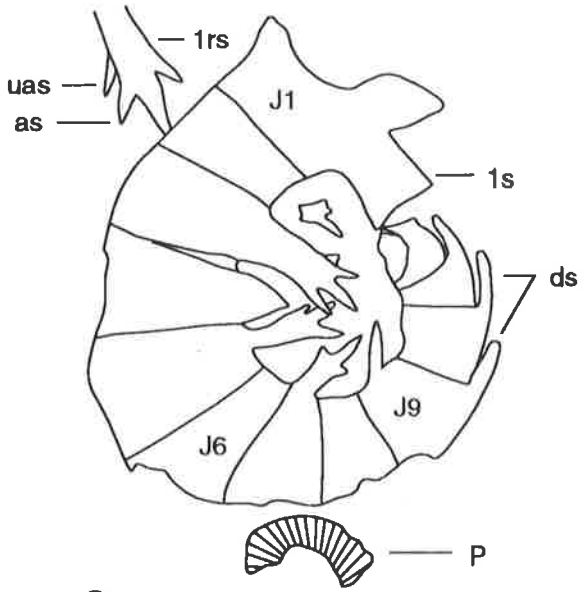

appendage as it overlies the ventral spines of the other. This indicates a degree of stiffness adequate to control struggling soft bodied prey. Given the interpretation that the mouth plates did not meet in the centre of the mouth (Whittington & Briggs, 1985), they probably acted in a durophagous role, assisting in the rupture of the carapace or cuticle of the prey. Ingestion was probably facilitated by peristaltic movements along the oesophagus as in *Limulus* (Manton 1977). The additional rows of teeth seen in the buccal cavity of other anomalocaridids may have assisted in food maceration (Whittington & Briggs, 1985). Unfortunately, no identifiable mouth parts have been found in the Big Gully assemblage, so that their exact configuration in *A. briggsi* remains unknown. A possible mouth apparatus documented by McHenry & Yates (1993) possesses transverse ribs and lacks a central opening. The similarity with anomalocaridid mouthparts appears, as they suggested, to be superficial.

The flexibility of the appendage in *Anomalocaris* sp. is graphically illustrated in Plates. 5.2 and 13. The flexure, while extreme due to the disarticulated nature of the specimen, probably does not greatly exceed that attainable in life. The overall size of the appendages indicates that the specimen was probably a juvenile, but larger than similar specimens reported from Chengjiang. A poorly preserved adult appendage length of 14 cm has been found, and the length of the organism is estimated to be approx. 60 cm (assuming allometric growth and an appendage to body ratio of 4.2 as calculated from Chen *et al.* 1994, fig. 2)

While *Anomalocaris* sp. appears to represent a new species, adding to the growing diversity of the group (e.g. Collins 1992), more complete specimens have been found from Chengjiang which would provide a more complete diagnosis. Thus no formal naming is attempted here.

### 3.3.3.2 *Myoscolex ateles*

The body of *Myoscolex* (Pl. 5.3, 14) is cigar-shaped, normally straight or very slightly curved. Rarely, specimens show pronounced curvature (e.g. Pl. 15.1) and this is

# Plate 13

**13.1** *Anomalocaris briggsi* (AUGD1046-340). Note spinules on proximal and distal margin of ventral spines. (x2.25)

**13.2** *Anomalocaris briggsi* (SAM P34554). Large appendage with spinules on ventral spines preserved as calcite or black fluorapatite. Note the 'halo' of bleached shale around the ventral spines. The presence of fluorapatite and the halo suggest that this represents an intact appendage and not a moult. (x1.5)

**13.3** *Anomalocaris briggsi* (SAM P31953). Two appendages, one lying on top of the other. Note the spinules on the upper proximal surface of the ventral spines at the upper left of the photograph. (x1.4)

**13.4** *Anomalocaris briggsi* (AUGD1046-638). Close up of the ventral spines showing auxiliary spines just above the end of the spine. (x3.5)

# PLATE 13

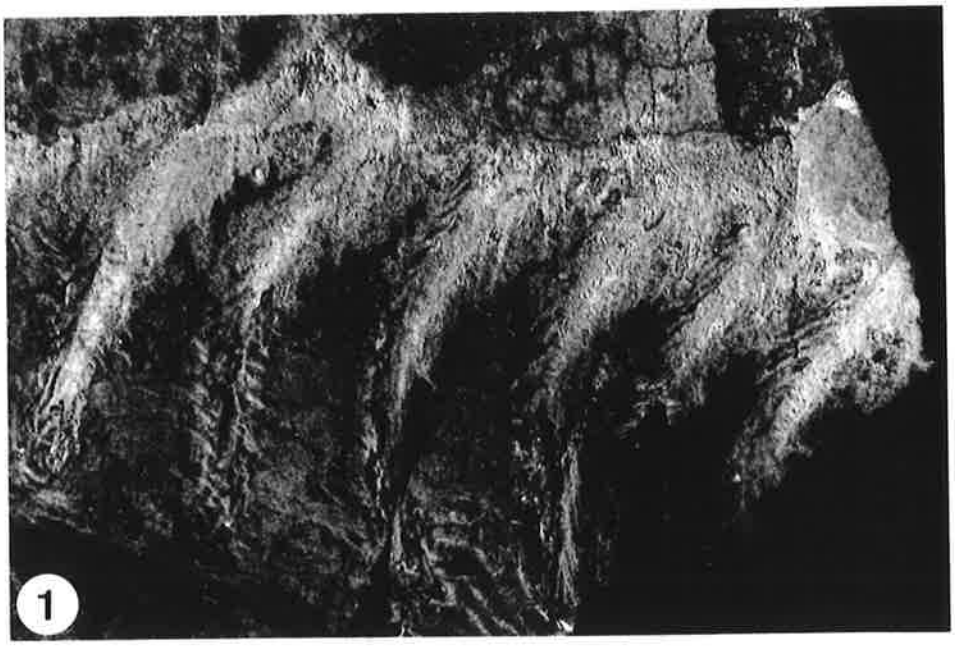


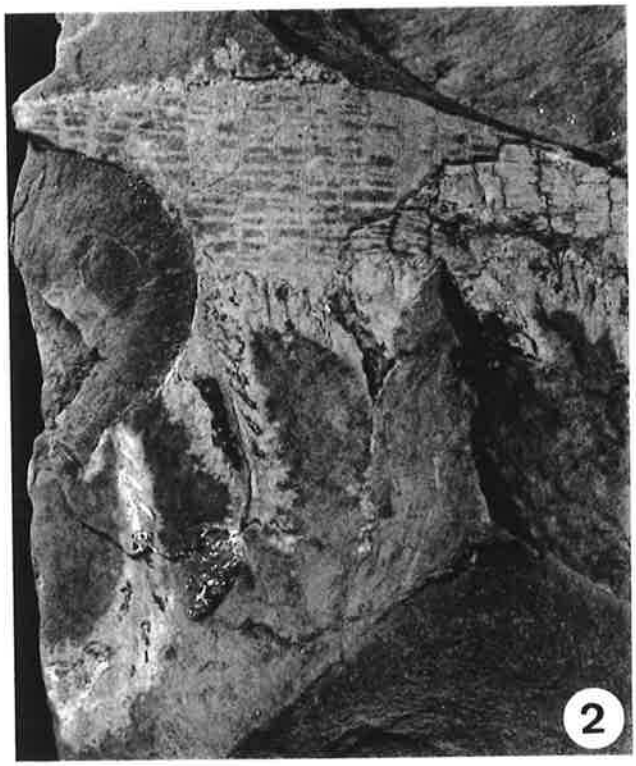


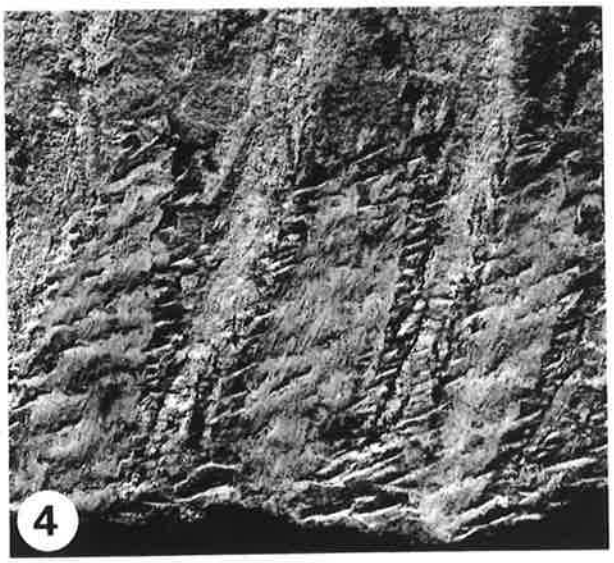


achieved by varying the length of the segments on opposite sides of the body. The number of segments is difficult to estimate due to the paucity of complete specimens, but the largest, with a preserved length of 104 mm, includes at least 35. Glaessner (1979) reported an incomplete juvenile only 25 mm long which includes 14 segments. As the animal becomes larger, so too does the number (Fig. 3.14) and length of the segments, which appear to be added to the trunk during growth. There are, however, sufficient

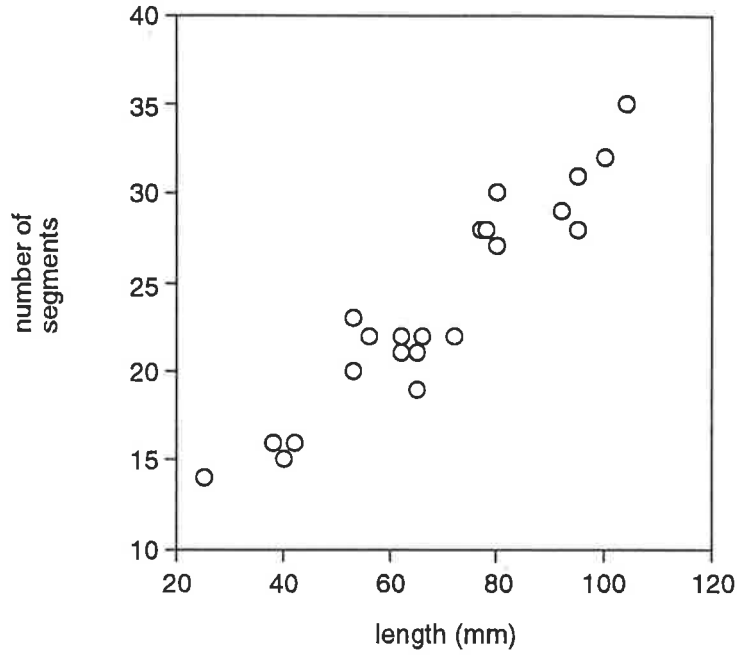


**Fig. 3.14** Plot of number of segments against overall length for *Myoscolex ateles* from the Emu Bay Shale Lagerstätte.

near complete specimens to show that the number of segments was variable, but it is not clear to what extent. The maximum height of *Myoscolex* lies well to the anterior of the mid-length. The trunk tapers very gradually posteriorly; the structure of the posterior region is essentially unknown. Anteriorly the trunk tapers much more abruptly to a narrow neck, beyond which projects the head. The body outline allows the anterior and posterior to be distinguished even where they are not preserved, as long as sufficient length of the trunk is present. There is no evidence that the body posterior of the head is divided into tagmata.

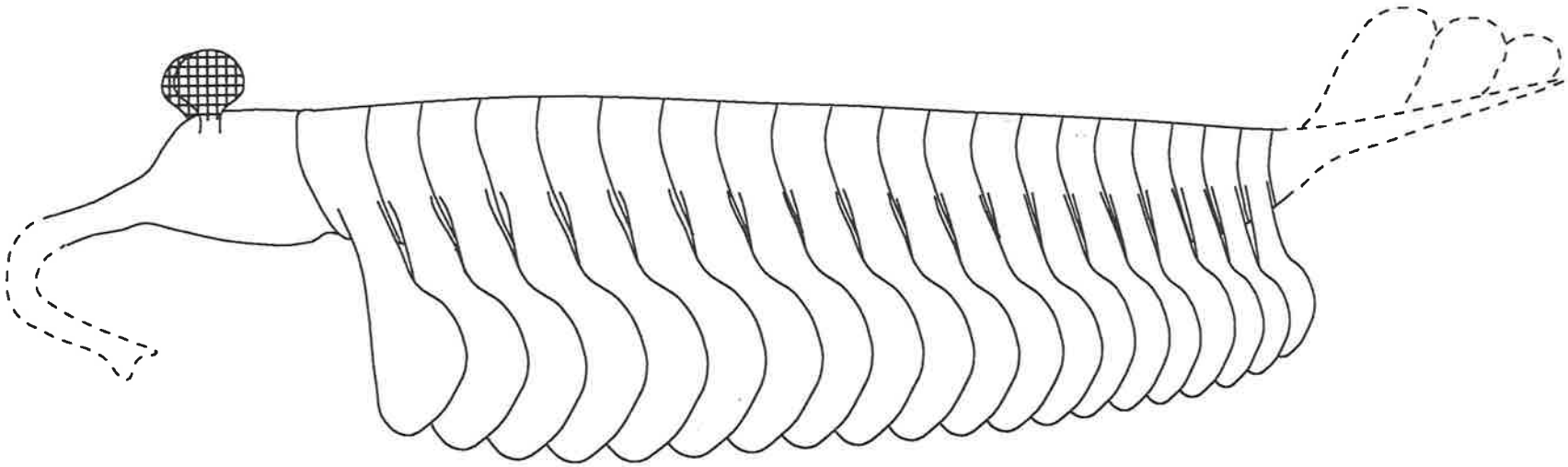

**Fig. 3.14** Reconstruction of *Myoscolex ateles* from the Emu Bay Shale Lagerstätte, left lateral view. Dotted area represents tentative reconstruction, based on *Opabinia* (Whittington 1975).

# Plate 14

**14.1** *Myoscolex ateles* (AUGD1046-239). View of posterior part of specimen showing preservation of muscle blocks and other soft tissue preservation, including ventral paddle-like appendages and part of the tail. Note appendages have been folded over and are thus reversed. (x1.5)

**14.2** Camera lucida drawing of AUGD1046-239.

# PLATE 14


1

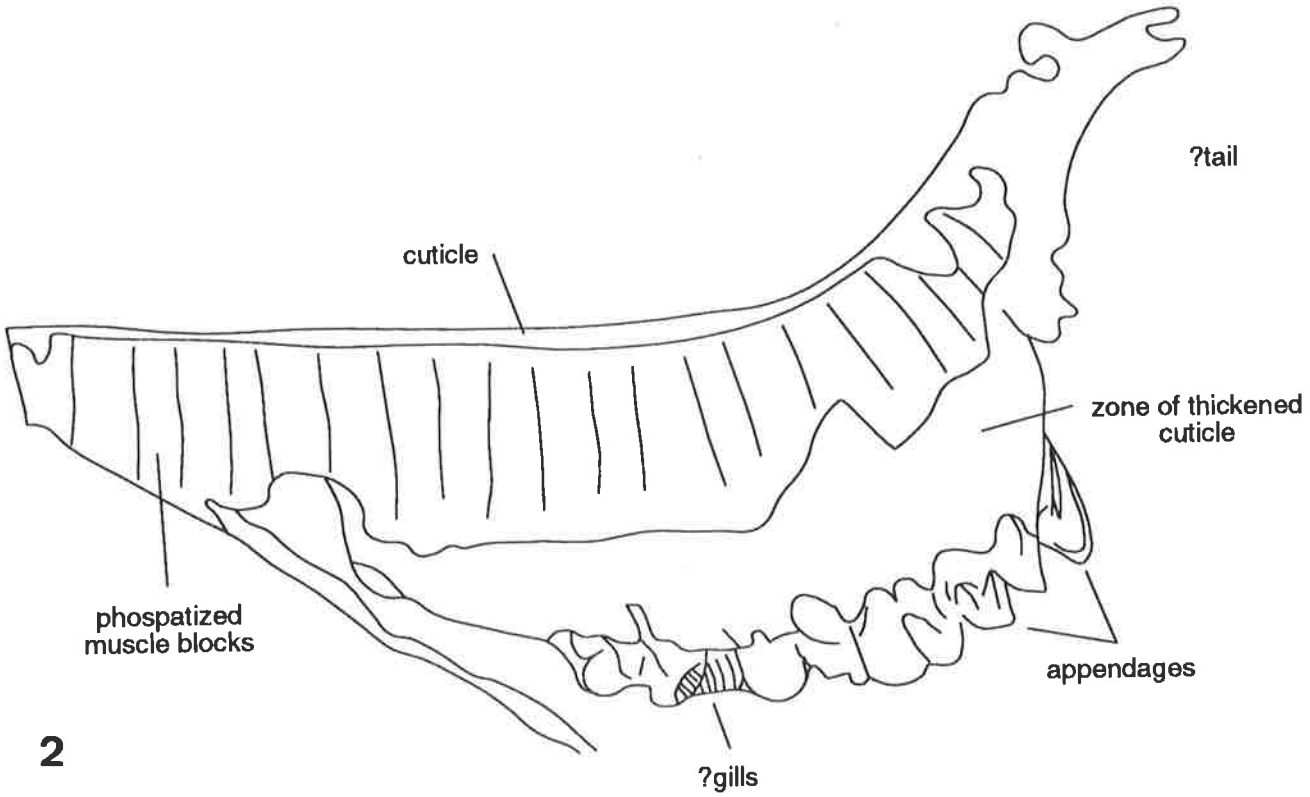
?tail
cuticle
zone of thickened cuticle
phospatized muscle blocks
appendages
?gills

2

The best preserved specimens of the head (Pls. 5.4, 15.2) shows the trunk narrowing rapidly anteriorly into a short projection flanked distally by structures here interpreted as eyes and a possible proboscis. The structures on the right side are preserved as two merging sub-circular features. These are thought to represent eyes. Although only two eyes are apparent, this may be an artifact of lateral compaction, for instance, in lateral aspect only two of the suggested five eyes possessed by *Opabinia* are visible (Whittington 1975, figs. 4-7). The outline of the head, and the structures interpreted as eyes, are preserved as a featureless film of fibrous calcite. No mineralised muscle tissue is evident in this area.

The apparent eyes and general habit of *Myoscolex* prompts possible comparisons with the Burgess Shale animal *Opabinia* (Briggs & Nedin In Prep.). Pl. 5.4 shows a suggestion, on the left hand side, that a proboscis-like structure curves backward along the side of, and partly obscured by, the trunk. There is a suggestion that this structure might taper and become digitate distally. A second specimen also preserves a possible proboscis (but this interpretation is equivocal given that no clear head or attachment is evident). The structure does, however, appear to originate in the head region and curve backward and upward through the sediment. Like the structure shown in Pl. 5.3, it appears to be annulated proximally and to taper, becoming digitate distally.

The trunk is the main feature preserved in specimens of *Myoscolex*, and its manner of preservation, as mineralised muscle tissue, is most unusual. Specimens in lateral aspect clearly show narrow bands of longitudinal muscle, the fibres running parallel to the axis of the body, along both dorsal and ventral margins of the trunk. These are separated by a wider band of dorso-ventral muscles, the fibres running at a high angle to the body axis. In the majority of cases both longitudinal and dorso-ventral muscles are fused together into a mineralised sheet. Occasionally, however, the individual muscles appear to remain discrete providing a clearer indication of their original configuration (Pls. 5.6, 15.4). Occasionally the dorso-ventral muscles seem to be overlapped at their extremities by the longitudinal muscles (PL. 15.5). Sometimes however, there is no evidence of the

# Plate 15

**15.1** *Myoscolex ateles* (AUGD1046-725). Specimen showing rare curved aspect. (x1)

**15.2** *Myscolex ateles* (AUGD1046-611). Specimen preserving a portion of the head as a carbonate film, with one round eye visible at right. The object at left is a small *Hsuaspis bilobata*. (x2)

**15.3** *Myoscolex ateles* (AUGD1046-646). Specimen preserving a portion of the head, two round eyes visible at left and proboscis-like organ at left. (x2.3)

**15.4** *Myoscolex ateles* (AUGD1046-648). Specimen in dorsal view, showing bilateral symmetry. (x1.75)

**5.5** *Myoscolex ateles* (AUGD1040-RS236). Specimen showing metameric phosphate structures. (x2.3)

# PLATE 15

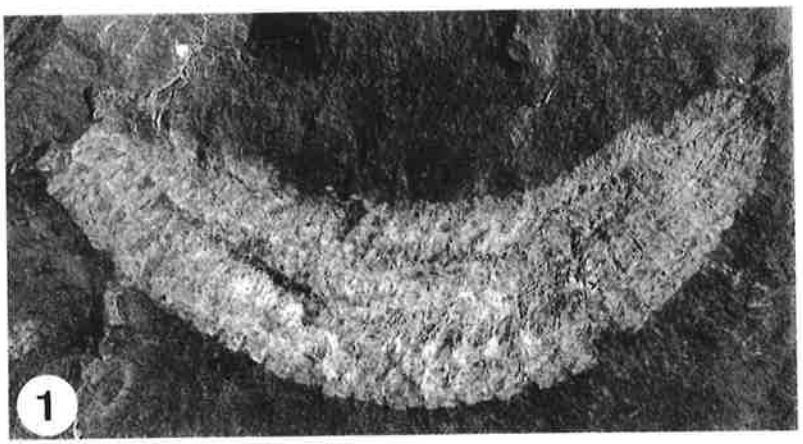




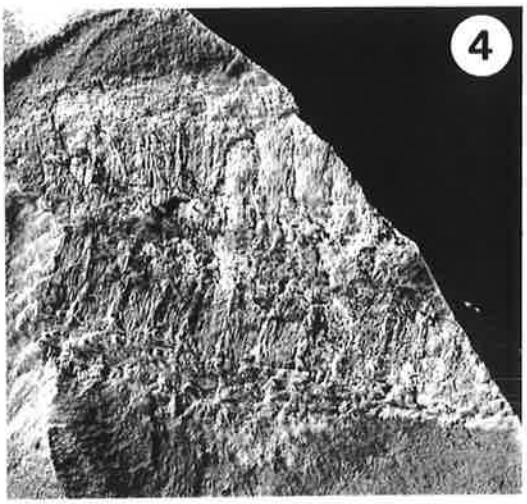


longitudinal muscles (Pl. 15.2). Where the muscles have been recrystallised the margins of the longitudinal muscles may be marked by a change in relief and in some cases the longitudinal and dorso-ventral muscles are distinguished by a sharp contrast in colour (grey as opposed to red: Pl. 5.3) (Briggs & Nedin In Prep).
In a number of specimens the trunk is very clearly segmented. This segmentation is marked not only by boundaries within the muscles but also by pronounced, if irregular, narrow ridges running roughly normal to the axis and usually gently concave anteriorly. Smooth curved lines may be evident connecting successive segment-bounding ridges, particularly ventrally, and the ventral part of each muscle segment may be overprinted by a consistent pattern of relief - usually a knob or projection. This regular pattern is assumed to be an imprint of the tergites that originally covered the muscle tissue.

A very small number of specimens are preserved in an attitude parallel to bedding (i.e. flattened dorso-ventrally). These specimens display a clear bilateral symmetry. In Pl. 15.4 the muscle segments are divided into two halves, presumably corresponding to the right and left dorso-ventral muscles, and converge anteriorly at an oblique angle to the mid line.

One unique specimen (Pl. 14 - collected by R.J.F. Jenkins) preserves a series of flap-like structures lying ventral of the mineralised muscle blocks. Unfortunately the specimen is both incomplete and weathered, so that it is difficult to interpret. The trunk curves abruptly dorsally at the posterior end, with scattered traces of cuticle below. The extremity of the body is too poorly preserved to allow any reliable conclusion to be drawn about the posterior region. The cuticle appears to have been preserved as an extremely thin layer, appearing darker than the surrounding rock. This occurrence is similar to that described by Whittington (1975) in specimens of *Opabinia*. In the posterior part of the trunk there is a series of 8 or 9 flap like projections (anterior of which the slab is missing). These are assumed to be right appendages evident in lateral view. Those lying furthest to the rear are straight along the posterior facing margin and

curved, convex forward, on the anterior. Those exposed furthest forward are preserved in the opposite sense (Briggs & Nedin In Prep). All, however, show the same relief (convex upward on the part) and hence they are unlikely to lie on opposite sides of the body. Striae visible on some appendages may represent gill structures. These structures are interpreted as appendages rather than as the pleural extremities of the tergites because they lie well below the muscle tissue which, on other specimens, retains an apparent impression of the tergites, and they vary in their facing direction - a feature unlikely to be present in stiffened tergites, but quite plausible in more flexible appendages which rotate as they swing forward and backward while the animal is swimming (cf. *Opabinia*; Whittington 1985, figs. 4, 55).

A number of other specimens preserve traces of structures along the ventral margin that may represent part of the appendages.

A number of specimens display the curved robust rod-like structures arranged segmentally along the margin of the trunk that Glaessner (1979) regarded as parapodial setae. In specimens preserved in lateral aspect these structures occur on one side only (assumed ventral) and are evidently paired (e.g. Pl. 15.5). There is clear evidence of variable mineralisation; the shape and extent of the structures varies. In lateral specimens they may extend ventrally beyond the mineralised muscle, or overlap it to a significant degree. They normally make an angle to the segmental boundaries, sloping forward and downward. These structures are also evident in the two specimens preserved in parallel aspect although here they are not as strongly mineralised. They appear to be arranged in pairs, one on either side of the mid-line, corresponding to the segments. There is no sign of them in association with the structures interpreted as appendages (Briggs & Nedin In Prep).

The nature of these curved rod-like structures is unknown. As Glaessner (1979) pointed out, in size and shape they are unlike the setae in any known polychaete. The position and the nature of their preservation is more consistent with them representing transverse structures, one pair present in the ventral part of each body segment. Their robust nature

suggests that they may have been structural elements, perhaps endoskeletal bars or sternites. This is consistent with the interpretation of *Myoscolex* as a possible arthropod, as indicated by the presence of eyes, the laterally flattened body, the impression of tergites, and the flap-like appendages.

*Myoscolex ateles* was first described by Glaessner (1979) on the basis of some 25 specimens in varying states of preservation and completeness. He noted the elongate body made of many short segments, interpreting mineralised material within the body as representing a median band of oblique muscles, flanked by two bands of longitudinal muscles. Curved robust rod-like structures arranged segmentally along the margin of the trunk were interpreted as parapodial setae, in spite of the fact that they are unlike any setae known. While admitting the difficulty of assigning *Myoscolex* to a higher taxon, Glaessner (1979, p. 29) regarded it as "of uncertain affinities among the Class Polychaeta".

*Myoscolex* has received little attention since Glaessner's original description was published. Its identification as a polychaete worm has generally been accepted (e.g. Hou & Chen 1989b), but a possible arthropod affinity was first suggested by Nedin (1992).

A number of factors prompt a reassessment of *Myoscolex*. A great deal of additional material has been collected at Big Gully in the 16 years since Glaessner studied the fauna. The preservation and environmental setting of the fauna as a whole has been the subject of an intensive study. The widespread occurrence of mineralised muscle tissue in the fossil record has been recognised (e.g. Allison 1988a; Allison and Briggs 1991) and its potential for preserving soft tissues in histological detail has been documented (e.g. Müller 1979; Martill 1988, 1990; Briggs & Kear 1993b). It should be noted that the remarkable Orsten faunas are preserved as a phosphatic coating (Müller 1979, 1985), with no phosphatised muscle tissue so far being documented. Finally progress has been made in understanding the controls on soft-tissue mineralisation and on the types of tissues likely to be preserved (e.g. Briggs *et al.* 1993; Briggs and Kear 1993a, b), and

this aids in the interpretation of fossils such as *Myoscolex*.

The extremities of *Myoscolex* appear were only weakly sclerotized and do not promote parting along bedding planes. For these reasons complete fossils of *Myoscolex* are rarely extracted from the shale. The preservation of *Myoscolex* tends to be incomplete in any event. Features on the periphery of the animal were either less prone to mineralisation, more prone to decay, or both.

The majority of specimens of *Myoscolex*, as preserved, are not bilaterally symmetrical. Thus they are assumed to be laterally flattened in the plane of the bedding. The presumed ventral margin (coinciding with the phosphatised ribs, previously interpreted as setae) tends to be straight to gently concave outward, the dorsal margin more strongly convex, but flexure of the body in the opposite sense also occurs. A small number of specimens are preserved in a dorso-ventral orientation (e.g. Pl. 15.4).

The animal is preserved mainly through mineralisation rather than as a result of the survival of organic material such as cuticle. The interpretation of the fossils is made difficult by the later recrystallisation of the minerals that replicate the soft-tissue, and by an external coating of fibrous calcite.

A transverse section normal to bedding shows that specimens of *Myoscolex* consist of four layers. The two central layers correspond to the muscle tissue, identified by its fibrous appearance, on either side (i.e. right and left) of the trunk. Normally the muscles on each side of the body have merged into a continuous sheet. In a few specimens, however, discrete muscles are evident, particularly those running dorso-ventrally, overlapping and cross cutting each other. The mineral ranges from black to pale grey to ochre in colour, and is apparently preserved in apatite/francolite $CaPO_4$. The morphology of the external surface of this muscle tissue is well preserved in most specimens, even though the recrystallisation has rendered the preservation of microstructure unlikely. In some specimens there has been more extensive diagenetic alteration to form a much more blocky, pale grey, discontinuous mineral sheet.

The outer surface of the muscle tissue is covered with a thin film of pink to pinkish-white fibrous calcite. This calcite is usually a very fragile open mesh which can be removed by gentle brushing. In some cases, however, it is more robust, perhaps as a result of recrystallisation. The calcite may fill in spaces between the phosphatised muscles. The fibrous calcite is aligned in a tectonic stress field, and its fabric bears no relationship to the fossils themselves. Where the phosphatised muscle tissue can be separated from the outer layer of calcite it is clear that the calcite retains an external mould of the muscle (Briggs & Nedin In Prep). No detail of the animal is retained on the outer surface of the calcite layer, however, nor on the matrix that abuts it. It is clear that the calcite grew on the muscle tissue after it had become mineralised. It must have grown early enough to displace the adjacent sediment (i.e. to create space for the crystals to form). The fabric related to the stress field must have been acquired at a much later stage of recrystallisation.

This is the first report of undoubted phosphatised muscle tissue in a Cambrian fossil Lagerstätten (whilst the possibility exists that phosphatised muscle tissue occurs in the Orsten faunas, none has so far been documented). The muscle tissue has been regarded as "calcified" (Glaessner 1979; Allison & Briggs 1991), but examination of paratype P21020, described by Glaessner as showing "a layer of calcified muscle tissue" (legend to figure 7: 1979, p. 28), shows this layer to be pink fibrous calcite that has grown external to the muscles (Pl. 5.6). On the other hand, Glaessner reported that the so-called setae were calcium phosphate. It prompts comparison with experiments on the fossilisation of the muscle and other tissues of shrimps (Briggs and Kear 1993, 1994a, b, Briggs *et al.* 1993) (see section 5.3).
Mineralisation of *Myoscolex* was probably similar to that reproduced in experiments, that decay induced phosphatisation followed by the formation of calcium carbonate on the outside of the specimen.

A small number of specimens of *Myoscolex* (e.g. Pl. 14) preserve traces of flap-like

appendages extending ventrally beyond the trunk. The absence of such structures in great majority of specimens indicates that the cuticle of this part of the body, at least, was very thin and normally decayed rapidly. If the cuticle of the axial part of the trunk was similarly thin and decay-prone it is likely to have survived only long enough to enclose the muscles and promote phosphate diffusion as they were becoming mineralised. If, on the other hand, the cuticle of the tergites covering the trunk muscles survived they can only have been very thin and flexible so as to take up the relief of the underlying muscles. Like them the tergites became phosphatised, but it is no longer possible to distinguish the very thin layer representing it, as it has become obscured by diagenetic recrystallisation. In a number of examples, however, it has clearly decayed, as the surface bounding the muscles is not continuous as would be expected if they were covered by a cuticle.

*Myoscolex* remains an enigmatic form. However, due to presence of lobe-like appendages and eyes, the original annelid assignation cannot be sustained and the form is here re-assigned to the Arthropoda.

*Myoscolex* (Fig. 3.14) appears to have been superficially similar to *Opabinia* in possessing a pair of, probably compound, eyes and a frontal process which appears to taper distally into what may be 'fingers' (Briggs & Nedin In Prep).

The trunk is divided into numerous segments, although the exact number is not known. There is some suggestion that the tergites covering the segments were separate and thin. Longitudinal and dorso-ventral muscle blocks are clearly preserved.

Segmentally arranged along the ventral margin are enigmatic curved, rod-like structures. These may have been endoskeletal bars or represent sternites. However, they may also represent support for the appendages. The lack of such obviously robust structures in the majority of specimens might be due to the uneven splitting tendency of the rock. The extremities of *Myoscolex* tend to be poorly mineralised at best, and so will not induce splitting along the plane on which they lie.

Comparisons with *Opabinia* are speculative, as the structural elements in *Myoscolex* regarded as similar are rarely found and poorly preserved. Nevertheless such a comparison merits documentation as a data point in ongoing research into the depth and breadth of Cambrian diversity, disparity and evolutionary turnover.

3.3.4.3 cf. *Opabinia* (Pl. 16)

In describing *Opabinia*, Whittington (1975) divided the organism into a cephalon and trunk in deference to its unknown affinities and to avoid the taxonomic implications of terms such as "thorax" and "telson". In his description, the trunk was divided into 15 segments bearing a pair of lateral lobes, each of which, except the first, bearing paddle shaped extensions and lamellae suggestive of gills. Each segment and the cuticle covering it appears to be separate from the immediately anterior and posterior segments. The posterior region of the trunk bore a tail fan with six lobe-like extensions.
The cephalon was reconstructed with five eyes and a tubular frontal process, which terminated in two groups of spines (Whittington 1975, fig. 82).
The unusual construction of the organism and it's rarity - only 10 reasonably intact specimens have been found, all from the 'Phyllopod bed' in the Burgess Shale (Whittington 1975) - has led to speculation as to its true affinities and the implications for the disparity of Cambrian bauplans. Gould (1989, 1991) has suggested, using the Burgess Shale fauna, that Cambrian faunas had higher taxanomic groups, up to phylum level, which are no longer represented, and that the variety or disparity of body plans was much greater. However, more recent finds have repositioned so-called 'odd-balls' back into pre-existing phyla, e.g. *Hallucigenia* (Ramsköld & Hou 1991). The possible affinity between *Opabinia* and *Myoscolex*, suggests that another 'odd-ball' from the Burgess Shale can be placed within a pre-existing phylum. Thus diminishing further the disparity, or number of extinct groups, in the Cambrian suggested by Gould.

Specimen 1046-240 appears similar to the Burgess Shale form *Opabinia*. If this is

# Plate 16

**16.1** cf. *Opabinia* (AUGD1046-240). Left lateral view. Specimen composed of 15 segments, the last segment is twisted back over the body. Basal part of tubular process visible. (x3.3)

**16.2** Camera lucida drawing of AUGD1046-240. Note apparently free tergites.

# PLATE 16


1

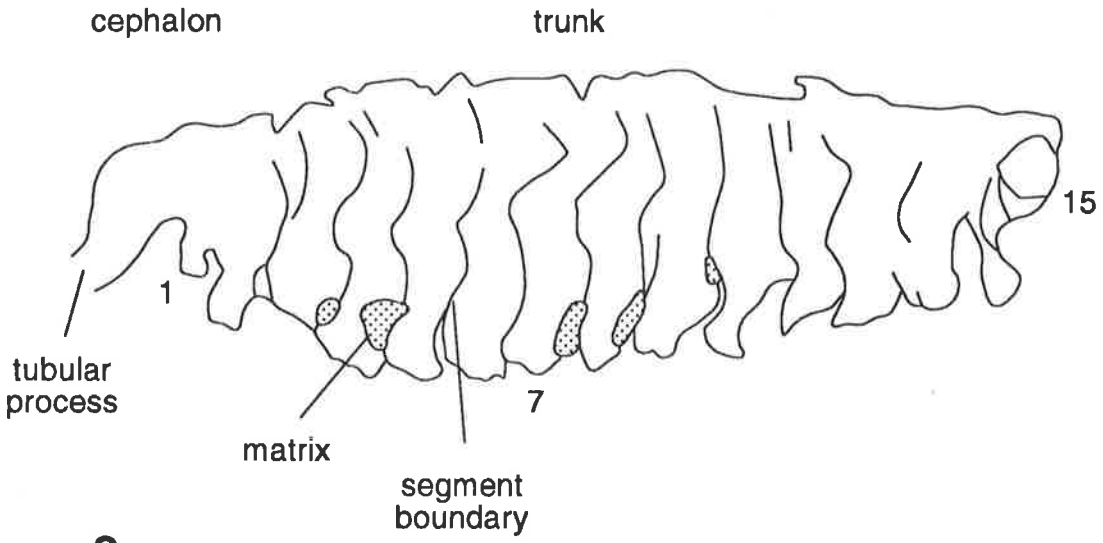
cephalon
trunk
15
1
tubular process
7
matrix
segment boundary
2
5 mm

correct, it extends the range of opabinids, both geographically and chronologically, representing the oldest example yet known. The presence of *Opabinia* in the Emu Bay Shale also strengthens the possible opabinid affinities of *Myoscolex*.

## 3.4 Incertae Sedis

### 3.4.1 (?)Annelids

#### 3.4.1.1 *Palaeoscolex antiquus*(Pl. 7.6)

The new material provides no additional information to augment the original description of the species (Glaessner 1979). The head region remains enigmatic. However, recent finds from the Georgina Basin in Queensland indicate that the head region is small and composed of four outwardly directed nipples (Müller & Hinz-Schallreuter 1994), and the preservation of such small parts is unlikely at Big Gully. When found, *Palaeoscolex* is always tightly coiled. This suggests exposure to environmental stress, such as low oxygen or salinity.

Palaeoscolecida are thought to be soft-bodied animals in which the cuticle was reinforced by sclerotized plates and platelets (Müller & Hinz-Schallreuter 1994). These consisted of rows of plates interspaced with tiny polygonal platelets. The plates did not form a complete cover, but lay in the soft tissue, allowing a certain degree of mobility.

The finds of Palaeoscolecida in current -washed sediments indicates that the plates were substantially toughened, possibly permitting an allochthonous origin for the fossils at Big Gully.

If the notion that Palaeoscolecida grew by moulting (Müller & Hinz-Schallreuter 1994) is correct, it is probable that the fossils of *P. antiquus* in the main, actually represent moults.

The placement of *Palaeoscolex* within the Annelida (e.g. Whittard 1953; Glaessner

1979), based upon their segmented appearance, was queried by Conway Morris & Robison (1986), and Müller & Hinz-Schallreuter (1994) postulated a possible relationship with the Priapulida or the Aschelminthes rather than the Annelida. The rejection of *P. antiquus* as a palaeoscolecian by Hou & Chen (1989a) is not sustained.

## 3.5 Trace Fossils

### 3.5.1 Coprolite (Pl. 10.5)

Material. AUGD1046-613, from the Emu Bay Shale at Big Gully, Kangaroo Island.

Coprolites can provide valuable information on the size and feeding habits of organisms. However, Cambrian coprolites are rare, and while rare to common small pelloidal masses may well be faecal material, only a few larger coprolites have been described (e.g. Durham 1971; Sprinkle, 1973; Conway Morris & Robison 1986, 1988). Circular Cambrian coprolites from the Stephen Formation in British Columbia (Sprinkle 1973) and from the Marjum and Spence Formations of Utah (Conway Morris & Robison 1986, 1988), are commonly 25 - 30 mm in diameter, but reach 45 mm in some instances. These are of a considerable size given the size range of known Cambrian predators. At approximately 0.5 m, *Anomalocaris* is the largest known Cambrian predator (Whittington & Briggs 1985). At this size the maximum gut diameter is approximately 20 mm (Briggs & Robison 1984; Whittington & Briggs 1985). The gut tapers to the rear and a terminal diameter of 10 mm has been suggested (Conway Morris & Robison 1988). There is a large degree of ambiguity in this figure, due in part to the unknown expansion limit of such a gut, making the passing of larger faeces possible. Also, recent anomalocaridid finds in China have prompted speculation of much larger individuals (Chen *et al.* 1994).

The coprolite from the Emu Bay Shale differs from the round compressed ones

previously mentioned in being an elongate mass some 43 mm in length and a maximum width of 28 mm. It contains a mass of trilobite fragments. Terrace lines are recognisable, indicating by the fragment length, that they represent the cephalic doublure. Also a large portion of one genal spine is present and one recognisable distal fragment of a pleuron, in close proximity to a short pleural spine. From the size of the cephalic doublure, the pleuron and the genal spine, the trilobite is estimated to have been some 4 cm in overall length. The size and shape of the elements and ornamentation indicate that the trilobite was probably *Redlichia takooensis*.

The coprolite is divided into two zones, a 'lower', coarse particulate zone crowded with exoskeletal fragments, and an area relatively free of coarse particulate exoskeletal material, composed of white and red fibrous calcite, with occasional small exoskeletal fragments. It is possible that the coarser part represents the solid, compacted portion of the expelled faeces. The finer part may represent the expansion or diffusion of a more fluid phase (either by fluids included with the faeces or by fluids adsorbed into the compacted faeces from the surroundings) into the sediment on the sea bed, in a possibly current induced direction. Therefore the actual width of the faeces, as expelled, may be more accurately represented by the coarser part, suggesting a maximum width of 15 mm. Assuming a 10 mm terminal diameter for a 0.5 m long anomalocaridid (Conway Morris & Robison 1988), a 15 mm terminal diameter suggests a total body length of approximately 0.75 m - a not unreasonable size given the estimate of 0.60 m for a specimen of *Anomalocaris* sp. found in the Big Gully assemblage, calculated from the length of the appendage (section 3.2.6.1).

## 3.6 Systematic Palaeontology

Superphylum ARTHROPODA Siebold & Stannius, 1845

Phylum TRILOBITA Walch, 1771

Order REDLICHIIDA Richter, 1933

Suborder REDLICHIINA Harrington, 1959

Superfamily REDLICHIACAE Poulson,1927

Family REDLICHIIDAE Poulson, 1927

Subfamily REDLICHIINAE Poulson, 1927

**Redlichia** Crossmann, 1902

Type species *Hoeferia noetlingi* Redlich, 1899 from the late Early Cambrian of the Salt Range, Pakistan.

*Redlichia takooensis* Lu, 1950 (Pls. 4.1, 6)
1950 Redlichia takooensis Lu, p. 166, pl. 1, fig. C-4.
1950 *Redlichia meitanensis* Lu, p. 167, pl. 1, fig. B-1.
1957 *Redlichia takooensis* Lu; Lu, p. 261, pl. 139, fig. 1.
1957 *Redlichia meitanensis* Lu; Lu, p. 261, pl. 138, fig. 16.
1965 *Redlichia takooensis* Lu; Lu *et al.*, p. 65, pl. 9, fig. 1.
1965 *Redlichia meitanensis* Lu; Lu *et al.*, p. 67, pl. 7, fig. 17.
1980 *Redlichia takooensis* Lu; Zhang W.T. *et al.*, p. 130, pl. 23, figs. 1-14
1980 *Redlichia meitanensis* Lu; Zhang W.T. *et al.*, p. 129, pl. 22, figs. 3,4.
1981 *Redlichia takooensis* Lu; Lu, p. 1, pl. 1, figs. 10-16.
1985 *Redlichia* sp. Conway Morris & Jenkins, p. 170, figs. 1,3.

Material: AUGD1046-246, -349,-359,-630; all from the Emu Bay Shale, Kangaroo Island, South Australia.

Description: Cephalon semicircular, moderately convex transversally and sagittally. Anterior border broad, slightly elevated,distinct sub-parallel terrace lines, occasionally anastomosing together, reaching genal spines. Preglabellar furrow shallow but distinct, becoming indistinct sagittally, merging with border furrow in larger individuals; preglabellar field very narrow. Glabella straight, conical, tapering gently forward to well rounded anterior; maximum width just before occipital furrow; three pairs of lateral

glabellar furrows, 3S pair transverse, short and weakly impressed, becoming more deeply impressed on flanks, discontinuous adaxially; 2S larger, directed inward and posteriorly transcurrent across glabella axis, connected by a shallow depression; 1S deep, directed inwards more strongly than other furrows, connected by more pronounced depression across glabella axis. Carinate projection posteriorly from 2L to 3L over 1S ; 1L and 2L sub-equal in size, 3L slightly narrower and smaller, 3L larger, semicircular, moderately convex sagittally and transversely. Occipital furrow recurved posteriorly, sub-parallel to 1S; deep behind 1L, shallowing sagittally and connected over axis by shallow furrow. Occipital ring large, maximum width sagittally; apodermal pits at postero-lateral corners; ring drawn out medially into a strong occipital spine extending to the 5th thoracic segment. Palpebral lobes convex in section, curved in outline, leaving axial furrow of glabella adjacent to 4L, does not extend far exsagittally, but long, reaching a level of the transverse medial line of the occipital lobe, almost to posterio-lateral corners of occipital lobe and posterior border. Palpebral furrow shallow, deep posteriorly, but indistinct from post-occular area. Facial suture leaving palpebral lobe close to axial furrow, then running in straight line a short distance at 75° to exsagittal, then curving adaxially to margin. Wide, flat to slightly convex genal field, with caecal ornamentation running away from palpebral lobe; border distinct, with furrow, sharp anterior marginal point where facial suture meets margin(?); margin uniformly wide, but widest at base of genal spine and narrowest behind spine, well developed, continuous terrace lines parallel with margin and extending length of genal spine. Genal spine gently tapering, long, extending to 8th thoracic segment. Post-occular area short and narrow, sub crescentic in shape, deep border furrow of librigenae, meets axial furrow at level of postero-lateral corners of occipital lobes; border long, narrow, approx. 0.5 width of librigena, widens adaxially, well developed, continuous terrace lines, parallel with margin. Hypostome ovoid, median body convex adventrally, pronounced anterior and lateral border furrows, becoming shallower posteriorly; narrow anterior border widens laterally into anterior wings; macula apparently absent; posterior border wide, smooth, bifurcate with two postero-lateral spines. Rostral plate long, crescentic, forming major

portion of cranidial doublure, anterior portion has terrace lines, slightly concave lateral margins.

Thorax of 15 segments, approx 0.6 length of dorsal exoskeleton, maximum width at level of 3rd segment, narrowing posteriorly, moderately convex; axis approx. 0.33 width of thorax, strongly convex; axial rings narrow sagittally, approx. 0.5 the width of pleurae, becoming wider towards axial furrow. Spines on each annulation, often only preserved as spine bosses; very large macrospine on 11th segment extends posteriorly over pygidium to distance equivalent of six axial segments; attitude in life is not certain, but appears to have been held at an angle to plane of body; large spine boss on 6th segment indicates a larger that average spine on this segment. Articulating half rings crescent shaped, narrower than axial ring, flange riding up on to preceding axial ring; more prominent adaxially along transverse furrow; transverse furrows deepest at abaxial extent, shallower and wider medially; axial furrows deep, deepest at junction between abaxial ends of transverse furrows and axial furrow; axial furrow on ventral surface represented by upraised ridges and peaks connected sagittally by a narrow platform. Anterior pleurae non-falcate, geniculate, outer part of posterior margin shows a narrow overlapping flange, disappearing adaxially; tips of pleurae extended into posteriorly directed spines; first six pleurae possess a notch in the posterior border close to spine, at the point of geniculation; seventh and subsequent pleurae lack this notch, become recurved and fulcate, terminal thoracic pleurae strongly recurved around, but not fused to, pygidium. Pleural spines show dense, sub-parallel, anastomosing terrace lines, curved exsagittally, extending from anterior to posterior margin. Deep pleural furrow, straight, slightly oblique; fine grained, pustulate surface texture over test, often coalescing to form short raised lines with random orientation, often more pronounced and parallel across articulating half-ring.

Pygidium micropygous, of three segments, with broad axis not reaching posterior border; anterior segment has short, single ring with short axial spine; in large specimens axial ring is deflected slightly anteriorly from median point of ring, this deflection

becoming more emphatic in second segment; transverse, deep axial furrows; pleurae strongly recurved with blunt tips resting posteriorly and exsagittally, fused to pygidial field and posterior doublure along posterior margin, anterior margin free, overlain by terminal thoracic segment. Narrow second segment, resembling axial ring, transverse furrow between second and posterior segments; no pleurae visible (recurved to form posterior border?). Posterior segment bilobed with prominent medial furrow, narrow posterior doublure, slight medial embayment in posterior border.

Superfamily PARADOXOIDEA Emmerich, 1830

Family ICHANGIIDAE Zhu, 1980

**Hsuaspis** Zhang, 1957

Type species *Lusatiops sinensis* Zang 1953, from the Early Cambrian of western Hupai, southwestern China.

*Hsuaspis bilobata* (Pocock 1964) (Pls. 4.2, 7)

1964 *Estaingia bilobata* Pocock, p. 463, pls 75-76.

1975b *Estaingia bilobata* Pocock; Öpik, p. 11, pl. 1.

Material: All from the Emu Bay Shale, Kangaroo Island, South Australia.

Merapsid 1 (AUGD1064-700)

Description: Cephalon semi-elliptical; length 0.78 mm ( 0.65 cranidial width), anterior sub-transverse; border relatively flat, narrow sagittally, widening exsagittally, passing into long, curved genal spine about 1.3 mm in length (1.7 cranidial length), presence of intergenal spines indeterminate ; border approx. 0.5 width of free cheeks at mid level across eyes. Marginal furrow distinct, narrow groove; rear margin of free cheek long,

border narrow and elevated, meeting posterior border of fixigena at an angle of 145°; posterior marginal furrow connects lateral marginal furrow of cheek in slightly abrupt curve at genal angle. Posterior facial suture short and delineates postero-lateral limbs with tips extending beyond posterior border and slightly beyond sagittal tangents of palpebral lobes. Anterior facial sutures diverge at 95°, curve slightly anteriorly towards anterio-lateral margin. Cranidial rim relatively narrow, widens laterally, marginal frontal furrow shallow and broad. Inter-ocular cheek and palpebral lobe together are much wider than glabella. Eye lobes extend tangentially away from 3L to where the anterior facial suture and ocular lobe meet, posterior of this the eye lobe curves slightly back; palpebral lobes arcuate, narrow, elevated and especially prominent towards rear, posterior tips do not reach posterior furrow of cranidium, palpebral furrows very weakly defined. Distance from anterior tip of palpebral lobe to glabella about 0.7 width of glabella at its widest. Distance between posterior eye lobe and axial furrow 0.50 cranidial length. Presence of bacculae indeterminate. Occipital lobe sub-equant, occipital furrow slightly convex anteriorly, posterior margin of lobe slightly convex posteriorly, lobe approx 0.15 glabellar length, width 0.65 glabella at widest point. Occipital furrow deep at margins, shallowing medially. Axial furrow at glabellar flanks moderate, shallowing and disappearing anteriorly. Glabella long, around 3.0 of its width at rear, clavate, reaching its maximal expansion of about 1.75 of its rear width just in front of anterior palpebral lobes. Anterior pre-ocular part of the glabella short, only some 0.2 of its total length. Front of glabella rounded, glabella contacts anterior border furrow. Glabellar furrows are not well preserved. Genal spines long, 1.7 cranidial length, thin, curved, possibly advanced.

Thorax of 1 segment, axial lobe as wide as 0.25 of shield across middle. Axis convex, axial furrows of thorax deeply incised at anterior and posterior margins of segment, shallowing medially, pleural furrows present but not well preserved. Segment bears long curving pleural spine about 1.7 mm (2.18 cranidial length).

Transitory pygidium is 0.42 mm long (0.54 cranidial length), 0.54 mm wide (0.36 cranidial width); axial furrow deep anteriorly, shallowing and disappearing posteriorly;

axis highly convex, shallowing posteriorly; axial rings indistinct, two segments discernible. First segment bears elongate pleural spines about 0.39 mm (0.5 cranidial length); second segment has pleura which end in short stout spines. Axis terminates in blunt point; pleural field smooth posteriorly of two anterior segments. Posterior border straight, apparently unadorned.

Meraspid 7 (AUGD1046-701)

Description: Cephalon semi-elliptical, length 1.3 mm (0.65 cranidial width), anterior gently curved; border relatively flat, narrow sagittally, widening exsagittally, passing into long, straight genal spine which curves sagittally near tip, >1.4 mm long (>1.08 cranidial length), intergenal spines absent; border approx. 0.4 width of free cheek at mid level across the eyes. Lateral border furrow distinct, narrow groove; rear margin of free cheek long, border narrow and elevated, posterior marginal furrow connects lateral marginal furrow of cheek in an abrupt curve at genal angle. Posterior facial suture short and delineate small postero-lateral limbs with tips extending only slightly beyond posterior border. Anterior facial suture diverge at approx. $105^{o}$, curves away from palpebral lobe towards antero-lateral margin. Cranidial rim relatively narrow and widens laterally, marginal frontal furrow defined. Inter-ocular cheek and palpebral lobe together at mid-line across eyes wider than glabella. Eye lobes extend tangentially away from 3L to where the anterior facial suture and ocular lobe meet, posterior of this the eye lobe curves back, palpebral lobes arcuate, narrow, elevated and prominent towards rear, posterior tips reach posterior furrow of cranidium, clear palpebral furrows absent. The distance from anterior tip of palpebral lobe to glabella about 0.8 the width of glabella at its widest. Distance between posterior eye lobe and axial furrow 0.40 cranidial length. Bacculae possibly present as convex swellings close to occipital furrow. Occipital furrow convex anteriorly, posterior margin of lobe convex posteriorly, curvature more pronounced than on anterior margin; lobe approx 0.2 glabellar length, width 1.0 glabella at its widest point. Occipital furrow deep, slightly shallower medially. Axial furrow at

glabellar flanks incised, shallowing and becoming indistinct at front. Glabella long, around 1.7 of its width at the rear, and clavate, reaching its maximal expansion of about 1.1 of its rear width just in front of palpebro- ocular ridge. Anterior pre-ocular part of glabella short, only some 0.23 of its total length. Front of glabella rounded; very short preglabellar field present. Three sets of glabellar furrows present, 1S are oblique, 2S straight and both sets contact axial furrows. 3S poorly defined, arched anteriorly and do not appear to contact axial furrows. Occipital ring large, semi-elliptical, maximum width sagittally, decreasing to zero at axial furrows. Genal spine moderate length, 1.2 cranidial length, curved, base becoming broader, strongly advanced.

Thorax of 7 segments, axial lobe as wide as 0.4 of the shield across the middle, axis tapers rearward to about 0.4 of its anterior width. Axial furrows moderately to deeply incised; apodemes present, well defined on anterior segments; pleural furrows oblique and moderately deep, widest at fulcra, petering out toward adaxial edge. Segments one and two bear long, straight pleural spines extending beyond length of body, total length unknown; other segments terminate in short spines. Fulcral points more pronounced in anterior segments, but still visible in rearmost segments. Distance of fulcra and fulcral lines from axial furrow is about 0.4 of width of axial lobe in anterior part of thorax. Geniculation along fulcral line apparently steep, with pleurae sloping down at relatively steep angle.

Transitory pygidium poorly preserved; 0.14 mm long (0.1 craidial length) and 0.35 mm wide (0.23 cranidial width) ; axial furrows shallow, disappearing posteriorly; axial rings not well preserved, but possibly three; axis terminates at blunt point. pleural field with insipid segmentation or pleural furrows. Posterior border not well preserved.

Meraspid 10 (AUGD1046-543a)

Description: Cephalon semi-elliptical, length 1.98 mm (0.75 cranidial width), anterior curved; border relatively flat, narrow sagittally, widening exsagittally, passing into long, curved genal spine about 2.5 mm long (1.25 cranidial length), intergenal spines absent;

border approx. 0.4 of width of free cheek at mid level across eyes. Lateral border furrow distinct, narrow groove, about 0.4 width of free cheek; rear margin of free cheek long, border narrow and elevated, joins posterior margin of fixigena at angle of 133°, posterior marginal furrow connects lateral marginal furrow of cheek in sharp curve at genal angle. Posterior facial suture short and delineate small postero-lateral limbs with tips extending only slightly beyond posterior border. Anterior facial sutures diverge at approx. 116°, curve slightly anteriorly towards antero-lateral margin. Cranidial rim relatively narrow and widens exsagittally. Inter-ocular cheek and palpebral lobe together at mid-line across eyes, wider than glabella. Eye lobes extend tangentially away from 3L for a short distance, to where the anterior facial suture and ocular lobe meet, posterior of this the eye lobe curves back, becoming strongly recurved distally, palpebral lobes, narrow, elevated and prominent towards rear, palpebral furrows weakly defined. Distance from anterior tip of palpebral lobe to glabella about 0.65 width of glabella at its widest. Distance between posterior eye lobe and axial furrow 0.35 cranidial length. Bacculae present as convex swellings close to occipital furrow. Occipital furrow convex anteriorly, lobe approx 0.23 glabella length, width 1.0 glabella at widest point. Occipital furrow deep. Axial furrow at glabellar flanks incised, shallowing anteriorly. Glabella long, around 1.6 of its width at rear and clavate, reaching its maximal expansion of about 1.1 of its rear width just in front of palpebro-ocular ridge. Anterior pre-ocular part of glabella short, only some 0.25 of its total length. Front of glabella rounded; very short preglabellar field present. Three sets of glabellar furrows are present, 1S oblique, 2S straight and both sets contact axial furrows. 3S are poorly defined, arched anteriorly and do not appear to contact axial furrows. Occipital ring large, semi-elliptical, maximum width sagittally, decreasing to zero at axial furrows. Genal spine moderate length, 1.1 cranidial length, slightly curved, stout, base broad, level with posterior margin of cranidium.

Thorax of 10 segments, axis highly convex, tapers rearward to about 0.5 of its anterior width. Axial furrows deeply incised; apodemes present, well defined on anterior segments; pleural furrows oblique and deep, widest at fulcra, petering out toward adaxial

edge. First segment bears short pleural spine, second segment bears long curving pleural spine about 2.6 mm (1.3 cranidial length); other segments terminate in short spines. Fulcral points more pronounced in anterior segments, but still visible in rearmost segments. Distance of fulcra and fulcral lines from axial furrow about 0.6 of width of axial lobe in anterior part of thorax. Geniculation along fulcral line apparently steep, with pleurae sloping down at relatively steep angle.

Transitionary pygidium not preserved.

Meraspid 12 (AUGD1046-547, -590)

Description: Cephalon semi-elliptical; length 2.15 mm ( 0.76 cranidial width); border relatively flat, narrow sagittally, widening exsagittally, passing into long, curved genal spine about 2.0 mm long (0.95 cranidial length), intergenal spines absent; border approx. 0.25 of width of free cheeks at mid level across eyes. Marginal furrow distinct, narrow groove; rear margin of free cheek long, border narrow and elevated, meets posterior border of fixagene at angle of 145°; a posterior marginal furrow connects lateral marginal furrow of cheek in a nearly abrupt curve at genal angle. Posterior facial suture short and delineate very small postero-lateral limbs with tips extending only slightly beyond sagittal tangents of the palpebral lobes. Anterior facial suture diverges at 115-117°, curves slightly anteriorly towards antero-lateral margin. Cranidial rim relatively narrow and widens laterally, marginal frontal furrow sharply defined and broad. Inter-ocular cheek and palpebral lobe together wider than glabella. Eye lobes extend tangentially away from 3L for a short distance, to where the anterior facial suture and ocular lobe meet, posterior of this the eye lobe curves back, becoming strongly recurved distally, palpebral lobes arcuate, narrow, elevated and especially prominent towards rear, palpebral furrows moderately defined. Distance from anterior tip of palpebral lobe to glabella about 0.6 width of glabella at its widest. Distance between posterior eye lobe and axial furrow 0.30 cranidial length. Bacculae present as convex swellings close to occipital furrow. Occipital furrow convex anteriorly; lobe approx 0.25 - 0.3 glabella

length, width 0.9 glabella at its widest point. Occipital furrow deep, slightly shallower medially. Axial furrow at glabella flanks and front incised. Glabella long, around 2.0 of its width at rear and clavate, reaching its maximal expansion of about 1.3 of its rear width just in front of anterior palpebral lobes. Anterior pre-ocular part of glabella short, only some 0.23 of its total length. Front of glabella rounded, glabella does not contact rim and very short preglabellar field present. Three sets of glabellar furrows are present, 1S oblique, 2S straight and both sets contact axial furrows. 3S arched slightly forward and do not contact axial furrows. Occipital ring large, semi-elliptical, maximum width sagittally, decreasing to zero at axial furrows. Genal spine short, 0.8 cranidial length, stout, base broad, level with posterior margin of cranidium.

Thorax of 12 segments, axial lobe as wide as 0.33 of shield across middle and tapers rearward to about 0.44 of its anterior width. Axial furrows of thorax deeply incised at anterior and posterior margins of segment, shallowing medially, apodemes strongly defined on dorsal surface, pleural furrows oblique and moderately deep, widest at fulcra, petering out at adaxial edge. Second segment bears long curving pleural spine about 2.25 mm (1.05 cranidial length). Pleural extremities in anterior segments are deflected sideways but become somewhat fulcate in middle and posterior segments. Fulcral points, although more pronounced in anterior segments, still visible in rearmost segments. Distance of fulcra and fulcral lines from axial furrow about 0.65 of width of axial lobe in anterior part of thorax. Geniculation along fulcral line apparently steep, with pleurae sloping down at relatively steep angle. Plural guides probably present. Transitory pygidium poorly preserved, axis containing 2 annulations and blunt weakly bilobed terminus, axial furrows weakly defined. Posterior margin has four pygidial spines. Test smooth.

Holaspid (F16441)

Description: Cephalon sub-semicircular, length 5.8 mm in holotype (0.84 cranidial width, gradually increasing to 0.9 in holaspids of cranidial length 10 mm). Border

slightly elevated, narrow sagittally, widening exsagittally, passing into genal spine about 4.6 mm long (0.8 cranidial length), intergenal spines absent; border approx. 0.25 of width of free cheeks at mid level across eyes. Marginal furrow distinct, narrow groove; rear margin of free cheek long, border narrow and elevated, meets posterior border of fixigena at angle of 145°; a posterior marginal furrow connects lateral marginal furrow of cheek in a nearly abrupt curve at genal angle. Posterior facial suture short and delineate very small postero-lateral limbs with tips extending only slightly beyond sagittal tangents of the palpebral lobes. Anterior facial suture diverges at 115-117° in holotype, curves slightly anteriorly towards antero-lateral margin. Cranidial rim relatively narrow and widens laterally, marginal frontal furrow sharply defined and broad. Inter-ocular cheek and palpebral lobe together wider than glabella. Eye lobes extend tangentially away from 3L for a short distance, to where the anterior facial suture and ocular lobe meet, posterior of this the eye lobe curves back, becoming strongly recurved distally, palpebral lobes arcuate, narrow but becoming broader distally, elevated and especially prominent towards rear, palpebral furrows moderately defined. Distance from anterior tip of palpebral lobe to glabella about 0.62 width of glabella at its widest. Distance between posterior eye lobe and axial furrow 0.25 cranidial length. Bacculae present as convex swellings close to occipital furrow. Occipital furrow convex anteriorly; lobe approx 0.2 glabellar length, width 0.9 - 1.0 glabella at its widest point. Occipital furrow deep, slightly shallower medially. Axial furrow at glabellar flanks and front incised. Glabella long, approximately 1.8 of its width at the rear and clavate, reaching its maximum expansion of about 1.3 of its rear width level with the anterior palpebral lobes. Anterior pre-ocular part of glabella short, only some 0.23 of its total length and highly arched. Front of glabella rounded, glabella does not contact rim and short preglabellar field present; preglabellar field gently convex, sloping from preglabellar furrow and eye ridges to anterior border furrow. Three sets of glabellar furrows present, 1S oblique, directed backward at adaxial end, 2S straight and horizontal, both sets contact axial furrows. 3S arched slightly forward and do not contact axial furrows. Occipital ring large, semi-elliptical, maximum width sagittally, decreasing to zero at axial furrows. Genal spine

short, 0.7 cranidial length, stout, straight, wide base, level with posterior margin of cranidium.

Thorax of 13 segments (not 12 as originally designated by Pocock 1964), maximum width at level of 4th segment, becoming widest at the 5th segment with growth. Axial lobe tapers rearward to about 0.44 of its anterior width. Axial furrows of thorax deeply incised at anterior and posterior margins of segment, shallowing medially, apodemes strongly defined on dorsal surface, pleural furrows oblique and moderately deep, widest at fulcra, petering out at adaxial edge. No elongate pleural spines present in holaspid. Plural extremities in anterior segments are deflected sideways but become somewhat fulcate in middle and posterior segments. Fulcral points, although more pronounced in anterior segments, still visible in rearmost segments. Distance of fulcra and fulcral lines from axial furrow about 0.65 of width of axial lobe in anterior part of thorax. Geniculation along fulcral line raised, with pleurae sloping down at an angle. Pleural guides probably present.

Pygidium poorly preserved, sub-semicircular in shape axis containing 2 annulations and blunt weakly bilobed terminus, axial furrows weakly defined. Posterior margin has four pygidial spines.

Order NEKTASPIDA Raymond, 1920

Family NARAOIIDAE Walcott, 1912

**Naraoia** Walcott, 1912

Type species. *Naraoia compacta* Walcott, 1912, from the Middle Cambrian Burgess Shale, British Columbia, Canada.

*Naraoia* sp. 1. (Pls. 4.3, 8)

Material. AUGD1046-622, 575; from the Emu Bay Shale, Big Gully, Kangaroo Island.

Description. Anterior shield approximately semicircular, overlapping posterior shield, significantly wider than long (sag.) although this could be an artifact of preservation. Prominent doublure present along lateral margin. External surface appears smooth with no evidence of eyes or sutures. Possible antennae preserved as indentations in presumed ventral surface of anterior shield. Point of attachment appears to be at the antero-lateral margin of ?hypostome and appears to taper progressively, becoming smaller away from basal attachment; extending beyond lateral margin of the anterior shield as evidenced by the indentations intersecting the margin. Centrally positioned ?hypostome. Several possible crease marks indicate a possibly flexible, convex shield in life.

Posterior shield only very slightly longer (sag.) than maximum width and slightly longer than the anterior shield. Axial region visible, maximum width unknown but appears to be approximately one third of the width of the posterior shield. At least eleven segments visible on the axial region, exact number unknown. External surface appears smooth with no evidence of transverse or oblique furrows. A prominent doublure is present. Posterior margin of posterior shield and axial region not preserved.

*Naraoia* sp. 2. (Pl. 8)

Material. AUGD1046-575; 1046-628, from the Emu Bay Shale, Big Gully, Kangaroo Island.

Description. Anterior shield approximately semicircular, overlapping posterior shield, significantly wider than long (sag.). Thin doublure present along lateral margin. External surface appears smooth with no evidence of eyes or sutures. Possible antennae preserved as indentations in presumed ventral surface of anterior shield, extending beyond lateral margin of the anterior shield as evidenced by the indentations intersecting the margin. Several possible crease marks indicate a possibly flexible, convex shield in

life.

Posterior shield longer (sag.) than maximum width and significantly longer than the anterior shield. Axial region visible, maximum width appears to be approximately one fifth of the width of the posterior shield. Number of segments unknown. External surface appears smooth with no evidence of transverse or oblique furrows. A very broad, prominent doublure is present. Posterior margin of posterior shield and axial region end in blunt point.

| | |
|---|---|
| Phylum | SCHIZORAMIA |
| Subphylum | ARACHNOMORPHA |
| Class | UNCERTAIN |
| Order | UNCERTAIN |

**Xandarella** Hou *et al.*, 1991.

Type Species. *Xandarella spectaculum* Hou *et al.*, 1991, Early Cambrian, Chengjiang, China.

*Xandarella* sp. (Pls. 4.4, 9)

Material. AUGD1046-320, from the Emu Bay Shale, Big Gully, Kangaroo Island.

Description. Cephalon semicircular, (?)eyes small, placed laterally, equidistant between (?)hypostome and lateral margin of cephalon. 'Thorax' of seven tergites, each ending in broad-based spine, with possible pleural furrows present. Three 'abdominal' tergites present, but total number unknown. 'Abdominal' tergites longer sagittally than 'thoracic' tergites, also ending in broad-based spines. Posterior margin not preserved.

Phylum CRUSTACEA Pennant, 1777

Class UNASSIGNED

Order UNASSIGNED

Family UNASSIGNED

**Isoxys** Walcott 1890

Type Species. *Isoxys chilhoweanus* Walcott, 1890, Middle Cambrian, Burgess Shale, British Columbia.

*Isoxys communis* Glaessner 1979. (Pls. 4.5, 10.1-2)

Material. AUGD 1046-316, AUGD 1046-710, from the Emu Bay Shale, Big Gully Kangaroo Island

Description. Carapace large, elongate, length to height ratio 3.3-3.4. Hinge margin slightly convex in anterior portion of margin, ventral margin with brim. Anterior portion of ventral margin strongly convex, posterior portion of ventral margin almost straight, tapering towards posterior spine. Spines on dorsal margin extending anteriorly and posteriorly. Anterior spine possesses thicker spine base the posterior spine. Length of posterior spine varied, but anterior spine can be >0.33 length of carapace. Two large, globate, stalked eyes protrude from antero-ventral margin. Cuticle apparently smooth.

**Tuzoia** Walcott 1912

Type Species. *T. retifera* Walcott, 1912, Middle Cambrian, Burgess Shale, British Columbia.

*Tuzoia australis* Glaessner 1979. (Pls. 4.6, 10.3-4)

Material. AUGD 1046-315, -281 from the Emu Bay Shale, Big Gully.

Description. Bivalved carapace, 1.5 longer than high, straight hinge line ending in small subequal triangular projections. Evenly developed reticulate ornamentation, triangular tooth on postero-ventral margin. Lateral ridge present, parallel to hinge line, traversing almost full length of the valve, positioned centrally to slightly ventrally.

| | |
|---|---|
| Phylum | UNCERTAIN |
| Class | UNCERTAIN |
| Order | UNCERTAIN |
| Family | ANOMALOCARIDIDAE Raymond 1935 |

**Anomalocaris** Whiteaves, 1892

Type Species. *Anomalocaris canadensis* Whiteaves, 1892

*Anomalocaris briggsi* sp. nov. (Pls. 5.1, 11, 13)
1993 *Anomalocaris* sp.; McHenry & Yates, p. 81, figs. 2-9.

Etymology. For D. E. G. Briggs.

Material. Holotype, AUGD1046-630; paratype: AUGD1046-335, from the Emu Bay Shale, Big Gully, Kangaroo Island. Other material P34554, P31953; AUGD- 340, 638 from the Emu Bay Shale, Big Gully.

Description. Appendage evidently of 14 segments, most specimens incomplete or too

poorly preserved to tell whether this number varied. Appendage predominantly straight, tapered distally with minor ventral curvature at the distal end. Longest segments positioned medially. Dorsal and lateral cuticle unadorned except where dorsal margin of segments 12 and 13 are produced distally into small dorsal spines. Intersegmental margins exhibit slight, proximally concave, arc at dorsal margin, indicating possibly sub-circular original aspect. A narrow triangular area, apex dorsal, occurs along the proximal margin of the segments, presumably facilitating movement and may represent an area of thinner, flexible cuticle. Segment 1 bears a pair of dagger-like, stout ventral blades, which curve distally and bears several minor teeth on its distal margin. A pair of slightly proximally curved spines projects from ventral margin of segments 2 to 13, always longer than the height of segment bearing it. Each pair of ventral spines bears a pair of ventrally positioned auxiliary spines. The distal margin of each ventral spine along with the upper, proximal margin and adjacent ventral segmental margin, appears spinulescent. Poor preservation limits resolution of the exact number of spinules or how this number varied. The ventral tips of the spines are poorly preserved. Segment 14 bears two terminal spines, the dorsal being more elongate relative to the ventral and while preservation is poor, both spines appear to bifurcate at the distal tip. In some specimens segment 1 appears continuous with indistinct cuticle, thought to represent the attachment to the body.

*Anomalocaris* sp. (Pls. 5.2, 12)

1991 *Anomalocaris canadensis* Whiteaves; Hou & Bergström 1991, p. 185-186, pl.2, figs 2,3.

1994 *Anomalocaris* sp. Chen *et al.* 1994, figs 1,2.

Material. AUGD1046-346, -600, from the Emu Bay Shale, Big Gully, Kangaroo Island.

Description. Appendage evidently of 14 segments. Appendage strongly recurved,

tapered distally with minor ventral curvature at the distal end. Longest segments positioned proximally. Dorsal and lateral cuticle unadorned except where dorsal margin of segments 9 to 14 were produced distally into small dorsal spines. Intersegmental margins exhibit slight, proximally concave, arc at dorsal margin, indicating possibly sub-circular original aspect. Segment 1 bore an enlarged pair of ventral spines, which curved slightly distally. Other segments, apart from the 14th, bore a pair of ventral spines at a point close to the distal margin of the segment and always equal to, or shorter than the height of the segment which bore them. These spines alternated in length on successive segments; those borne on the odd segments being consistently longer than those on the even. Each pair of ventral spines bore a pair of ventrally positioned auxiliary spines, below this the ventral spine tapered rapidly. A narrow triangular area, apex dorsal, occurs along the proximal margin of the segments, presumably facilitating movement and may represent an area of thinner, flexible cuticle. The distal segments are poorly preserved, but segment 14 appears to have borne two terminal spines. Segment 1 appears continuous with indistinct cuticle, but the attachment to the body remains obscure.

| | |
|---|---|
| Phylum | ARTHROPODA? |
| Class | UNCERTAIN |
| Order | UNCERTAIN |
| Family | UNCERTAIN |

**Myoscolex** Glaessner, 1979

Type species. *Myoscolex ateles* Glaessner, 1979, from the Early Cambrian Emu Bay Shale, Kangaroo Island, South Australia.

*Myoscolex ateles* Glaessner 1979. (Pls. 5.3-6, 14, 15)

Material. AUGD1046-239, -611, -646, -648, -725; P21029, from the Emu Bay Shale, Big Gully, Kangaroo Island.

Description. Trunk tapers abruptly anteriorly into a short projection flanked distally by two merging sub-circular features, possibly eyes. Possible proboscis-like structure, annulated proximally, curving backward along the side of the trunk, distally terminating in possible spines.

There is no evidence that the body posterior of the head is divided into tagmata. Body cigar-shaped, normally straight or very slightly curved, rarely pronounced curvature occurs. The maximum height well anterior of the mid-length. The trunk tapers very gradually posteriorly; the structure of the tail region is essentially unknown. Trunk composed of segments separated by deep grooves. Number variable, length of segments increasing with size of animal. Narrow bands of muscle present running parallel to the axis of the body, along both dorsal and ventral margins of the trunk. These are separated by wider bands of muscle running at a high angle to the body axis.

Ventrally positioned flap-like structures, straight along anterior margin, curved convex backwards on the posterior, convex upward.
Curved, robust, segmentally arranged, smooth rod-like structures extending ventrally only. Set at angle to the segment boundaries, sloping forward and downward

| | |
|---|---|
| Phylum | ARTHROPODA? |
| Class | UNCERTAIN |
| Order | UNCERTAIN |
| Family | UNCERTAIN |

**Opabinia** Walcott, 1912

Type species. *Opabinia regalis* Walcott, 1912, from the 'Phyllopod bed', Burgess Shale, British Columbia.

cf. *Opabinia* Walcott 1912. (Pl. 16)

Material. AUGD1046-240, from the Emu Bay Shale, Big Gully, Kangaroo Island.

Description. Specimen is poorly preserved, but appears to be divided into a cephalon and trunk. The trunk is divided into 15 segments, each of which terminates in an apparently structureless lateral lobe. Segmental boundaries appear strongly defined and curved, but do not reach the dorsal margin. Segments appear largest just anterior of medially, tapering anteriorly and posteriorly, although tapering is more pronounced anteriorly. Nothing is preserved posterior of the 15th segment.

The cephalon appears to taper anteriorly into a tubular frontal process, only the proximal portion of which is preserved. No eyes are evident.

# Chapter 4: Geochemistry of the Emu Bay Shale Lagerstätte at Big Gully

*"It is better to study the changes in the data which are preserved than to bemoan that which has been lost."*

(Wignall 1990a, p. 16)

## 4.1 **Introduction**

In recent years, the upsurge in oceanographic research has provided a greatly enhanced understanding of the precipitation of minor and trace elements under the differing redox conditions in the ocean environment (e.g. Goldberg & Arrhenius 1958; Boyle *et al.* 1976; Calvert & Price 1977; Brutland 1980; Klinkhammer *et al.* 1982; Piper 1988). This work has clearly shown that seawater provides a major component of the minor and trace elements present in sediments, and that the concentrations of minor and trace elements are influenced by the depositional environment. However, does this permit the accurate reconstruction of past environments? Does the depositional environmental 'signature' survive early diagenesis in sediments, not to mention lithification and rock forming processes, and thus have the potential to assist in delineating ancient depositional environments?

Geochemical analyses of modern and ancient shales show that ancient shales often exhibit extreme enrichment of certain trace elements, far in excess of enrichments occurring today (e.g. Brumsack 1989). Several environmental conditions have been suggested to account for these anomalous concentrations, with anoxic, or in some instances oxic, conditions being largely accepted as essential to promote enrichment (e.g. Demaison & Moore 1980). Recently it has been suggested that enrichment can occur in

other environments, such as upwelling zones (Calvert & Pederson 1993; Piper 1994). A major problem in this debate is the difficulty in deducing the original depositional settings. The utilisation of normalised Mn v. Mo plots used here represents a novel approach to answering this question, as it appears to differentiate between oxic, suboxic and anoxic depositional environments.

While the use of such apparently diagnostic, minor and trace elements might well be useful, it is important to understand the factors which control the physical and chemical characteristics of near shore marine sediments before utilising such data to interpret ancient depositional environments.

Marine sediments are highly fractionated crustal materials, supplied to the ocean from a number of different sources. Nearshore sediments in particular are very heterogenic and are important removal sites for several elements in sea water due to the rapid accumulation rate and physio-chemical conditions being different from the open ocean (Calvert 1976). The minor and trace elements in such sediments are thus controlled, both by the terrigenous material via riverine and eolian transport, and marine volcanic debris; and by seawater-derived material such as metal oxides, hydroxides or sulphides and absorbed phases (hydrogenous factors), as well as $CaCO_3$, opal and organic material (biogenic factors) (Piper 1994).

The composition of the detrital fraction represents the provenance from which the debris is derived. The influence of sedimentary detritus upon minor and trace elements in fine grained, marine sediments can be quantified by normalising elemental concentrations against average shale values (Wedepohl 1971; Taylor & McLennan 1985). These average values effectively represent the composition of the solid fraction being eroded from the continents and thus are representative of minor and trace element concentrations entering the marine environment via sediment debris. This allows the elemental concentration of the marine sediment to be compared with concentrations expected from

detrital influences alone. Any depletion and/or enrichment due to other factors and sources can therefore be identified.

The composition of the seawater-derived fraction is, on the other hand, highly dependent on the chemical conditions pertaining during deposition. Therefore, an understanding of the chemical conditions found in the marine environment is needed before it's influence upon minor and trace element accumulations can be established.

## 4.2 Chemical conditions in the marine environment

The modern ocean is generally stratified with respect to density, temperature, salinity and light. Biological activity is most prolific within the surficial photic zone. The oxygen concentration in the water column varies significantly with depth (Fig. 4.1). The upper waters (≈ 0-500 m) are oxygenated by turbulent mixing with the atmosphere. For averaged modern ocean conditions the saturated oxygen concentration is 7.45 ml $l^{-1}$. However, the mean oxygen concentration is 3.3 ml $l^{-1}$ (Quinby-Hunt & Turekian 1983), less than half the saturated value. This variation is due to the balance between photosynthesis (net oxygen production) and respiration/decay (net oxygen utilisation). Since the present atmospheric level (PAL) of oxygen is 200 ml $l^{-1}$, it can be seen that the saturation concentration of dissolved oxygen in the modern ocean is less than 5% of the concentration in the atmosphere.

The value of dissolved oxygen in the surface layers declines from close to oversaturation (in areas where photosynthesis outstrips respiration) near the surface, to a minimum value that is both a function of the utilisation of oxygen by decaying organic matter sinking from the surface (Berry & Wilde 1978; Chester 1990), and the lack of photosynthesis. This decline in dissolved oxygen has been quantified by Richards (1965) (eq. 4.1). An example is the Northern Peru upwelling zone where an

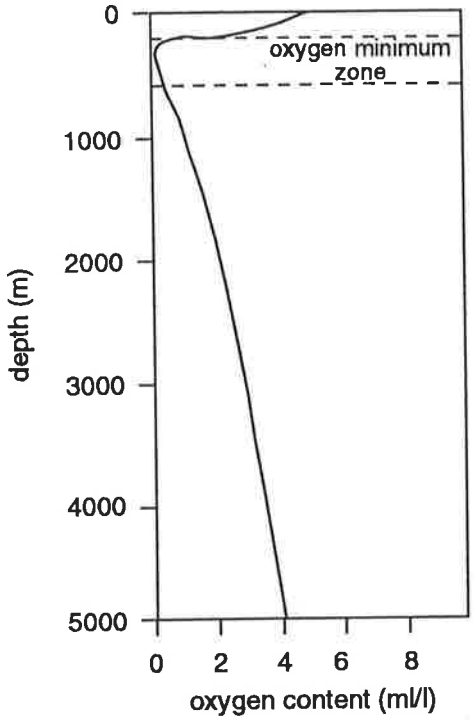


**Fig. 4.1** Change in the amount of dissolved oxygen with depth, showing the position of the Oxygen Minimun Zone. (after Ingmanson & Wallace 1985)

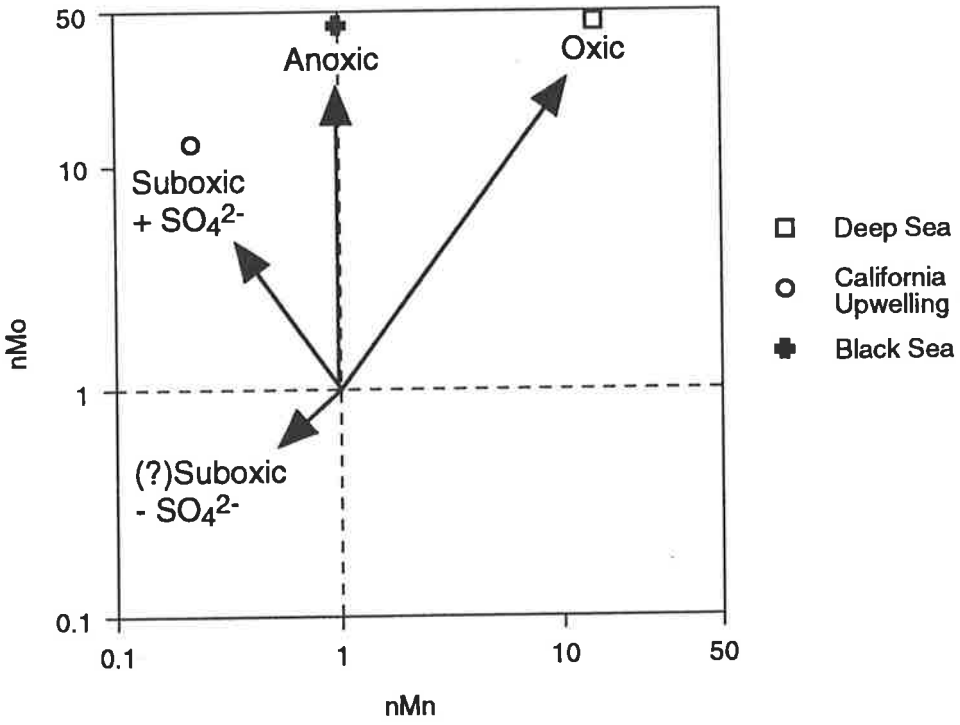


**Fig. 4.2** Plot of nMo/nMn values from the deep sea (oxic), California upwelling zone (suboxic) and the Dead Sea (anoxic), showing that nMo/nMn plots can be used to resolve depositional environment based on bottom water dissolved oxygen levels.

$$(CH_2O)_{106}(NH_3)_{16}(H_3PO_4) + 138O_2 \rightarrow 106CO_2 + 122H_2O + 16HNO_3 + H_3PO_4 \quad [4.1]$$

oxygen deficient zone between 100 - 400 m is present (Packard *et al.* 1983). Below this Oxygen Minimum Zone, the value of dissolved oxygen increases with depth (Fig. 4.1) due to the ventilation from deep waters (Wyrtki 1962). This deep ventilation is a result of effects at the surface in high latitudes during winter (Berry & Wilde 1978).
The water column above the majority of modern deep water sediments is rich in dissolved oxygen which provides oxygen for both epi- and infaunal animals, leading to the bioturbation of deep sea sediments (Menzies *et al.* 1973). Also the positive Eh or oxidising chemical potential means that most modern, open ocean sediments are oxidised (Berry and Wilde 1978). A highly negative Eh or reducing chemical potential is required to preserve organic matter. In the modern environment, this preservation occurs primarily in nearshore areas, where a combination of high organic content in sediments, anaerobic bacteria and little or no oxygen, is found (Berger 1976; Berry & Wilde 1978) and in restricted basins such as the Black Sea (Richards 1965).

In Oxygen Minimum Zones, where the concentration of dissolved oxygen falls below ≈ 0.2 ml $l^{-1}$ (the Pasteur Point, the minimum concentration of oxygen needed for aerobic respiration), the marine organisms inhabiting the area must respond to the changing environment.in order to avoid death. Thus organisms migrate out of the zone, encyst, or switch their respiratory chemistry from an oxygen-based oxidation to another oxidation system. In the modern ocean, the thermodynamic sequence of available oxidants, after free oxygen, are the oxygenated nitrogen species, followed by $MnO_2$, $Fe_2O_3$ and then the oxygenated sulfur species, principally sulphate (Chester 1990; Wilde *et al.* 1990b; Allison & Briggs 1991) (eq. 4.2),with hydrogen sulphide produced as a

$$(CH_2)_{106}(NH3)_{16}H_3PO_4 + SO_4^{2-} \rightarrow CO_2 + HCO_3^- + HS^- + 16NH_3 + H_3PO_4 \quad [4.2]$$

by-product of sulphate reduction (Froelich *et al.* 1979). In anoxic basins such as the Black Sea, the concentration of dissolved hydrogen sulphide can reach levels of 425 μM (Murray *et al.* 1989).

Thus the ocean environment experiences chemical (or redox) conditions varying from fully oxic, in shallow waters and in the deep sea, to dysaerobic, in Oxygen Minimum Zones, to anoxic in restricted basins and rarely below Oxygen Minimum Zones. Organic matter is the primary reducing agent in the oceans, with $O_2$, $NO_3^-$ and $SO_4^{2-}$ being the most important electron acceptors. The hierarchy of these reactions is determined by the reaction yielding the greatest free energy per mole of carbon used (Froelich *et al.* 1979). Thus, oxygen respiration (eq. 4.1) proceeds until the concentration of $O_2$ decreases to a point at which denitrification yields equal free energy and so on (Piper 1994).

The concentrations of minor and trace elements reflect a range of chemical, oceanographic and sedimentary controls. Of these, the chemical controls appear to be the most important in the partitioning of minor and trace elements, and in particular the redox conditions of the water column. Many minor and trace elements have multiple valency states characterised by solubilities that vary with dissolved oxygen levels, or are partitioned between the solid and solution phases to different extents under different redox conditions (Calvert & Pederson 1993). Behavioural characteristics of minor and trace elements in modern sedimentary settings, where the chemical environment is known, can result in a distinctive signature. This signature may be diagnostic for a particular chemical state of the environment of deposition and provide information of the depositional and chemical environment of ancient sediments, provided these sediments retained the original minor and trace element abundances.

Those rocks most likely to retain the original depositional minor and trace element signal are those which incorporate a relatively high marine fraction. These are metalliferous shales, phosphorites and sediments which accumulated under conditions of primary productivity. The content of minor and trace elements in these sediments, above levels

which can be assigned to a detrital fraction, is attributable to the accumulation of biogenic debris (organic matter) and the precipitation and/or absorption of minor and trace elements from seawater under various redox potentials (Piper 1994). Recent interest in the environment of deposition of organic-rich rocks has focused attention on the mechanisms of organic enrichment in marine sediments. It has been widely accepted that anoxic bottom waters are needed to preserve deposited organic matter, namely anoxic basins or beneath Oxygen Minimum Zones (e.g. Demaison & Moore 1980). For example, finely laminated, pyrite-rich and organic rich Cretaceous shales have been associated with a stagnant ocean (de Graciansky *et al.* 1984), or, where they occur on basin margins, assigned to enhanced and expanded Oxygen Minimum Zones (Schlanger & Jenkyns 1976). However, the presence of alternating black and green or red shales and marls in some areas have necessitated the invoking of repeated episodes of oxic and anoxic conditions. This appears to be a case of forcing the interpretation of the depositional environment to be consistent with a model linking enhanced accumulation of organic matter with water column anoxia. The view of Parrish (1982), that enhanced preservation of organic matter can be explained by deposition under sites of upwelling, negates the need for water column anoxia. This, along with the models of Sarmiento *et al.* (1988) casting doubt on the probability of deep water anoxia in the Cretaceous ocean, indicates that water column anoxia may be unnecessary for enhanced organic matter preservation (Pederson & Calvert 1990), or for the enhancement of minor and trace element concentrations. It is becoming increasingly apparent that organic-rich sediments can be formed under oxic conditions, below zones of increased primary production within the photic zone, where the increased settling and burial flux of organic matter leads to its preservation (Calvert & Pederson 1993).

Studies on element geochemistry show that recent and ancient sediments with high total organic carbon (TOC) values are often enriched in specific trace elements such as copper, molybdenum, nickel, vanadium, zinc etc. (Brumsack 1980, 1989). If this enrichment is of a syngenetic origin, then a relationship between the palaeoenvironment of deposition,

fauna, tectonic position and oceanographic parameters should exist (Vine & Tourtelot 1970, Brumsack 1989).

In practice, two differing palaeoenvironments which support the production of a TOC-rich sediment may be delineated, and these have characteristic chemical, oceanographic and biological parameters. By far the most important factor is that a significant fraction of the organic matter which is being produced in the photic zone, or is brought in from elsewhere, must survive depositional transit through the water column and the benthic boundary layer. Once buried, the preservation potential of the organic matter is much higher. This survival may be achieved by either decreasing the residence time in the water column or at the sediment water interface, or reducing the level of oxygen available (Brumsack 1989).

The first condition can occur in areas of high primary productivity, or upwelling zones. High productivity leads to an increase in the amount of organic matter impinging on the sediment surface and concomitant rapid burial, resulting in increased preservation. commonly, in such areas, biological activity produces an Oxygen Minimum Zone, in which the dissolved oxygen level may fall to 0.1 ml $l^{-1}$ (Berry & Wilde 1978; Chester 1990). In this environment it is the sediment which is anoxic rather than the water column, as the burial rate of organic matter exceeds the rate of oxygen replenishment from bottom waters by diffusion or irrigation (Calvert & Pederson 1993).

The second exemplar occurs in anoxic environments such as the Black Sea. Here, oxygen is absent from the deeper waters, allowing hydrogen sulphide to diffuse upward from the sediment into the water column and to be produced within the water column by the active reduction of sulphate. This environment commonly occurs where a topographical barrier restricts the replacement of deep water so that the rate of dissolved oxygen consumption exceeds the rate of replenishment. (Anderson 1987; Richards 1965). Preservation of organic carbon under such anoxic conditions can be high, even if productivity is low (Anderson 1987) and such sediments often exhibit evidence of long residence times.

The minor and trace element chemistry of recent sediments may provide the tools to extract information regarding the palaeoenvironment of fossil organic-rich sediments (Brumsack 1989). In many settings, the reasons for minor and trace element enhancement in sediments remains equivocal. Such enhancement, above levels which can be attributed to detrital input, have been attributed to local hydrothermal input of minor and trace elements (Arrhenius & Bonatti 1965) or unusual chemical conditions and/or severe water column anoxia in the open marine environment. Recent work has indicated that hydrothermal input or unusual conditions are not only exceedingly rare, but are not necessary for minor and trace element enrichment to occur (Packard *et al.* 1983; Calvert & Pederson 1993; Piper 1994). Thus enrichment can be brought about by the accumulation of biogenic debris, and the precipitation and/or absorption of elements from seawater under differing redox conditions commonly found in the present marine environment.

If minor and trace elements are to be used as indicators of past depositional environments, then their properties under differing redox conditions need to be established.

## 4.3 Geochemical Significance of Certain Elements

### 4.3.1 Manganese

Manganese involved in the geochemical cycle has two main sources, as oxide coatings on particulate material delivered by wind or rivers; and via diffusion from shelf sediments. Surface waters are normally enriched in manganese and the element is scavenged throughout much of the underlying water column (e.g. Bender *et al.* 1977). A dissolved manganese maximum is often observed coincident with the Oxygen Minimum Zone, wherever oxygen concentrations fall below 100 $\mu m\ l^{-1}$. This correlation

has been ascribed to reduction, and hence dissolution, of manganese oxyhydroxides from settling particles and/or from dissolved manganese diffusing out of anoxic shelf and slope sediments (Klinkhammer & Bender 1980). Johnson *et al.* (1992) showed that this anoxic shelf and slope source is inadequate to account for the concentration of dissolved manganese found within the Oxygen Minimum Zone and concluded that processes within the water column must be responsible.

Dissolved Mn (II) accumulates in the deep sulphide-rich waters of anoxic basins due to the reduction of Mn (IV) oxides settling from overlying aerobic waters. Concentrations of manganese are commonly higher immediately below the oxygen/sulphide boundary than in deeper waters. This is due to the reduction and dissolution of insoluble manganese oxides on settling particulate matter from a particle concentration maximum just above the oxygen-sulphide boundary. This maximum is the result of the oxidation and precipitation of upwardly diffusing Mn (II) from the anoxic waters (Calvert & Pederson 1993). Manganese, therefore, displays an active redox recycling of oxidized and reduced forms across the redox boundary within the Oxygen Minimum Zone.

Manganese is concentrated in the aerobic sediments of the deep sea and in surface sediment horizons of the continental shelf. In these sediments, solid manganese occurs as the oxyhydroxides $MnO_2$ and MnOOH (Murray *et al.* 1984). The enrichment of manganese in pelagic sediments is due to the slow accumulation rates of terrestrial and biogenic particulate matter relative to the precipitation of $MnO_2$ and winnowing of Mn-bearing fine particles allowing the build-up of $MnO_2$ in the surficial sediments. A similar mechanism was suggested for manganese enrichment in the Holocene sediments of Sigsbee Knoll, in the Mississippi Delta area of the USA (Trefry & Presley 1982). The small settling rate of organic particulate matter, coupled with its often extreme refractory nature, ensures that aerobic conditions are maintained, often to great depth within the deep sea sediments (e.g. Canfield 1989a; Thomson *et al.* 1993).

In continental margin environments where the accumulation of organic matter is higher, oxygen is completely consumed at relatively shallow depths within the sediments. Burial of surface oxyhydroxides transports Mn (IV) into the reducing environment, where it

dissolves. Trefly & Presley (1982) found a 45% decrease in manganese levels in rapidly deposited Mississippi delta sediments compared with river suspended matter. This depletion was caused by the mobilisation of manganese in the suboxic sediments as a result of $MnO_2$ reduction and the subsequent flux of reduced manganese out of the sediments. The concentration of reduced Mn (II) is therefore usually much higher in pore waters of sediments immediately below horizons which contain oxyhydroxides. Dissolved Mn (II) diffuses downward into the anoxic sediments and upward into the overlying aerobic zone. Here it is oxidized and precipitated as $MnO_2$ and MnOOH (Froelich *et al.* 1979). This zonal refining results in a surficial solid manganese concentration that is often much higher that in pelagic sediments (Calvert & Pederson 1993). Burial of this manganese-rich layer results in greatly enhanced pore water concentrations of dissolved manganese in the anoxic sediments underlying surficial, aerobic sediments. In some instances, the concentration of dissolved manganese may reach levels where the ion activity product of Mn (II) and dissolved bicarbonate exceeds the solubility product of the carbonate phase and $MnCO_3$ (rhodochrosite) is precipitated. In fact, Mn (II) carbonates commonly form in such settings (Calvert & Price 1970, Shimmield & Price 1986). This is due to the manganese pump, which delivers abundant reducible Mn (IV) to the anoxic horizon. Where such authogenic carbonates are below detection limits, pore water manganese profiles commonly show clear evidence of manganese removal from the sediments (Calvert & Price 1972). The carbonate precipitated is invariably a mixed Mn-Ca phase rather that pure rhodochrosite. The presence of $CaCO_3$ can also lead to manganese enrichment, since $CaCO_3$ can act as a preferred surface for the catalysis of $MnO_2$ precipitation (Trefry & Presley 1982).

In environments where the bottom waters are anoxic, the accumulation of dissolved manganese does not reach the levels that would permit the precipitation of a Mn (II) solid, either in the water column or within the underlying sediments. Under these conditions, any solid manganese concentration is controlled entirely by the aluminosilicate fraction (Calvert & Pederson 1993).

From these considerations, it can be concluded that high sedimentary concentrations of

solid manganese in the form of Mn-carbonate is indicative of the sediment originally accumulating under oxic bottom waters. This can be explained due to the fact that the mechanism for increasing the concentration of dissolved manganese in sediment pore waters only operates where the surface sediments accumulate manganese oxyhydroxides. These are pumped into the subsurface horizons on burial (Calvert & Pederson 1993). This can only occur beneath oxygenated bottom waters.

By contrast, where bottom waters are anoxic, the surface sediments are in contact with sulphidic waters. These sediments do not, then, have authigenic manganese enrichment due to the fact that no effective mechanism exists for producing dissolved manganese concentrations which could exceed the solubility product of $MnCO_3$. Similarly, Mn-carbonates cannot be precipitated from waters within the Oxygen Minimum Zone. While such waters contain elevated concentrations of dissolved manganese (Klinkhammer & Bender 1980), the concentrations are still several orders of magnitude lower than that required for the precipitation of Mn-carbonates (Calvert & Pederson 1993).

### 4.3.2 Molybdenum and Uranium

These elements are grouped together because of their conservative behavior in the ocean. Their concentrations are more or less constant from ocean to ocean and with water depth (e.g. Morris 1975; Ku *et al.* 1977; Collier 1985). The uptake by plankton in the photic zone and remineralisation at depth are insufficient to affect its vertical distribution in the water column (Piper 1994). This consistency is due to the unreactive nature of the dissolved species, $MoO_4^{2-}$ and $UO_2(CO_3)_3^{4-}$, in oxygenated sea water (Calvert & Pederson 1993). While these elements show a lack of chemical reactivity under aerobic conditions, they are enriched to a greater extent in anoxic sediments relative to almost all other elements. This provides potential for them to be used as indicators of anoxia.

In sulphidic waters, molybdenum may exist as the (V) species $MoO^{2+}$, as the thiooxymolybdate species $MoO_2S_2^{2-}$ and as the insoluble (IV) phase $MoS_2$ (Brutland 1983; Emerson & Huested 1991). Accordingly, dissolved molybdenum concentrations

tend to decrease in the deeper sulphidic waters of anoxic basins. However, concentrations vary widely in individual settings, with no relationship between dissolved molybdenum and dissolved sulphide levels. This is possibly due to removal of molybdenum into anoxic sediments (Emerson & Huested 1991).

In marine sediments, the geochemistry of molybdenum is known to be related to manganese. Molybdenum is also known to be greatly enriched in the sediments of anoxic basins (Calvert & Pederson 1993). In contrast to the conservative behavior and its speciation in oxygenated sea water, molybdenum is significantly enriched in ferromanganese nodules and in surficial manganese oxyhydroxides in nearshore sediments (Calvert & Price 1977, Shimmield & Price 1986), in the absence of dissolved sulphide. Molybdenum is released from the solid phase when manganese oxyhydroxides are reductively dissolved during burial in more reducing sediments. Where dissolved sulphide occurs, dissolved molybdenum is removed. Molybdenum may possibly form a separate insoluble sulphide phase, possibly $MoS_3$, when FeS is converted to pyrite (Berner 1984). It is also possible that the reduced form $MoO^{2+}$ is more effectively scavenged by negatively-charged organic matter than the oxidized form $MoO_4^{2-}$ (Bertine 1972). The bottom anoxic sediments of Saanich Inlet, British Columbia, exhibit great enrichment of molybdenum (128 ppm) compared with a concentration of molybdenum in settling particulate matter of < 5 ppm (Francois 1988). These findings suggest that dissolved sulphide must be present in bottom sediments for significant enrichment to occur. It is possible that molybdenum released during sulphide diagenesis may be taken up or associated with the higher molecular weight organic fraction ( Pilipchuk & Volkov 1974; Malcolm 1985).

Molybdenum signals oxygenated bottom waters (e.g. Pederson 1988), contrary to previous suggestions nominating anoxic or suboxic bottom waters (e.g. Emerson 1985). Dissolved uranium concentrations are slightly lower in the suboxic and anoxic waters in Saanich Inlet (Todd *et al.* 1988) and 30% lower in the anoxic water column of the Black Sea (Anderson *et al.* 1989), compared with oxygenated waters. This suggests that uranium is being removed from the water column in these basins. However, the

oxygenation state of uranium is almost entirely U (VI) throughout the anoxic waters (e.g. Anderson *et al.* 1989). The unreactive nature of uranium in these anoxic basins is confirmed by the fact that little authigenic uranium is found in settling particulate matter. One explanation for the lack of U (VI) reduction to U (IV) in these sulphidic waters, despite the fact that it is thermodynamically favoured, might be that particulate surfaces are required to catalyze the reaction. If this is so, then the reaction would be more likely to proceed in the bottom sediments. Allied to this is the possibility that, although non-enzymic reduction of U (VI) by sulphide has been the traditional explanation for U (VI) reduction in anoxic sediments, recent studies have demonstrated that enzymic reduction by U (VI)-reducing microorganisms is a more likely mechanism (Lovely & Phillips 1992). This mechanism would be favoured in the sediments compared with the water column due to much higher concentrations of bacteria in surface sediments (Kris 1963). Uranium also appears to be removed from oxygenated bottom waters by diffusion across the sediment/water interface into organic-rich, continental margin sediments. Klinkhammer & Palmer (1991) showed a decrease with depth of uranium dissolved in pore water and a concomitant increase in the solid phase precipitated uranium in suboxic sediments, probably occurring where sulphate reduction begins. There is no requirement for bottom waters to be fully anoxic to explain uranium enrichment. An increase in the carbon flux is required, whether by a decrease in clastic input or increased productivity. With increased productivity such as in upwelling zones, a reduction in the dissolved oxygen concentration is likely.

### 4.3.3 Chromium and Vanadium

These elements occur in sea water in several oxidation states (Murray *et al.* 1983), with Cr (VI) making up 95% of total chromium. With more reducing conditions V (IV) and V (III) are more stable and chromium exists as the Cr (III) ion ($Cr(H_2O)_4(OH)_2^+$) under denitrification conditions (Murray *et al.* 1983). Aging leads to the complex forming insoluble $Cr(OH)_3$ (Calvert & Pederson 1993). With high concentrations of dissolved

sulphide, V (IV) is reduced to V(III) which precipitates as $V_2O_3$ or $V(OH)_3$ (Wanty & Goldhaber 1992), indicating the possibility of removal of vanadium in to the sediment under anoxic conditions.

The vertical distribution of dissolved chromium and vanadium in the ocean shows modest depletion in surface waters, indicative of removal by biological processes. A relatively small increase in concentration with depth for chromium, is suggestive of regeneration within the water column. Vanadium, however, shows a relatively consistent concentration with depth (Collier 1985). In anoxic conditions, chromium and vanadium are rapidly reduced and removed from solution, probably by adsorption onto particulate surfaces (Emerson *et al.* 1979; Emerson & Huested 1991).

The behavior of chromium and vanadium indicates that they should be removed from sea water into anoxic sediments due to the fact that the reduced species of both elements precipitate as sparingly soluble oxides/hydroxides or are strongly absorbed onto particulate matter.

### 4.3.4 Copper, Nickel and Zinc

These chalcophyle elements are commonly enriched in sedimentary rocks as disseminated sulphides, especially in black shales. Nickel and zinc behave as micronutrients, being depleted in surface waters by plankton uptake and exhibiting a linear relationship with the major nutrients $PO_4^{3-}$ and $NO_3^-$ (Collier 1985) Liberation from settling organic debris in the water column results in increasing concentrations with depth (Calvert & Pederson 1993). Copper is somewhat unique amongst trace elements in sea water as it behaves partially like a micronutrient, but is scavenged from solution in deep water. Its depth distribution shows only a slight surficial depletion compared with the other nutrients. This is due to the fact that the concentration of copper in the water column is much higher than that needed for plankton growth (Piper 1994). Below the photic zone, a more or less linear increase in concentration with depth occurs, leading to high concentrations in bottom waters (Collier 1985; Piper 1994), implying a sediment

source (Boyle *et al.* 1981).

Measurements of dissolved copper, and zinc levels in anoxic basins, such as the Cariaco Trench, Framvaren Fjord, Saanich Inlet and the Black Sea, indicates levels decrease by a factor of 2 to 10 in anoxic waters compared with levels in overlying oxygenated waters (e.g. Jacobs *et al.* 1987, Landing & Lewis 1991). This decrease appears due to the precipitation of the respective sulphides in the presence of dissolved sulphide in the anoxic waters. However, nickel does not show any decrease in concentration in anoxic waters possibly reflecting the need for solid surfaces to initiate precipitation (Calvert & Pederson 1993). Therefore, bottom sediments of anoxic basins should display enrichment of at least copper and zinc above the levels of detrital sediment input.

Copper, nickel and zinc are enriched in the bottom sediments of some anoxic basins, although not all basins show significant enrichment for these metals (Jacobs *et al.* 1987). These differences in enrichment patterns are due to a balance between detrital aluminosilicate supply to the sediments and the magnitude of transport of authigenic fractions of the metals from the oxic waters to the deep anoxic waters of the basins (Jacobs *et al.* 1987). Since the enrichment process is diffusion dependent, low sedimentation rates will maximise residence time, thus maximising enrichment. Authigenic copper, nickel and zinc appear to be added to the solid fraction of many nearshore sediments by the diffusion of the dissolved metals from the overlying oxygenated waters or pore waters into the subsurface anoxic horizons.

The burial of large amounts of organic matter will produce a redox boundary at relatively shallow depths. This can result in the enrichment of copper, nickel and zinc as sulphides in the sediments (Calvert & Pederson 1993). Studies on the sediments of the Southern California Borderland suggest that copper is being released from organic carriers into pore waters within surficial sediments and fixed in underlying anoxic sediments (Shaw *et al.* 1990). Copper appears to be less sensitive to redox conditions

sediments (Shaw *et al.* 1990). Copper appears to be less sensitive to redox conditions than other elements and an important fraction of copper is added to sediments due to its binding capacity with sediment (Shaw *et al.* 1990). Thus copper may be enriched in rapidly deposited sediments regardless of redox conditions. Nickel, on the other hand, is strongly associated with surface oxyhydroxides and while not enriched in pore waters, is released upon the burial of the oxyhydroxides into the anoxic zone, where the oxyhydroxides are dissolved. This process pumps nickel into the anoxic environment where it is precipitated. Shaw *et al.* (1990) found that solid state phase enrichment of nickel and copper was positively linked to bottom water oxygenation. The largest enrichment occurring where the bottom water level of dissolved oxygen was highest.

### 4.3.5 Phosphorus

Phosphorus is an essential nutrient and its availability in seawater is considered a dominant factor in limiting marine biological productivity (Holland 1978; Smith 1984). Organic phosphorus is quantitatively one of the most important reservoirs in marine sediments as organic matter is often the principle carrier of phosphorus to the sediments (Froelich *et al.* 1982). Another method of supplying phosphorus to the sediments is by the authigenic production of solid phase phosphates, with phosphorus derived originally from sea water.

Under oxic conditions iron from detrital sources complexes to produce iron oxyhydroxide (FeOOH). Dissolved phosphate strongly absorbs onto FeOOH and precipitates with it into the surface sediments as $FeOOH{\cdot}PO_4$ (Froelich *et al.* 1988; Ruttenberg & Canfield 1988; Heggie *et al.* 1990; Ingall *et al.* 1993). As the $FeOOH{\cdot}PO_4$ is reduced in the underlying sediments, $Fe^{2+}$ and $PO_4^{3-}$ are released to the pore fluids. The dissolved $Fe^{2+}$ can either diffuse upward to the oxic zone and be recycled or, in the presence of sulfide, precipitate out as FeS. The dissolved $PO_4^{3-}$ can likewise diffuse upward or, provide an extraneous source for dissolved phosphate and become involved in processes leading to carbonate fluorapatite precipitation. A dissolved $PO_4^{3-}$ minimum

has been measured just below the sediment-water interface in sediments on the continental margin underlying the Peru upwelling zone; indicating active phosphate precipitation at this level (Froelich *et al.* 1988). Such a minimum would also stop dissolved phosphate sited deeper in the sediment diffusing to the surface, effectively trapping phosphate at this level. This iron-phosphate redox cycling has been shown to effectively trap phosphate in the Black Sea (Shaffer 1986). Thus phosphorus would be expected to be concentrated in sediments where iron is actively being recycled, specifically where the oxic-anoxic boundary is either at or just below the sediment-water interface.

Since phosphorus absorbs strongly onto FeOOH, phosphorus can be expected to concentrate in oxic sediments, provided there were high concentrations of FeOOH. In anoxic bottom water conditions, phosphorus released by the decay of organic matter and from the reduction of any FeOOH, will remain in solution and diffuse from the sediment into the anoxic bottom waters. Under anoxic bottom waters, sediment phosphate levels would depend on detrital apatite levels settling through the water column.

## 4.4 Discussion

From the above arguments, it can be seen that the concentrations of minor and trace elements are initially supplied to the site of deposition from terrestrial sources, from biological activity within the ocean and from ocean bottom waters. It is the latter authigenic fractions, with their dependence on redox conditions at or close to the sediment/water interface, which are important in characterising depositional environments. After reviewing the redox parameters of several minor and trace elements, it is apparent that the most useful elements aiding in the identification of past depositional environments are manganese and molybdenum.

Using nMn (Eq. 4.3) and nMo (Eq. 4.4) plots, three principal depositional environments can be delineated (Fig. 4.2).

$$Mn_{(Emu\ Bay\ Shale)} / Mn_{(PAAS\ Normalised)} = nMn \qquad [4.3]$$

$$Mo_{(Emu\ Bay\ Shale)} / Mo_{(PAAS\ Normalised)} = nMo \qquad [4.4]$$

### 4.4.1 Oxic

- exhibiting manganese and molybdenum enrichment (nMn, nMo >1)

Oxic environments are characterised as having bottom waters with dissolved oxygen levels of > 1.0 ml per litre of water (Rhodes & Morse 1971; Ekdale & Mason 1988) and typify conditions at the bottom of the deep sea and on oxic continental shelf margins. In the deep sea, the highly refractory nature of particulate organic matter reaching the sea floor results in a permanently oxic redox state. The oxic/anoxic boundary is relegated to several metres below the sediment/water interface. Manganese, brought to the deep sea on fine, winnowed, particles and re-precipitating as manganese oxyhydroxides, is concentrated in such oxic sediments. The low detrital input results in long residence times for surface sediments and prolongs the enrichment process. This same effect also results in molybdenum enrichment. Detrital input is so low that other elements are also enriched in deep sea oxic sediments purely as a function of the prolonged residence time of sediments at or near the sediment/water interface.

On continental margins, where accumulation of organic matter is higher, rapid burial leads to anoxic conditions within the sediment. The surficial sediments, being oxic, accumulate manganese and molybdenum in the form of oxyhydroxides and carbonates. Burial of these enriched sediments into suboxic and anoxic environments liberates manganese and molybdenum, which migrate back into the oxic sediments and precipitate, enriching the sediments further. Detrital input, in this environment is high and so other elements will not become enriched due to lower residence times.

### 4.4.2 Anoxic

- exhibiting manganese shale normal values, but molybdenum enrichment (nMn =1, nMo >1).

These environment are characterised as having bottom waters with dissolved oxygen levels of < 0.1 ml per litre of water (Rhodes & Morse 1971; Ekdale & Mason 1988), and are typified by euxinic basins such as the Black Sea and Framvaran Fjord. Here, the oxic/anoxic boundary is present within the water column, often a considerable distance above the sediment/water interface. Anoxic bottom waters, the result of barred or silled circulation, contain abundant dissolved sulphides below the oxic/anoxic boundary. Immediately underlying the oxic/anoxic boundary is a dissolved manganese maximum, due to the reductive dissolution of settling particulate manganese oxides and carbonates. Thus the redox recycling of manganese proceeds within the water column and is remote (up to kilometres) from the underlying sediments. Manganese oxyhydroxides and carbonates are reductively dissolved as they pass through the oxic/anoxic boundary leaving only that manganese associated with the aluminosilicate fraction of settling particulate matter to impinge on the sea floor. The concentration of dissolved manganese, although high, does not reach sufficiently high levels to initiate precipitation as manganese carbonate. The sediments then, acquire only the aluminosilicate fraction of manganese, resulting in manganese concentrations close to normal shale values.
The reductive dissolution of molybdenum, on the other hand, provides a source of dissolved molybdenum which can co-precipitate with pyrite. This results in the enrichment of molybdenum in sediments below anoxic waters.

### 4.4.3 Suboxic

- exhibiting manganese depletion but molybdenum enrichment or depletion (nMn <1, nMo >1 - <1).

The suboxic environment is characterised as having bottom waters with dissolved oxygen levels of between 1.0 ml and 0.1 ml per litre of water (Rhodes & Morse 1971; Ekdale & Mason 1988) and can further be subdivided into :

4.4.3.1 Suboxic without dissolved sulphide

- exhibiting manganese depletion and molybdenum shale normal values or depletion (nMo $\leq$1)

This environment can be described as having the oxic/anoxic boundary within the sediment. The bottom layers of the water column have depleted dissolved oxygen levels and possibly depleted dissolved nitrate levels (denitrification). This situation is analogous to that under upwelling zones such as along the California coast (e.g. Calvert & Pederson 1993). Here, high primary production in the photic zone results in enhanced oxygen requirements in the underlying water column, thus depleting dissolved oxygen levels and initiating nitrate reduction. A minor, but significant portion of the topmost sediments are characterised by having manganese and iron reduction as the major cause of organic matter degradation. Sulphate reduction and hence available sulphides, are confined to a level some millimetres (to rarely centimetres) below the sediment surface. Manganese and iron reducing redox conditions result in the reductive dissolution of manganese and molybdenum within the topmost sediments. The concentration of dissolved manganese in pore waters is augmented by dissolved manganese diffusing up from below the oxic/anoxic boundary. This sets up a concentration gradient between the sediment and the overlying water column resulting in the migration of dissolved manganese out of, and subsequent manganese depletion within, the sediments. Molybdenum geochemistry closely mirrors that of manganese as has been shown above. In sediments underlying suboxic conditions, molybdenum is reductively dissolved along with manganese in the sediments. With no significant sulphide available, molybdenum remains in the dissolved state and is lost from the sediments, resulting in molybdenum depletion. After burial below the oxic/anoxic boundary, the amount of molybdenum

remaining which could be available to co-precipitate with pyrite is insufficient to markedly affect molybdenum levels within the sediment.

4.4.3.2 Suboxic with dissolved sulphide

- exhibiting manganese depletion but molybdenum enrichment (nMo >1).

This environment represents a variant of the suboxic environment, where the oxic/anoxic boundary is at, or very close to, the sediment/water interface. Below the interface, the sediment is essentially anoxic. Immediately underlying the oxic/anoxic boundary, within the sediment, is a dissolved manganese maximum, due to the reductive dissolution of manganese oxides and carbonates. The presence of dissolved sulphide within the sediments, as a product of sulphate reduction, has little effect on dissolved manganese levels, resulting in dissolved manganese migrating out of the sediment into the bottom waters, resulting in sedimentary manganese depletion.

However, the concomitant reductive dissolution of molybdenum does not result in molybdenum loss. The presence of dissolved sulphides allows the co-precipitation of molybdenum with sulphides - especially in the presence of pyrite precipitation. The removal of molybdenum from the pore waters results in a concentration gradient between the sediment and the overlying water column. Dissolved molybdenum diffuses into the sediments, augmenting and enhancing molybdenum precipitation. Thus under these conditions the concentration of solid molybdenum within the sediment increases, producing molybdenum enrichment.

For the majority of elements discussed here, the passage of time is one of the main criteria which controls enrichment or depletion. Over extended periods of time, most elements will show significant enrichment or depletion in a number of differing environments. The exception appears to be manganese, which apparently is only significantly enriched when surface sediments are oxic. Other factors also come into play, such as the concentration of organic matter in the surficial sediments - a factor not

strictly controlled by oxygen levels. However, by combining the results from various elements with the apparent constant reaction of manganese to differing environments, a more accurate reconstruction of the environments of deposition pertaining at the time can be made. The reaction of manganese and molybdenum to different environments of deposition (Table. 4.1) will be used in this study as the primary indicator of depositional

**Table 4.1** Suggested effect on the concentration of manganese and molybdenum due to the redox state of the depositional environment.

| Element | Oxic | Suboxic ($-SO_4$) | Suboxic ($+SO_4$) | Anoxic |
|---|---|---|---|---|
| Mn | enriched | depleted | depleted | normal |
| Mo | enriched | depleted | enriched | enriched |

environment. Other elements can be used to support the environment of deposition suggested by the manganese and molybdenum results, but cannot be considered definitive by themselves.

Many areas containing sediments with enhanced or depleted minor and trace element concentrations have been studied geochemically. Such areas are commonly associated with high primary productivity (upwelling zones) or anoxic bottom waters (euxinic basins) and the sediments themselves contain elevated TOC levels. An analysis of these studies may go some way to establishing the veracity of using minor and trace element signatures in ascertaining the actual depositional environments of ancient sediments.

## 4.5 Emu Bay Shale Geochemistry

For the purpose of making environmental studies utilising trace element concentrations, the 'average shale' values of Wedepohl (1971) are commonly used. However, with

regard to the Emu Bay Shale, it has been found that Post-Archean average Australian Shale (PAAS) values vary significantly in a few instances from 'average shale' values (Table 4.2). Thus PAAS values are used in this study.

**Table 4.2** Comparison of Average Shale and PAAS values for certain elements. Concentrations in ppm. ([1] from Wedepohl 1971, [2] from Taylor & McLennan 1985)

| Element | Average Shale[1] | PAAS[2] |
|---|---|---|
| Mn | 850 | 900 |
| Mo | 2.6 | 1.0 |
| Cu | 45 | 28.26 |
| Ni | 68 | 36.9 |
| P | 700 | 1700 |
| V | 130 | 90.6 |

### 4.5.1 Section 1: 0.00 - 1.80 metres

Section appears altered, nMo high (x2.6) (Fig. 4.3); very high enrichment of zinc (x33) (Fig. 4.4) and lead (x26) (Fig. 4.5). Copper shows fluctuating levels between 1.3 and 2.4 of PAAS values (Fig. 4.6). No perturbation in other elemental concentrations.

In the absence of significant enrichment of copper and other elements, the high values of lead and zinc possibly indicate post-depositional enrichment, probably by lead/zinc-rich fluids. Manganese levels show little deviation from PAAS values (Fig. 4.3), therefore fluids may well have been sulphidic. Towards the top of the section, manganese and molybdenum depletion is evident, indicating a possible return to original depositional values. Molybdenum and copper levels fluctuate and it is apparent that a certain amount of overprinting has occurred, obscuring the original depositional signature, especially in the lower part of the section. Since the base of the section rests unconformably upon the

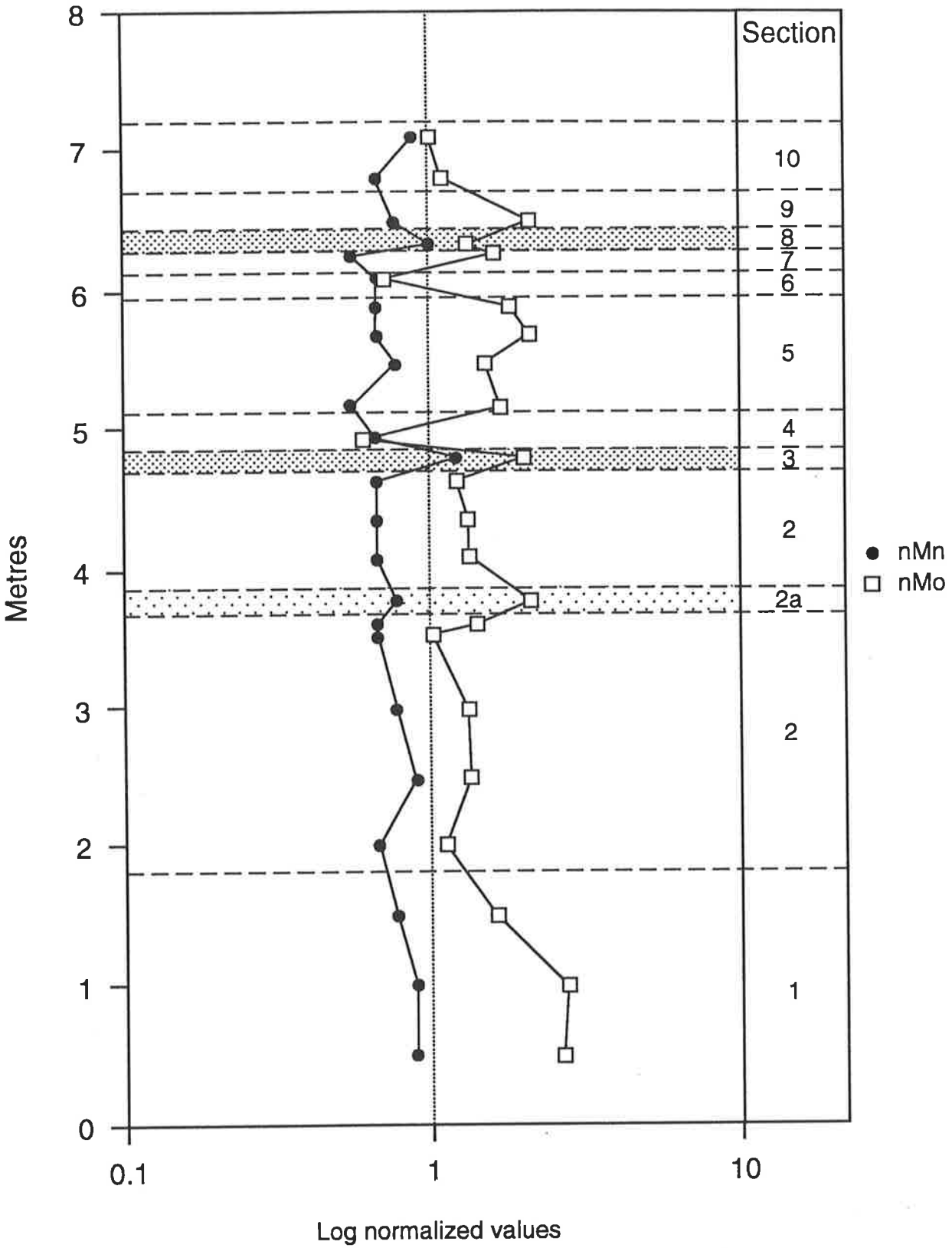


**Fig. 4.3** Manganese and molybdenum concentrations in the lower 8 metres of the Emu Bay Shale at Big Gully, normalized against Post Archean Australia Shale values. Probable anoxic zones are shaded, lighter shading highlights possible anoxic excursion.

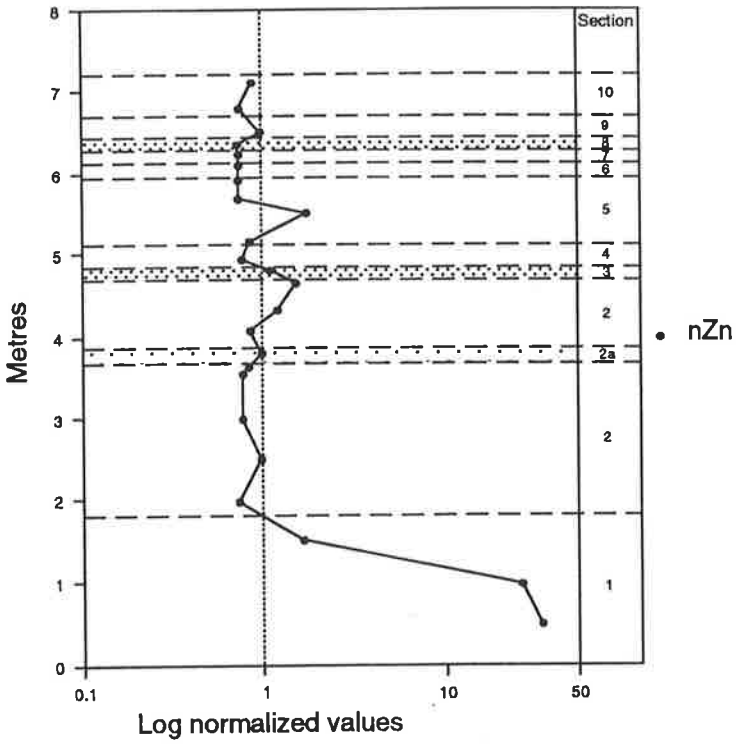


**Fig 4.4** Zinc concentration in the lower 8 metres of the Emu Bay Shale at Big Gully, normalized against Post Archean Australian Shale values.

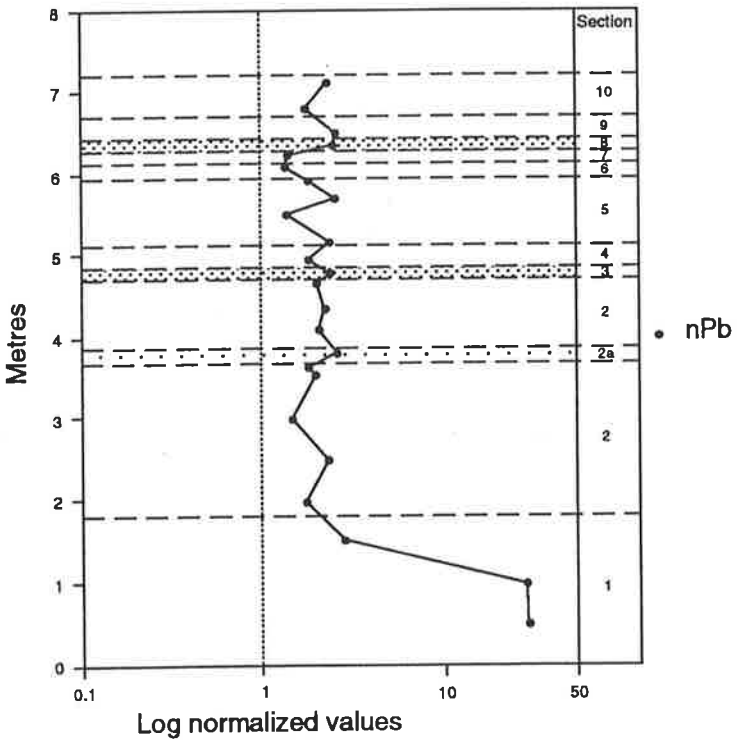


**Fig 4.5** Lead concentration in the lower 8 metres of the Emu Bay Shale at Big Gully, normalized against Post Archean Australian Shale values.

White Point Conglomerate, it is possible that this unconformity could have acted as a post-depositional conduit for fluids. Lead/zinc enrichment is common in Cambrian sediments of South Australia (e.g. Seccombe *et al.* 1985; Horn & Morris 1988). Thus, in this interval, an enrichment process divorced from the original conditions of deposition is a possible explanation for the anomalous lead and zinc levels. Other elements measured show little deviation from PAAS values (e. g. Figs. 4.8, 4.9, 4.10), which also indicates enrichment from a fluid enriched in specific elements.
In outcrop the section weathers with a characteristic green sheen, suggestive of sulphide breakdown (McKirdy 1967).

### 4.5.2 Section 2: 1.80 - 4.70 metres

At the base of this section, manganese shows apparent depletion (0.6), but this figure then increases, before falling again and reaching another low at 3.70 metres (0.67) (Fig. 4.3). Molybdenum values show only a slight enrichment over PAAS normal values at the base of the sequence, a value which rises before falling to PAAS normal values at 3.70 metres. Copper values show an enrichment (>2) at the base of the section, which falls through the section to a low of approximately PAAS values at 3.00 metres. Above this, copper values rise sharply (Fig. 4.6). Uranium levels towards the base of the section are approximately twice PAAS values and retain this level throughout the section (Fig. 4.6).

The depletion of manganese, coupled with the PAAS values for molybdenum, suggests the possible onset of suboxic conditions without significant sulphate availability (see 4.4.3.1 above). The suboxic condition results in the reductive dissolution of manganese and molybdenum. However, in the absence of dissolved sulphide, the dissolved molybdenum remains in solution and is lost from the sediments. Prolonged exposure of the sediments to this environment will result in the depletion of both manganese and molybdenum. Molybdenum normalised values do not show depletion, suggesting short-

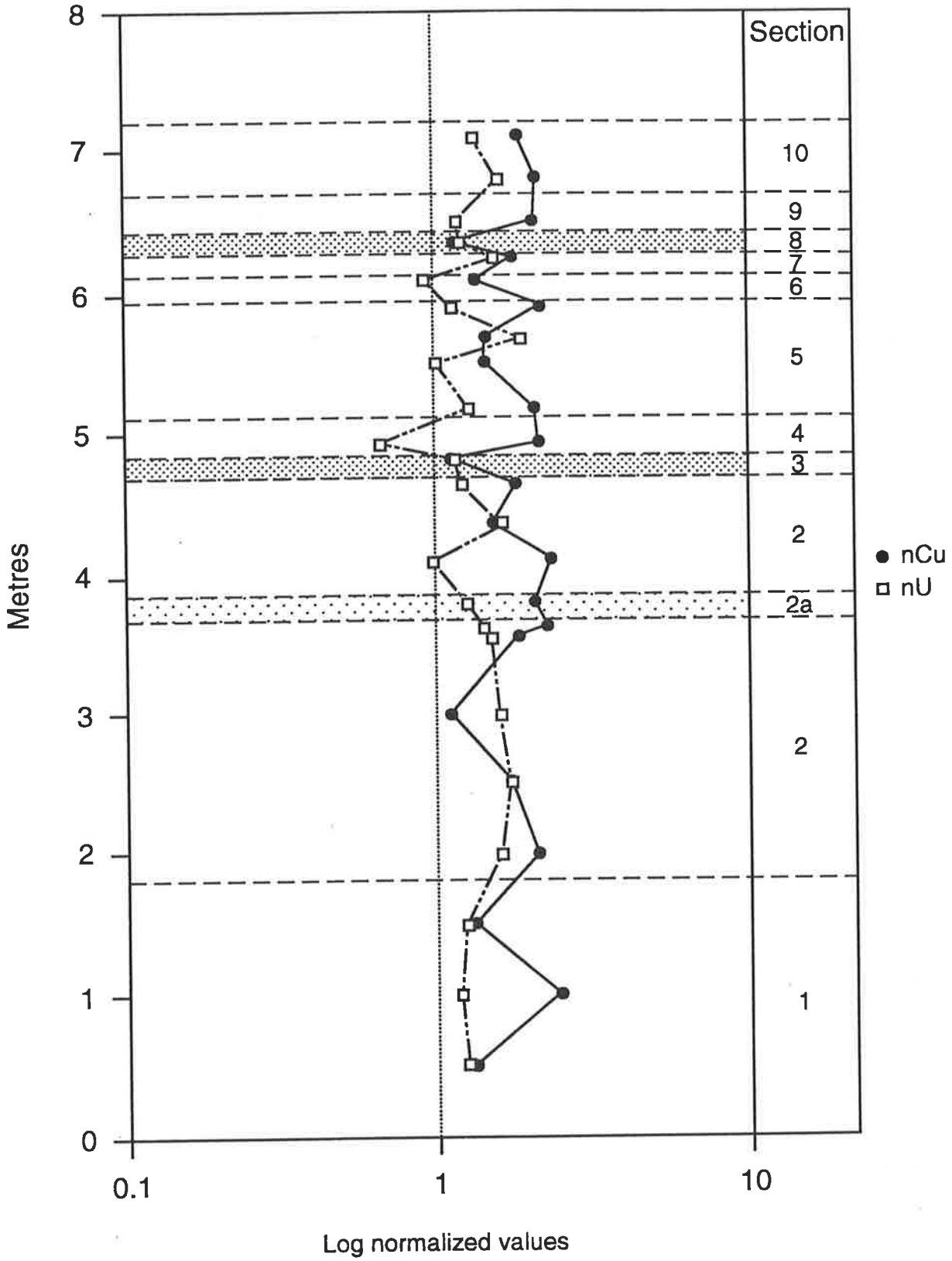


**Fig 4.6** Copper and uranium concentration in the lower 8 metres of the Emu Bay Shale at Big Gully, normalized against Post Archean Australian Shale values.

term stability of this environment. The fact that copper also shows slight enrichment (>2) is also suggestive of short-term stability. The large sediment binding capacity of copper, plus its high concentration in sea water, means that copper can become enriched in environments with rapid detrital influx, whereas other elements are not concentrated. The enrichment of uranium is linked with the increase in the amount of organic matter being deposited as sedimentation rates decrease. Since uranium complexes with organic matter, an increase in the rate of organic matter being buried will increase the amount of uranium entering the sediments. Therefore, uranium enrichment supports an decrease in sedimentation rate.

While these conditions appear to predominate through the sequence, some minor excursions perhaps indicate that the overall chemical signature is an amalgam of small fluctuations. For instance around 3.50 metres the depletion of manganese coupled with the return of molybdenum to PAAS normal values may be indicative of suboxic conditions with a small but significant suboxic sedimentary veneer (4.5.3.1 above). Thus manganese is depleted as is molybdenum. Copper, however, shows increased enrichment (>2) and uranium levels remain enriched. This may indicate a retreat of the oxic/anoxic boundary down into the sedimentary column. The increased residence time of the suboxic sediments allows manganese and molybdenum to become depleted, while enhancing the addition of other elements in the sediment. Copper especially, with its high relative concentration in sea water would be expected to show significant enrichment as residence time increases.

The concentration of phosphate in the two sections remains enriched, but relatively constant (Fig. 4.8).

4.5.3.1 Section 2a: 3.75 - 3.85 metres

Within section 2, a nMo enrichment spike occurs between 3.75 - 3.85 metres. An increase in nMn levels also occurs, but this is only slight and nMn values still remain depleted (0.78). Copper levels remain high, but uranium levels fall to near PAAS

values.

The enriched molybdenum concentration clearly stands out from the rest of section 2. The weak increase in manganese concentration suggests a short-lived enrichment event. The lower relative uranium concentration suggests an increase in sediment supply, diluting the concentration of organic matter and thus uranium, per unit volume of sediment. These results suggest a short-lived either anoxic or oxic event. The low concentration of manganese suggests that this was an anoxic event, however, not enough geochemical information is available to be certain. This section is, therefore, kept as a sub-division of section 2 rather than comprising a separate section.

### 4.5.3 Section 3: 4.70 - 4.82 metres

Here, manganese shows slight enrichment (1.22) for the first time in the sequence and molybdenum continues to show significant enrichment (2.0) (Fig. 4.3). Copper shows a decrease to PAAS values (Fig. 4.6), while uranium shows only slight enrichment (1.17) (Fig. 4.6). Other elements show minor negative excursions (e.g. Figs. 4.9 & 4.10).

Manganese levels appear to increase from depleted levels in the underlying sediments to slightly enriched values. Molybdenum concentrations show elevated enrichment over immediately underlying values. A manganese concentration slightly higher than PAAS values plus enriched molybdenum values appears indicative of anoxic bottom waters (see 4.5.2 above). The magnitude in the increase of manganese concentration is slightly larger (80%) than that for molybdenum (67%). This is in accord with the fact that manganese recycling exceeds that of molybdenum (e.g Calvert & Pederson 1993). While manganese and molybdenum oxyhydroxides and carbonates are not precipitated and redox recycling occurs within the water column, manganese associated with the aluminosilicate fraction of settling particulate matter is not affected and PAAS manganese

concentrations result. Molybdenum, reductively dissolved at the oxic/anoxic boundary within the water column, is removed from the water column by co-precipitation with pyrites. This enriches the bottom sediments with respect to molybdenum. The decline in copper and uranium levels towards PAAS values seems to indicates a reduction in the amount of organic matter being buried. This would seem to mitigate against the influx of organic matter as being the main cause of the anoxic conditions. Low levels of other elements such as copper indicate that detrital input was low, and therefore the anoxic event was caused by an extraneous event such as the influx of anoxic bottom water across the continental shelf. Prolonged exposure to these conditions would result in the extensive enrichment of molybdenum and several other elements. This is not seen, suggesting therefore, that this environment was probably temporary, possibly seasonal, with the anoxic environments masked by the longer lasting suboxic ones. The phosphate concentration also declined in this section (Fig. 4.7), as may be expected in an anoxic environment, since phosphate is soluble in reducing conditions.

### 4.5.4 Section 4: 4.82 - 5.13 metres

Manganese shows a return to depleted values (0.67) while molybdenum exhibits a significant reversal from the underlying sections and for the first time depleted levels (0.6) are recorded (Fig. 4.3). Copper shows an increase to enriched levels (2.09) (Fig. 4.6), but uranium exhibits a depleted level, also for the first time in the sequence (0.66) (Fig. 4.6).

This section is delineated from only one analysis, but it seems to indicate suboxic conditions without major dissolved sulphide (see 4.4.3.1 above). Thus the manganese concentration returns to depleted levels as manganese is dissolved and lost from the sediments. Pore water and bottom water conditions are suitably suboxic to not allow the precipitation of manganese oxyhydroxides or carbonates. Molybdenum exhibits a marked reduction in concentration. This is indicative of the suboxic oxidation of reduced

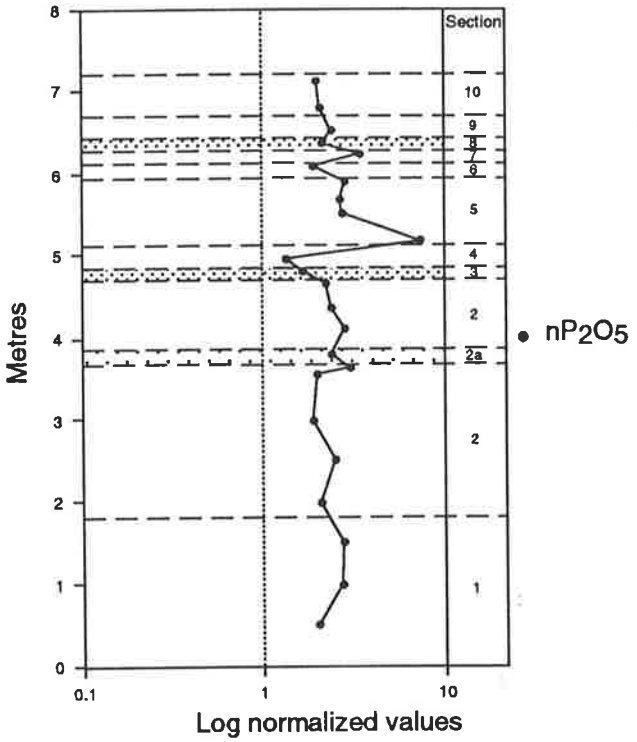


**Fig 4.7** Phosphate concentration in the lower 8 metres of the Emu Bay Shale at Big Gully, normalized against Post Archean Australian Shale values.

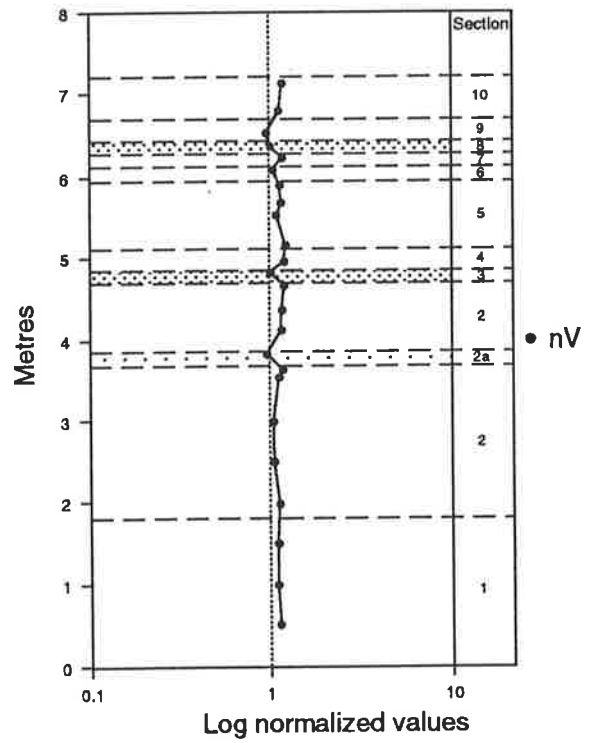


**Fig 4.8** Vanadium concentration in the lower 8 metres of the Emu Bay Shale at Big Gully, normalized against Post Archean Australian Shale values.

molybdenum sulphides and the entry of dissolved molybdenum into the pore waters and bottom waters. The absence of dissolved sulphides from the topmost sediments results in molybdenum depletion within them as dissolved molybdenum is lost to the overlying bottom waters. The enrichment of copper seen in this section, coupled with the marked depletion of uranium indicates that little detritus and very little organic matter is being delivered to the sediments. This can be expected to increase the residence time of the sediments at the sediment/water interface, allowing the depletion of manganese and molybdenum to proceed. Copper with its high concentration in sea water, compared with other elements would show enrichment if residence times increased. Uranium, with its large depleted value, indicates that most of the organic matter which impinged on the sediment was oxidised before burial.

The other elements under investigation show slight positive excursions back to or slightly above PAAS values. This effect seems to support the possibility of increased residence times. The concentration of phosphate in this section is the lowest measured in this study (Fig. 4.8). The relatively low level compared with other sections may be due to the lack of suitable redox conditions conducive to precipitate phosphate. In other words, redox conditions at or near the sediment-water interface did not support the precipitation of calcium phosphate and thus dissolved phosphate was lost to the overlying water column.

### 4.5.5 Section 5: 5.13 - 5.95 metres

This section exhibits manganese depletion and molybdenum enrichment (Fig. 4.3). Copper shows continued enrichment through the section, although towards the middle, levels are lower than towards the top and bottom (Fig. 4.6). Uranium shows initial slight enrichment, then PAAS values before becoming enriched again towards the top of the section (Fig. 4.6).

The overall pattern of manganese depletion and molybdenum enrichment indicates a

suboxic environment with dissolved sulphide (see 4.4.3.2 above). The separation between the manganese and molybdenum curves is largest at the base of the section suggesting active recycling and high sulphide levels. Towards the middle of the section (5.50 m), the general movement towards PAAS values shown by manganese, molybdenum, copper and uranium concentrations, may well be indicative of relatively rapid sedimentation , inhibiting extensive depletion/enrichment. Uranium concentrations equal PAAS values at one point in this part of the section, which also indicates that organic matter input was low, supporting the idea of a relatively high detrital input at this time. A trend to slightly lower concentrations of other trace elements also supports a higher detrital input, minimising residence time at the sediment/water interface. Eighteen centimetres above this point, uranium exhibits a enrichment of 1.9. This excursion is concomitant with an increase in manganese depletion and molybdenum enrichment, indicating an influx of organic matter which increases the suboxic conditions of the bottom waters and immediately underlying sediments. Towards the top of the section, uranium concentrations fall to near PAAS with little coeval movement in manganese or molybdenum concentrations. Thus towards the top of the section the amount of organic matter impinging on the sediment falls, resulting in a slight lessening on suboxic conditions in the bottom waters. The highest concentration of phosphate was recorded from the base of this section (Fig. 4.7) which is also suggestive of active recycling in a redox environment conducive to the precipitation of calcium phosphate. Phosphate concentrations above the base are lower, possibly indicating a more rapid sedimentation rate and thus shorter residence time.

### 4.5.6 Section 6: 5.95 - 6.15 metres

Manganese concentrations in this section show similar depletion levels to the underlying section. However, molybdenum exhibits a strong, depletion trend (0.70) (Fig. 4.3). Copper concentrations show a drop in enrichment levels relative to the underlying section and uranium concentrations approximate PAAS values (Fig. 4.6).

While this section is also only delineated from one analysis, the levels of molybdenum differ markedly from those immediately above and below. This environment approximates that described in 4.4.3.1 above, whereby bottom waters are suboxic, but dissolved sulphide is absent, due to the oxic/anoxic boundary being depressed within the sediment column. Under these conditions manganese settling to the sea floor will reductively dissolve and escape from the sediment. Molybdenum present as sulphides or associated with manganese will also reductively dissolve. With no dissolved sulphide present in pore waters or the bottom water, molybdenum too will be lost from the sediment and depletion results. The depression of the oxic/anoxic boundary within the sediment suggests that labile organic matter is absent. This is supported by uranium concentrations which approximate PAAS levels. Copper enrichment is less than in the immediately underlying section. This indicates that detrital input is also low and, since copper levels are still enriched, relatively long residence times are indicated. The absence of any significant enrichment in the other trace elements also points to a lack of anoxic conditions within the sediment and, by implication, a lack of significant amounts of organic matter. Phosphate concentrations drop in this section (Fig. 4.7) and, as in section 4, suggest a depositional environment not conducive to phosphate precipitation.

### 4.5.7 Section 7: 6.15 - 6.34 metres

This section shows a trend towards manganese depletion, but a reversal from molybdenum depletion in the previous section to enrichment (Fig. 4.3). Copper and uranium both exhibit an increase (Fig. 4.6).

The combination of increasing manganese depletion and molybdenum enrichment is indicative of an environment similar to that in section 4.4.3.2 above, whereby the oxic/anoxic boundary is close to, or at the sediment/water interface and bottom waters are markedly suboxic. Molybdenum enrichment is due to the precipitation of molybdenum

sulphides possibly associated with pyrite precipitation. The enrichment of uranium could indicate that the environmental conditions have been brought about by an increase in the amount of organic matter being buried, the oxidation of which results in the migration of the oxic/anoxic boundary towards the sediment/water interface. The increase in copper concentrations is suggestive of an increase in precipitation possibly due to the formation of insoluble copper sulphides. The increase in phosphate concentration (Fig. 4.7) is also suggestive of a depositional redox environment conducive to the precipitation of phosphate.

### 4.5.8 Section 8: 6.34 - 6.45 metres

Manganese in this section shows a departure from the depleted levels of the previous section, whereas molybdenum, while still exhibiting enriched values, shows a decrease from the previous section (Fig. 4.3). Copper and uranium concentrations fall to near PAAS values (Fig. 4.6).

This section probably represents a period of anoxic bottom waters (see 4.4.2 above) as in section 6. Manganese concentrations show a shift from depleted to PAAS values, an increase of almost 100% on the levels in the immediately underlying section. Interestingly, the molybdenum concentration, while still somewhat enriched, are less than those in the preceding section. An anoxic environment would be expected to be conducive to molybdenum enrichment and manganese normal values. The small level of molybdenum enrichment may be an overprinting effect from the proceeding section, whereby molybdenum is scavenged from this section and concentrated in the higher section. The PAAS values for copper and uranium tend to support a short-lived anoxic bottom water event with little detrital input. This section may represent a sequence of anoxic to suboxic, seasonal events. A decrease in the supply of detritus would mean that the enrichment of bottom sediments would have to occur via diffusion across the sediment/water interface. Since this is a time dependent process, the lack of such enrichment could indicate that insufficient time elapsed during the instigation of these

conditions to allow this. The thinness of this section also suggests this. The low levels of uranium point to a low input of organic matter, thus indicating that the onset of anoxic conditions was, once again, due to extraneous conditions. The low levels of phosphate relative to the previous section (Fig. 4.7) may also be explained by an anoxic depositional environment, which would not favour the precipitation of phosphate, allowing dissolved phosphate to enter the overlying water column. An alternative explanation would be that this interval represents a brief return to normal oxic conditions. However, considering that nMo values show considerably more fluctuation than nMn values, it would seem likely that if conditions were oxic for a brief period, then the nMo values would tend toward PAAS normal values more rapidly than the nMn values. Thus an anoxic event is favoured.

### 4.5.9 Section 9: 6.45 - 6.67 metres

This section shows a return to depleted levels for manganese concentrations and an increase in enrichment levels for molybdenum (Fig. 4.3). Uranium levels remain close to PAAS, but copper shows a marked increase from PAAS levels in the preceding section to enriched (2.09) (Fig. 4.6).

Manganese depletion and molybdenum enrichment indicate a return to suboxic bottom and an oxic/anoxic boundary close to the sediment/water interface (see 4.4.3.2. above). The PAAS levels of uranium indicate that little organic matter was being added to the sediments, a possible indicator that depleted oxygen levels are the result of extraneous circumstances and not the reduction of organic matter. The enrichment of copper could be caused by the precipitation of reduced copper, although it may indicate low detrital input and thus longer residence times for surficial sediments at the sediment/water interface. The slightly higher concentration of phosphate compared with the previous section (Fig. 4.7) may be explained by a longer residence time combined with a depositional environment which would allow the retention of some iron oxyhydroxides

by the sediments.

### 4.5.10 Section 10: 6.67 - 7.20 metres

The enrichment of manganese intensifies in this section, while molybdenum concentrations decrease to PAAS values from the enriched value of the previous section (Fig. 4.3). At the top of the sequence, both molybdenum and manganese approach PAAS normal values. Uranium concentrations increase to a slightly more enriched level and copper concentrations remain enriched (Fig. 4.6).

The depletion of manganese coupled with the decrease in molybdenum concentration to PAAS values indicates that this section represents a slight relaxation of suboxic conditions in the water column and the depression of the oxic/anoxic boundary within the sediment (see 4.4.1. above). This means that manganese and molybdenum are reductively dissolved, but without dissolved sulphide, molybdenum is lost from the sediment. Uranium concentrations are slightly enriched and copper concentrations remain enriched, possibly indicating that residence times were long enough for diffusion across the sediment/water interface to occur. Towards the top of the sequence the section exhibits a return to normal oxic conditions and rapid deposition. Both manganese and molybdenum concentrations approach PAAS values. This indicates that residence times and the sediment environment did not promote enrichment or depletion. Most other elements figured also show a trend towards PAAS concentrations. Phosphate concentrations appear to level out at a slightly enriched level (Fig. 4.7) which might approximate background values for the Emu Bay Shale.

Above this level, the last 80 cm of the lower Emu Bay Shale comprises fine grained, laminated sandstones alternating red and green in colour. The colour alternation indicates that a cycling between oxic and suboxic depositional environments continued despite the slightly more proximal nature of the sediments

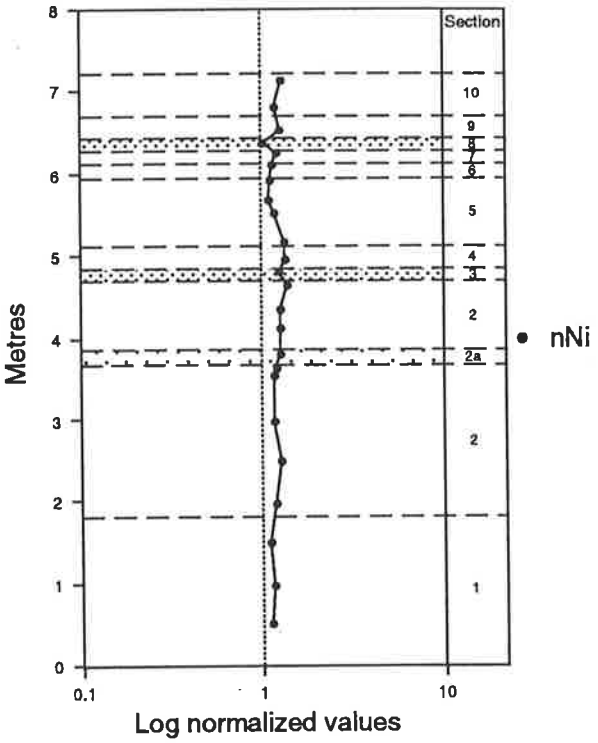


**Fig 4.9** Nickel concentration in the lower 8 metres of the Emu Bay Shale at Big Gully, normalized against Post Archean Australian Shale values.

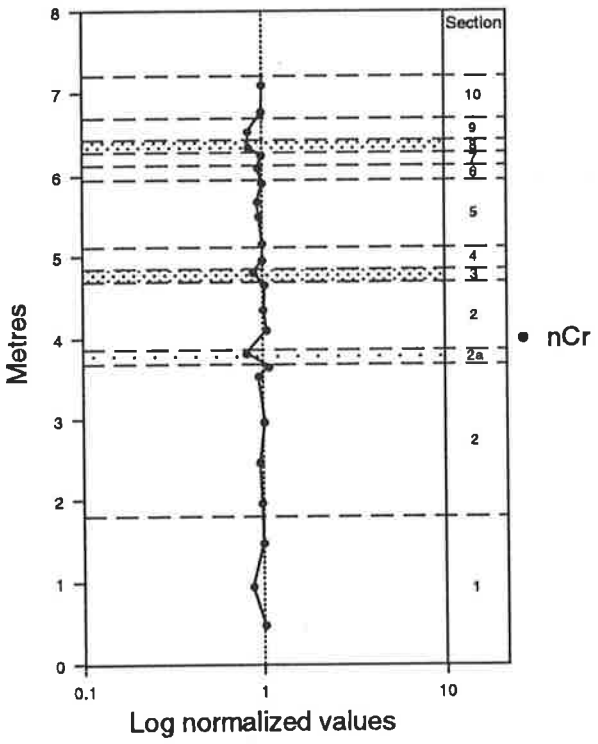


**Fig 4.10** Chromium concentration in the lower 8 metres of the Emu Bay Shale at Big Gully, normalized against Post Archean Australian Shale values.

## 4.6 Discussion

The environments delineated above almost certainly do not a form a true picture of the total variability. Bottom water conditions can alter, quite dramatically, within weeks and commonly within months. Even changes on a seasonal basis would be far too rapid to be detected using this method. All that might be achieved is to pick out major trends within the sequence and hope that these secular trends accurately reflect longer term bottom water oxygen levels. There have undoubtedly been a considerable number of anoxic events which have not been delineated in this study. This is suggested by the absence of bioturbation and sessile organisms.

Molybdenum for the most part remains enriched throughout the sequence, whereas manganese is predominantly depleted (Fig. 4.3). This is probably a reflection of the common state of the surficial sediments. Where the oxic/anoxic boundary is close to, or at, the sediment/water interface, the suboxic environmental conditions result in the precipitation of molybdenum, but the dissolution of manganese. When the environment reverts to an anoxic environment (whether seasonally or due to other factors), only the manganese associated with the aluminosilicate fraction of the detritus is incorporated into the sediments (sections 3 and 8). Molybdenum, however, co-precipitates with sulphides, thus enriching sediments under anoxic or deep suboxic conditions. This is reflected in the grouping of the normalised values mostly within the suboxic part of the nMo/nMn plot (Fig. 4.11). The nMo/nMn plot represents a possible method for delineating past depositional environment utilising the differing response characteristics of manganese and molybdenum in varying chemical environments. In this plot the Emu Bay Shale samples cluster close to normal values but within the suboxic zone with sulphate. The only two samples which plot in the suboxic zone without sulphate, come from sections 4 and 6. These results can be compared with measurements of nMo and

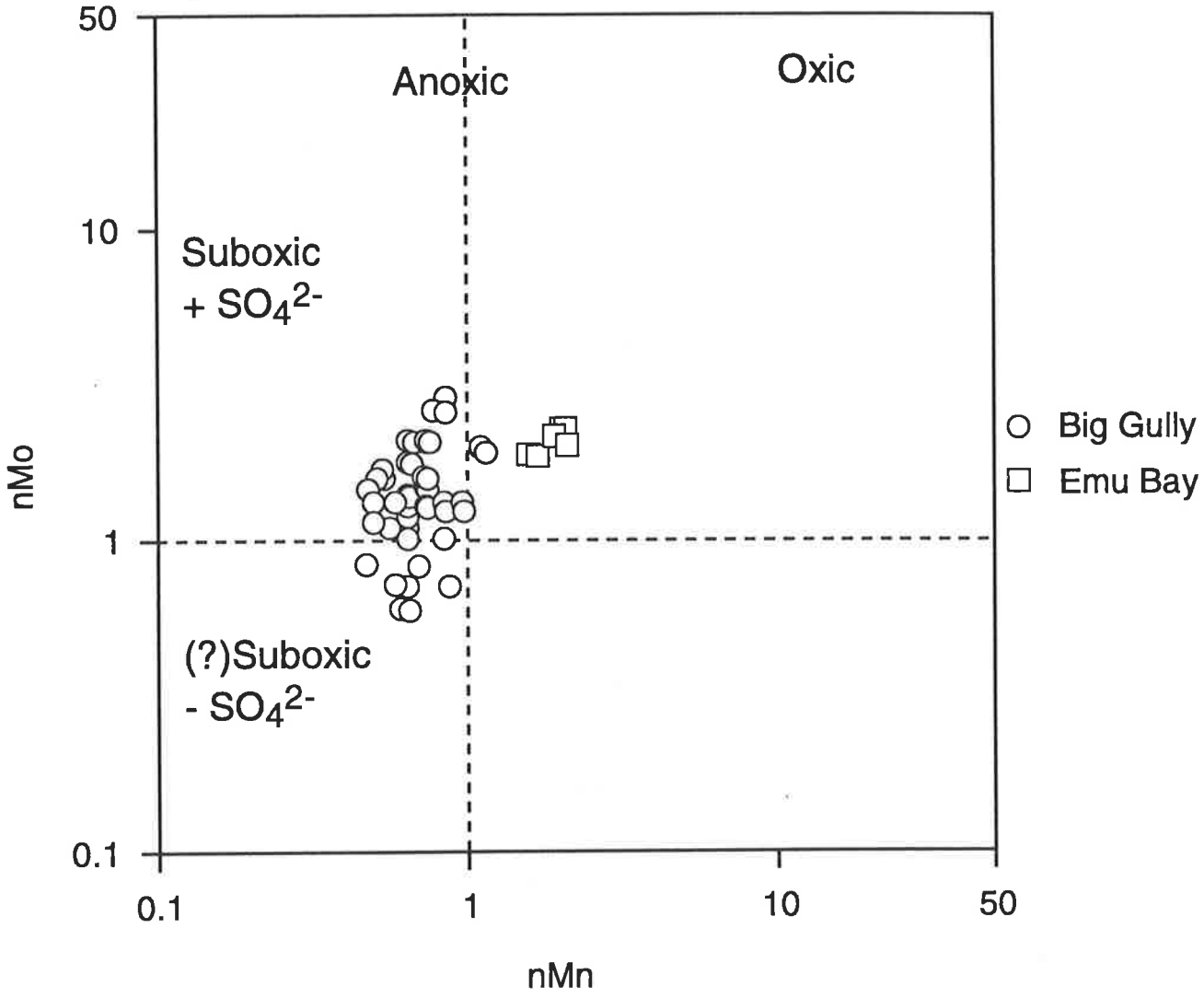


**Fig. 4.11** Plot of nMo/nMn values from the Emu Bay Shale at Big Gully and at Emu Bay, showing the shale at Big Gully indicates a predominantly suboxic depositional environment compared with an oxic depositional environment at Emu Bay.

nMn taken from the Emu Bay Shale at its type section, in Emu Bay. In this instance the values plot within the oxic zone and do not overlap the results from the Emu Bay Shale samples from Big Gully. This suggests an oxic depositional environment for the Emu Bay Shale at Emu Bay, a suggestion supported by the fossil assemblage.

Unlike all other trace elements with the exception of uranium and molybdenum, copper concentrations fluctuate through the sequence (Fig. 4.6). This is, in all probability, linked to both the higher concentration of copper in the water column and its large sediment binding capacity. Low levels probably correlate with short periods of low sedimentation, since copper enrichment depends on either relatively large detrital input (due to the high binding capacity of copper to sediment) or a long residence time (due to the high concentration of dissolved copper in sea water). More enriched levels indicate larger detrital input or longer residence times, which allow the enrichment of copper, often before other elements become enriched.

The concentration of uranium is, by and large, related to the rate of burial of organic matter. Therefore, the lack of enhanced uranium levels is indicative of low burial rates of organic matter. Uranium concentration, with one or two minor exceptions, is uniformly low throughout the sequence (Fig. 4.6). This indicates that organic matter was not the main cause of the reduced oxygen levels experienced at the time of deposition of the sediments. The remarkable consistency of vanadium concentrations throughout the sequence at or around normalised values (Fig. 4.8) suggests that organic matter input was low, since vanadium concentration can be correlated with organic matter content (Brumsack 1986; see also section 4.5.6). Any elevated average uranium concentrations may be caused by the fact that the sediment is derived from igneous and metamorphic basement, which would be expected to contain elevated levels of uranium compared with sedimentary rocks.

The source of minor and trace element concentrations above that supplied from the

detrital fraction can be attributed to the accumulation of biogenic debris and the precipitation or adsorption of minor and trace elements from seawater, which will vary under differing redox conditions (Piper 1994). Since the concentration of organic matter in the Emu Bay Shale is low, it appears that that this has not produced the observed concentrations of some minor and trace elements. Therefore, enrichment or depletion must be derived from precipitation/dissolution or adsorption from seawater. This process will only produce significant enrichment/depletion under conditions of extremely slow bulk sediment accumulation (e.g. Calvert & Price 1977; Piper 1994), since this process is dependent on long term exposure of bottom sediments to bottom waters. Weak enrichment/depletion over levels brought in via detrital material is indicative of rapid sedimentation. Such an example is provided by the Cariaco Trench, where the high detrital accumulation rate has resulted in only weak enrichment of minor and trace elements (Piper 1994). This is analogous to the Emu Bay Shale depositional environment at Big Gully. The normal shale values exhibited by the minor elements (Figs. 4.8, 4.9, 4.10), indicate that the residence time of sediments at the sediment/water interface is insufficient to allow wholesale enrichment/depletion. The sedimentological and geochemical information is indicative of periods of rapid sedimentation which allowed only weak enrichment/depletion, possibly interspersed with periods of relative depositional quiescence. Copper, by virtue of its higher concentration in sea water relative to other elements and its sediment binding capacity, would be expected to show enrichment even when other elements do not. This is indeed what is found. Phosphate enrichment (Fig. 4.7) may indicate active recycling of ferric oxyhydroxide in a suboxic environment. The fact that phosphate enrichment does not coincide with iron oxic enrichment (Fig. 4.12) suggests that phosphate enrichment is not due to the retention of ferric oxyhydroxides within the sediment and thus the result of enrichment in an oxic environment.

The picture being painted by the geochemical data is one of a predominantly suboxic environment with the oxic/anoxic boundary close to, or at, the sediment/water interface (see 4.4.3.2. above). Doubtless periodic anoxic episodes occurred. However, the data

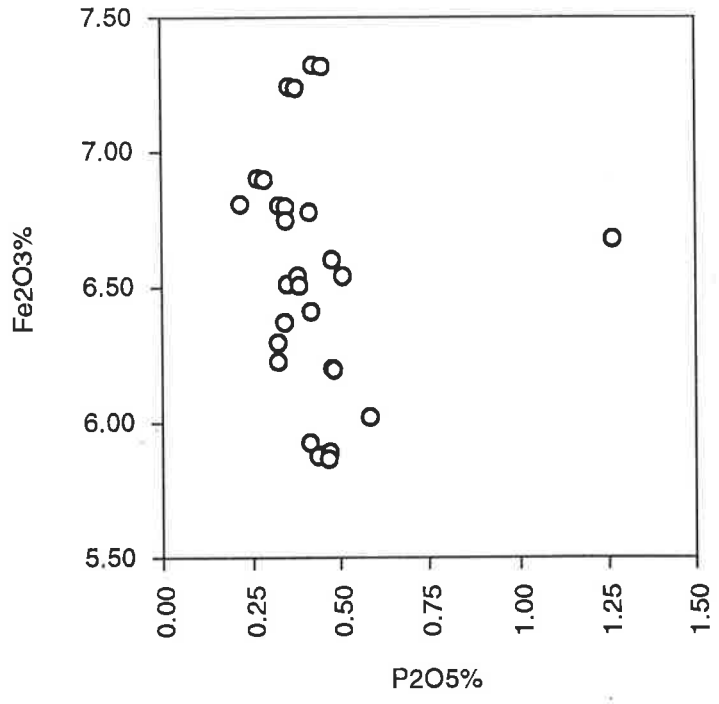


**Fig. 4.12** Plot of phosphate concentration against iron concentration, showing that the occurrence of phosphate is not linked to the occurrence of iron.

does not allow a fine-tuned analysis of redox fluctuations, due mainly to the number and spacing of the samples and the distortion of the preserved signal, to some degree, by subsequent depositional environments and diagenetic processes.

Comparing nMn and nMo values with trilobite distributions (Fig. 4.13), it can be seen that where the geochemical evidence suggests anoxia, the trilobite occurrence drops to zero. This drop in trilobite numbers would be expected if bottom waters were anoxic and hence inhospitable to benthonic life. The continued presence of free swimming forms during these intervals (Fig. 4.13), suggests that the water column as a whole remained oxic to suboxic and shows that only benthonic forms were apparently affected. Fossil distributions therefore, support the interpretation based on geochemical studies, that there were periods of bottom water anoxia during the deposition of the Emu Bay Shale Lagerstätte.

While the signal might be considered somewhat equivocal and the measured

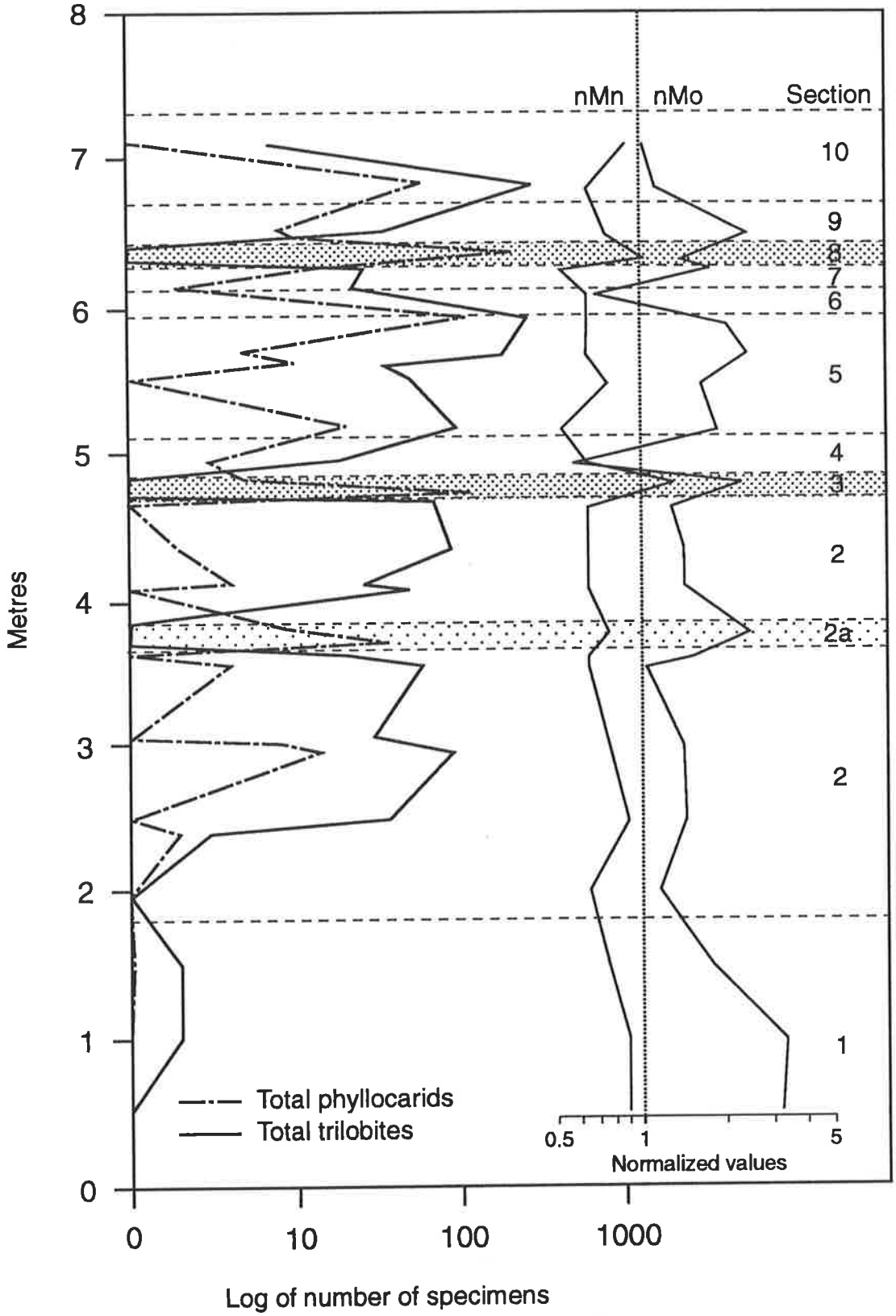


**Fig. 4.13** Comparison plot of total trilobite and total phyllocarid occurrence from the lower 8 metres of the Emu Bay Shale at Big Gully against geochemical zonation with nMn and nMo curves (from Fig. 4.3).

enrichment/depletion of questionable statistically validity, it should be pointed out that most of the elements show deviation which can be attributed to environmental conditions at or shortly after deposition. Also the amount of deviation is in line with the reactivity of the elements over time (e.g. Jacobs *et al.* 1987). In other words, the elements with the shortest "reaction time" are slightly altered, but the elements with longer "reaction times" are not. In order to argue that this signal could be an artifact of post depositional processes divorced from the processes detailed above, a polyphase process would have to be invoked which affected each section differently, yet the overall affect of which, on the elements, was to produce a signature similar to that for the differing reactivities of the elements over time.

It is difficult to conceive of a post-depositional process which would affect what are essentially identical lithological sequences to differing extents, producing enrichment in some while depleting others.

The overall signature of depleted manganese and enriched molybdenum, along with a slight signal trend amongst the other elements indicates that deposition can be equated with a suboxic environment with occasional anoxic episodes in a nearshore environment with rapid, if inconsistent, sedimentation.

# Chapter 5: Taphonomy of the Big Gully Assemblage

*"Carbonate preservation can be envisaged as a transient state because carbonates can be destroyed by a single dissolution event occurring at any time in the depositional-burial-uplift cycle. It is surprising that carbonate material is preserved at all."*

(Canfield & Raiswell 1991b, p. 433)

## 5.1 Introduction

While structural tissues such as plant and animal cuticle may be preserved via organic diagenesis as complex biopolymers (Butterfield 1990), the more readily metabolised 'soft' tissues generally decay too rapidly to be preserved. Soft body parts provide a rich source of nutrients and as such are avidly consumed by predators, scavengers and microbes, making such nonmineralised organic tissues rare in the fossil record. Indeed decay of some soft parts is often required to produce the chemical conditions conducive to the preservation of other tissues.

Preservation of soft, and/or poorly mineralised tissues does occur in the fossil record, with the most common methods of tissue preservation being mineralisation via carbonate, phosphate or sulphide. Pocock (1964, p. 461) characterised the preservation of trilobites within the Emu Bay Shale at Big Gully as being replacement by calcite and commented that some of the fossils, "also seem to serve as a locus of deposition for cryptocrystalline haematite." Glaessner (1979) described soft tissue (muscle bundle) preservation in *Myoscolex* as plates composed of elongate iron stained calcite. It is now appears that the soft tissue preservation in *Myoscolex* is due to phosphate mineralisation and not carbonate (Briggs & Nedin in prep). This represents the earliest known occurrence of muscle tissue mineralisation by phosphate in the fossil record. All other

fossils in the Emu Bay Lagerstätte appear to be preserved via carbonate mineralisation. Here, as in other such instances, the mineralisation is dependent on a critical balance between decay and precipitation. This is controlled by the chemical characteristics of the immediate surroundings (Allison 1988a; Briggs & Kear 1993a, b, 1994; Briggs *et al.* 1993), to a certain extent bottom water conditions, but principally the first few centimetres of the sediment.

It is the chemical characteristics of sediments undergoing early diagenesis which have the major bearing on whether or not organisms are preserved and the amount of detail retained. In order to appreciate the processes which ultimately result in the preservation of an organism, an understanding of the conditions experienced by sediments undergoing early diagenesis is needed.

## 5.2 Early diagenesis in sediments

In marine sediments microorganism communities compete for organic matter. Oxidation of organic matter provides energy for maintenance, growth and reproduction. Successful competition for the organic substrate depends, to a large degree, on the availability of the oxidant utilised by the microorganism and the redox state of the sediment, which determines the particular oxidant thermodynamically favoured. In marine environments, oxygen respiration, nitrate, iron and manganese reduction, sulphate reduction and methane production, approximately in that order thermodynamically, all contribute to organic carbon [C(org)] oxidation. The sequence follows the decreasing energy yield which organisms gain from the utilisation of these substances, with methanogenesis as the terminal microbal metabolism (Froelich *et al.* 1979; Bender & Heggie 1984; Jørgensen & Revsbech 1989). Oxygen respiration and sulphate reduction are by far the two most important reactions (Jørgensen 1982; Bender & Heggie 1984; Canfield 1989b; Allison and Briggs 1991). Microorganisms tend to

concentrate in areas where their particular method of oxidation is favoured. Thus, microorganisms which utilise oxygen respiration are concentrated at or near the sediment-water interface, in sediments with a positive Eh (oxidizing environment), whereas those utilising sulphate reduction (e.g. *Disulfovibrio* and *Desulfotomaculum*), normally obligate anaerobes, will be concentrated below this zone, in sediments having a negative Eh (reducing environment).

The relative dominance of one oxidative method over the other depends on several factors, chief amongst which are rate of sedimentation and primary production (Berner 1978, 1980; Jørgensen 1982; Canfield 1989b, 1991). Where sedimentation rates are about 0.1g $cm^{-2}$ $y^{-1}$, sulphate reduction and aerobic respiration are equally important (Canfield 1989b). However as sedimentation rates fall from 0.1g to 0.01g $cm^{-2}$ $y^{-1}$, sulphate reduction becomes less important as C(org) becomes progressively less available to sulphate reducing microorganisms. Aerobic respiration becomes dominant, until at sedimentation rates below 0.001g $cm^{-2}$ $y^{-1}$, aerobic respiration decomposes 100-1000 times as much C(org) as sulphate reduction (Canfield 1989b). Thus in deep sea pelagic sediments, where sedimentation rates are very low, the aerobic respiration zone can be ≥ 1 μ thick, and the sulphate reduction zone, although much thicker, contributes very little to the overall decomposition of C(org). This is due to the relatively long residence time of C(org) within the aerobic respiration zone which results is only the most refractory C(org) being made available for sulphate reduction (Jørgensen 1982).
Nearer shore, with higher sedimentation rates, decomposition of C(org) via sulphate production may dominate. At sedimentation rates above ≈ 0.1g $cm^{-2}$ $y^{-1}$ the aerobic respiration zone is maximally only a few decimetres thick (Jørgensen 1982), but is commonly only a few centimetres thick; and in coastal sediments the zone is only a few millimeters thick (Jørgensen & Revsbech 1985, 1989). Thus, rapid burial and a thin aerobic respiration zone, ensures labile C(org) will be available for sulphate reduction and this process predominates (Jørgensen 1982; Jørgensen & Revsbech 1985, 1989; Canfield 1989b). Berner (1980, fig. 6.6) noted a linear correlation between sulphate

reduction and the rate of deposition and also concluded that rapid burial resulted in an increase in the amount of labile organic material being made available for oxidation via sulphate reduction.

There also appears to be a close correlation between primary production in the oceans and the preponderance of sulphate reduction, indicating that the input of C(org) is an important factor (Canfield 1991). This appears to be related to the increase in the amount of C(org) in the depositing sediment. Primary production is concentrated at sites of ocean upwelling, and these show an increase both in the percentage of C(org) decomposed by sulphate reduction and the rate of reduction (Canfield 1991). It is important to note that at sites of enhanced primary production, excess C(org) causes rapid utilisation of available oxygen by aerobic respirers, leading to euxinic environments and the production of an Oxygen Minimum Zone in the water column (Morse *et al.* 1992) (see section 4.2).

Thus, the relative importance of sulphate reduction in diagenesis is dependant on the sedimentary influx of carbon (the total carbon available) and sedimentation rate (the net amount of carbon available for sulphate reduction).

### 5.2.1 Diagenesis in modern sediments

Sediments below modern, normally aerated marine waters can be partitioned into three zones depending on the kind of process involved in the biologically mediated degradation of organic matter. This, by and large, is a reflection of the distribution of oxygen and oxidized products. These zones are, (i) oxic; (ii) suboxic and (iii) anoxic (e.g. Jørgensen & Revsbech 1989) (Fig. 5.1). Whilst these zones are similar to those described in section 4.4 - being based on the levels of dissolved oxygen - in this instance, they have a pronounced effect on the constituents which are already present in the sediment and less influence on which constituents will be incorporated into the

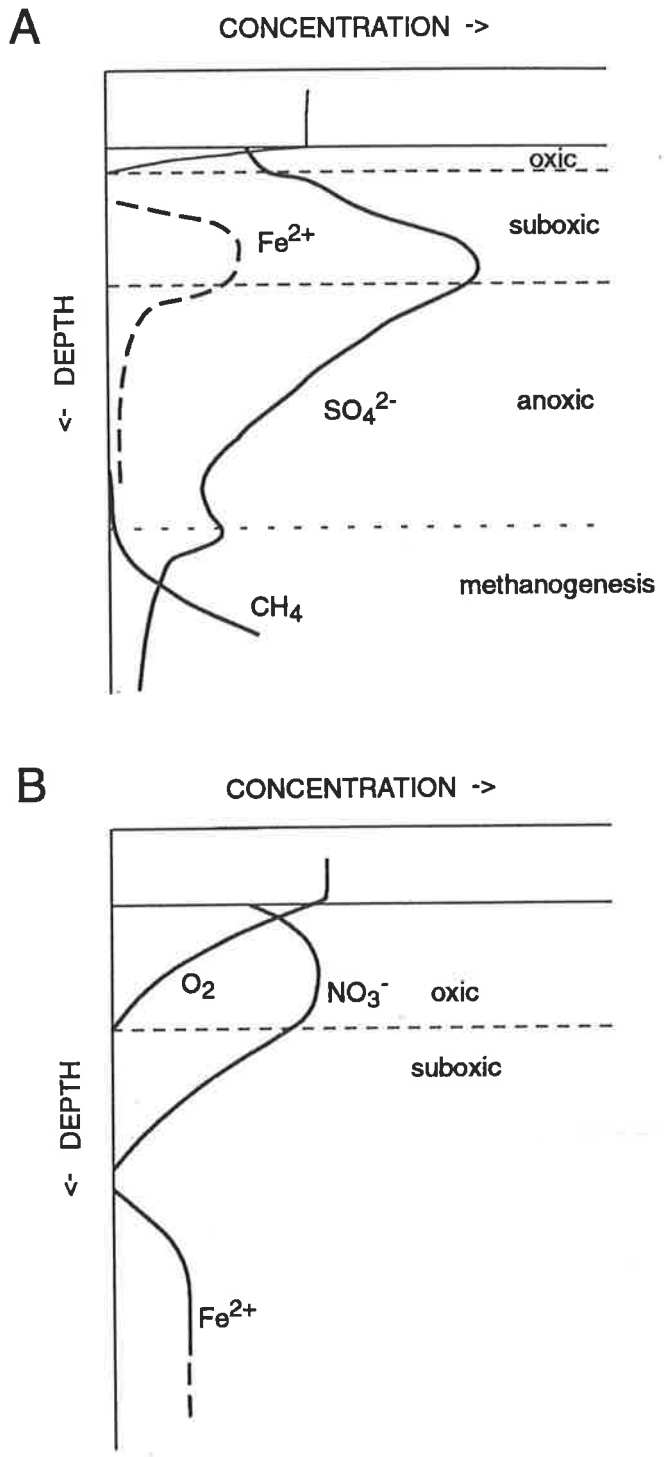


**Fig. 5.1** **A**. Redox zones within marine sediments showing relative sizes and pore water concentration of major species. **B**. Expanded view of oxic and suboxic zones.

sediment. Also the zones delineated below are affected by different criteria, for example bioturbation, as well as oxic and anoxic bacteria.

5.2.1.1 Oxic zone

This zone represents the depth of oxygen penetration into the sediment from the surface. It has been measured as being between 1.3 - 5.6 mm thick along a transect from the Belt Sea to Skagerrak (Jørgensen & Revsbech 1989), but in deep sea sediments where deposition is slow the zone can be much thicker. Within this zone active aerobic oxidation of organic matter occurs. Aerobic oxidation (eq. 5.1) has a profound effect on

$$(CH_2O)_{106}(NH_3)_{16}(H_3PO_4) + 138O_2 \rightarrow 106CO_2 + 122H_2O + 16HNO_3 + H_3PO_4 \quad [5.1]$$

$$\downarrow$$

$$CO_2 + H_2O + CO_3^{2-} \leftrightarrow 2HCO_3^- \quad [5.1]$$

$$\uparrow\downarrow$$

$$CaCO_3 \leftrightarrow Ca^{2+} + CO_3^{2-} \quad [5.2]$$

the chemistry of pore water fluids and thus the preservation potential of both calcium carbonate and organic matter within the sediment. The products are mostly acids, which lower the pH of the surrounding pore fluids, and $CO_2$ which rapidly reacts with the dissolved $CO_3^{2-}$ (eq. 5.2). The need to replenish the dissolved $CO_3^{2-}$ and the lower pH values results in the dissolution of calcium carbonate (eq. 5.3) (Berger 1976; Emerson & Bender 1981; Moulin *et al.* 1985). Thus the saturation state of the pore fluids with respect to carbonate is a direct function of the $CO_3^{2-}$ concentration (eq. 5.3 - the $Ca^{2+}$ ion is essentially non-limiting). The liberation of $CO_2$ during oxic organic matter decay (aerobic respiration) decreases the saturation state of carbonate in the pore fluids and thus will enhance or initiate carbonate dissolution (Emerson & Bender 1981; Boudreau 1987). In continental margin sediments, where the oxic zone is commonly only a few millimetres to a few tens of millimetres thick, the base of the oxic zone, where the

concentration of free oxygen reaches zero, is often associated with a pronounced pH minimum (Murray *et al.* 1980; Boudreau 1987; Jørgensen & Revsbech 1989). The cause of this pH minimum is the production of acids by aerobic respiration within the oxic layer and the oxidation of reduced molecules diffusing up from the suboxic and anoxic sediment. The thinness of the oxic layer allows more organic matter to be buried in the suboxic and anoxic zones, thus fueling sulphate reduction and the production of sulphides (see 5.2.2 below). Oxidation of upwardly diffusing $NH_3$ and $H_2S$ produces nitric and sulfuric acids respectively, resulting in a net drop in pH. This pH minimum indicates a lack of solid calcium carbonate and undersaturated pore fluids, since the presence of carbonate would buffer the chemical system with no resultant drop in pH (Ben-Yaakov 1973; Murray *et al.* 1980).

Despite the fact that oxidative reduction of organic matter predominates within the oxic zone, sulphate reduction has been documented as occurring there. Jørgensen (1977) reported sulphate reduction occurring in microniches within the oxic zone, "almost at the surface of the sediment" (Jørgensen 1977 p. 15). The sulphide oxidizing bacteria *Beggiatoa* sp. and the sulphate reducing, obligate anaerobe *Desulfovibrio* sp. were found within these microniches and it is thought that the oxygen level begins to fall some hundreds of micrometres away from these bacterial concentrations, possibly caused by the oxidation of sulphides emanating from within them.

#### 5.2.1.2 Suboxic Zone

Respiratory ventilation within burrows and general bioturbation of the sediment maintain an oxidized zone which is much deeper than the oxic zone (Fig. 5.1), although oxidizing conditions may also be established by occasional re-suspension of surface sediment during storms. This is the zone associated with positive redox potentials and is characterised by a brown colouration due to the presence of ferric oxides and oxyhydroxides (Jørgensen 1988; Jørgensen & Revsbech 1989)

The zone is mostly anoxic and organic matter is oxidized via nitrate, manganese and iron

reduction. The lower limit of the zone is taken as the depth to the +100 mV redox potential and has been measured at between 5 - 64 mm thick (Jørgensen & Revsbech 1989). However in the deep sea, the zone may be several decimetres thick. Denitrification, or organic matter decay utilising nitrate (eq. 5.4, simplified but

$$5CH_2O + 4NO_3^- \rightarrow CO_2 + 2N_2 + 3H_2O + 4HCO_3^- \qquad [5.4]$$

sufficiently accurate to model the major products), is responsible for up to 10% of organic carbon oxidation. However, the reaction has no net effect on pH levels or alkalinity (Murray *et al.* 1980) and thus no net effect on carbonate dissolution (Canfield & Raiswell 1991b). Manganese reduction (eq. 5.5, simplified) has a marked effect both

$$CH_2O + 2MnO_2 + 3CO_2 + H_2O \rightarrow 4HCO_3^- + 2Mn^{2+} \qquad [5.5]$$

on the pH and the carbonate saturation state of surrounding pore fluids. The reaction uses up $CO_2$ producing $HCO_3^-$, thus driving eq. 5.2 in the reverse direction, toward carbonate saturation. Also the overall alkalinity of the pore fluids increases, raising pH (Boudreau 1987). The increase in $Mn^{2+}$ within pore fluids can lead to carbonate oversaturation since excess $Mn^{2+}$ is known to inhibit carbonate precipitation at saturated and low oversaturated levels (Berner 1975; Murray *et al.* 1980; Styles 1985). Interestingly, during deep sea core recovery, calcium carbonate is precipitated even though no solid carbonate is present . Therefore, at least in pressure mediated carbonate precipitation, no solid carbonate is needed to act as a nucleating surface (Murray *et al.* 1980). The suboxic zone is perpetuated and enhanced by burrowing and bioturbation (Jørgensen & Revsbech 1989). Without these processes and in low oxygen environments the suboxic zone becomes very thin.

5.2.1.3 Anoxic Zone

The zone below the +100 mV redox potential line comprises the vast majority of the biologically active sediment column (Jørgensen & Revsbech 1989). Sediments are black due to the presence of reduced compounds, primarily FeS, since the dominant organic matter degradation reaction is that involving sulphate reduction. Below the sulphide reduction zone, which is always significantly larger than the oxic and suboxic zones, is the zone of methane fermentation. Methane is produced by the anoxic decay of organic matter and diffuses upward to the base of the sulphate reduction layer where it is used by sulphate reduction bacteria as a source of organic carbon, often causing a marked increase in the rate of sulphate reduction at the sulphate-methane interface (Devol 1983).

All $C_{(org)}$ oxidization reactions destroy organic matter. However, the chemistry of sulphate reduction produces ancillary reactions which can enhance preservation of some organic matter as carbonate, phosphate or sulphide. The processes within the anoxic zone then, are the key to understanding of the diagenetic pathway which led to the exceptional preservation at Big Gully.

### 5.2.2 Sulphate reduction in the anoxic zone

In areas of high productivity and/or rapid deposition, the water column can undergo sufficiently rapid decomposition of organic matter as to entirely consume oxygen and nitrate, leaving suboxic and anoxic conditions within the sediment. Bacteria, with their large surface area per unit mass of protoplasm, are by far the most important agents of metabolic reactions within such sediments since, due to the low levels of oxygen, macrofauna are generally absent (Berner 1980). In such environments sulphate is used as an energy source by sulphate reducing bacteria to oxidize organic matter (eq. 5.6). However, since these bacteria only utilise small organic molecules (Berner 1980),

$$(CH_2)_{106}(NH3)_{16}H_3PO_4 + SO_4^{2-} \rightarrow CO_2 + HCO_3^- + HS^- + 16NH_3 + H_3PO_4 \qquad [5.6]$$

other processes must occur to break down the most labile organic matter before sulphate reduction can start. This probably occurs within the water column and the aerobic respiration zone of the sediment, resulting in the loss of more labile tissues.

The consumption of sulphate from pore fluids (eq. 5.6) produces a variety of protolytic and non-protolytic species, including the weak acids $H_2S$ and $H_3PO_4$, the weak base $NH_3$, and the amphoteric species $HCO_3^-$, and $CO_2$. Although the products may be present in considerable quantities and the composition of the pore fluid deviate markedly from that of normal marine water as a result, the pH of the pore fluids remains confined within narrow limits, typically between 7.0 - 8.2. (Ben-Yaakov 1973). For example, while in normal marine water the amount of dissolved $CO_2$ present is approximately 2.0 mM $kg^{-1}$ and the amount needed to shift the pH by one pH unit is 0.5 mmoles $kg^{-1}$ (Ben-Yaakov 1973), the amount of dissolved $CO_2$ in pore fluids is commonly 10 times the normal levels (Morse *et al.* 1992), and has been recorded at 30 times the normal levels (Presley 1969), with no change in pH values. This points to a complex buffering system acting on the pore fluid and it is this buffering system which can lead to increased preservation potential. The buffering system is controlled by four major processes:-

(i) the high concentration of weak acids and bases as byproducts of organic decomposition;

(ii) the transfer of charge from the non-protolytic species to the protolytic species (e.g. $SO_4^{2-} \rightarrow HS^-$);

(iii) precipitation of metal sulphides;

(iv) precipitation of calcium carbonate.

Processes (i) and (ii) are dependant on bacterial sulphate reduction and will tend to shift the pH of pore fluids downward. Process (iii) will increase the pH by removing $HS^-$, thus controlling the lower limit of the pH range. Process (iv) controls the upper limit of the pH range since the concentration of $CO_3^{2+}$ increases exponentially at higher pH levels (Ben-Yaakov 1973), thus pushing eq. 3 in the reverse direction. The possibility exists, therefore to model conditions conducive to soft tissue mineralisation in order to

ascertain likely conditions favouring such an event.

## 5.3 Soft tissue mineralisation

While a certain amount of decay is required to initiate the process of preservation, if too much decay occurs, information is lost. The preservation of such labile tissues as muscle can only occur where mineralisation is rapid and decay minimal (Allison 1988a; Allison & Briggs 1991; Briggs & Kear 1993a, b; Briggs *et al.* 1993).

Early work recognised 3 main influences on soft-tissue preservation; oxygen levels, rapid decay and microbial films (Seilacher *et al.* 1985). These factors do not prevent decay, but merely inhibit scavenging, and create geochemical gradients essential for diagenesis (Briggs & Kear 1993a, b). Scavenging is considered to be the primary cause of carcass destruction (Plotnick 1986). Thus its prevention does enhance preservation. Where decay is faster than mineralisation, only decay-resistant tissues will preserve.

The rate of mineralisation is dependent on a variety of controls which include concentration and oxidation state of the mineral ions, size and kind of the organic substrate, and the pH (Briggs *et al.* 1993).

The mineralisation of such soft tissues as muscle, which preserve the highest degree of fidelity, commonly involves calcium phosphate or apatite (Briggs & Kear 1993a, b, 1994; Briggs *et al.* 1993).

### 5.3.1 Phosphate Mineralisation

Ocean waters usually contain only trace quantities of phosphorus, commonly about 0.27 mg $l^{-1}$ (Lucas & Prévôt 1991), but in pore waters organic matter decomposition may increase phosphate to much higher levels (Burton & Walter 1990).

Biogenic phosphorus occurs in both soft and mineralised tissues in amounts between two and ten times that in sea water. Marine animals for instance, contain between 0.5 -

3.2% phosphorus dry weight in their soft tissues, 90% of which is in the organic phase (ATP, ADP, DNA, RNA, etc.) (Lucas & Prévôt 1991). Such tissues offer a rich source of phosphorus and upon the death of the organism, this phosphorus is quickly liberated into pore waters (Scharpf 1974; Berner 1980).

A series of laboratory experiments have been carried out, to analyse the decay and mineralisation process (Allison 1988a; Briggs & Kear 1993a, b). Initial experiments revealed that oxygen levels dropped to only a few percent within 1-2 days, regardless of the initial amount of oxygen present or the availability of oxygen throughout the experiment (Allison 1988a), indicating that decay within the carcass became anoxic within hours. In open conditions (where oxygen was freely available), oxygen levels returned to normal after the labile tissues had decayed (Briggs & Kear 1983a, b), otherwise anoxic conditions prevailed.

pH fell rapidly from approx. 8 to between 6 and 7 in closed systems, within 3 days Briggs & Kear 1993a, b, 1994). The ph recovered to 8.0 after 4 weeks, when all labile tissues had decayed. Reduction in pH was due to anoxic decay of labile tissues and the buildup of $CO_2$ and volatile fatty acids (Briggs & Kear 1994). Under open conditions, pH dropped initially, but then rose to 8.3 after 3-5 days and remained at those levels for the duration of the experiments.

Briggs and Kear (1993a, 1994) found that in most instances mineralisation had occurred and appeared to be of two kinds;

i) crystal bundles of acicular or dumbbell shaped $CaCO_3$ , which form within carcasses and moults - particularly within envelopes formed by the cuticle (see section 5.3.2 below);

ii) microspheres, occurring in various parts of the organism and replicating soft tissues - especially muscle.

The microspheres appear to be amorphous calcium phosphate and were concentrated around the more labile tissues such as muscle, where it replicated the fine structure, even

down to muscle fibres. This mineralisation started within 1-2 weeks and continued up to 4-8 weeks, by which time blocks of mineralised tissues reached 1-3 mm in size. The end of phosphate mineralisation appears to coincide with the rise in pH back to normal values (Briggs & Kear 1993a, b 1994; Briggs *et al.* 1993).

The phosphatisation of soft tissues appears to only occur when conditions were closed with respect to oxygen and labile tissues are present, since phosphatisation did not occur at all in moults (Briggs & Kear 1994). Phosphatisation appears linked with the initial drop in pH associated with the onset of soft tissue decay. Where phosphatisation did occur, it occurred in stages and mineralisation increased with time, provided pH levels remained depressed (Briggs & Kear 1994). Mineralisation was concentrated on muscle tissue and where muscle tissue contacted the surface of the tergites, but tended to be more widespread where oxygen was actively excluded. In instances where extraneous phosphorus was limiting, organisms provided up to 80% of the phosphorus present (a byproduct of sulphate reduction is $H_3PO_4$ - see eq. 5.6), and in examples where extraneous phosphorus was not limiting, up to 65% of available phosphorus was provided from the decay of the organism (Briggs & Kear 1994). This indicates that phosphatisation can occur even when the only source of phosphorus is the organism itself. However, an extraneous source would probably be needed for whole organism mineralisation.

Whilst the precise circumstances of mineralisation is unknown, it is apparent that early diagenetic mineralisation is a major factor (Allison 1988a; Briggs *et al.* 1993). From field and laboratory observations, it is clear that the two main conditions effecting phosphate mineralisation are oxygen levels and pH. Where oxygen is eliminated, the pH falls rapidly with the onset of anoxic decay. This drop in pH is most evident in the larger masses of soft tissue, but not in the extremities. The depressed pH levels and the presence of excess dissolved phosphate from soft tissue decay, inhibit $CaCO_3$ precipitation (Burton & Walter 1990) and increases the stability of apatite relative to

$CaCO_3$. In fact, the liberation of $PO_4^{3-}$ increases the acidity of the localised pore waters and encourages carbonate dissolution. The $Ca^{2+}$ thus liberated, is free to combine with the $PO_4^{3-}$ and thus precipitate $CaPO_4$ (Nathan & Sass 1981: Froelich *et al.* 1988; Prévôt & Lucas 1990). After the decay of soft tissues is complete, the pH rises, initiating $CaCO_3$ bundle precipitation in various parts of the carcass and over phosphatised tissues. Where conditions remain open to oxygen, pH remains high and $CaCO_3$ bundles are precipitated. Also, in moults, which lack labile tissues, only $CaCO_3$ bundles are precipitated (Briggs & Kear 1994).

As mentioned above, while a large proportion of the dissolved phosphate needed for mineralisation, can be provided by the decaying tissues, a significant proportion must come from extraneous sources. Such a source may be the phosphate "pump trap" of Froelich *et al.* (1988), which is intimately associated with the redox recycling of iron (see section 4.4.6.).

Froelich *et al.* (1988) proposed a two step phosphate precipitation process (Fig. 5.2)

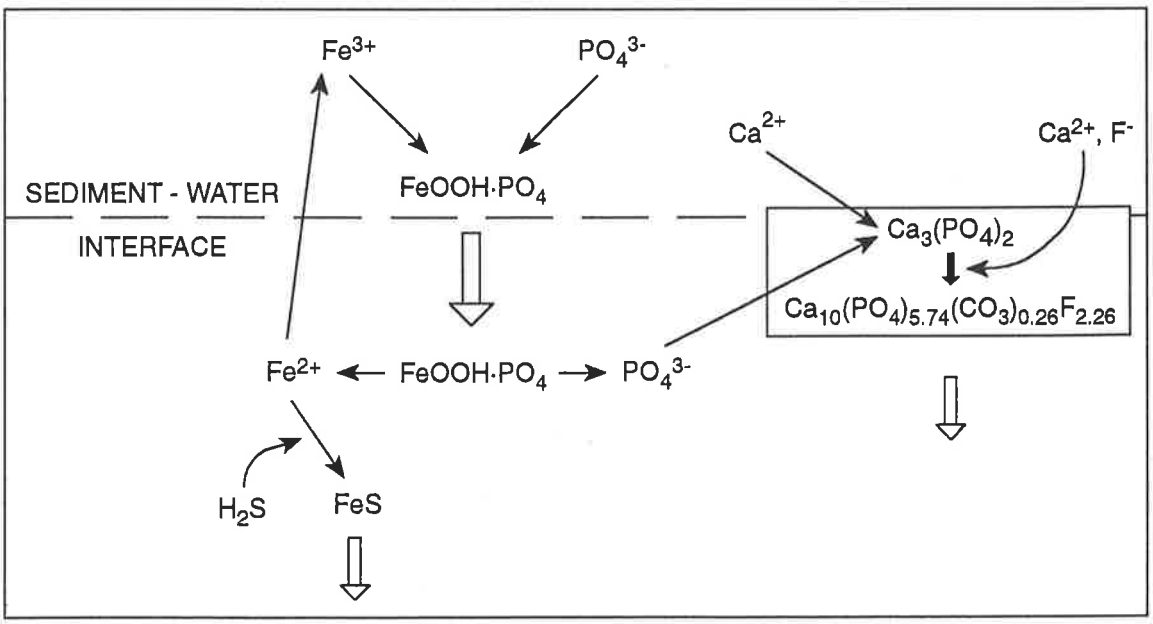


**Fig. 5.2.** Iron redox cycle and phosphate pump trap. Adapted from Froelich *et al.* (1988).

including a rapidly deposited, metastable calcium phosphate precursor phase (eq. 5.7),

$$3Ca^{2+} + 2PO_4^{3-} \rightarrow Ca_3(PO_4)_2 \qquad [5.7]$$

precipitated within the first centimetre of the sediment. This precursor phase is apparently oversaturated at typical pore-water calcium and phosphate concentrations. The second step is the conversion of the precursor phase to carbonate fluorapatite (CFA) by uptake of pore-water carbonate and fluoride (eq. 5.8). This can occur most typically

$$3Ca_3(PO_4)_2 + Ca^{2+} + 0.26CO_3^{-} + 2.26F^{-} \rightarrow Ca_{10}(PO_4)_{5.74}(CO_3)_{0.26}F_{2.26} \qquad [5.8]$$

in situations where there is a zone of mixed suboxic to anoxic diagenesis to allow the redox recycling of Fe and P and where sulphate reduction is present in the first few centimetres of the sediment (Froelich *et al.* 1988). Such conditions occur under upwelling zones or in areas where bottom waters are suboxic. Ruttenburg and Berner (1993) noted a peak in dissolved fluoride concentration coincided with a similar peak in dissolved iron in anoxic sediments from the FOAM site in Long Island Sound and in sediments from the Mississippi delta. Thus, they suggested that, since fluoride also adsorbs onto FeOOH, the fluoride was being released during the reduction of FeOOH at or below the oxic-anoxic boundary. This implies a source of fluoride and the potential for CFA precipitation below the first few centimetres of the sediment. However, at these depths within the sediment, dissolved carbonate concentrations are high enough to dissolve the metastable calcium phosphate precursor phase, since the solubility of the precursor phase increased dramatically with increasing pore-water carbonate ion concentration (Froelich *et al* 1988). The precipitation of CFA therefore occurs primarily in the first few centimetres of the sediment. Thus it is an sediment-water interface-linked phenomenon, when the oxic-anoxic boundary lies at or just below the sediment-water interface. Below this level, the high carbonate ion concentration dissolves the precursor phase and so does not allow CFA to precipitate.

Whilst CFA precipitation was thought to only occur under upwelling zones Ruttenburg and Berner (1993) recently showed in studies from the FOAM site in Long Island Sound and from the Mississippi delta, that CFA precipitation can occur in a number of non-upwelling environments and may well be a common process in marine, continental margin sediments.

5.3.1.1 Ancient Examples

Phosphatisation of soft tissues is rare and apparently requires exceptional conditions (Allison 1988a). Where it does occur however, spectacular preservation results (e.g. Müller & Walossek 1985; Martill 1989).

Preservation of soft tissues by phosphate in the fossil record has been known for some time (e.g. Reis 1888, 1893; Dean 1902) and include shark muscle from the Devonian Cleveland Shale (Dean 1902); arthropod cuticle, pterosaur wing membrane, fish, coleoid cephalopod and annelid muscle from the Lower Jurassic, Solnhofen Limestone (Viohl 1990); pterosaur wing membrane, arthropod cuticle, fish muscle, stomach lining and eggs from the Lower Cretaceous, Santanna Formation of Brazil (Martill 1988, 1989; Martill & Unwin 1989; Wilby & Martill 1992); fish, crustacean, polycaete and nematode tissues in the Lower Jurassic Osteno Formation of Italy (Pinna 1985); fish muscle from the Upper Jurassic of Chile (Schultze 1989); cephalopod muscle from the Middle Jurassic (Callovian) of Wiltshire, England (Donovan 1983; Allison 1988c); concavicarid muscle from the Upper Devonian (Frasnian) Gogo Formation, Western Australia (Briggs & Rolfe 1983); the soft integument of arthropods from the Orsten of Sweden (Müller 1979, 1985; Müller & Walossek 1985) and Georgina Basin of Australia (Walossek *et al.* 1993; Müller & Hinz-Schallreuter 1994) and cuticle and body infilling of shrimp from the Granton "Shrimp-Bed" and Gullane "Shrimp-Bed" from the Lower Carboniferous of Scotland (Briggs & Clarkson 1983, 1985) and algae, fungi and fecal pellets (e.g. Riggs 1982; Hirschler *et al.* 1990).

Of these, the most comprehensive studies have been on the Santanna Formation of

Chapada do Araripe, northeast Brazil (Martill 1988, 1989, 1990; Martill *et al.* 1992; Wilby & Martill 1992) and the Osteno of Italy (Pinna 1985).

Within the Santanna Formation, a number of fish species, such as *Lepidotes*, *Aspidorhynchus* and *Microdon*, have been found in laminated, carbonate-rich concretions with abundant pyrite. Phosphate, in this instance francolite, occurs as a replacement for soft tissues such as muscle and gills, and as a surface coating on bone (Martill 1988). Some phosphatised muscle fibres remain as myotomes and in some instances cell nuclei are preserved (Martill 1989). However, some myotomes have clearly begun to decompose before phosphatisation occurred and are represented as an amorphous mass. It is obvious that phosphatisation has preceded all other diagenetic mineral phases (Martill 1988). Phosphate is concentrated in the body, the extremities appear to be only partially phosphatised. SEM analysis of the phosphate indicates that the mineralisation consists of aggregated clusters of microspherical apatite (Allison 1988a).

It has been suggested that occasional mass mortalities, caused by migration of the halocline, resulted in the rapid deposition of large numbers of fish in the sediments. The hypersaline conditions, together with the rapid removal of oxygen by the decaying fish evidently inhibited predation and instigated conditions conducive to phosphate mineralisation (Martill 1988).

The Osteno Formation from the Sinemurian (Lower Jurassic) of Italy has produced fossil fish, crustaceans, polychaetes and nematodes, preserved via "molecule-by-molecule" replacement by calcium phosphate (Pinna 1985 p. 171). The fauna comprised 50.39% decapod crustaceans; 28.90% thylacocephala crustaceans; 11.55% fish; 3.49% land plants; 2.40% Ophiuroidia; 1.89% cephalopods; 0.94% polychaetes and 0.44% nematodes (Pinna 1985). The taxonomic diversity is low, with some groups being represented by only one or two species (e.g. the crustacean thylacocephala are mainly represented by *Ostenocaris cypriformis*). Fossilisation is characterised by the

dissolution of calcite and aragonite leaving only moulds, and the replacement by phosphate of muscle tissue and branchiae in thylacocephala crustaceans, the arms of coleoidea cephalopods, the muscle tissue of fish and the digestive tracts of polychaetes and nematodes (Pinna 1985). In all instances, the phosphate occurs as spherulites. The fossils are found in unbedded, grey, spongolithic micrites, containing pyrite granules and limonitic material. The absence of post mortem transport in indicative of an environment of deposition similar to a restricted basin with little current activity. Oxygen levels were low, but not anoxic, allowing the basin floor to be occupied by a sparse fauna of low taxanomic diversity, which was tolerant of low oxygen levels (Pinna 1985). The oxic-anoxic boundary was placed close to the sediment-water interface, allowing no avenue for infaunal, metazoan activity. The low oxygen levels and the proximity of the oxic-anoxic boundary were conducive to low pH levels, which resulted in the dissolution of $CaCO_3$ and the precipitation of phosphate and pyrite

While the chemical conditions necessary for the precipitation of phosphate in large-scale Cambrian phosphorites may well be similar to that discussed above, other factors, such as high carbon and phosphorous concentrations and sedimant reworking, appear important (Cook & Shergold 1986). These are not factors in the occurrence of phosphate in the Emu Bay Shale.

5.3.1.2 Phosphate mineralisation in the Emu Bay Shale

Examples of extensive phosphatisation within the Emu Bay Shale fauna appear confined to *Myoscolex ateles*, a form which was described as a polychaete worm (Glaessner 1979). This classification has been questioned (Nedin 1992) and it now appears to represent an arthropod (see section 3.2.6.2). Thin films of fluorapatite have been found associated with the trilobite *Redlichia takooensis* and the phyllocarid *Isoxys communis* (D. E. G. Briggs pers comm. 1994).

A transverse section normal to bedding shows that specimens of *Myoscolex* consist of four layers. The two central layers on either side of the trunk correspond to the muscle tissue, identified by its fibrous appearance. Mineralisation ranges from black to pale grey apatite/francolite. Where more extensive diagenetic alteration has occurred, the mineral is a much more blocky, discontinuous sheet which is characteristically pale grey in colour (Pl. 5.6).

Phosphatisation appears confined to the trunk of the organism, and is not found in the extremities. In lateral aspect, well preserved specimens clearly show narrow bands of longitudinal muscle, the fibres running parallel to the axis of the body, along both dorsal and ventral margins of the trunk. These are separated by a wider band of dorso-ventral muscles, the fibres running at a high angle to the body axis. In the majority of instances, both longitudinal and dorso-ventral muscles are fused together into a mineralised sheet. Occasionally, the individual muscles appear to remain discrete providing a clearer indication of their original configuration (Pl. 5.6).

In the post Cambrian examples discussed above, and in the cited experimental work, the phosphate was present as aggregated clusters of microspheres. In the Emu Bay Shale however, the phosphate occurs as blocky, flat sheets (Pl. 5.6). This is taken as indicative of recrystallisation.

It is possible that an indication of the original tergites may be evident in specimens where the phosphate has a blocky recrystallised form.

The apparent lack of individual muscle bundles does indicate that some decay before mineralisation occurred, as would be expected from the experimental results discussed above (Section 5.3.1)

While it appears that phosphatisation and thus preservation of muscle tissue has occurred in *Myoscolex*, there does not seem to be a concomitant preservation of the cuticle. Rare specimens preserve traces of flap-like appendages extending ventrally beyond the trunk (e.g. Pl.14). The absence of such structures in the majority of specimens indicates that the cuticle of this part of the body, at least, was very thin and normally decayed rapidly.

If the cuticle of the axial part of the trunk was similarly thin and decay-prone, it is likely to have survived only long enough to enclose the muscles and promote phosphate diffusion as they were becoming mineralised. However, it is also likely that the cuticle covering the tergites might have been very thin and flexible and has taken up the relief of the underlying muscles. Like the muscles, it then became phosphatised and is no longer possible to distinguish the thin layer as it has become obscured by diagenetic recrystallisation. In a number of examples it has clearly decayed, as the surface bonding the muscles is not continuous as would be expected if they were covered by a cuticle.

With a better understanding of the processes leading to and controlling phosphatisation, a more accurate taphonomic history can be established. The key controls on phosphate mineralisation appear to be pH and anoxia (Briggs & Kear 1993a, b), thus the environmental conditions which produced the mineralisation of soft tissues can be constrained to one in which rapid anoxia and lowering of pH occur in the presence of dissolved phosphate. Counter-intuitively, an anoxic water column, i.e. an environment where the oxic-anoxic boundary enters the overlying water column, will not enhance phosphate mineralisation. Conditions conducive to such mineralisation occur where the oxic-anoxic boundary is at, or immediately below, the sediment-water interface. Such conditions allow the redox recycling of iron oxyhydroxides and thus provides an extraneous source of dissolved phosphate. In such an environment, active decay of soft tissues, even at the sediment-water interface above the oxic-anoxic boundary, will quickly become anoxic, leading to sulphate reduction and a concomitant lowering of pH inside the tissues (Briggs & Kear 1993b). These conditions allow for rapid mineralisation by phosphate to occur.

No phosphate has been found in association with *Anomalocaris* specimens. Since these specimens are most likely moults, the absence of phosphate mineralisation may be explained by the lack of labile tissues needed to produce the anoxic, low pH environment necessary for phosphate mineralisation (e.g. Briggs & Kear 1993b). It is likely that

phosphatisation has occurred in all forms to greater or lesser degrees where labile tissues existed.

It is important to note that the presence of high concentrations of dissolved phosphate inhibits the precipitation of calcium carbonate, especially at low pH (see Burton & Walter 1990 and references therein).

This is the first record of phosphatised muscle tissue in a Cambrian Konservat-Lagerstätte (muscle tissue reported within the Sirius Passet fauna from the Lower Cambrian of Greenland appear to have been replaced by silica - although probably after apatite). Phosphate mineralisation in the Orsten faunas appears to have been via a different process than that occurring within the Emu Bay Shale. In the Orsten faunas, phosphatisation is confined to external tissues, with no phosphatised muscle tissue being reported. The process appears to have been via the impregnation of the integument, commonly resulting in the formation of hollow carcasses. Also, phosphatisation is restricted to organisms or parts of organisms <2mm in size.

Glaessner (1979) regarded the muscle tissue in *Myoscolex* as being "preserved as plates composed of elongate calcite crystals" (Glaessner 1979, p. 22). However, examination of P21020, described by Glaessner as showing "a layer of calcified muscle tissue" (legend to fig. 7: 1979, p. 28) shows that the layer in question is pink fibrous calcite which has grown external to the muscles (see section 5.3.2.4 below). However, Glaessner did report that so-called setae were preserved as calcium phosphate.

### 5.3.2 Carbonate Mineralisation

Whilst the phosphatisation of soft tissues remains rare and phosphatised hard parts somewhat more common in the fossil record, by far the most common mode of fossil preservation is as calcium carbonate (e.g. Runnegar in Bengtson *et al.*1990). Indeed, the preservation of soft parts is more commonly associated with carbonate mineralisation than with any other authigenic mineral phase (Allison 1988b) and extraordinary detail

can be preserved (e.g. Baird *et al.* 1985a, b).

From the previous arguments (section 5.2.1) it can be seen that sulphate reduction in sediments undergoing early diagenesis can profoundly affect carbonate precipitation or dissolution (Berner 1971; Stoessell 1992). Therefore, it is this process more than any other which dictates the possibility of fossilisation via carbonate mineralisation.

Changes in carbonate chemistry involved with the diagenesis of anoxic marine sediments involve complex interrelationships with other minerals, mediated by pH, salinity and temperature. Where the concentration of $CaCO_3$ dissolved in pore water exceeds approximately $4.3 \times 10^{-7}$ (the apparent equilibrium constant for calcite), the pore waters are said to be supersaturated with respect to $CaCO_3$ and carbonate precipitation may be initiated from solution. Where the concentration of dissolved $CaCO_3$ is below the apparent equilibrium constant, the pore waters are said to be undersaturated with respect to $CaCO_3$ and solid carbonate dissolution may be initiated. (Canfield & Raiswell 1991b).

5.3.2.1 Sulphate reduction and carbonate chemistry

An important relationship is that between carbonate and sulphate. Sulfate reduction in sea water can enhance the precipitation of carbonate minerals (Berner 1971; Stoessell 1992). However, during early diagenesis, initial sulphate reduction results in carbonate pore water undersaturation and thus the dissolution of carbonate (Fig. 5.3). This is brought about by the accumulation of the byproducts of sulphate reduction in the pore waters and the resultant depression of the pH (Morse & Mackenzie 1990; Canfield & Raiswell 1991b). The decrease in pH has a greater impact than the increase in alkalinity (Ben-Yaakov 1973; Canfield & Raiswell 1991b; Morse *et al.* 1992). Also, back-oxidation of produced sulphide to sulphuric acid increases carbonate dissolution (Smart *et al.* 1988). Where the build-up of dissolved sulphate is allowed to continue, pH values can be depressed to below 7 and carbonate undersaturation can persist for extended

periods. However, where dissolved sulphate is removed from pore waters, the waters remains less acidic and pore water carbonate supersaturation occurs very rapidly (Canfield & Raiswell 1991a). Under these conditions carbonate dissolution is minimalised and carbonate precipitation may result.

The byproduct of sulphate reduction which has the most significant effect on pore water pH is $HS^-$ (eq. 5.6). Where reactive iron is available, $HS^-$ is removed from pore waters as FeS and/or $FeS_2$ (Berner 1971; Canfield 1989b; Canfield & Raiswell 1991a, Morse *et al.* 1992; Hendry 1993) (see section 5.3.2.2 below). In many coastal sediments less than 10% of the total $HS^-$ ($H_2S + HS^-$) is preserved as FeS or $FeS_2$ and the remainder is oxidized (Jørgensen 1983; Fossing & Jørgensen 1990).

Canfield and Raiswell (1991b) found that a model of pore water carbonate saturation consistently overestimated pore water carbonate saturation in the initial stages of sulphate reduction compared with field observations of the FOAM site. A factor not included in the model, which was put forward as a possible reason for this, was sulphide oxidation. Sulphide oxidation occurs to a great extent in continental margin sediments (Jørgensen 1977), the products of which are acidity and $CO_2$. Although difficult to quantify, the process of sulphide oxidation can, on a seasonal basis, dominate in nearshore areas, generating acidity and resulting in carbonate dissolution (e.g. Aller 1982). The oxidation of sulphide can bring about significant increases in the levels of dissolved iron and influence the pH levels, of pore waters. After a hurricane passed through Long Island Sound, high concentrations of dissolved iron (near millimolar) and low sediment pH were measured. This compares with average values before and two weeks later of $\leq 80$ $\mu M$ l-1 of dissolved iron and a pH of 7.5 (Canfield 1989b). The rise in dissolved iron concentration and the fall in pH were thought to be related to surficial sediment mixing with the overlying water, resulting in the oxidation of sulphides.

It was thought that such back-oxidation of sulphide was chemically controlled and confined to the oxic and suboxic zones. Oxidation of $HS^-$ has since been observed at all depths, even in highly reducing sediments (Fossing & Jørgensen 1990). A new pathway in this cycle has been discovered which incorporates a thiosulphate shunt

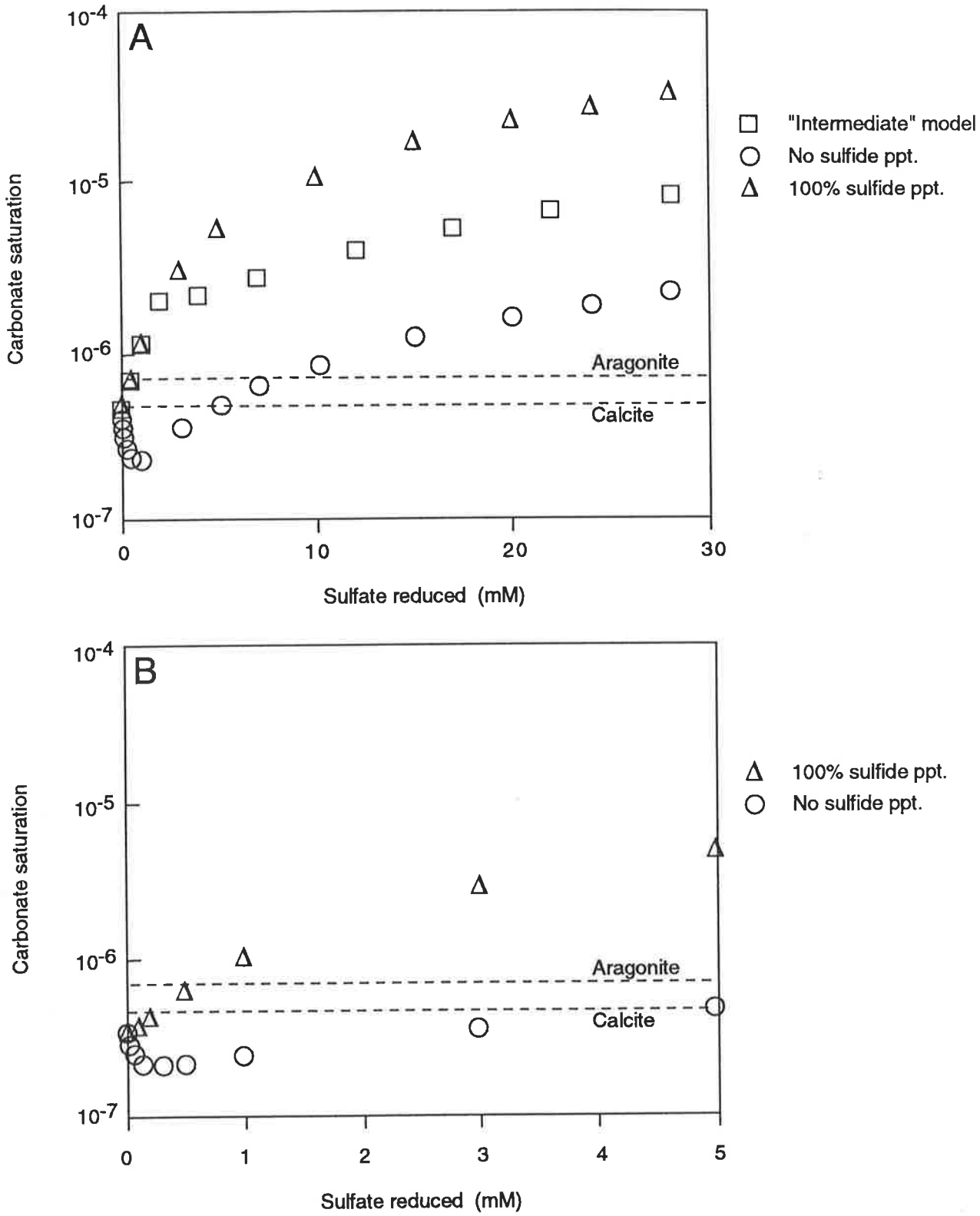


**Fig. 5.3 A**. Results from a sulfide reduction model considering three cases, one where all the sulfide produced accumulates in solution, one where all of the sulphide precipitates with iron, and an intermediate case where the first 2 mM of sulphide produced precipitates after which 25% of the sulphide accumulates in solution. Carbonate saturation is expressed by ion molarity product. Dashed lines represent the saturation level of pore fluids with respect to calcite and aragonite. The models show rapid initial carbonate undersaturation, leading to carbonate dissolution and eventual carbonate supersaturation and precipitation. **B**. Expanded scale of the first few nM of sulphate reduced. The intermediate model mirrors field measurements from the FOAM site in Long Island Sound, Connecticut. From Canfield & Raiswell (*in* Allison & Briggs 1991, Taphonomy: Releasing the Data Locked in the Fossil Record. Plenum Press, with permission).

(Fossing & Jørgensen 1990; Jørgensen *et al.* 1990). This shunt activates on the inorganic oxidation of $HS^-$, whereby the dominant product is thiosulphate ($S_2O_3^{2-}$) and $SO_4^{2-}$ is only a minor product (Fossing & Jørgensen 1990; Jørgensen *et al.* 1990). Of this thiosulphate, more than 50% is recycled to $HS^-$ via disproportionation (Fossing & Jørgensen 1990; Jørgensen *et al.* 1990) (eq. 5.9). This shunt can keep $HS^-$ levels high,

$$S_2O_3^{2-} + CH_3COO^- + H^+ \rightarrow 2HS^- + 2CO2 + H20 \qquad [5.9]$$

even during oxidative recycling and hence is an important factor in carbonate precipitation. The oxidation of thiosulphate produces sulphate and iron as byproducts (eq. 5.10). The sulphate is free to re-enter at the sulphate reduction stage of the sulphur

$$S_2O_3^{2-} + 8FeOOH + 14H^+ \rightarrow 2SO_4^{2-} + 8Fe^{2+} + 11H_2O \qquad [5.10]$$

cycle, whilst the free iron can react with dissolved $HS^-$ and precipitate as pyrite. The thiosulphate shunt therefore, plays an important role in the sulphur cycle, especially during early diagenesis, where reactions which increase pore water pH are critical in providing an environment conducive to carbonate precipitation.

In a series of experiments set to analyse conditions conducive to mineralisation, Briggs & Kear (1994) found that where conditions remained open to oxygen and/or the pH levels remained high, $CaCO_3$ bundles stated forming within 1 week, with no evidence of phosphate mineralisation. The crystal bundles were formed of acicular or dumbbell shaped $CaCO_3$ crystals and formed on the inner surface of the cuticle rather than in the soft tissues. Where large numbers of these bundles precipitated in close proximity, they coalesced to form a sheet. With continued precipitation, sheets formed in all parts of the moults but rarely in eyes and antennae.

Bundle formation occurred more readily, in a variety of positions within the carcass and under a wide range of conditions compared with phosphatisation, but appeared to be

correlated with a rise in pH after initial soft tissue decay (Briggs & Kear 1993a, 1994). This link with the rise in pH was especially marked in the instance of $CaCO_3$ bundle overgrowths of phosphatic mineralisation (Briggs & Kear 1994). In some enclosed experiments, $CaCO_3$ crystal bundles 100-200 μm long precipitated over $CaPO_4$ mineralised muscle tissue. Briggs & Kear (1993a, 1994) found this to be representative of a latter phase of mineralisation which only occurred in specimens which had been decaying for over 8 weeks and where the pH had risen to 8.0. This late phase of $CaCO_3$ precipitation over phosphatised tissues, was not found in specimens that had been decaying for less than 8 weeks.

Clearly then, the pH levels found in sediments undergoing early diagenesis is critical in controlling the concentration of dissolved carbonate in pore waters and thus the potential for carbonate precipitation or dissolution. A major influence on pH in pore waters is the presence of dissolved sulphide. This is controlled in turn, by the rate of sulphate reduction and the availability of reactive iron.

5.3.2.2 The role of iron

Reactive iron - the fraction of iron in marine sediments which readily reacts with sulphides from sulphate reduction to form various iron sulphide minerals (Raiswell & Berner 1984) - is effective in buffering pore water sulphides to very low levels, even during active sulphide production via sulphate reduction. This reactive iron is mainly in the form of iron oxides and oxyhydroxides (Goldhaber & Kaplan 1974), not iron silicates which have very much slower reaction times. Bacterial mediated iron production via iron oxide reduction is the most important source of dissolved, reactive iron (Canfield 1988). When iron is present, the presence of dissolved sulphide causes the precipitation of iron sulphides (eq. 5.11). With the subsequent removal from the

$$9CH_2O + 4SO_4^{2-} + 4FeOOH \rightarrow 4FeS\downarrow + 9HCO_3^- + H^+ + 6H_2O \qquad [5.11]$$

pore waters of $HS^-$, the pH rises (Canfield & Raiswell 1991a; Morse *et al.* 1992) Also, the production of $HCO_3^-$, not only enhances the increase in alkalinity and thus the saturation state of the pore fluids, but also helps push equation 5.3 in the reverse direction. This results in the rapid establishment of carbonate supersaturation and the possibility of carbonate precipitation.(Fig. 5.3). Thus an often complex diagenetic relationship exists between pyrite and carbonate.

This relationship can be seen by the reaction of carbonate in the presence or absence of pyrite precipitation (no free iron) during the early stages of sulphate reduction. Where free iron is absent, a major decrease in the saturation state with respect to carbonate minerals occurs, due to the impact of lowered pH values (Canfield & Raiswell 1991a, b; Morse *et al.* 1992). The combination of sulphate reduction and pyrite precipitation, on the other hand, can lead to significant calcium carbonate precipitation (Berner 1971; Canfield 1988; Canfield & Raiswell 1991a, b; Morse *et al.* 1992) (Fig. 5.3).

Thus, under anoxic conditions in the presence of reactive iron, carbonate supersaturation occurs, which can lead to carbonate precipitation.

5.3.2.3 Ancient examples

Whilst the above model appears to accord well with what is found in experiments, the rock record does not show this simple pattern. Indeed, in some instances, the rock record appears counter-intuitive (e.g. the Posidonienschiefer - see below). An understanding of the geochemical environment applicable in these cases, indicates that the model described above does indeed hold and can be used to explain the presence of carbonate in the Emu Bay Shale at Big Gully.

Some Jurassic shales in Europe exhibit variable aragonite preservation seemingly unrelated to depositional oxygen and organic carbon levels. The Upper Oxford Clay in

England is a grey, bioturbated shale with low organic carbon and pyrite, and aragonite is only rarely preserved (Fisher & Hudson 1987). The Lower Oxford Clay is much less bioturbated, has higher sulphide and organic carbon levels and contains well preserved aragonite (Fisher & Hudson 1987). However, within the classic black shale of the Posidonienschiefer, which is rich in organic carbon and contains pyrite, aragonite has been completely removed (Raiswell & Berner 1985).

These differences may be explained, not just in terms of bioturbation (and hence oxygenation), but by the diagenetic pathways undergone by each sediment (Hudson, quoted in Canfield & Raiswell 1991b). The loss of aragonite from the Upper Oxford Clay occurred primarily as a result of bioturbation. This prevented the build-up of alkalinity by promoting the aerobic reduction of organic carbon, whilst allowing oxidation of the accumulated sulphides. This produced acidic conditions conducive to undersaturation and hence aragonite dissolution. The occurrence of calcite within the Upper Oxford Clay is due to the higher dissolution constant of calcite compared to aragonite.
The preservation of aragonite within the Lower Oxford Clay is due primarily to much weaker bioturbation, resulting in low dissolved oxygen levels, increased sulphate reduction and overall carbonate supersaturation.

The loss of aragonite from the Posidonienschiefer, which would be expected to retain any precipitated aragonite, may be explained by the lack of reactive iron, leading to a buildup of $H_2S$. This initially results in carbonate undersaturation, leading to aragonite dissolution (Canfield & Raiswell 1991b). This idea is supported by comparisons with coeval Jet Rock sediments in northeast England in which aragonite is preserved and which contains much more pyrite. The higher pyrite content indicates that the initial reactive iron content of the Jet Rock was much higher than in the Posidoneinschiefer. High levels of reactive iron leads to rapid removal of sulphide from the pore fluids and bottom waters via iron sulphide precipitation (eq. 5.9). Thus promoting supersaturation

with respect to carbonate and so, carbonate preservation.

From these examples it can be seen that in order to precipitate and preserve carbonate, it is not enough to have low dissolved oxygen levels and a concomitant increase in sulphate reduction. It is also important to have freely available reactive iron to facilitate the removal of the acidic products of sulphate reduction, as shown by the Jet Rock deposits above compared with the Posidonienschiefer. The presence or absence of carbonate mineralisation and its preservation within the Emu Bay Shale, can therefore, provide information of its depositional and early diagentic environment.

5.3.2.4 Carbonate Mineralisation in the Emu Bay Shale

The majority of fossils within the Emu Bay Shale at Big Gully are preserved by calcium carbonate (e.g. Glaessner 1979) in what appears to be two separate forms. The the main expression of fossilisation is pink to white, acicular calcite fibres fibres, 0.3 - 0.4 mm long and ≤0.02 mm wide (Pl. 5.6). Rarely, cuticle is preserved as light pink to white blocky sheet-like calcite, which produces a flat pavement-like surface approx, 0.02 mm thick.

The carbonate precipitation model put forward by Canfield and Raiswell (1991b) (see section 5.3.2.1), seems applicable. Bacterial mediated sulphate reduction in the presence of dissolved iron results in carbonate supersaturation and carbonate precipitation.

With *Myoscolex*, pH levels appear to have been keep low during the initial stages of sulphate reduction. This may have been due to the concentrated mass of labile muscle tissue available as a substrate compared with other elements in the fauna. Probably depressed pH levels inhibited carbonate precipitation and even may have encouraged carbonate dissolution, whilst promoting phosphate precipitation. With the decline in available labile tissues, the concomitant decline in sulphate reduction allows the removal of substantial amounts of $HS^-$ via pyrite precipitation. This may elevate the pH of the pore waters, resulting in carbonate supersaturation and carbonate precipitation.

The fact that, where the two are found together, carbonate always overlies phosphate (Pl. 5.6) suggests primary carbonate precipitation postdates phosphate precipitation. This is in accord with the Canfield& Raiswell and the Briggs and Kear models discussed above.

An interesting anomaly in the application of these models is the lack of pyrite - or its oxidized products - *at the site of carbonate precipitation.* Logically, if the precipitation of pyrite is needed to elevate pH levels and initiate carbonate precipitation, pyrite should be precipitated at the site of carbonate precipitation. Occasionally in the Emu Bay Shale phosphate/carbonate fossils are found closely associated but *spatially separated* from iron oxide concretions or crusts. These concretions and crusts may well be the oxidized remnants of primary pyrite. Canfield (1989), found that the most likely source of dissolved iron in sediments was not the reaction between dissolved organic matter and iron oxides as was previously thought, but was in fact due to bacterial reduction of iron oxides. He speculated that bacterial sulphate reduction and bacterial iron reduction could occur in different microniches within the sediment, since the two bacterial populations are vying for separate substrates (labile organic matter for one, oxidized iron surfaces for the other). The cause of this separation between centres of carbonate precipitation and pyrite precipitation in the Emu Bay Shale is likely to be the result of microniche separation between bacteria which utilise sulphate reduction as a primary source of energy and thus produce $HS^-$, and those which utilise iron oxide and thus produce dissolved $Fe^{2+}$. It is possible that, with *Myoscolex*, the intensity of sulphate reduction due to the presence of large quantities of labile tissues was such that production of $HS^-$ was greater than its capacity to diffuse away, resulting in excess $HS^-$ in and around labile tissues and hence low pH. Away from the centre of sulphate reduction, $HS^-$ may soon have come into contact with dissolved $Fe^{2+}$ from disseminated iron reducing bacteria production, and precipitation of disseminated pyrite would result. There are rare examples of what could possibly be oxidized iron sulphide halos around some fossils (e.g. Pl. 13.2). Occasionally, centres of iron reducing bacteria would occur close to centers of sulphate reduction and large concretions of pyrite would be precipitated, later

to oxidize to iron oxide.

Thus the centres of carbonate precipitation are spatially separate from the sites of iron reduction. Since iron precipitates are extremely rare intimately associated with carbonate precipitation in the Emu Bay Shale, it can be assumed that the rate of sulphate reduction around labile tissues (and hence the rate of $HS^-$ production) exceeded the rate of iron reduction, leading to a $HS^-$ gradient and the diffusion of $HS^-$ away from the centre of sulphate reduction. Any pyrite which precipitated very close to the centre of sulphate reduction will, in all probability, be re-oxidized to thiosulphate and thence, eventually to sulphate and re-entry into the sulphur cycle. This can only occur in small amounts, since the main by-product of such oxidation is thiosulphate and then $HS^-$, which can be expected to lower the pH if such a reaction were to occur in bulk.

The fibrous form of the calcite is somewhat unusual. Whilst the preservation of fossils by fibrous calcite is rare, its occurrence in the rock record is not. Fibrous calcite has been reported from numerous locations and its occurrence has been linked to; precipitation under the influence of fresh water after emergence (e.g. Ginsburg 1957), precipitation below the low-tidal level (e.g. Newell 1955) and precipitation under sedimentary cover by connate waters or brines derived from compaction of neighbouring basinal shales of from lagoonal sediments. In all known examples however, precipitation was an early diagenetic feature.

The formation of calcite fibres, as in other crystal morphologies, is influenced by chemical environment and rate of crystallisation. The presence of sulphate and magnesium favours the formation of fibrous crystals (Folk 1974). This is due to the 'poisoning' effect of these species on the x- and z-axes of the crystal, resulting in growth only along the c-axis.

Crystallisation rate is governed by the relative growth of its faces, which is dependent on the internal order of the crystal and the medium. Initial precipitation of carbonate is characterised by a brief surge of crystal growth caused by surface and bulk nucleation. After the initial precipitation, a period of steady addition from solution following a

second order surface controlled reaction (Nancollas & Reddy 1971).

Since crystal growth takes place exclusively on the solid-liquid interfaces, the morphology of the crystal is directly related to the structure of the interface, or how rough it is (Sunagawa 1982). Where the interface is atomistically rough, continuous growth occurs. High saturation leads to increased roughness of the solid-liquid interface and thus to changes in the growth mechanism from continuous growth controlled by dislocations, to continuous growth controlled by two dimensional nucleation (Sunagawa 1981). A similar progression, albeit from a silica gel, from single polygonal crystals to polycrystalline rhombic aggregates to spicular forms was shown to occur experimentally (McCavley & Roy 1974). Sunagawa (1982) found that in slightly supersaturated fluids, the nature of the seed crystal or substrate becomes important.

As growth proceeds, by addition of reactants along the c - oblique faces, competitive growth results in the selective elimination of those crystals whose c-axes are not sub-perpendicular to the substrate. A compromise boundary parallel to the c-axis is eventually attained, resulting in a fibrous array of crystals (González *et al.* 1993). Thus it is the fluid chemistry, especially supersaturation, which will determine the form and fibrous habit of the precipitating crystals.

It is apparent that the present form of the calcite, as with the phosphate, is the result of at least one episode of recrystallisation given the unusual tectonically aligned fibrous habit. There are several possibilities to explain the fibrous nature of the recrystallised carbonate; pseudomorphed after fibrous aragonite; recrystallised into dilating voids or as slickenfibres growing along a displacement plane.

5.3.2.4.1 Carbonate fibre alignment

It is difficult to say, but it is probable that the calcite was originally aragonite and that during the episode of recrystallisation, the original aragonite may have been pseudomorphed by acicular calcite. A similar occurrence has been documented from modern sediments along the Trucial Coast of the Persian Gulf (Evemy 1973). Briggs

and Kear (1994) found that carbonate precipitated during experiments on tissue decay and mineralisation, took the form of aragonite.

Alternatively, the fibrous nature of the calcium carbonate may well be suggestive of a somewhat unusual chemical and/or structural environment during recrystallisation.

The fibrous calcite appears similar to crystal vein fibres which are formed by antitaxial growth. This occurs where the growth fibre is of a crystal species that is uncommon or absent in the wall rocks of the vein, for example calcite veins forming in shale (Durney and Ramsay 1973). The fibres appear to grow from a median suture line towards the walls (hence 'antitaxial'). Where the principal strain direction changes, the fibres curve. However, the direction of earliest increments are recorded by the fibre directions at the central median surface, compared with those of the last increments which are recorded by the fibre directions at the vein walls (Durney & Ramsay 1973; Davis 1984). Thus where there is no change in fibre direction from the median to the walls, the principal strain direction has remained constant throughout the formation of the vein. The fibres found in the Big Gully fossils consistently align in the same direction ( S -> N) regardless of the alignment of the fossil. This is consistent with other data, indicating that the direction of principal strain was toward the north. Also the straightness of the fibres indicates that the strain was constant during the precipitation of the fibrous calcite. In certain instances a medial line exists within the calcite fibres. Thus the fibrous calcite might represent the recrystallisation of original aragonite within a tectonically active stress field.

An alternative hypothesis is that the fibrous calcite represents slickenfibres sub-parallel to $\partial i$. Here, crystal fibres grow along a fault, or displacement plane. If crystal growth keeps pace with the progressive separation of the adjacent walls, the morphology of the crystals will be similar to those which grow in tensile fissures (Durney & Ramsay 1973). The result will be a series of overlapping needlelike fibres aligned in the direction of the last differential displacement. However, crystal fibres will tend to be precipitated on the leeward side of tiny ridges and bumps. Thus microtopography will control, to a certain extent, the area and thickness of crystal growth.

In the Emu Bay Shale fossils, the $CaCO_3$ fibres continue at the same thickness over the microtopography of trilobite morphology with no discernable preference for the leeward side. Also, there is no evidence of fracturing within the sediment, apart from well defined cleavage planes, two of which are orientated at a high angle to the longitudinal axis of the fossils. Thus, it appears that the fibres do not represent slickenfibres.
A stable isotopic analysis of of the fossil calcite and vein calcite, shows a significant difference between them. Fossil calcite has a $\partial C^{13} = -2.734$ compared with that for vein calcite of $\partial C^{13} = +0.821$. This indicates that fluids which deposited calcite in cleavage and joint planes did not homogenise with that which produced the fossil calcite. Also, the fossil calcite still retains a remnant of its original low $\partial C^{13}$ value, a value indicative of a biogenic source for the carbonate (e.g. Hendry 1993).

# Chapter 6: Palaeoenvironment of the Emu Bay Shale Lagerstätte

*"One principle of research probably comes nearer than any other to being without exceptions: no matter what your problem is, there is never enough data to solve it. That applies with bitter force to paleoecology."*

G. G. Simpson (1969, p. 163)

## 6.1 Introduction

The environment of deposition is clearly the most important single factor in the formation of fossil lagerstätten (e.g. Seilacher *et al.* 1985). Innumerable factors combine to produce the many modern environments that have been documented. Some of these are quite subtle and the exact interplay which occurs is extremely difficult to unravel, even when viewed at first hand. How much more difficult it is then, to reconstruct past environments using only the few relic clues remaining in the rock record after the ravages of diagenesis, lithification, metamorphosis and tectonic upheaval.

Nevertheless, in recent years great strides have been made in our understanding of the chemistry of early diagenesis, thanks to the work of Berner (1971, 1978, 1984), Canfield (1988, 1989b, 1991), Jørgensen (1983, 1988) and others, and to a few important observational sites - including the aptly named FOAM site (Friends Of Anoxic Mud!).

A more complete understanding of modern environments has shown that they contain recognisable biological, physical and chemical factors which, when preserved in the rock record, point the way to a more accurate reconstruction of past conditions (e.g. Calvert & Pederson 1993; Piper 1994). Information on such factors can be gained from an integrated study of the sedimentology, palaeontology and geochemistry of a deposit. This type of integrated approach has been successfully used in a study of the Late Jurassic Kimmeridge Clay in England, where a study of species composition and trophic

groups, geochemistry and environmental controls produced a detailed subdivision of the strata and a better understanding of the palaeoenvironment during deposition (Wignall 1990a).

In order to reconstruct the palaeoenvironment at Big Gully during Emu Bay Shale deposition, an understanding of the main influences on the environment is needed. Once these are established, they can be compared with the information obtained from the sedimentological, palaeontological and geochemical analyses in order to construct a depositional environmental model for the Emu Bay Shale Lagerstätte.

## 6.2 Orientation of Fossils

Soft-bodied and poorly mineralised organisms are usually in a compressed state. The orientation of such fossils in the sediment can provide important information, not only as to original shape, but also to the mode of deposition. The reconstruction of the original shape of the compressed fossils can be enhanced by the utilisation of specimens preserved at differing attitudes, allowing structures concealed by one orientation to be revealed (e.g. Briggs & Williams 1981).

However, the orientation of fossils in an assemblage can also provide depositional information. Beds containing fossils in a number of differing orientations suggest rapid deposition in a sediment slide or slump. For example, the fauna of the Burgess Shale is preserved in a wide variety of orientations, with some forms preserved with their longitudinal axes steeply inclined or vertical to bedding (e.g. Conway Morris 1986). As a consequence of this and other sedimentological evidence, it has been suggested that the Burgess Shale represents a distal slide deposit whereby organisms have been transported downslope by slumping and deposited within turbiditic deposits in an anoxic basin (Whittington 1971a, Whittington 1977; Conway Morris 1986).

In contrast, the Chengjiang fauna appears to have been preserved either parallel or lateral

to bedding (e.g. with the long axis of the body parallel to bedding) (Hou *et al.* 1991) (Table 6.1). The great majority of the organisms which were inferred to be dorso-ventrally flattened in life, for example the 'trilobitomorphs', are preserved parallel to bedding (i.e. the lateral margins of the organism are orientated parallel to bedding). Bivalvate organisms, e.g. *Isoxys*, are preserved in lateral aspect (with the organism lying on its side, parallel to bedding). A few organisms exhibit both preservational aspects, for example, 70% of *Alalcomenaeus*? *illecebrosus* individuals are preserved in lateral aspect, while 30% exhibit parallel aspect (Hou *et al.* 1991). To a certain extent this pattern is repeated in *Canadaspis perfecta* and *Odaraia alata* from the Burgess Shale (Briggs 1978, 1981). It was concluded that this pattern occurred due to the possession of a rounded cross-sectional body plan rather than a dorso-ventrally or laterally flattened one (Briggs 1978, 1981; Hou *et al.* 1991). The orientation of the Chengjiang fauna, the in situ preservation of lingulids (Chen *et al.* 1989) and *Facivermis* (Hou & Chen 1989b) and the lack of abrasion and disarticulation, support the view that the fauna was not buried within a mud slide or mud-laden slurry as has been suggested for the Burgess Shale. Rather it was buried in situ, possibly by wind blown material settling through the water column, with weak current activity (Chen & Erdtmann 1991; Hou *et al.* 1991). The lack of bioturbation and the rarity of trace fossils, despite their presence both above and below the occurrence of soft-bodied fossils, and the lack of decay suggests a suboxic or anoxic environment of deposition (Chen & Erdtmann 1991; Hou *et al.* 1991).

The orientation of fossils in the Big Gully assemblage is almost exclusively parallel or lateral (Table 6.1). Rarely *Isoxys* and *Tuzoia* occur in parallel aspect, due presumably to the gape allowing the carapace to settle on the sea bed in parallel aspect. Significantly, only one form exhibits more than one aspect, this is *Myoscolex*, which occur mainly in lateral, but occasionally in parallel and very rarely in an oblique aspect. This is inferred to result from a rounded cross-sectional body plan (see section 3.3.4.2).

**Table 6.1.** Some arthropod orientations from Chengjiang, Big Gully and the Burgess Shale. Chengjiang data from Hou *et al.* (1991), Burgess shale data from Whittington (1971b) and Briggs (1981). [1] high oblique orientation percentage for *Odaraia* caused partially by ovate body plan of organism. [2] percentages taken from figured specimens, thus, with a bias towards oblique figured specimens, the actual percentage of parallel orientated specimens is probably higher.

| | No. of specimens | Parallel % | Lateral % | Oblique % |
|---|---|---|---|---|
| **Chengjiang** | | | | |
| *Naraoia* | c. 600 | 97.5 | 2.5 | - |
| *Xandarella* | 2 | 100 | - | - |
| *Isoxys* | c.809 | 2 | 98 | - |
| *Branchiocaris*? | c. 100 | 2 | 98 | - |
| *Alalcomenaeus*? | c. 300 | 30 | 70 | - |
| | | | | |
| **Big Gully** | | | | |
| *Redlichia* | c. 750 | 100 | - | - |
| *Hsuaspis* | c. 870 | 100 | - | - |
| *Naraoia* | 2 | 100 | - | - |
| *Xandarella* | 1 | 100 | - | - |
| *Isoxys* | c. 375 | 1 | 99 | - |
| *Tuzoia* | c. 300 | 5 | 95 | - |
| *Myoscolex* | c. 434 | 20 | 79 | 1 |
| *Anomalocaris* | c. 25 | - | 100 | - |
| *Palaeoscolex* | c. 40 | - | 100 | - |
| | | | | |
| **Burgess Shale** | | | | |
| *Canadaspis* | c. 301 | 32 | 51 | 17 |
| *Odaraia*[1] | c. 26 | 46 | 8 | 46 |
| *Marella*[2] | 47 | 81 | - | 19 |

### 6.3 Fossil Distribution within the Emu Bay Shale at Big Gully

Although the Big Gully assemblage appears to be one of low diversity, the elements within the assemblage cover a wide range of environmental niches. These include; epifaunal vagrants (*Redlichia* and *Hsuaspis*); pelagic swimmers (*Isoxys* and *Tuzoia*); nectobenthic (*Anomalocaris* and ?*Myoscolex*) and ?infaunal vagrant (*Palaeoscolex*). The absence of sessile organisms (infaunal or epifaunal) is again highlighted and can be contrasted with the Burgess Shale, where approximately 40% of the genera in the fauna were sessile forms (Conway Morris 1986, fig. 8). The distribution of organisms from various habitats within the Emu Bay Shale Lagerstätte may provide information on environment pertaining at the time of deposition.

The occurrence of the trilobites *Redlichia takooensis* and *Hsuaspis bilobata* appears consistent above the 2 metre level (Fig. 6.1, Appendix 3). However, there appears to be three levels where the occurrence drops to zero. These are between 3.7 - 3.8 metres above the base, 4.7 - 4.8 metres above the base and 6.35 - 6.45 metres above the base. Since the trilobites are benthonic, their absence can be explained either by rapid sedimentation of the interval, or that the benthic environment could not support life.

The occurrence of *Isoxys communis* and *Tuzoia australis* appears low throughout the 8 metre sequence (Fig. 6.2). However, there are 5 levels where higher numbers occur. Interestingly, three of these occurrences overlap to a certain extent, levels where the numbers of trilobites drop to zero (Fig. 4.13). This may indicate that lack of surface bioturbation by trilobites enhances the preservation of *Isoxys* and *Tuzoia*. However, at 6.25 metres above the base, an abundance of phyllocarids and trilobites occur together, showing that large numbers of trilobites are not necessarily detrimental to the preservation of the phyllocarids. The relatively large numbers of phyllocarids occurring at a level where the numbers of trilobites drop off to zero might also suggest that the environment at the sediment-water interface became unsuitable for benthonic life, but that the water column remained unaffected. This would allow the free swimming phyllocarids to flourish, while the benthic environment became untenable.

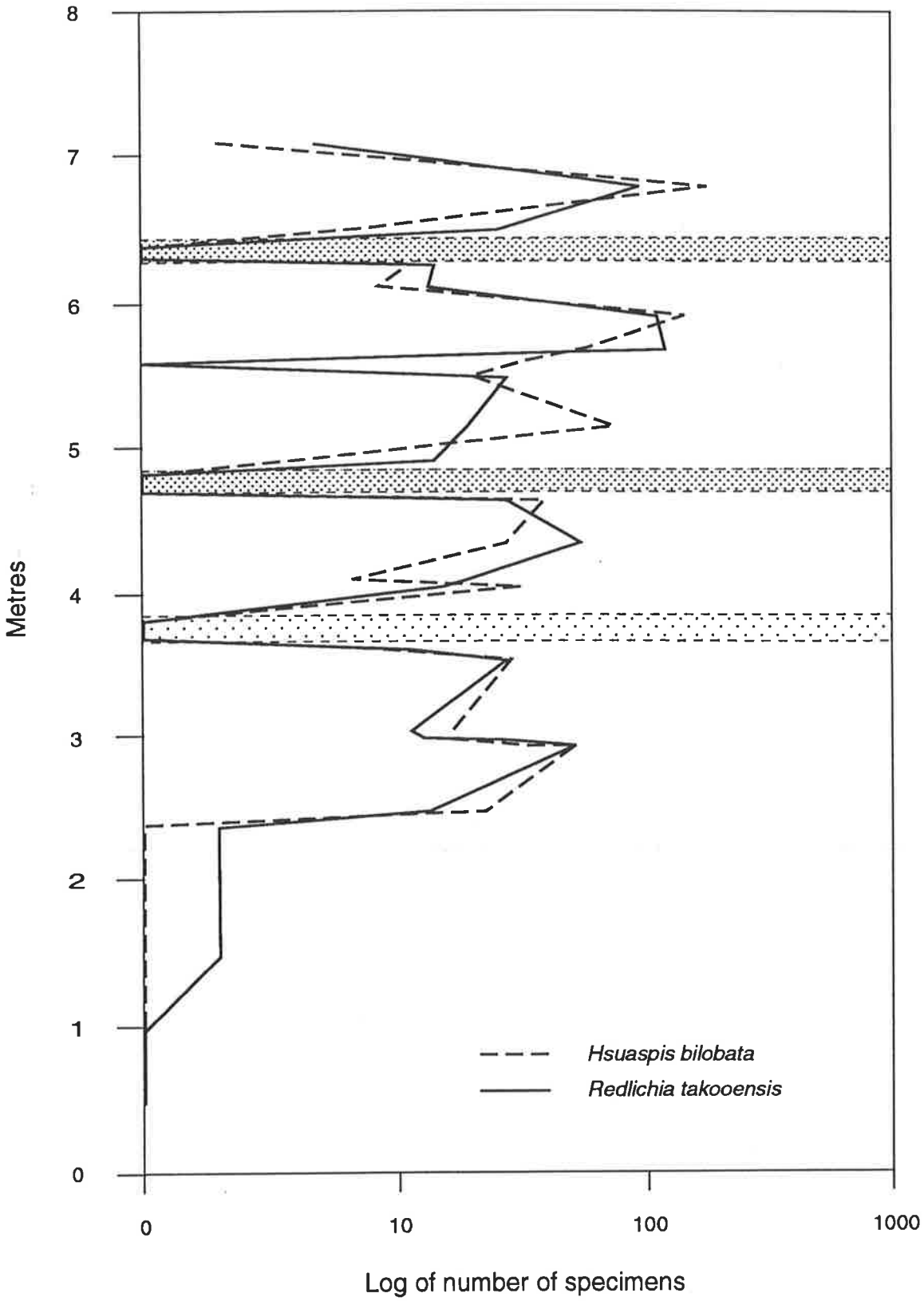


**Fig 6.1** Plot of the abundance of *Redlichia takooensis* and *Hsuaspis bilobata* in the basal 8 metres of the Emu Bay Shale at Big Gully.

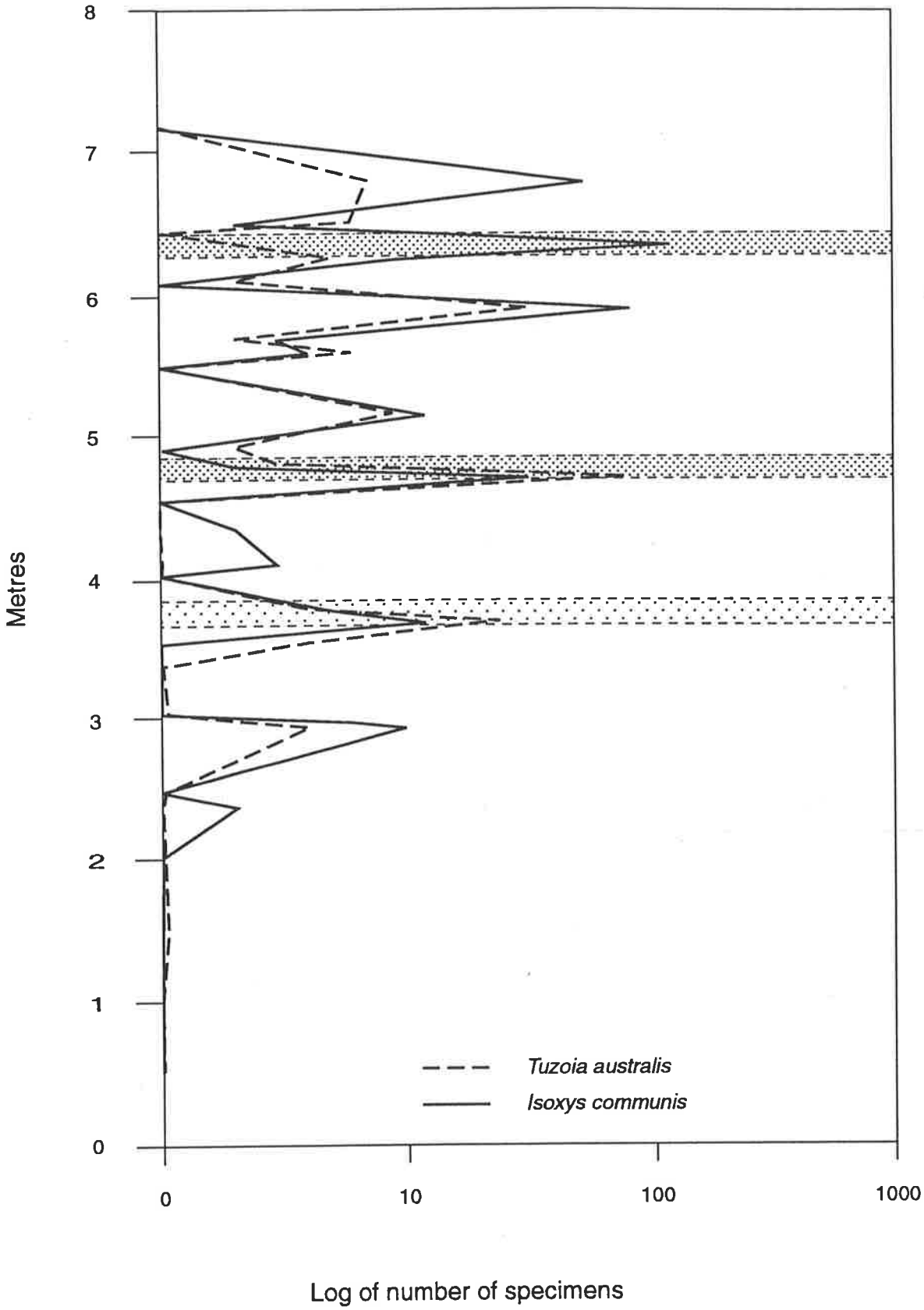


**Fig 6.2** Plot of the abundance of *Isoxys communis* and *Tuzoia australis* in the basal 8 metres of the Emu Bay Shale at Big Gully.

The occurrence of *Anomalocaris* in the Big Gully assemblage is rare and concentrated between 4.6 and 6.1 metres above the base (Fig. 6.3). The majority of specimens appear to be of moults and all specimens are of appendages only. In some examples there is evidence of both appendages being present (Pl. 13.3), indicating that the moult took place *in situ*, at or near the sediment-water interface, since the moults would be expected to become easily disarticulated with transport. Although sporadic, the trends in the occurrence of *Anomalocaris* tend to follow the trend for the trilobites rather than the phyllocarids. Since there is evidence of predation on trilobites from the Big Gully assemblage (Conway Morris & Jenkins 1985), a link between *Anomalocaris* and the trilobites would be expected. However, no firm link in occurrences can be established. This may be due to the fact that the majority of forms found are referable to *A. briggsi*, which is not considered to have preyed on trilobites (see section 3.3.4.1). The lack of substantial sclerotization may mean that the preservation of *Anomalocaris* would depend, to a large extent, on the occurrence of moulting at or just above the sediment-water interface and environmental conditions during deposition. This and their presumed position at the top of the food chain, would mean that despite their possible presence within the community throughout the deposition of the lower Emu Bay Shale, their preservation would be rare.

*Myoscolex* remains an enigmatic member of the assemblage, although the annelid affinity suggested by Glaessner (1979) appears invalid. *Myoscolex* may have been a nectobenthic arthropod, superficially similar to the Burgess Shale form *Opabinia.* Its nectobenthic habit is suggested by the presence of large, lobe-like appendages and its distribution, which more closely follows that of the free-swimming forms *Isoxys* and *Tuzoia* in occurring where the numbers of trilobites initially drop to zero (Fig 6.4). However, *Myoscolex* appears to be much more common in the lower part of the section than the phyllocarids. The largest concentration of *Myoscolex* occurs at approximately 5.10 metres above the base.

*Palaeoscolex* occurs very rarely in the lagerstätte, but appears to persist throughout the sequence (Fig. 6.3). When found it is usually coiled, suggesting environmental stress.

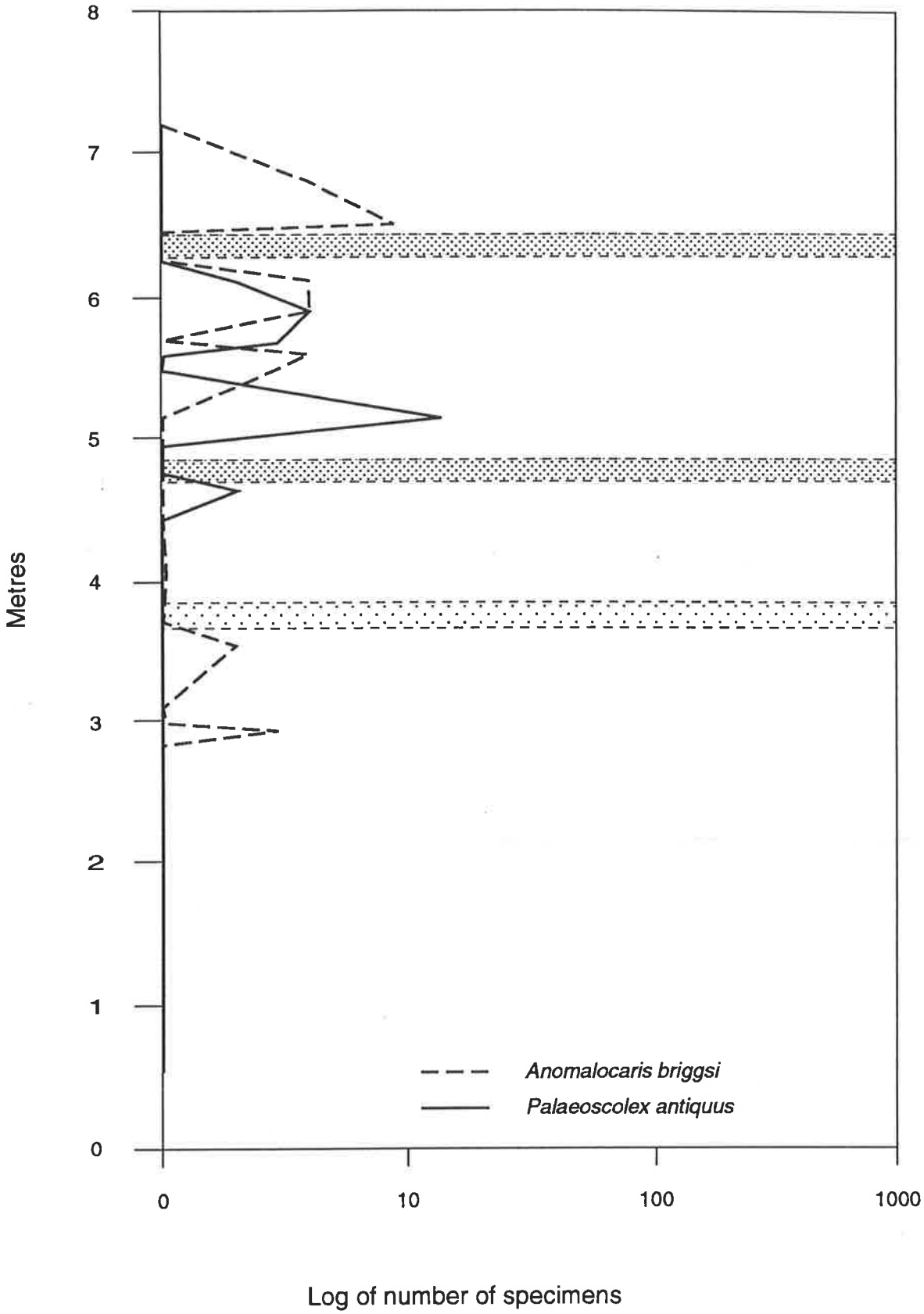


**Fig 6.3** Plot of the abundance of *Anomalocaris briggsi* and *Palaeoscolex antiquus* in the basal 8 metres of the Emu Bay Shale at Big Gully.

Other elements of the assemblage occur too rarely and randomly for their occurrence to be statistically meaningful.

## 6.4 Environmental controlling factors

These factors which control the make-up of the biota often have a significant input on which parts of that biota will be preserved. Environmental conditions are the result of the interplay of three main factors, physical, chemical and biological (Ager 1963; Rayment 1971). Each factor is dependant on a number of components and it is the variation of these components which produces differing environments. Contributing factors include; geographic location, temperature, bottom sediment or substrate, turbidity, water movements, depth, salinity, redox potential, hydrogen ion concentration, oxygen, carbon dioxide, sulphur and sulphide group ions, trace elements, organic matter, food supply, population dynamics and dispersal.
Whilst it is possible to quantify most of these factors in the modern environment, clearly many can never be assessed satisfactorily for any palaeoenvironmental study. However, there are some influences which, under favourable circumstances, can be assessed.

### 6.4.1 Physical Factors

#### 6.4.1.1 Geographic Location

Most workers place Australia at or close to the equator during much of the Cambrian (e.g. Zeigler *et al.* 1979; Scortese 1986; McKerrow *et al.* 1992), which would imply a tropical to sub-tropical, equable climate (Frakes 1979), and would influence the environment of deposition via water temperature and by effecting the oceanic currents.

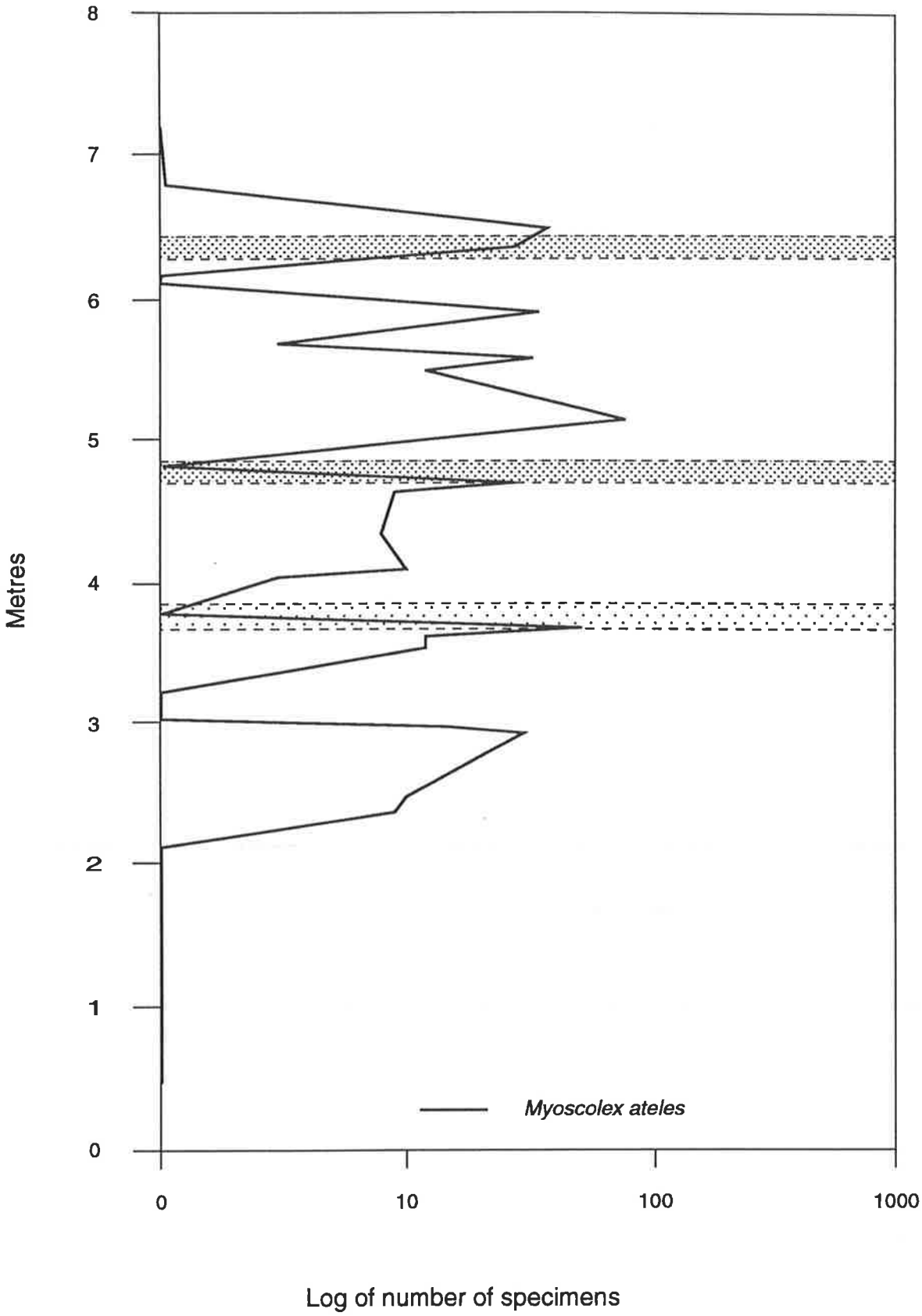


**Fig 6.4** Plot of the abundance of *Myoscolex ateles* in the basal 8 metres of the Emu Bay Shale at Big Gully.

6.4.1.2 Temperature

Temperature can affect organisms in a variety of ways, such as limiting reproduction, larval success and even death (Boucot 1981). This effect is partially caused by the increase or decrease in the rate of chemical reactions with the change in temperature. In many instances, it is not so much the change in temperature which is detrimental, but the *rate* of that change.

The tropical position of most of the continents in the Cambrian (e.g. McKerrow *et al.* 1992) is thought to have induced a broad band of warm water which encompassed most of the land masses (Frakes 1979). Such a warm, stable water temperature would tend to extend the period of larval settling (Boucot 1981) to almost all the year round. Also, such prolonged settling periods may encourage the occupation of all available niche-space. Growth tends to be faster, and the onset of reproduction occur earlier in warm waters (Valantine 1973). Thus larval settling would not be expected to limit the composition of the community. Also the concentration of dissolved oxygen is sea water is inversely linked to water temperature, suggesting lower dissolved oxygen availability.

6.4.1.3 Substrate

Whilst there has been considerable study on the effect of various factors as a moderator of trophic structure and thus the impact on the environment, the role of substrate consistency, especially in fine grained sediments, has received little attention. For example, fine grained sediments are commonly categorised as representing soft substrates even though fine grained, firm substrates can occur (Hattin 1986). It has become apparent that substrate consistency exerts an important influence on the the attendant biota (e.g. Rhoads & Young 1970; Wignall 1993). Criteria for recognising soft substrates are;

(i) Decline in shelly benthonic diversity;

(ii) Decline in the depth of bioturbation;

(iii) Change in faunal composition to known soft-substrate tolerant taxa.

These can often be confused with the criteria for oxygen deficiency, since the first two also occur in association with oxygen deficient gradients (see 6.4.2.1. below). The third criterion, whilst pertaining only to substrate controlled changes, is hard to substantiate for Early Palaeozoic assemblages in which taxonomic affinities and ecological adaptations are sometimes poorly constrained (Wignall 1993).

Another influence of the substrate in respect of the environment, is in controlling the trophic groups making up the biota. Within the marine benthonic biota two main strategies are adopted in the quest for food, allowing division into two general trophic groups; suspension feeding and deposit feeding. Under oxygen mediated conditions, both trophic groups co-exist. However, where substrate consistency factors play a role, a different pattern emerges. Deposit feeder-dominated ecotomes would be expected to be concentrated on fine grained, organic rich muds, which contain an abundant food supply. The distribution of suspension feeder-dominated ecotomes was thought to be influenced solely by the quantity and quality of suspended organic material (e.g. Turpaeva 1959, Driscoll 1967). It has since been shown that suspension feeders can occur in low numbers and diversity even when particulate organic matter is abundant (Rhoads & Young 1970). Also, the boundary between deposit feeder-dominated ecotomes and suspension feeder-dominated ecotomes is frequently abrupt, without noticeable changes in the gradient of suspended food supply and as a general rule, suspension feeder-dominated ecotomes are absent from soft substrates (Rhoads & Young 1970). Indeed, solid objects such as anchors, cans, etc, which project above soft mud substrates are commonly fouled with suspension and epifaunal feeders, whilst the surrounding substrate is devoid of such forms. Clearly, there are other factors affecting the distribution of suspension feeder-dominated ecotomes, with the exception of a small number of forms which appear especially adapted to fine grained, soft sediments (e.g. Wignall 1990b, 1993; Doyle & Whitham 1991; Fürsich *et al.* 1991), discouraging suspension feeders and attached epifauna from populating soft substrates despite the

presence of an adequate food supply (Rhoads & Young 1970; Wignall 1993).

The problems of attachment and stability of suspension feeders on soft substrates have been long recognised (e.g. Savilov 1959). Soft substrates do not provide a stable base, a prerequisite for sessile organisms, and floundering may result. Also, strong attachment is impossible on soft, unstable substrates unless specialist attachment methods are employed (e.g. Bromley & Surlyk 1973; Franzen 1977).

#### 6.4.1.4 Turbidity

The action of deposit feeders on soft substrates tends to decrease cohesiveness, increasing the amount of resuspended sediment and thus increasing turbidity. Whilst suspension feeders feed most efficiently in relatively clear water (Loosanoff 1962), some forms show a wide tolerance range to turbidity (Maurer 1967; Rhoads & Young 1970). Indeed, some forms can live in turbid environment quite successfully (Urban & Kirchman 1992), so that turbidity alone cannot be considered as limiting. In general an abundance of suspension feeders should correlate with clear waters, whereas an abundance of deposit feeders may correlate with more turbid conditions (Aller & Dodge 1974).

### 6.4.2 Chemical Factors

#### 6.4.2.1 Oxygen

Dissolved oxygen levels are considered to be the most fundamental of environmental constraints, especially on the make-up and ecology of benthonic communities where bottom waters become oxygen deficient (e.g Rhodes & Morse 1971; Oschmann 1993; Wignall 1993). The tripartite division, aerobic (>1.0 ml $O_2$ $l^{-1}$ sea water), dysaerobic (1.0 - 0.1 ml $l^{-1}$) and anaerobic (<0.1 ml $l^{-1}$) of Rhoads and Morse (1971) has become a

well known classification describing the declining oxygen gradient and associated faunal changes. These are, by necessity, only the end members of what in nature is a gradational sequence from fully oxygenated (aerobic) to essentially zero oxygen (anaerobic), as recent subdivisions have shown (e.g. exaerobic of Savrda & Bottjer 1987, 1991; poikiloaerobic of Oschmann 1991). Oxygen availability during past deposition cannot be measured directly, but, inferences can be made utilising carbon content, the presence or absence of pyrite, sediment grain size and faunal make-up (Boucot 1981). The decline in oxygen gradient can be characterised by:

(i) a decrease in benthic diversity, down to zero at the dysaerobic-anaerobic boundary (Rhodes and Morse 1971);

(ii) a decrease in the depth of bioturbation (Rhoads & Morse 1971; Savrda & Bottjer 1991; Wignall 1993).

In the decline of benthonic shelly diversity caused by oxygen deficiency, a point is reached (the Pasteur Point) when the oxygen level will no longer support an oxygen dependent metabolism - the dysaerobic-anaerobic boundary condition (Rhoads & Morse 1971; Savrda *et al.* 1984; Sageman 1989; Sageman *et al.* 1991), or the 'zero point' of Wignall (1993). This differs from a soft substrate induced decline in shelly benthonic diversity, since in this instance *no zero point is reached* (Wignall 1993, emphasis added) and an impoverished soft-substrate tolerant fauna continues to flourish (e.g. Rhoads & Young 1970, Lewy & Samtleben 1979). Thus in an environment controlled by substrate consistency, a fauna, however reduced, would still be present.

Low levels of dissolved oxygen is not in itself a barrier to the presence of a shelly benthonic macrofauna. Adaptive strategies used by benthonic forms include reducing metabolic rate, for example mytilid molluscs in tidal flats (de Zwaan 1991) and the use of a succinate metabolic pathway by some polychaete worms and bivalve molluscs, thus allowing survival of anoxic events lasting up to a few weeks (Livingstone 1983; de Zwaan 1991). Even the presence of the potent neurotoxin $H_2S$ does not entirely preclude benthonic macrofauna. Some organisms living in relatively $H_2S$-rich

environments have $H_2S$-binding pigments which prevent blockage of cytochrome *c*. This protection only lasts until the pigments are saturated and so is only useful when the presence of $H_2S$ is temporary such as in tidal mud flats (e.g. Vetter *et al.* 1991). Another, secondary, adaptive strategy in $H_2S$-rich areas is chemosymbiosis, involving chemo-autotrophic bacteria which oxidize $H_2S$ to sulphate. Some four phyla have members which show some adaptation to chemosymbiosis (Conway *et al.* 1992) including 26 species of bivalves from five families (Vetter *et al.* 1991). Whatever the adaptive strategy used, the key is *simultaneous* access to $O_2$ and reduced sulfur compounds (Conway *et al.* 1992, emphasis added). Chemosymbiotic bivalves, for instance, whilst undergoing such fundamental modifications as the loss of feeding appendices and diminution of the digestive system, still retain their dependence on an oxygen-mediated metabolism. Thus the strategy is only applicable to low (dysaerobic) oxygen levels, not to prolonged anaerobic conditions. At $O_2$ levels less than 0.1 ml $l^{-1}$ (the Pasteur Point) oxidative metabolic processes can no longer be sustained and macrofauna are absent. This represents the anaerobic facies of Rhoads and Morse (1971).

Whilst some organisms which possess a calcareous shell can exist in low oxygen environments, a diverse calcareous fauna is absent. Those organisms which do occur often show some facility for periodic anaerobic respiration. During this time, calcium is removed from the inside of the shell to buffer the acidic products of anaerobic glycolysis (lactic acid, pyruvic acid, succinic acid etc.) resulting in marked shell erosion (e.g. Rhoads & Pannella 1970). This may be a common process in dysaerobic environments (Rhoads & Morse 1971). Repair of the shell in these circumstances, requires a period of aerobic respiration. Extended (seasonal ?) periods of anaerobic respiration in dysaerobic environments could cause sustained shell dissolution due to the build-up of acidic glycolysis products, resulting in shell weakness and even rupturing (e.g. Kuwatani & Nishii 1969; Bamber 1989).

Whilst the low oxygen levels associated with organic-rich soft sediments can

significantly reduce both diversity and overall numbers, it has been shown above that low oxygen levels alone are not an insurmountable barrier to successful colonisation.

6.4.2.2 Trace Elements

The geochemistry of cadmium, copper, manganese, molybdenum, nickel, zinc and uranium in the ocean and unconsolidated sediments result in important indicators as to the likely depositional environment of sedimentary rocks (e.g. Brumsack 1980, 1986) (see 4.4 above). One problem is that ancient black shales often have metal concentrations greatly in excess of any modern sediments. While explanations such as epigeneric enrichment from hydrothermal or volcanic sources remain a possibility in some instances (Gustafson & Williams 1982), a clearer understanding of the mechanisms of enrichment indicates that authigenic processes can also produce higher concentrations (Pederson & Calvert 1990; Calvert & Pederson 1993; Piper 1994). Minor and major elements all behave distinctly differently under oxic and anoxic environments. This can be used to identify the possible depositional environment pertaining at the time of enrichment. Manganese in not enriched in modern sediments being deposited under anoxic and sulphidic bottom waters. It is enriched in oxic deep-sea sediments as Mn (IV) oxyhydroxides, and in subsurface anoxic sediment on continental margins as a mixed carbonate phase. Thus manganese enrichment can be used as an indicator of sedimentation under oxic bottom waters. This is at odds with previous interpretations of the depositional environment of manganiferous black shales, where the presence of the Mn (II) solid phase was assumed to be indicative of formation under anoxic bottom waters or Oxygen Minimum Zones (e.g. Fan *et al.* 1992, Jenkyns *et al.* 1991).

Cadmium, copper, molybdenum, nickel, zinc and uranium all appear to be precipitated under anoxic bottom waters. It also appears that these metals are also removed from sea water by diffusion into anoxic sediments underlying thin, surficial oxic sediments. Thus sediments which receive large fluxes of detrital marine organic matter, such as those on

continental margins, also act as sinks for these metals. Since these metals are enriched both in anoxic surface sediments and subsurface anoxic sediments overlain by thin, surficial oxic sediments. Absence of enrichment indicates significantly oxygenated bottom waters and a probable lack of large amounts of detrital organic matter, or rapid deposition of organic poor sediments.

### 6.4.3 Biological Factors

Community structure is often diagnostic of particular environments, for instance the presence or absence of sessile suspension feeders, the diversity of the community, etc. Where evidence of this structure survives taphonomic processes, important information can be gained as to the environment of deposition.
Also the degree of disarticulation found in fossil shells and skeletal elements can provide information on the strength of currents and residence time on the surface, as well as giving an indication whether the organisms were transported before final burial.

Recruitment patterns play an important role in determining community structure (Luckenbach 1984) and thus the effect of the community on the environment. The process involves at least two components, larval settlement, and equally important, post-larval survival (Thorson 1966).

#### 6.4.3.1 Larval Settlement

It has long been thought that the larvae of suspension feeders exhibit a significant preference for settling on firm substrates (e.g. Butman *et al.* 1988) compared with soft substrates. However, recent experiments on larval settlement in still water have shown that settling may well be non-selective, with no significant difference in the choice of substrate (Bachelet *et al.* 1992). This indicates that in an environment where currents are lacking, the larvae of suspension feeders have little control over the kind of substrate

they settle on and hence this should not result in the lack of suspension feeders on soft substrates. If suspension-feeder larvae show non-selective settling, then it is within the post-settlement processes of larval survival, metamorphosis and the survival of the young juvenile that recruitment fails (Holme 1961; Dalby & Young 1992). This failure only occurs on organic-rich, soft substrates, and given the abrupt boundaries between some deposit feeder dominated and suspension feeder dominated ecotomes, the causes must be inherently linked with the properties (physical and/or chemical) of the soft substrate.

#### 6.4.3.2 Post-Settlement Survival

One factor affecting post-settlement survival may be the action of deposit feeders. Predation of larvae/young juveniles (accidental or otherwise) may occur, but the resuspension and subsequent burial of larvae and young juveniles due to deposit feeder activity may be an even greater factor (Rhoads & Young 1970), especially since burial has a significantly higher adverse affect on young juveniles compared with adults (Glude 1954). Although some forms do exhibit the ability to rapidly burrow several centimetres back to the surface (Rhoads & Young 1970).

## 6.5 Discussion

Benthonic conditions are not usually controlled absolutely by one factor. Rather it is the interplay of factors which produces the varied conditions and thus the varied biotas found both in the modern environment and in the rock record. The identification and interpretation of these subtle interplays is the challenge confronting taphonomists and palaeoecologists.

With a knowledge of the interplay of the depositional environment and a number of key

factors, it is now possible to marshal several lines of evidence, which when combined may hopefully lead to an accurate assessment of the environment during deposition of the Emu Bay Shale.

The low faunal diversity, the absence of sessile forms and the rarity of juveniles point to a stressed depositional environment.

Low faunal diversity is indicative of unusual conditions and can be caused by extremes of salinity, temperature or low oxygen levels (e.g. Valentine 1973). Chemical analyses of the Emu Bay Shale indicate normal or near normal marine saline conditions as reflected in the sodium, barium and sulphate levels (Appendix 4). The geographic position of Australia during the Cambrian tends to suggest warm, equable sea temperatures, thus implicating oxygen levels as the primary environmental limiting factor.

The geochemical data, whilst appearing somewhat equivocal, gives an overall picture of a suboxic to anoxic environment, which is apparently in accord with the biological and physical evidence.

The poor sorting and the overall fine grain size of the sediment, tends to indicate a soft substrate. None-the-less, by themselves these characters are not definitive (e.g. Hattin 1986). Combined with sedimentary structures indicative of soft sediment slumping (Pl. 3.5), they comprise a compelling argument for a soft, muddy substrate. Such soft substrates tend to discourage colonisation by sessile forms. Thus, to account for the low diversity and lack of sessile organisms, a combination of low oxygen levels and soft substrates can be invoked. This is not an unusual setting, since soft substrates are often associated with low oxygen levels (e.g. Rhoads & Morse 1971, Wignall 1990a, 1993).

It is very difficult to quantify sedimentation rates in past environments, but certain considerations can be brought to bear in an attempt at an estimation. Presuming that deposition was occurring within an active tectonic zone, rapid sedimentation rates may be anticipated. The presence of articulated skeletons and *in situ* moults also offer clues to

the sedimentation rate during the deposition of the Emu Bay Shale Lagerstätte. Perkins & Tsentas (1976) indicated that in shallow marine environments, shells and skeletons experience substantial degradation in a short time, Brett & Baird (1986) suggested only a few tens of years even for the more robust elements. Therefore in order to preserve intact skeletons and *in situ* moults a very rapid sedimentation rate of between 1-50 cm per 100 years is needed (Brett & Baird 1986). The presence of fully articulated forms and *in situ* moults also suggests that little or no transport has occurred prior to burial. Thus, unlike the Burgess Shale fauna, the Big Gully assemblage appears to have lived in and around the area of deposition, at least long enough to undergo successful moulting. This implies that the environment could not have been consistently anoxic.
Geochemical studies have shown little or no enrichment in the Emu Bay Shale Lagerstätte. This suggests low residence times for sediments at the sediment-water interface, also supporting rapid sedimentation rates. The absence of precompactional nodules also suggests rapid sedimentation, since their formation requires considerable periods of time with little or no sediment input (Wignall 1990a).

The available evidence then, suggests rapid deposition. Sedimentation rate is an important factor in controlling substrate stability since low rates allow firm substrates to develop. Rapid sedimentation rates would tend to result in soft substrates.

This environmental interpretation can be used to explain the apparent lack of juvenile forms in the fauna. There appears to be no taphonomic bias against the preservation of juvenile forms, since well preserved specimens have been found (Section 3.2.1.2). However, the rarity of the finds is out of proportion to the presumed abundance of juveniles compared with adults represented by survivorship curves. With no taphonomic filter in operation, exclusion of juveniles must be due to environmental factors.

In a series of still water experiments, Bachelet *et al.* (1992) found that the apparent preference for firm substrates exhibited by settling larvae was in fact an artifact of

increased post-settling mortality on organic-rich soft sediments. Larval shell material from those forms which had settled on the organic-rich soft substrate exhibited significant dissolution. The experiments, carried out in the absence of deposit feeders and turbidity, and in similar oxygen levels over all substrates, indicated that the cause of the dissolution and hence the increased mortality, is due to the chemical properties of the organic-rich soft substrate and, more importantly, the diffusive boundary layer immediately above the sediment.

Within the large scale marine environment, turbulent eddy diffusion is the dominant mode of mass molecular transport. However, fluid mechanical forces are quite different over small scales. At small distances from the sediment-water interface, the internal friction of the water creates a viscous layer which tends to coat the surface like a blanket and does not participate in the general circulation of the bulk water (Vogel 1981). Within this diffusive boundary layer, eddy diffusion becomes insignificant and molecular diffusion dominates as the mechanism for mass transport across the sediment-water interface (Santschi *et al.* 1983; Archer *et al.* 1989). The introduction of microelectrodes with a spatial resolution of 10-100 μm and with a sensing tip of only a few microns have allowed this layer to be accurately measured (Revsbech *et al.* 1983; Revsbech 1983), thus making possible detailed investigations of this a very important microenvironment. The layer starts, on average, some 0.4 - 0.5 mm above the sediment-water interface and is marked by a sudden change in dissolved oxygen concentration (Fig. 6.5). A gradient is set up caused by aerobic respiration at the sediment-water interface and within the first few millimetres of the sediment. Where respiration rates are high, oxygen is used up more rapidly than it can diffuse through the diffusive boundary layer, leading to a sharp gradient, steepest just above the sediment-water interface. If the surface has a sufficiently high oxygen uptake (i.e. on organic-rich muds) the result is an essentially anaerobic environment, despite the overlying aerobic bulk water (Jørgensen & Revsbech 1989). Aerobic respiration is thus limited by the rate of diffusion through the diffusive boundary layer.

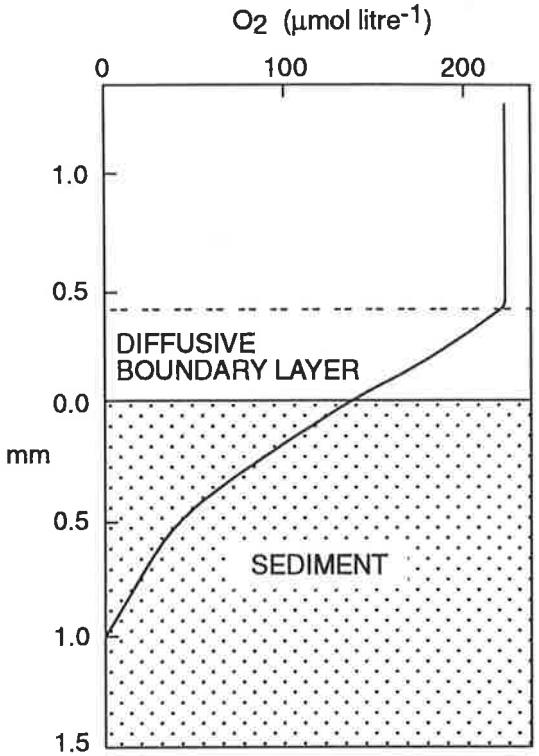


**Fig. 6.5** Oxygen micro-gradient in a diffusive boundary layer over organic-poor sediments 1 mm oxic zone. (After Jørgensen and Revsbeth 1985, 1989)

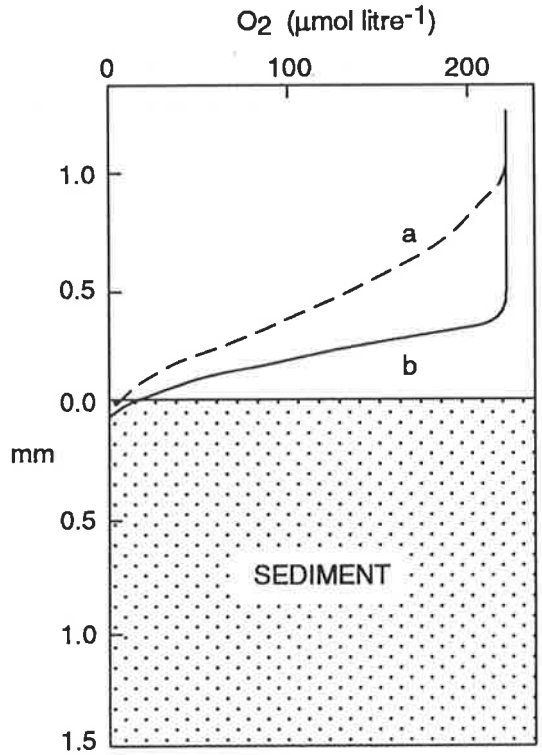


**Fig. 6.6** Oxygen micro-gradient in a diffusive boundary layer over organic-rich sediments showing change of thickness with a) low current flow and b) high current flow. (After Jørgensen and Revsbeth 1985, 1989)

The thickness of the layer depends on the flow régime occurring within the bottom waters. Its thickness varies from 0.1 - 0.2 mm in high flow régimes to ≈1 mm in low flow régimes, especially in the deep sea (Boudreau & Guinasso 1982; Santschi *et al.* 1983, Jørgensen & Revsbech 1989; Jørgensen & Des Marais 1990) (Fig. 6.6). Since diffusion time increases with the square of the diffusive path, diffusion through thick layers is much slower than through thin layers. Thus a 1 mm thick diffusive boundary layer has a diffusion time of 9 minutes compared with 73 seconds for a 0.36 mm thick layer (Jørgensen & Revsbech 1989). Diffusion times are important since oxygen levels can be reduced from fully saturated to minimal values (7%) in only 80 seconds by aerobic respiration over organic-rich substrates (Jørgensen & Revsbech 1989). Small particles (>0.2 mm) do not seem to affect the layer, but particles approximately half the thickness of the film or greater do have a noticeable effect on layer dynamics (Jørgensen & Revsbech 1989).

The diffusive boundary layer then is a very thin film in which molecular diffusion is the dominant mode of mass transport. This creates not only a steep dissolved oxygen gradient, but also allows a very dynamic chemical microenvironment at the sediment-water interface, separating the solid surface from the overlying, oxygen saturated, bulk water (Jørgensen & Revsbech 1989; Gundersen & Jørgensen 1990; Jørgensen & Des Marais 1990). Thus the composition and concentration of dissolved species at the sediment-water interface is not necessarily the same as in the overlying bulk water (Morse 1974). The diffusive boundary layer has the greatest influence over organic-rich sediments in low flow régimes, a situation commonly found where muds are deposited. Thus the surface of these fine grained, unconsolidated, organic rich sediments may experience conditions markedly different from those in the surrounding bulk water.

When present, larvae will try to settle and colonise if the opportunity arises. In the Kimmeridge Clay, bedding planes covered with larval shells and small juveniles attest to larval swarm settlement. These events have been taken as indicative of settlement in temporarily oxygenated waters, eventually failing with the return of anaerobic conditions

(Oschmann 1988, 1991). It is equally plausible that the event represents a lowering of sedimentation rates leading to lower levels of available organic carbon and a temporary firming of the substrate. This may lead to an increase in the oxygen levels within the diffusive boundary layer and the topmost sediment creating a buffer zone, stopping reduced compounds reaching the surface. This creates a temporary environmental window, conducive to larval settlement. With the restoration of 'normal' sedimentation rates, the increase in organic carbon availability quickly re-establishes long term dysaerobic to anaerobic conditions likely to produce mass mortality quite quickly, especially given the lengthy recovery times of benthonic faunas exposed to relatively short anaerobic episodes (e.g. Austin & Wibdom 1991).

Sulphides produced from sulphate reduction in the anaerobic zone, when transported upward into the topmost layers of sediment, by bioturbation or storm activity for instance, has resulted in mass mortality (Brongersma-Sanders 1957). However, no physical processes are necessary to produce this. The waning of oxygen levels, with the return of dysaerobic conditions, results in a shrinkage of the aerobic and subaerobic zones which would normally buffer the topmost layers of the sediment from the reduced products of the anaerobic oxidation of organic matter. Indeed, the dysaerobic conditions at the bottom of the water column may be exacerbated by the diffusive boundary layer to such an extent that the amount of dissolved oxygen at the sediment-water interface reaches zero. The aerobic and subaerobic zones may then become insignificant, allowing reduced compounds access to the surface. Thus, whilst there is still sufficient oxygen available to organisms above the diffusive boundary layer, within the layer a lethal mixture of $H_2S$ and sulfuric acid accrues. The oxidation of sulphides and other reduced compounds also acts as a dissolved oxygen sink, reinforcing the effect.
Amongst the byproducts of the anaerobic reduction of sulphate, which occurs within organic-rich muds are weak acids (eq. 6.1). One of these, $H_2S$, is lost from the

$$2CH_2O + SO_4 \rightarrow H_2CO_3 + H_2S \qquad [6.1]$$

system, diffusing along concentration gradients and even forming bubbles (Coleman 1985). Oxidation of $H_2S$ by oxygen at the sediment-water interface not only enhances the depletion of oxygen within the diffusive boundary layer, but has the potential to dramatically lower the pH by producing sulfuric acid (eq. 6.2). The presence of acid

$$H_2S + O_2 \rightarrow H_2SO_4 \leftrightarrow SO_4^{2-} + 2H^+ \qquad [6.2]$$

depresses the dissolution constant of carbonate, changing the saturated state of the overlying diffusive boundary layer to an undersaturated one (section 5.3.2). This produces a much more corrosive environment, encouraging carbonate dissolution. The $SO_4^{2-}$ produced in the oxidation of $H_2S$ is then available for the sulphate reduction reaction, producing more $H_2S$ (Fig. 6.7).

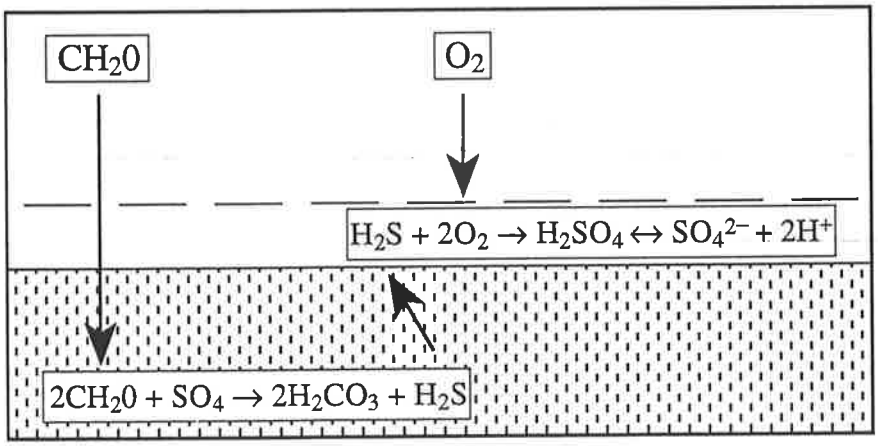


**Fig. 6.7** Carbonate corrosive microenvironment produced within the diffusive boundary layer due to the production of $H_2S$ as a byproduct of sulphate reduction.

Keir (1982) found no evidence for carbonate dissolution within the diffusive boundary layer. However, this work was carried out in the deep sea where bottom waters are rich in dissolved oxygen and, more importantly, the organic matter content of the sediment is low. Under these conditions, the lower levels of organic matter reduces the rate of

respiration within the topmost sediment. This allows adequate oxygen to diffuse through the layer to balance that lost through respiration, maintaining an oxic microenvironment within the diffusive boundary layer. An oxic diffusive boundary layer will allow dissolved oxygen to penetrate the surface layers of sediment to a level of ≈ 2.0 mm, even with insignificant bioturbation (Jørgensen & Revsbech 1985). This produces an oxic layer (Fig. 6.5) sufficient to buffer the sediment-water interface and hence the diffusive boundary layer from the reduced products of the suboxic and anoxic zones. However, it has been shown that gypsum dissolution does take place within the diffusive boundary layer (Santschi *et al.* 1983) and that the layer may well have a controlling influence on carbonate dissolution (Archer *et al.* 1989; Gundersen & Jørgensen 1990).

Larvae have thin, fragile shells and thus are very susceptible to carbonate dissolution and are not only at risk from outside influences. Given the lack of dissolved oxygen within the diffusive boundary layer the larva may be forced into anaerobic respiration, the acidic byproducts of which will attack and dissolve the shell (e.g. Calabrese & Davis 1966). This process is most effective upon areas of the shell adjacent to the surface of the organism. Once the integrity of the shell has been violated, death soon follows. It seems likely then, that a microenvironment could form at the sediment-water interface, within the diffusive boundary layer, which would be conducive to carbonate dissolution and to subsequent post-settlement mortality. The final result is the mass mortality of the larval and early juvenile fauna and thus a failure in recruitment. During the early stages of suboxia therefore, recruitment failure may occur, whilst the onset of anoxia would result in the mortality of the surviving adult population.

The lack of juveniles and sessile forms in the Emu Bay Shale at Big Gully can therefore be explained as being due to the conditions pertaining during deposition. Specifically, conditions of low dissolved oxygen availability, rapid sedimentation and soft substrates, effectively stop settlement and recruitment, allowing only motile adult forms to colonise from adjacent areas.

The distribution of fossils through a sequence has been successfully used to delineate anoxic intervals. Indeed, fossil distribution was taken as the main criterion for distinguishing the aerobic, dysaerobic and anaerobic facies of Rhoads and Morse (1971) and has also an important factor in recent studies to determining available benthic dissolved oxygen gradients.

The Emu Bay Shale Lagerstätte appears unusual in that it possesses no sessile forms. Also, common elements of the assemblage are free swimming forms (*Isoxys*, *Tuzoia*, ?*Myoscolex*) and thus not bound by conditions at the sediment-water interface. A comparison of trilobite and phyllocarid occurrences against geochemical zonation (Fig, 4.13) shows when trilobite numbers drop to zero, there is a significant increase in the number of phyllocarids compared with their numbers when trilobites occur. These occurrences appear to coincide with periods of anoxia suggested by the geochemical evidence. Thus it appears that during times of presumed benthic anoxia, trilobite numbers drop to zero whilst phyllocarid numbers increase. This increase may be due to the greater preservation potential afforded by the lack of trilobites (and hence surface bioturbation) and the chemical environment at the sediment-water interface.

The distribution of *Myoscolex* through the Lagerstätte (Fig. 6.4) appears most similar to that of the free swimming forms, suggesting a nectobenthic rather than a benthic niche. However, the occurrence of *Myoscolex* drops to zero during the anoxic events, suggesting that the form was not wholly independent of the benthic environment. Peaks in the occurrence of *Myoscolex* coincide with increased phosphate levels (Fig. 6.8), suggesting a link between phosphate levels and *Myoscolex* preservation, although high levels of phosphate do not appear to be a prerequisite for preservation.

The low occurrence of *Anomalocaris* and *Palaeoscolex* precludes any meaningful discussion of their distribution, except that, in part the distribution of *Anomalocaris* is similar to the free-swimming phyllocarids, suggesting a possible nektonic lifestyle for

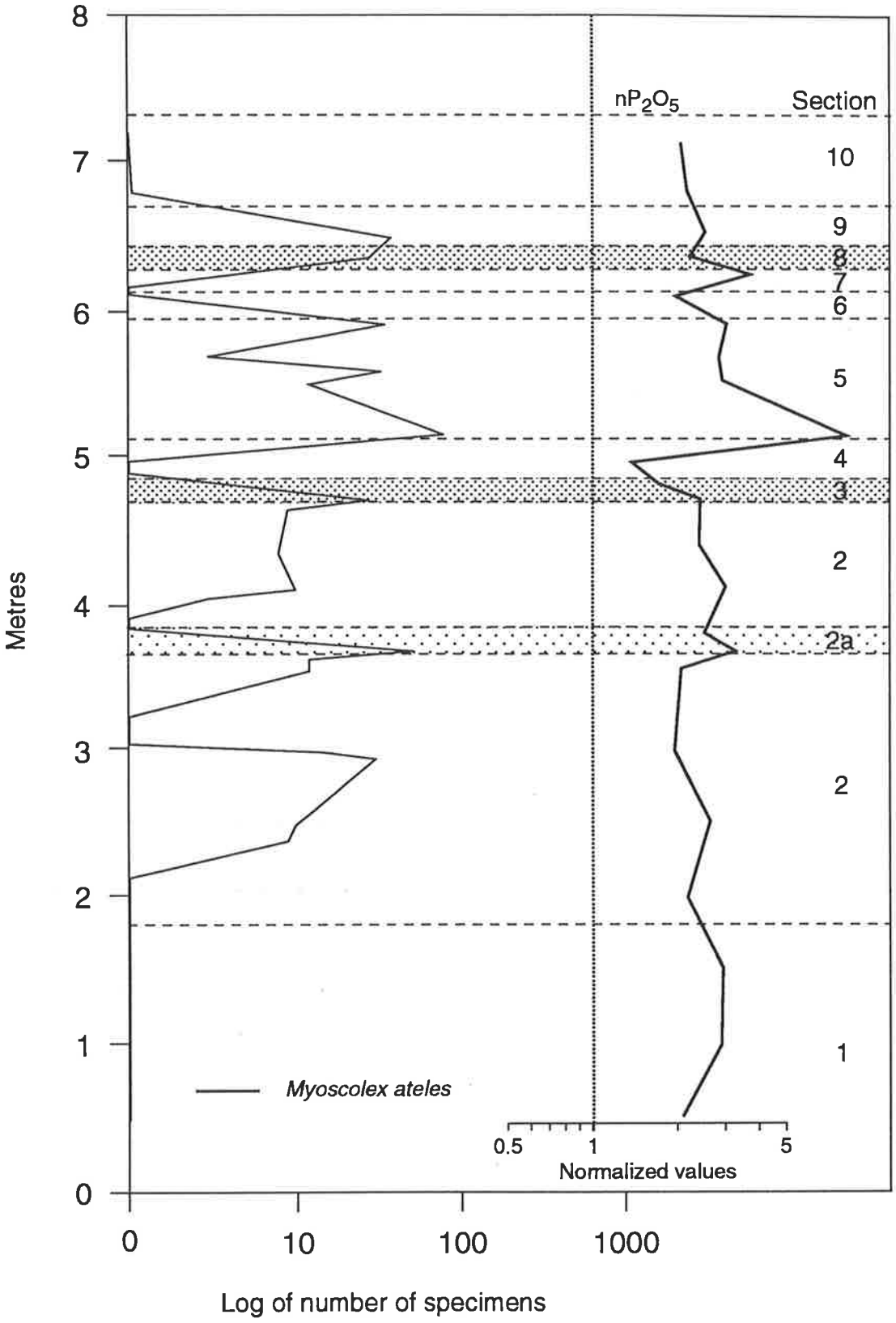


**Fig. 6.8** Comparison plot of *Myoscolex ateles* occurrence from the lower 8 metres of the Emu Bay Shale at Big Gully against geochemical zonation with $P_2O_5$ curve (from Fig. 4.7).

*Anomalocaris*.

This palaeoenvironment model can be used to explain the taphonomy of *Myoscolex* (Fig. 6.9). Dead individuals lying on or just under the sediment begin to decay. Intense sulphate reduction around the muscle tissue microenvironment initiates phosphate mineralisation. However, tissues in the extremities, having very little muscle tissue, do not experience such intense reduction and so no phosphate mineralisation occurs. The next stage in the process causes a rapid increase in local pH, resulting in carbonate precipitation around the phosphatised muscle tissue and around any other remaining tissues.

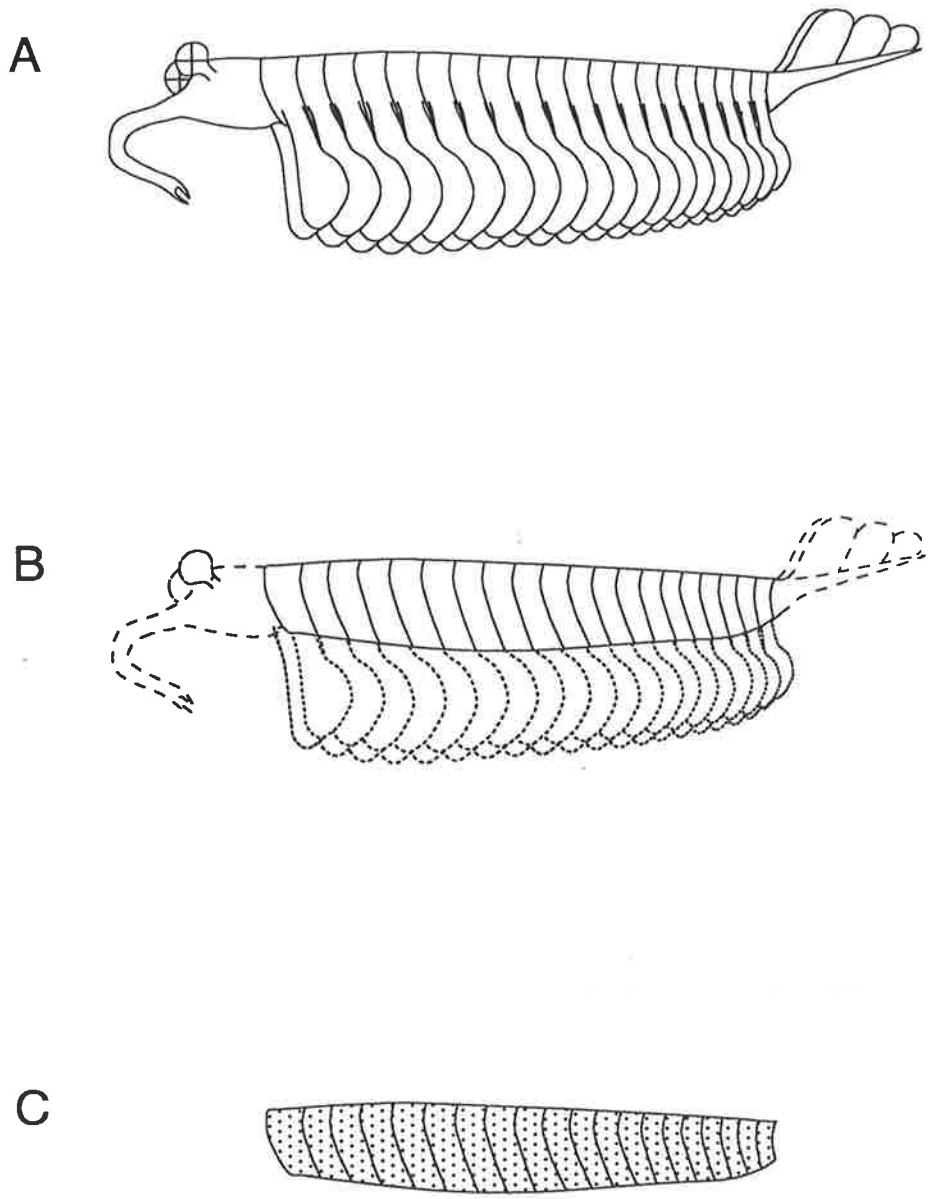


**Fig. 6.9** Taphonomy of *Myoscolex ateles* in the Emu Bay Shale Lagerstätte. **A**. Dead organism lying on or in the sediment. **B**. Highly labile tissues decay causing collapse of organism, but muscle blocks stay intact. Tissues at the extrmities of the body start to decay. **C**. Intense decay within the trunk causes phophatization of muscle blocks. Less intense decay in extremities does not lead to mineralization and results in loss of tissues. Increasing pH at the end of phosphate mineralization initiates carbonate precipitation around mineralized muscle blocks and rarely around any surviving tissues in extremities (compare with Plate 5.3-6 and Plate 14 - note the posterior appendages`in AUDG1046-239, figured in Plate 14, were reversed after death).

# Chapter 7: Conclusions

*"Well, it did make sense when I first started . . ."*

Pooh Bear

The Lower Kangaroo Island Group appears to represent deposition on a shallow tidal to subtidal shelf, representing an overall shallowing upward cycle from the lower Mt. McDonnell Formation to the Stokes Bay Sandstone. The transtensional Kangarooian Movements appear to have initiated a series of localised, rapidly subsiding, westwardly migrating basins which accumulated subtidal to alluvial sediments, represented by the Upper Kangaroo Island Group. These movements appear to have continued into the early Middle Cambrian until a switch to a compressional tectonic regime, initiated the Delamerian Orogeny, earlier than previously considered.

Fossil evidence suggests an upper Early Cambrian age for the majority of the Kangaroo Island Group, with actual fossil occurrences allowing a potential correlation between the Mt. McDonnell Formation and the Sellick Hill Formation and Fork Tree Limestone on Fleurieu Peninsula, the upper Kulpara Formation and lower Parara Limestone on Yorke Peninsula and the upper Wirrapowie Limestone, the lower Parara Limestone, and the lower Wilkawillina Limestone in the Flinders Ranges. The White Point Conglomerate may be correlated with the Oraparinna Shale and overlying Billy Creek Formation in the Flinders Ranges and the Koolywurtie Member and the overlying Minlaton Formation on Yorke Peninsula. Correlation with Fleurieu Peninsula is difficult, with no fossils found in this part of the sequence there. However, a tentative correlation is made between the White Point Conglomerate and the Carrickalinga Head and the Backstairs Passage Formations, which represent the onset of deposition into the newly opening Kanmantoo Trough. The Emu Bay Shale and the fossil Lagerstätte it contains, is here considered uppermost Botomian in age and a suggested correlated is made with the upper Minlaton Formation on Yorke Peninsula and the Billy Creek Formation in the Flinders Ranges.

Correlation with the sequence on Fleurieu Peninsula is tentative, but the Emu Bay Shale may correlate with the Talisker Calc-Siltstone/Karinya Shale.

The Emu Bay Shale at Big Gully appears to have been initially deposited into a localised basin, in an environment of sluggish currents and low dissolved oxygen availability. Basal shales being quickly buried by prograding units until sub- to inter-tidal conditions were re-established during the deposition of the conformably overlying Boxing Bay Formation. The top of the Boxing Bay Formation is not exposed but appears to extend into the early Middle Cambrian. The unconformably overlying Bald Rock Beds may contain clasts of metamorphosed Kanmantoo metasediments, in which instance its deposition must post-date the Delamerian Orogeny and thus the Bald Rock Beds may represent the youngest early Palaeozoic rocks on in the Southern Adelaide Fold-Thrust Belt.

The Emu Bay Shale Lagerstätte contains a low diversity fauna, with arthropods overwhelmingly dominant. These are represented by the trilobites *Redlichia takooensis*, *Hsuaspis bilobata*, the trilobite/trilobitomorph *Naraoia*, the crustacean *Xandarella*, the phyllocarids *Isoxys communis* and *Tuzoia australis* and the presumed arthropod *Anomalocaris*. The only other forms which occur with any frequency in the lagerstätte are *Myoscolex ateles*, which is here reassigned to the Arthropoda, and the presumed annelid *Palaeoscolex antiquus*.

All forms occurring occupy either benthonic or nectonic niches. Sessile forms are absent. The fact that sessile forms are a common element in Early Cambrian strata and are present in the presumed correlative deposits at Emu Bay suggests that their absence from the Emu Bay Shale Lagerstätte owes more to environmental, than taphonomic factors. The lack of sessile forms and the extreme rarity of juveniles, points to a lack of recruitment at the Big Gully locality. Environmental conditions when the oxic-anoxic boundary is at the sediment water interface would not be conducive to either recruitment or post settlement survival. This appears to have resulted in colonisation by motile forms in other areas, thus precluding sessile forms and young juveniles.

Fossil occurrence throughout the Emu Bay Shale Lagerstätte suggest several episodes of bottom water anoxia which is indicated by the absence of benthonic forms such as *Redlichia takooensis* and *Hsuaspis bilobata*, but the continued presence of free swimming nectonic forms such as *Isoxys communis* and *Tuzoia australis*. These fluctuating occurrences and the mode of preservation support a low oxygen environment prone to frequent anoxic episodes, since the presence of an anoxic sediment with a benthonic epifauna suggests a sharp oxygen gradient which would, most likely, be unstable. The enigmatic form *Myoscolex ateles* appears similar to the Burgess Shale form *Opabinia*, and exhibits an unusual style of preservation, phosphate mineralisation of muscle tissues. The distribution of *Myoscolex* within the Emu Bay Shale Lagerstätte, similar to *Isoxys* and *Tuzoia*, suggests that it was a free swimming form.
The forms *Naraoia*, *Xandarella* and *Anomalocaris* sp. all appear closely related to forms occurring in the Early Cambrian Chengjiang fauna of China, suggesting a close link between the two areas during this period.

The geochemistry of the Emu Bay Shale Lagerstätte is probably a reflection of the common state of the surficial sediments during deposition. The oxic/anoxic boundary appears to have been close to, or at, the sediment/water interface resulting in a suboxic to anoxic water column immediately above the sediment surface, and as is reflected in the grouping of the normalised values mostly within the suboxic part of the nMo/nMn plot (Fig. 4. 12). In this plot the Emu Bay Shale samples cluster close to normal values but mostly within the suboxic zone with sulphate. These results can be compared with measurements of nMo and nMn taken from the Emu Bay Shale at its type section in Emu Bay, which plot within the oxic zone and do not overlap the results from the samples from Big Gully. This suggests an oxic depositional environment for the Emu Bay Shale at Emu Bay, a suggestion supported by the fossil assemblage found there.

Since the concentration of organic matter in the Emu Bay Shale appears low, even allowing for post depositional oxidation, enrichment or depletion of minor and trace

elements must be derived from precipitation/dissolution or adsorption from seawater. This process will only produce significant enrichment/depletion under conditions of extremely slow bulk sediment accumulation, since this process is dependent on long term exposure of bottom sediments to bottom waters. Weak enrichment/depletion is indicative of rapid sedimentation. The normal shale values exhibited by most of the minor elements measured, indicate that the residence time of sediments at the sediment/water interface is insufficient to allow wholesale enrichment/depletion. The sedimentological and geochemical information is indicative of periods of rapid sedimentation which allowed only weak enrichment/depletion, possibly interspersed with periods of relative depositional quiescence.

As indicated by the absence of bioturbation and sessile organisms, periodic anoxic episodes occurred. However, the data does not allow a detailed analysis of rapid redox fluctuations, due mainly to the number and spacing of the samples and the distortion of the preserved signal, to some degree, by subsequent depositional environments and diagenetic processes.

The overall signature of depleted manganese and enriched molybdenum, along with a slight, related signal trend amongst the other elements, indicates that conditions during deposition can be considered suboxic with occasional anoxic episodes in a nearshore setting with rapid, if inconsistent, sedimentation.

The geochemistry of the sediment and overlying sea-water plays a pivotal role in the processes leading to fossilisation. Extraordinary levels of palaeontological detail can occur as a result of the preservation of organisms by early diagenetic mineralisation. Work done on early diagenetic mineralisation of soft tissues in the the laboratory appear to be a good corollary for these ancient fossilisation events. Thus the conditions which optimise mineralisation, can be applied with some confidence to ancient examples. These laboratory studies provide a good framework in which to base an analysis of the taphonomic processes which have occurred within the Emu Bay Shale at the Big Gully locality.

Phosphatisation of soft tissues appears to be a very rapid process, occurring immediately after the onset of soft tissue decay. Martill & Harper (1990) suggested a time frame as low as 5 hours for phosphatisation of Santanna fish muscle. However, under favorable conditions, longer time frames are possible, up to 4 weeks (Briggs & Kear 1993a, b, 1994). During this period, the presence of dissolved phosphate in pore waters, possibly released from decaying tissues or sourced extraneously, from the redox recycling of iron oxyhydroxides and dissolved sulphate inhibits calcite growth. Thus in early diagenesis at the Big Gully locality, the low pH, the presence of sulphate and the presence of dissolved phosphorus all contribute to inhibit the precipitation of calcite, resulting in high concentrations of dissolved carbonate in pore-waters. As sulphate reduction proceeds, phosphate is precipitated and sulphate is removed from pore waters by the precipitation of pyrite. This results in an increase in pH leading to eventual carbonate supersaturation and calcite precipitation.

Thus it appears that almost immediately after the onset of decay, conditions at or immediately underlying the sediment-water interface - which presumably approximated the oxic-anoxic boundary - supported the depression of pore water pH.

Once the decay of large blocks of tissue had proceeded towards completion, the precipitation of phosphate and the removal of $HS^-$ from pore waters may elevate pH levels and initiate calcite precipitation.

Under conditions where Fe is not limiting, as appears to have been the state during deposition of the Emu Bay Shale, dissolved sulphide produced from sulphate reduction is quickly extracted from pore waters by precipitation with Fe. Thus pH levels are not depressed, or are not depressed for significant periods, and carbonate supersaturation is quickly reached. Only under conditions of high sulphate reduction in essentially closed conditions, such as within significant masses of labile tissues, will periods of extended, depressed pH levels occur, resulting in phosphate precipitation. Normally, conditions would not be conducive to sustained, depressed pH levels. This means that in the

majority of instances phosphate mineralisation would be absent or slight and the most common expression of fossilisation will be via the precipitation of $CaCO_3$.

A model for the palaeoenvironment of the Emu Bay Shale at Big Gully can now be constrained using factors gained from palaeontological, geochemical and geological analyses. These indicate deposition into a small, faulted, nearshore basin (Fig. 2.6). Erosion of uplifted areas would have been rapid due to the lack of vegetation, providing abundant sediments to depocentres. Current activity appears to have been sluggish, except during storm activity, allowing the deposition of predominantly silt-sized sediments and occasional sand bodies. Such deposition resulted in fine grained, soft substrates and probably turbid waters which would have discouraged settlement of the larval stages of sessile organisms.

Sluggish currents in the warm tropical waters would probably have resulted in low dissolved oxygen availability. The oxic-anoxic boundary appears to have been close to, if not at, the sediment-water interface during most of the depositional period, allowing *in situ* communities to develop, before probably frequent anoxic events rendered the benthic environment uninhabitable. Such excursions were brief however, being insufficient to allow marked enrichment of the underlying sediment in elements known to accumulate under anoxic conditions, but enhancing the preservational potential of dead and dying free swimming forms falling to the sea floor.

Such factors as soft substrate, turbidity and low dissolved oxygen availability, would be detrimental to the settlement and recruitment of any larval/young juvenile stages, causing recruitment failure and resulting in an 'adults only' assemblage, recruited via migration and containing only motile elements, including *Myoscolex*, which appears to have been a nectobenthic arthropod.

Redox conditions at and/or immediately below the sediment-water interface appears to have been conducive to the rapid mineralisation of tissues by phosphate, quickly followed by calcium carbonate precipitation. In instances where soft tissues were absent (e.g.

moults) or conditions did not allow phosphate mineralisation, only calcium carbonate precipitation occurred, most probably after burial, close to the sediment-water interface.

All fossils seem to have undergone at least one remineralisation event. This is indicated by the platy form of the phosphate - as opposed to the spherulite form of newly deposited phosphate - and the apparently tectonically aligned fibrous carbonate.
Recrystallisation has made it difficult to determine whether primary mineralisation occurred pre or post sediment compaction. Certainly the larger elements of the fauna show little evidence of compaction and the observation of Briggs & Kear (1994) that decaying tissues cause the collapse of overlying mineralised tissues, indicates that mineralisation could well have occurred before significant compaction. This is also indicated given the time frame involved in early diagenetic mineralisation.

The results of this study support the interpretation that the Emu Bay Shale at Big Gully was rapidly deposited into a small suboxic-occasionally anoxic basin. The redox conditions at the sediment-water interface restricted larval settlement and provided a chemical environment conducive to the early diagenetic precipitation of calcite and occasionally phosphate.

## References


Ager, D. V. (1963) *Principles of Paleoecology*. McGraw-Hill, New York. 371 pp.

Alberch, P.; Gould, S. J.; Oster, G. F. & Wake, D. B. (1979) Size and shape in ontogeny and phylogeny. *Paleobiology*, **5**: 269-317.

Allen, J. R. L. (1972) Intensity of deposition from avalanches and the loose packing of avalanche deposits. *Sedimentology*, **18**: 105-111.

Aller, R. C. (1982) Carbonate dissolution in near-shore muds: the role of physical and biological reworking. *Journal of Geology*, **90**: 79-95.

Aller, R. C. & Dodge, R. E. (1974) Animal-sediment relations in a tropical lagoon, Discovery Bay, Jamaica. *Journal of Marine Research*, **32**: 209-232.

Allison, P. A. (1988a) The decay and mineralization of proteinaceous macrofossils. *Paleobiology*, **14**: 139-154.

Allison, P. A. (1988b) *Konservat-Lagerstätten*: cause and classification. *Paleobiology*, **14**: 331-344.

Allison, P. A. (1988c) Phosphatized soft-bodied squids from the Jurassic Oxford Clay. *Lethaia*, **21**: 403-410.

Allison, P. A. & Briggs D. E. G. (1991) Taphonomy of nonmineralized tissues. In: Allison, P. A. & Briggs , D. E. G. (eds.), *Taphonomy: Releasing the Data Locked in the Fossil Record*. 25-70. Plenum Press, New York.

Allison, P. A. & Briggs, D. E. G. (1993) Exceptional fossil record: Distribution of soft-tissue preservation through the Phanerozoic. *Geology*, **21**: 527-530.

Anderson, R. F. (1987) Redox behavoir of uranium in an anoxic marine basin. *Uranium*, **3**: 145-164.

Anderson, R. F.; Fleisher, M. Q. & Murray, J. W. (1989) Concentration, oxidation state and particulate flux of uranium in the Black Sea. *Geochimica et Cosmochimica Acta*, **53**: 2205-2224.

Archer, D.; Emerson, S. & Smith, C. R. (1989) Direct measurement of the diffusive boundary sublayer at the deep-sea floor using oxygen microelectrodes. *Nature*. **340**: 623-626.

Arrhenius, G. & Bonatti, E. (1965) Neptunism and vulcanism in the ocean. In: M. Sears (ed), *Progresses in Oceanography, Vol 3*. 7-22. Permagon Press, London.

Austin, M. C. & Wibdom, B. (1991) Changes in and slow recovery of a meiobenthic nematode assemblage following a hypoxic period in the Gullmar Fjord basin, Sweden. *Marine Biology*. **111**: 139-145.

Bachelet, G.; Butman, C. A.; Webb, C. M.; Starczak, U. R. & Snelgrove, P. V. R. (1992) Non-selective settlement of *Mercenaria mercenaria* (L.) larvae in short term, still water, laboratory experiments. *Journal of Experimental Marine Biology and Ecology*. **161**: 241-280.

Bayne, B. L. (1971) Oxygen consumption by tree species of lamellibranch mollusc in declining ambient tension. *Comparative Biochemistry and Physiology*, **40A**: 955-970.

Belperio, A. P. &. Flint, R. B. (1993). Geological Note. The southeastern margin of the Gawler Craton. *Australian Journal of Earth Sciences*, **40**: 423-426.

Bamber, R. N. (1989) The effects of acidic sea water on young carpet-shell clams *Venerupis decussata* (L.) (Mollusca: Veneracea). *Journal of Experimental Marine Biology and Ecology*, **108**: 241-260.

Bender, M. L. & Heggie, D. T. (1984) Fate of organic carbon reaching the deep sea floor: a status report. *Geochim et Cosmochim Acta*. **48**: 977-986.

Bender, M. L.; Klinkhammer, G. P. & Spencer, D. W. (1977) Manganese in seawater and the marine manganese balance. *Deep-Sea Research*, **24**: 799-812.

Bengtson, S. (1990) Crustaceans. *Memoir of the Association of Australasian Palaeontologists*, **9**: 322-330.

Bengtson, S.; Conway Morris, S.; Cooper, B. J.; Jell, P. A. & Runnegar, B. N. (1990) Early Cambrian fossils from South Australia. *Memoir of the Association of*

*Australasian Palaeontologists*, **9**: 1-364.

Ben Yaakov, S. (1973) pH buffering of pore water of recent anoxic marine sediments. *Limnology and Oceanography*, **18**: 86-94.

Berger, W. H. (1976) Biogenous deep-sea sediments: production, preservation and interpretation. In: Ripley, J. P. & Chester, R. (eds.), *Chemical Oceanography Vol 5*. 266-372. Academic Press, London.

Bergström, J. (1986) *Opabinia* and *Anomalocaris*, unique Cambrian "arthropods". *Lethaia*, **19**: 241-246.

Berner, R. A. (1971) *Principles of Chemical Sedimentology*. McGraw-Hill, New York. 240 pp.

Berner, R. A. (1975) The role of magnesium in the crystal growth of calcite and aragonite from sea water. *Geochimica et Cosmochimica Acta*, **39**: 489-504.

Berner, R. A. (1978) Sulfate reduction and the rate of deposition of marine sediments. *Earth and Planetary Science Letters*, **37**: 492-498.

Berner, R. A. (1980) *Early Diagenesis: A Theoretical Approach*. Princton University Press, Princton. 250 pp.

Berner, R. A. (1984) Sedimentary pyrite formation: an update. *Geochimica et Cosmochimica Acta*, **48**: 605-615.

Berry, W. B. N. &. Wilde, P. (1978) Progressive ventilation of the oceans - an explanation for the distribution of the Lower Paleozoic black shales. *American Journal of Science*. **278**: 257-275.

Bertine, K. K. (1972) The deposition of molybdenum in anoxic waters. *Marine Chemistry*, **2**: 43-53.

Blackstone, N. & Yund, P. (1989) Morphological variation in a colonial marine hydroid: A comparison of size-based and age-based heterchrony. *Paleobiology*, 15: 1-10

Boucot, A. J. (1981) *Principles of Benthic Marine Paleoecology*. Academic Press, New

York. 463 pp.

Boudreau, B. P. (1987) A steady-state diagenetic model for dissolved carbonate species and pH in the pore waters of oxic and suboxic sediments. *Geochimica et Cosmochimica Acta*, **51**: 1985-1996.

Boudreau, B. P. & Guinasso, N. L. (1982) The influence of a diffusive sublayer on accretion, dissolution and diagenesis at the sea floor. In: Fanning, K. A. & Manheim, F. T. (eds.), *The Dynamic Environment of the Sea Floor*. 115-145. Lexington Books, Lexington.

Boyle, E. A.; Huested, S. S. & Jones, S. P. (1981) On the distribution of copper nickel and cadmium in the surface waters of the North Atlantic and North Pacific Oceans. *Journal of Geophysical Research*, **86**: 8048-8066.

Boyle, E. A.; Sclater, F. R. & Edmond, J. M. (1976) On the marine geochemistry of cadmium. *Nature*, **263**: 42-44.

Brasier, M. D. (1992) Background to the Cambrian Explosion. *Journal of the Geological Society of London*, **149**: 585-587.

Brett, C. E. & Baird, G. C. (1986) Comparative taphonomy: a key to paleo-environment interpretation based on fossil preservation. *Palaios*, **1**: 207-227.

Briggs, D. E. G. (1976) The arthropod *Branchiocaris* n. gen., Middle Cambrian, Burgess Shale, British Columbia. *Bulletin of the Geological Survey of Canada*, **264**: 1-29.

Briggs, D. E. G. (1978) The morphology, mode of life, and affinities of *Canadaspis perfecta* (Crustacea: Phyllocarida), Middle Cambrian, Burgess Shale, British Columbia. *Philosophical Transactions of the Royal Society of London*, **B281**: 439-487.

Briggs, D. E. G. (1979) *Anomalocaris*, the largest known Cambrian arthropod. *Paleontology*, **22**: 631-634.

Briggs, D. E. G. (1981) The arthropod *Odaraia alata* Walcott, Middle Cambrian, Burgess Shale, British Columbia. *Philosophical Transactions of the Royal*

*Society of London*, **B291**: 541-585.

Briggs, D. E. G. & Clarkson, E. N. K. (1983) The Lower Carboniferous Granton "shrimp-bed", Edinburgh. *Special Publications in Palaeontology*, **30**: 161-177.

Briggs, D. E. G. & Clarkson, E. N. K. (1985) The Lower Carboniferous shrimp *Tealliocaris* from Gullane, East Lothian, Scotland. *Transactions of the Royal Society of Edinburgh, Earth Sciences*, **76**: 173-201.

Briggs, D. E. G. & Fortey, R. A. (1989) The early radiation and relationships of the major arthropod groups. *Science*, **146**: 241-243.

Briggs, D. E. G. & Kear, A. J. (1993a) Fossilization of soft tissue in the laboratory. *Science*, **259**: 1439-1442.

Briggs, D. E. G. & Kear, A. J. (1993b) Decay and preservation of polychaetes: taphanomic thresholds in soft-bodied organisms. *Paleobiology*, **19**: 107-135.

Briggs, D. E. G. & Kear, A. J. (1994) Decay and mineralization of shrimps. *Palaios*, **9**: 431-456.

Briggs, D. E. G. & Mount, J. D. (1982) The occurrence of the giant arthropod *Anomalocaris* in the Lower Cambrian of southern California, and the overall distribution of the genus. *Journal of Paleontology*, **56**: 1112-1118

Briggs, D. E. G. & Nedin, C. (In Prep) The taphonomy and affinities of the problematic fossil *Myoscolex* from the Cambrian Emu Bay Shale of South Australia.

Briggs, D. E. G. & Robison, R. A. (1984) Exceptionally preserved nontrilobite arthropods and *Anomalocaris* from the Middle Cambrian of Utah. *University of Kansas, Paleontological Contributions*, **111**: 1-23.

Briggs, D. E. G. & Rolfe, W. D. I. (1983) New Concavicarida (new Order: ?Crustacea) from the Upper Devonian of Gogo, Western Australia, and the palaeoecology and affinities of the group. *Special Publications in Palaeontology*, **30**: 249-276.

Briggs, D. E. G. & Williams, S. H. (1981) The restoration of flattened fossils. *Lethaia*, **14**: 157-164.

Briggs, D. E. G.; Fortey, R. A. & Willis, M. A. (1992) Morphological disparity in the Cambrian. *Science*, **256**: 1670-1673.

Briggs, D. E. G.; Kear, A. J.; Martill, D. M. & Wilby, P. R. (1993) Phosphatization of soft tissue in experiments and fossils. *Journal of the Geological Society of London*, **150**: 1035-1038.

Brock, G. A. & Cooper, B. J. (1993) Shelly fossils from the Early Cambrian (Toyonian) Wirrealpa, Aroona Creek and Ramsay Limestones of South Australia. *Journal of Paleontology*, **67**: 758-787.

Bromley, R. G. & Surlyk, F. (1973) Borings produced by brachiopod pedicles, fossil and recent. *Lethaia*, **6**: 349-365.

Brongersma-Sanders, M. (1957) Mass mortality in the sea. *Geological Society of America, Memoir*. **67**: 941-1010.

Brown, H. Y. L. (1898) Kangaroo Island. *Annual Report of the Government Geologist. Parliamentary Papers South Australia, 1898*, **36**: 1-5.

Brown, H. Y. L. (1908) A short account of the chief geological features of the state of South Australia. *Record of the Mines of South Australia*, **4**: 1-7.

Brutland, K. W. (1980) Oceanographic distribution of cadmium, zinc, nickel and copper, in the North Pacific. *Earth and Planetary Science Letters*, **47**: 176-198.

Bruland, K. W. (1983) Trace elements in sea-water. In: Riley, J. P. & Skirrow, G. (eds.), *Chemical Oceanography Vol 8*. 157-220. Academic Press, New York.

Brumsack, H.-J. (1980) Geochemistry of Cretaceous black shales from the Atlantic Ocean (DSDP Legs 11, 14, 36 & 41). *Chemical Geology*, **31**: 1-25.

Brumsack, H.-J. (1986) The inorganic geochemistry of Cretaceous black shales (DSDP Leg 41): comparison to modern upwelling sediments from the Gulf of California. *Geological Society of London Special Publication*, **21**: 447-462.

Brumsack, H. J. (1989) Geochemistry of recent TOC-rich sediments from the Gulf of California and the Black Sea. *Geologische Rundschau*, **78**: 851-882.

Budd, G. (1993) A Cambrian gilled lobopod from Greenland. *Nature*, **364**: 709-711.

Burton, E. A. & Walter, L. M. (1990) The role of pH in phosphate inhibition of calcite and aragonite precipitiation in seawater. *Geochimica et Cosmochmica Acta*, **54**: 797-808.

Butman, C. A.; Grassle, J. P. & Webb, C. M. (1988) Substrate choices made by marine larvae settling in still water and in a flume flow. *Nature*, **333**: 771-773.

Butterfield, N. J. (1990) Organic preservation of non-mineralizing organisms and the taphonomy of the Burgess Shale. *Paleobiology*, **16**: 272-268.

Butterfield, N. J. (1994) Burgess Shale-type fossils from a Lower Cambrian shallow-shelf sequrnce in northwest Canada. *Nature*, **369**: 477-479.

Butterfield, N. J. (1995) Secular distribution of Burgess Shale-type preservation. *Lethaia*, **28**: 1-13

Calabrese, A. & Davis, H. C. (1966) The pH tolerance of embryos and larvae of *Mercenaria mercenaria* and *Crassostrea virginica*. *Biological Bulletin*, **131**: 427-436.

Calvert, S. E. (1976) The mineralogy and geochemistry of nearshore sediments. In: Riley, J. P. & Chester, R. (eds.), *Chemical Oceanography*. 187-280. Academic Press, London.

Calvert, S. E. & Pederson, T. F. (1993) Geochemistry of recent oxic and anoxic marine sediments: Implications for the geological record. *Marine Geology*, **113**: 67-88.

Calvert, D. E. & Price, N. B. (1970) Composition of manganese nodules and manganese carbonates from Loch Fyne, Scotland. *Contributions to Minerology and Petrology*, **29**: 215-233.

Calvert, D. E. & Price, N. B. (1972) Diffusion and reaction profiles of dissolved manganese in the pore waters of marine sediments. *Earth and Planetary Science Letters*, **16**: 245-249.

Calvert, D. E & Price, N. B. (1977) Geochemical variation in ferromanganese nodules and associated sediments from the Pacific Ocean. *Marine Chemistry*, **5**: 43-74.

Canfield, D. E. (1988) Reactive iron in marine sediments. *Geochimica et Cosmochimica Acta*, **53**: 619-632.

Canfield, D. E. (1989a) Diffusion and reaction profiles of dissolved manganese in the pore waters of marine sediments. *Earth and Planetary Science Letters*, **16**: 245-249.

Canfield, D. E. (1989b) Sulfate reduction and oxic respiration in marine sediments: implications for organic carbon preservation in euxinic environments. *Deep-Sea Research*, **36**: 121-138.

Canfield, D. E. (1991) Sulfate reduction in deep-sea sediments. *American Journal of Science*, **291**: 177-188.

Canfield, D. E. &. Raiswell, R. (1991a) Pyrite Formation and Fossil Preservation. In: Allison, P. A. & Briggs, D. E. G. (eds.), *Taphonomy: Releasing the Data Locked in the Fossil Record.* 337-387. Plenum Press, New York.

Canfield, D. E. &. Raiswell, R. (1991b) Carbonate precipitation and dissolution: its relevance to fossil preservation. In: Allison, P. A. & Briggs, D. E. G. (eds.), *Taphonomy: Releasing the Data Locked in the Fossil Record.* 411-453. Plenum Press, New York.

Chapman, F. (1929) On some trilobites and brachiopods from the Mt. Isa district, N.W. Queensland. *Procedings of the Royal Society of Victoria*, **41**: 206-216.

Chen Junyuan & Erdtmann, B-D. (1991) Lower Cambrian Lagerstätte from Chengjiang, Yunnan, China: Insights for reconstructing early metazoan life. In: Simonetta, A. M. & Conway Morris, S. (eds.), *The Early Evolution of Metazoa and the Significance of Problematic Taxa.* 57-76. Cambridge University Press, Cambridge.

Chen Junyuan Hou Xiangguang & Erdtmann, B. D. (1989) New soft-bodied fossil fauna near the base of the Cambrian System at Chengjiang, eastern Yunnan, China. In: *Developments in Geoscience, Contributions to 28th International*

*Geological Congress*. p. 265-277. Science Press, Beijing.

Chen Junyuan, Ramsköld, L. & Zhou Guiqing (1994) Evidence for monophyly and arthropod affinity of Cambrian giant predators. *Science*, **264**: 1304-1308.

Christie-Blick, N. & Biddle, K. T. (1985) Deformation and basin formation along strike-slipe faults. *Society of Economic Paleontologists and Mineralogists, Special Publication*, **37**: 1-34.

Clifton, H. E. (1981) Progradational sequences in Miocene shoreline deposits, southeast Caliente range, California. *Journal of Sedimentary Petrology*, **51**: 165-184.

Coleman, M. L. (1985) Geochemistry of diagenetic non-silicate minerals: kinetic considerations. *Philosophical Transactions of the Royal Society of London,* **A315**: 39-56.

Collier, R. W. (1985) Molybdenum in the northeast Pacific Ocean. *Limnology and Oceanography*, **30**: 1351-1254.

Collins, D. H. (1987) A new Burgess Shale-type fauna in the Middle Cambrian Stephen Formation on Mt. Stephen, British Columbia. *Geological Society of America, Abstracts with Programs*, **17**: 550.

Collins, D. H. (1992) Whither Anomalocaris? The search in the Burgess Shale continues. 5th. North American Paleontological Convention. Abstracts with Programs. *The Paleontological Society Special Publication*, **6**: 66.

Collins, D. H.; Briggs, D. E. G. & Conway Morris, S. (1983) New Bugess Shale fossil site reveals Middle Cambrian faunal complex. *Science*, **222**: 163-167

Collinson, J. D. (1986) Alluvial Sediments. In: Reading, H. G. (ed.), *Sedimentary Environments and Facies*. 20-62. Blackwell Scientific, Oxford.

Coney, P. J.; Edwards, A.; Hine, R.; Morrison, F. & Windrim, D. (1990) The regional textonics of the Tasman orogenic system, eastern Australia. *Journal of Structural Geology*, **12**: 519-543.

Connard, P. D. (1967) The Cambrian Stratigraphy of Kangaroo Island in Relation to the

Hydrocarbon Potential of O.E.L. 24 (St. Vincent Gulf), S. Aust. *University of Adelaide Honours thesis* (*unpublished*).

Conway, N. M.; Howes, B. L.; Capuzzo, J. E. M.; Turner, R. D. & Cavanaugh, C. M. (1992) Characterisation and site description of *Solemya borealis* (Bivalvia; Solemyidae), another bivalve-bacteria symbiosis. *Marine Biology*, **112**: 601-613.

Conway Morris, S. (1985) Concluding remarks-Extraordinary fossil biotas: Their ecological and evolutionary significance. *Philosophical Transactions of the Royal Society of London, B*, **311**: 187-192.

Conway Morris, S. (1986) The community structure of the Middle Cambrian Phyllipod Bed (Burgess Shale). *Palaeontology*, **29**: 423-467.

Conway Morris, S. (1989a) Burgess Shale Faunas and the Cambrian Explosion. *Science*, **246**: 339-346.

Conway Morris, S. (1989b) The persistence of Burgess Shale-type faunas: implications for the evolution of deeper-water faunas. *Transactions of the Royal Society of Edinburgh: Earth Sciences*, **80**: 271-283.

Conway Morris, S. & Jenkins, R. J. F. (1985) Healed injuries in Early Cambrian trilobites from South Australia. *Alcheringa*, **9**: 167-177.

Conway Morris, S. & Robison, R. A. (1986) Middle Cambrian pirapulids and other soft-bodied fossils from Utah and Spain. *University of Kansas, Paleontological Contributions*, **117**: 1-22.

Conway Morris, S. & Robison, R. A. (1988) More soft-bodied animals and algae from the Middle Cambrian of Utah and Spain. *University of Kansas, Paleontological Contributions*, **117**: 1-22.

Conway Morris, S.; Peel, J. S.; Higgins, A. K.; Soper, N. J. & Davis, N. C. (1987) A Burgess Shale-like fauna from the Lower Cambrian of North Greenland. *Nature*, **326**: 181-183.

Cook, P. J. & Shergold, J. H. (1986) Proterozoic and Cambrian phosphorites - nature

and origin. In: Cook, P. J. & Shergold, J. H. (eds.), *Phosphate Deposits of the World, Vol. 1*. 369-386. Cambridge University Press, CAmbridge.

Cooper, J. A.; Jenkins, R. J. F.; Compston, W. & Williams, I. S. (1992) Ion Probe zircon dating of a tuff in the South Australian Lower Cambrian. *Journal of the Geological Society of London*, **149**: 185-192.

Daily, B. (1956) The Cambrian of South Australia. *International Geological Congress*, **21**(2): 91-147.

Daily, B. (1957) Progress report on the Cambrian sequence met with in the Minlaton Stratigraphic Bore 1, section 210, Hd. Ramsey, Yorke Peninsula, South Australia. *South Australia Department of Mines, open file Env.* **48** (*unpublished*)

Daily, B. (1963) Appendix 3B. In Harrison, J.; Campbell, I. R. and Higginbotham, G. T. Delhi-Santos Pandieburra 1 *Well Completion Report, SA Department of Mines and Energy Env.* **813** (unpublished).

Daily, B. (1968) Stansbury Town No. 1 Well - subsurface stratigraphy and palaeontology of the Cambrian sequence. *South Australia Mines Department, Open File Env.* **916** (unpublished).

Daily, B. (1969) Fossiliferous Cambrian sediments and low-grade metamorphics, Fleurieu Peninsula, South Australia. In: Daily, B. (ed.), *Geological Excursions Handbook.*, ANZAAS, Section 3, p. 49-54.

Daily, B. (1976) The Cambrian of the Flinders Ranges. In: Thomson, B. P.; Daily, B.; Coats, R. P. & Forbs, B. G. (eds.), *Late Precambrian and Cambrian Geology of the Adelaide 'Geosyncline' and Stuart Shelf. 25th International Geological Congress, Excursion Guide*, **33A**: 15-19

Daily, B. (1977) Notes on the geology of Kangaroo Island. Kangaroo Island Field Conference, October 1977. *Geological Society of Australia, South Australian Branch* (unpublished).

Daily, B. & Forbes, B. G. (1969) Notes on the Proterozoic and Cambrian, southern and central Flinders Ranges, South Australia. In: Daily, B. (ed.), *Geological*

*Excursions Handbook.*, ANZAAS, Section 3: 23-30.

Daily, B. & Milnes, A. R. (1971) Stratigraphic notes on Lower Cambrian fossiliferous metasediments between Campell Creek and Tunkalilla Beach in the type section of the Kanmantoo Group, Fleurieu Peninsula, South Australia. *Transactions of the Royal Society of South Australia*, **95**: 199-214.

Daily, B & Milnes, A. R. (1972a) Revision of the stratigraphic nomenclature of the Cambrian Kanmantoo Group, South Australia. *Journal of the Geological Society of Australia*, **19**: 197-202.

Daily, B. & Milnes, A. R. (1972b) Significance of basal Cambrian metasediments of andalusite grade, Dudly Peninsula, Kangaroo Island, South Australia. *Search*, **3**: 89-90.

Daily, B.; Jago, J. B. & Milnes, A. R. (1973) Large-scale horizontal displacement within Australo-Antartica in the Ordovician. *Nature*, **244**: 61-64.

Daily, B.; Moore, P. S. & Rust, B. R. (1980) Terrestrial-marine transition in the Cambrian rocks of Kangaroo Island, South Australia. *Sedimentology*, **27**: 379-399.

Daily, B.; Milnes, A. R.; Twidale, C. R. & Bourne, J. A. (1979) Geology and Geomorphology. In: Tyler, M. J.; Twidale, C. R. & Ling, J. L. (eds.), *Natural History of Kangaroo Island.* 1-38. Royal Society of South Australia, Adelaide.

Dalby, J. E. Jr. & Young, C. M. (1992) Role of early post-settlement mortality in setting the upper limit of ascidians in Florida epifaunal communities. *Marine Ecology Progress Series*, **80**: 221-228.

Dean, B. (1902) The preservation of muscle-fibres in sharks of the Cleveland Shale. *American Geologist*, 30: 373-378.

Debrenne, F. & Gravestock D. I. (1990) Archaeocyatha from the Sellick Hill Formation and Fork Tree Limestone on Fleurieu Peninsula, South Australia. *Geological Society of Australia Special Publication*, **16**: 290-309.

Devol, A. H. (1983) Methane oxidation rates in the anaerobic sediments of Saanich Inlet.

*Limnology and Oceanography*, **28**: 738-742.

Dinnick, M. (1985) Stratigraphy, sedimentology and palaeontology of a Cambrian molassic sequence, Cape D'Estaing to Point Marsden, north east coast of Kangaroo Island, South Australia. *University of Adelaide Honours thesis (unpublished)*.

Donegan, D. & Schrader, H. (1982) Biogenetic and abiogenetic components of laminated hemipelagic sediments in the central Gulf of California. *Marine Geology*, **48**: 215-237.

Donovan, D. T. (1983) *Mastigophora* Owen 1856: a little known genus of Jurassic coleoids. *Neues Jahrbuch für Geologie und Paläontologie*, **165**: 484-495.

Doyle, P. & Whitham, A. G. (1991) Palaeoenvironments of the Nordenskjold Formation: an Antartic Late Jurassic-Early Cretaceous black shale-tuff sequence. *Geological Society of London, Special Publication*, **58**: 397-414.

Driscoll, E. G. (1967) Attached epifauna-substrate relations. *Limnology and Oceanogaphy*, **12**: 633-641.

Ekdale, A. A. & Mason, T. R. (1988) Characteristic trace-fossil associations in oxygen-poor sedimentary environments. *Geology*, **16**: 720-723.

Emerson, S. R. (1985) Organic carbon preservation in marine sediments. In: Sundquist, E. T. & Broecker, W. S. (eds.), *The Carbon Cycle and Atmospheric $CO_2$: Natural variations Archean to Present*. 78-87. American Geophysical Union, Washington.

Emerson, S. & Bender, M. (1981) Carbon fluxes at the sediment water interface of the deep-sea: calcium carbonate preservation. *Journal of Marine Research*, **39**: 139-162.

Emerson, S. R. & Huested, S. S. (1991) Ocean anoxia and the concentrations of molybdenum and vanadium in seawater. *Marine Chemistry*, **34**: 177-196.

Emerson, S. R.; Cranston, R. E. & Liss, P. S. (1979) Redox species in a reducing fjord: equilibrium and kinetic considerations. *Deep-Sea Research*, **26A**: 859-

878.

Endo, R. & Resser, C. E. (1937) The Sinian (pre-Cambrian) and Cambrian formations and fossils of southern Manchoukou. *Bulletin of the Manchurian Science Museum*, **1**: 474 pp.

Etheridge, R. (1897) Official contributions to the palaeontology of South Australia, No. 9: On the occurrence of *Olenellus* in the Northern Territory. *South Australian Parliamentary Papers*, **63**: 13-16.

Evemy, B. D. (1973) The precipitation of aragonite and its alteration to calcite on the Trucial Coast of the Persian Gulf. In: Purser, B. H. (ed.), *The Persian Gulf: Holocene Carbonate Sedimentation and Diagenesis in a Shallow Epicontinental Sea*. 329-341. Springer-Verlag, Berlin.

Fan, D.; Liu, T. & Ye, T. (1992) The process of formation of manganese carbonate deposits hosted in black shale series. *Economic Geology*, **87**: 1419-1429.

Fisher, I. St. J. & Hudson, J. D. (1987) Pyrite formation in Jurassic shales of contrasting biofacies. *Geological Society of London, Special Publication*. **26**: 69-78.

Flöttmann, T.; James, P. (1994) Tectonic evolution of the southern Adelaide Fold Belt: a strain and balanced-section approach. *Geological Society of Australia, Abstracts*, **32**: 241.

Flöttmann, T.; James, P.; Rogers, J. & Johnson, T. (1994) Early Palaeozoic forelend thrusting and basin reactivation at the southeast Palaeo-Pacific margin of the Australian Precambrian Craton: a reappraisal of the structural evolution of the Southern Adelaide Fold-Thrust Belt. *Tectonophysics*, **234**: 95-116.

Flöttmann, T.; James, P.; Mempes, R.; Cesare, P.; Twinning, M.; Fairclough, M.; Randabel, J. & Marshak, S. (1995) The structure of Kangaroo Island (South Australia); strain and kinematic patitioning during Delamarian basin and platform reactivation. *Australian Journal of Earth Sciences*, **42**: 35-49.

Folk, R. L. (1974) The natural history of crystalline calcium carbonate: effect of magnesium content and salinity. *Journal of Sedimentary Petrology*, **44**: 40-53.

Foote, M.; Gould, S. J. & Lee, M. S. Y. (1992) Cambrian and recent morphological disparity - comment. *Science*, **258**: 1816-1817.

Fortey, R. A. (1990) Ontogeny, hypostome attachment and trilobite classification. *Palaeontology*, **33**: 529-576.

Fossing, H. & Jørgensen, B. B. (1990) Oxidation and reduction of radiolabeled inorganic sulfur compounds in an esturine sediment, Kysing Fjord, Denmark. *Geochimica et Cosmochimica Acta*, **54**: 2731-2742.

Frakes, L. A. (1979) *Climates Throughout geologic Time*. Elsevier, Amsterdam. 310 pp.

Francois, R. (1988) A study on the regulation of the consentration of some trace elements (Rb, Sr, Zn, Pb, Cu, V, Cr, Ni, Mn, and Mo) in Saanich Inlet sediments, British Columbia, Canada. *Marine Geology*, **83**: 285-308.

Franzen, C. (1977) Crinoid holdfasts from the Silurian of Gotland. *Lethaia*, **10**: 219-234.

Froelich, P. N.; Klinkhammer, G.; Bender, M. L.; Luedtke, N. A.; Heath, G. R.; Cullen, D.; Dauphin, P.; Hammond, D.; Hartman, B. & Maynard, V. (1979) Early oxidation of organic matter in pelagic sediments of the eastern equatorial Atlantic: suboxic diagenesis. *Geochimica et Cosmochimica Acta*, **43**: 1075-1090.

Froelich, P. N.; Bender, M. L.; Luedtke, N. A.; Heath, G. R. & DeVries, T. (1982) The marine phosphorus cycle. *American Journal of Science*, **282**: 474-511.

Froelich, P. N.; Arthur, M. A.; Burnett, W. C.; Deakin, M.; Hensley, V.; Jahnke, R.; Kaul, L.; Kim, K.-H.; Soutar, A. & Vathakanon, C. (1988) Early Diagenesis of organic matter in Peru continental margin sediments: phosphorite precipitation. *Marine Geology*, **80**: 309-343.

Fürsich, F. T.; Oschmann, W.; Jailty, A. K. & Singh, I. B. (1991) Faunal response to transgressive-regressive cycles: examples from the Jurassic of western India. *Palaeogeography, Palaeoclimatology, Palaeoecology*, **85**: 149-159.

Gatehouse, G. G. (1983) Stratigraphic units in the Warburton Basin in South Australia. *South Australian Geological Survey Quarterly Geological Notes*, **86**: 5-8.

Gatehouse, G. G. (1986) The geology of the Warburton Basin in South Australia. *Australian Journal of Earth Sciences*, **33**: 161-180.

Ginsburg, R. N. (1957) Early diagenesis and lithification of shallow water carbonate sediments in South Florida. *Society of Economic Paleontologists and Mineralogists, Special Publication*, **5**: 80-99.

Glaessner, M. F. (1952) A Cambrian fauna from Kangaroo Island, South Australia. *South Australia Department of Mines Report (unpublished)*.

Glaessner, M. F. (1979) Lower Cambrian crustacea and annelid worms from Kangaroo Island, South Australia. *Alcheringa*, **3**: 21-31.

Glude, J. B. (1954) Survival of soft-shelled clams *Mya arenaria*, buried at various depths. *Research Bulletin of the Department of Sea Shore Fisheries, Maine*. **22**: 2-26.

Goldberg, E. D. & Arrhenius, G. O. S. (1958) Chemistry of Pacific pelargic sediments. *Geochimica et Cosmochimica Acta*, **13**: 3-25.

Goldhaber, M. B. & Kaplan, I. R. (1974) The sulfur cycle. In: Goldberg, E. D. (ed.), *The Sea, Vol 5*. 569-655. John Wiley & Sons, New York.

González, L. A.; Carpenter, S. J. & Lohmann, K. C. (1993) Inorganic calcite morphology: roles of fluid chemistry and fluid flow. *Journal of Sedimentary Petrology*, **62**: 382-399.

Gould, S. J. (1989) *Wonderful Life*. Penguin, London. 347 pp.

Gould, S. J. (1991) The disparity of the Burgess Shale arthropod fauna and the limits of cladistic analysis: why we must strive to quantify morphospace. *Paleobiology*, **17**: 411-423.

de Graciansky, P. C.; Deroo, G.; Herbin, J. P.; Montadent, L.; Müller, C.; Schaaf, A. &

Sigal, J. (1984) Ocean-wide stagnation episode in the Late Cretaceous. *Nature*, **308**: 346-349.

Gravestock, D. I. (1984) Archaeocyatha from the lower parts of the Lower Cambrian carbonate sequence in South Australia. *Association of Australasian Palaeontologists, Memoir*, **2**: 1-139.

Gravestock, D. I. (1995) Early and Middle Palaeozoic. In *The Geology of South Australia*, Vol 2. In press.

Gundersen, J. K. & Jørgensen, B. B. (1990) Microstructure of diffusive boundary layers and the oxygen uptake of the sea floor. *Nature*, **345**: 604-607.

Gustafson, L. B. & Williams, N. (1981) Sediment-hosted stratiform deposits of copper, lead, and zinc. *Economic Geology*, **75**: 139-178.

Hallam, A. (1984) Pre-Quaternary sea-level change. *Annual Review of Earth and Planetary Sciences*, **8**: 205-243.

Harrington, H. J. (1959) Arhtropoda. p. 191-216. In: *Treatise of Invertebrate Paleontology (O)*. University of Kansas Press, Lawrence, Kansas

Hattin, D. E. (1986) Carbonate substrates of the Late Cretaceous Sea, Central Great Plains and Southern Rocky Mountains. *Palaios*. **1**: 347-367.

Heggie, D. T.; Skyring, G. W.; O'Brien, G. W.; Reimers, C.; Herczeg, A.; Moriarty, D. J. W.; Burnett, W. C. & Milnes, A. R. (1990) Organic carbon cycling and modern phosphorite formation on the East Australian continental margin: an overview. *Geological Society Special Publication*, **52**: 87-117.

Hirschler, A.; Lucas, J. & Hubert, J. C. (1990) Bacterial involvement in apatite genesis. *Microbiology and Ecology*, **73**: 211-220.

Holland, H. D. (1978) *The Chemistry of the Atmosphere and Oceans*. Wiley Interscience, New York. 351 pp.

Holme, N. A. (1961) The bottom fauna of the English Channel. *Journal of the Marine Biology Association of the United Kingdom*, **41**: 397-461.

Horn, C. M. & Morris, B. J. (1988) Summary review of lead-zinc mineralization in South Australia. *Department of Mines and Energy, South Australia.* Report Book 87/7628 pp.

Horwitz, R. C. & Daily, B. (1958) Yorke Peninsula. *Journal of the Geological Society of South Australia*, **5**: 46-60.

Hou Xian-Guang & Bergström, J. (1991) The arthropods of the Lower Cambrian Chengjiang fauna, with relationships and evolutionary significance. In: Simonetta, A. M. & Conway Morris, S. (eds.), *The Early Evolution of Metazoa and the Significance of Problematic Taxa.* 179-187. Cambridge University Press, Cambridge.

Hou Xian-Guang & Chen Junyuan (1989a) Early Cambrian arthropod-annelid intermediate sea animal, *Luolishania* gen. nov. from Chengjiang, Yunnan. *Acta Palaeontologica Sinica*, **28**: 1-15. [In Chinese with English summary].

Hou Xian-Guang & Chen Junyuan (1989b) Early Cambrian tentacled worm-like animals (*Facivermis* gen. nov.) from Chengjiang, Yunnan. *Acta Palaeontologica Sinica*, **28**: 32-41. [In Chinese with English summary].

Hou Xian-Guang & Sun Wei-Guo (1988) Discovery of Chengjiang fauna at Meisuchun, Jinning, Yunnan. *Acta Palaeontologica Sinica*, **27**: 1-12 . [In Chinese with English summary]

Hou Xian-Guang, Bergström, J. & Ahlberg, P. (1995) *Anomalocaris* and other large animals in the Lower Cambrian Chengjiang fauna of southwest China. *Geologiska Foreningen i Stockholm Forhandlinger*, **117**: 163-183.

Hou Xian-Guang, Ramköld, L. & Bergström, J. (1991) Composition and preservation of the Chengjiang fauna - a Lower Cambrian soft-bodied biota. *Zoologica Scripta*, **20**: 395-411.

Howchin, W. (1899) Notes on the geology of Kangaroo island, with special reference to evidences of extinct glacial action. *Transactions of the Royal Society of South Australia*, **23**: 198-207.

Howchin, W. (1903) Further notes on the geology of Kangaroo Island. *Transactions of the Royal Society of South Australia*, **27**: 75-90.

Ingall, E. D.; Bustin, R. M. & Van Cappellen, P. (1993) Influence of water column anoxia on the burial and preservation of carbon and phosphorus in marine shales. *Geochimica et Cosmochimica Acta*, **57**: 303-316.

Ingmanson, D. E. & Wallace, J. W. (1985) *Oceanography: an introduction*. Wadsworth Publishing Co., Belmont , California. 530 pp.

Jacobs, L.; Emerson, S. & Huested, S. S. (1987) Trace metal geochemistry in the Cariaco Trench. *Deep-Sea Research*, **34**: 965-981.

Jago, J. B.; Daily, B.; Von Der Borch, C. C.; Cernovskis, A & Saunders, N. (1984) First reported trilobites from the Lower Cambrian Normanville Group, Fleurieu Peninsula, South Australia. *Transactions of the Royal Society of South Australia*, **108**: 207-211.

Jell, P. A. (1990) Trilobita. In: *Early Cambrian Fossils from South Australia. Memoir of the Association of Australasian Palaeontologists*, **9**: 257-322.

Jell, P.A.; Jago, J. B. & Gehling, J. G. (1992) A new conocoryphid trilobite from the Lower Cambrian of the Flinders Ranges, South Australia. *Alcheringa*, **16**: 189-200.

Jenkins, R. J. F. (1990) The Adelaide Fold Belt: Tectonic reappraisal. *Geological Society of Australia Special Publication*, **16**: 396-420.

Jenkins, R. J. F. & Hasenohr, P. (1989) Trilobites and their trails in a black shale: Early Cambrian of the Fleurieu Peninsula, South Australia. *Transactions of the Royal Society of South Australia*, **113**: 195-203.

Jenkyns, H. C.; Geczy, C. B.& Marshall, J. D. (1991) Jurassic manganese carbonates of Central Europe and the Early Toarcian anoxic event. *Journal of Geology*, **99**: 137-149.

Johnson, H. D. (1975) Tide- and wave-dominated inshore and shoreline sequences from the late Precambrian of Finmark, North Norway. *Sedimentology*, **22**: 45-74.

Johnson, K. S.; Berelson, W. M.; Coale, K. H.; Coley, T. L.; Elrod, V. A.; Fairey, W. R.; Iams, H. D.; Kilgore, T. E. & Nowicki, J. L. (1992) Manganese flux from continental margin sediments in a transect through the oxygen minimum. *Science*, **257**: 1242-1245.

Jørgensen, B. B. (1977) Bacterial sulphate reduction within reduced microenvironments of oxidised marine sediments. *Marine Biology*, **41**: 7-17.

Jørgensen, B. B. (1982) Mineralisation of organic matter in the sea-bed - the role of sulfate reduction. *Nature*, **296**: 643-645.

Jørgensen, B. B. (1983) The microbal sulfur cycle. In: Krumbein, W.E. (ed.), *Microbal Geochmistry*. 91-124. Blackwell, London.

Jørgensen, B. B. (1988) Ecology of the sulfur cycle: oxidative pathways in sediments. *Society for General Microbiology, Symposium*, **42**: 31-63.

Jørgensen, B. B.; Bang, M. & Blackburn, T. H. (1990) Anaerobic mineralization in marine sediments from the Baltic Sea-North Sea transition. *Marine Ecology Progress Series*, **59**: 39-54.

Jørgensen, B. B. & Des Marais, D. J. (1990) The diffusive boundary layer of sediments: oxygen microgradients over a microbal mat. *Limnology And Oceanography*, **35**: 1343-1355.

Jørgensen, B. B. & Revsbech, N. P. (1985) Diffusive boundary layers and the oxygen uptake of sediment and detritus. *Limnology and Oceanography*, **30**: 111-122.

Jørgensen, B. B. & Revsbech, N. P. (1989) Oxygen uptake, bacterial distribution, and carbon-nitrogen-sulfur cycling in sediments from the Baltic Sea-North Sea transition. *Ophelia*, **31**: 29-49.

Kasting, J. F. (1986) Theoretical constraints on oxygen and carbon dioxide concentrations in the Precambrian atmosphere. *Precambrian Research*, **34**: 205-229.

Keir, R. S. (1982) Dissolution of calcite in the deep-sea: theoretical prediction for the

case of uniform size particles settling into a well mixed sediment. *American Journal of Science*, **282**: 193-236.

Keynton, N. H. & Stride, A. H. (1970) The tidal-swept continental shelf sediments between the Shetland Isles and France. *Sedimentology*, **14**: 159-175.

Klein, G. D. (1970) Tidal origin of a Precambrian quartzite: the lower fine-grained quartzite (Middle Dalradian) of Islay, Scotland. *Journal of Sedimentary Petrology*, **40**: 973-985.

Klinkhammer, G. P. & Bender, M. L. (1980) The distribution of manganese in the Pacific Ocean. *Earth and Planetary Science Letters*, **46**: 361-384.

Klinkhammer, G. P.; Heggie, D. T. & Graham, D. W. (1982) Metal diagenesis in oxic marine sediments. *Earth and Planetary Science Letters*, **61**: 211-219.

Klinkhammer, G. P. & Palmer, M. R. (1991) Uranium in the oceans: where it goes and why. *Geochimica et Cosmochimica Acta*, **55**: 1799-1806.

Kobayashi, T. & Kato, F. (1951) On the ontogeny and the ventral morphology of *Redlichia chinensis* with description of *Alutella nakamurai* new gen. and sp. *Journal of the Faculty of Science, Imperial University of Tokyo, Section 2*, **8**: 99-143.

Kris, A. E. (1963) *Marine Microbiology*. Oliver & Boyd, Edinburgh, 536 pp.

Kruse, P. D. (1982) Archaeocyathan biostratigraphy of the Gnalta Group at Mt. Wright, New South Wales. *Palaeontographica A*, **177**: 1-212.

Kruse, P. D. (1991) Cyanobacteria-archaeocyathan-radiocyathan bioherms in the Wirrealpa Limestone of South Australia. *Canadian Journal of Earth Sciences*, **28**: 601-615.

Ku, T-L.; Knauss, K. G. & Mathieu, G. G. (1977) Uranium in the open ocean: Concentration and isotopic composition. *Deep-Sea Research*, **24**: 1005-1017.

Kuwatani, Y. & Nishii, T. (1969) Effects of pH of culture water on the growth of the Japanese pearl oyster. *Bulletin of the Japanese Society of Scientific Fisheries*,

**35**: 342-350.

Landing, E.; Myrow, P.; Benus, A.P. & Narbonne, G. M. (1989) The Placentian Series: appearence of the oldest skeletalized faunas in southeast Newfoundland. *Journal of Paleontology*, **63**: 739-769.

Landing, W. M. & Lewis, B. L. (1991) Thermodynamic modeling of trace metal speciation in the Black Sea. In: Murray, J. W. & Izdar, E. (eds.), *Black Sea Oceanography*.125-160. Kluwer, Dordrecht.

Laws, R. A. & Heisler, H. H. (1967) Stansbury Town No. 1 Well - well completion report. Beach Petroleum N. L. *South Australia Mines Department, Open File 784 (unpublished)*.

Lewy, Z. & Samtleben, C. (1979) Functional morphology and paleontological significance of the conchiolin layers in corbulid pelecypods. *Lethaia*, **12**: 341-351.

Lin Tian-Rui & Jago, J. B. (1993) *Xystridura* and other early Middle Cambrian trilobites from Yaxian, Hainan Province, China. *Transactions of the Royal Society of South Australia*, 117: 141-152.

Livingstone, D. R. (1983) Invertebrate and vertebrate pathways of anaerobic metabolism: evolutionary considerations. *Journal of the Geological Society of London*, **140**: 27-37.

Loosanoff. V. L. (1962) Effects of turbidity on some larval and adult bivalves. *Proceedings of the Gulf Caribbian Fisheries Institute*, **14**: 80-95.

Lovely, D. R. & Phillips, E. J. P. (1992) Reduction of uranium by *Desulfovibro desulfuricans*. *Applied Enviromental Microbiology*, **58**: 850-856.

Lu Yanhou (1950) New species of Redlichia. *Geological Review*, **15**. Geological Publishing House, Beijing.

Luckenbach, M. W. (1984) Settlement and early post-settlement survival in the recruitment of *Mulinia lateralis* (Bivalvia). *Marine Ecology Progress Series*, **17**: 245-250.

Lucas, J. & Prévôt, L. E. (1991) Phosphates and fossil preservation. In: Allison, P. A. & Briggs, D. E. G. (eds.), *Taphonomy: Releasing the Data Locked in the Fossil Record*. 389-409. Plenum Press, New York.

Ludbrook, N. H. (1967) Permian deposits of South Australia and their fauna. *Transactions of the Royal Society of South Australia*, **91**: 65-87.

Madigan, C. T. (1928) Preliminary notes on new evidence as to the age of formations on the north coast of Kangaroo Island. *Transactions of the Royal Society of South Australia*, **52**: 210-216.

Malcolm, S. J. (1985) Early diagenesis of molybdenum in esturine sediments. *Marine Chemistry*, **16**: 213-225.

Mancktelow, N. S. (1990) The structure of the southern Adelaide Fold Belt, South Australia. *Geological Society of Australia, Special Publication*, **16**: 215-229.

Manheim, F. T. & Chan, K. M. (1974) Interstitial waters of Black Sea sediments: new data and review. *American Association of Pertroleum Geologists, Memoir*, **20**: 155-180.

Manspeizer, W. (1985) The Dead Sea Rift: impact of climate and tectonism on Pleistocene and Holocene sedimentation. *Society of Economic Paleontologists and Mineralogists, Special Publication*, **37**: 143-158.

Manton, S. M. (1977) *The Arthropoda: habits, functional morphology and evolution.* Clarandon Press, Oxford. 527 pp.

Martill, D. M. (1988) The preservation of fishes in concretions from the Santanna Formation (Cretaceous) of Brazil. *Palaeontology*, **31**: 1-18.

Martill, D.M. (1989) The Medusa effect: instantaneous fossilisation. *Geology Today*, **5**: 201-205.

Martill, D.M. (1990) Macromolecular resolution of fossilized muscle tissues from an elopomorph fish. *Nature*, **346**: 171-172.

Martill, D.M. & Harper, E. (1990) Critical point drying, a technique for

palaeontologists. *Palaeontology*, **33**: 423-428.

Martill, D. M. & Unwin, D. M. (1989) Exceptionally well preserved pterosaur wing membrane from the Cretaceous of Brazil. *Nature*, **340**: 138-140.

Martill, D.M.; Wilby, P.R. & Williams, N. (1992) Elemental mapping: a technique for investigating delicate phosphatized fossil soft tissues. *Palaeontology*, **35**: 869-874.

Maurer, D. (1967) Filtering experiments on marine pelecypods from Tomales Bay, California. *Veliger*, **9**: 305-309.

McCavley, J. W. & Roy, R. (1974) Controlled nucleation and crystal growth of various $CaCO_3$ phases by the silica gel technique. *American Mineralogist*, **59**: 947-963.

McHenry, B. & Yates, A. (1993) First report of the enegmatic metazoan *Anomalocaris* from the Southern Hemisphere and a trilobite with preserved appendages from the Early Cambrian of Kangaroo Island, South Australia. *Records of the South Australian Museum*, **26:** 77-86.

McKerrow, W. S.; Scotese, C. R. & Brasier, M. D. (1992) Early Cambrian continental reconstructions. *Journal of the Geological Society of London*, **149**: 599-606.

McKinney, M. L. & McNamara, K. J. (1991) Heterochrony: The Evolution of Ontogeny. Plenum Press, New York. 437 pp

McKirdy, D. M. (1967) A preliminary investigation of the alkane hydrocarbon content of two Australian sedimentary rocks. *Honours thesis, University of Adelaide (unpublished)*

McKirdy, D. M. (1971) An organic geochemical study of Australian Cambrian and Precambrian sedimentary rocks. *University of Adelaide MSc. thesis (Unpublished)*.

McNamara, K. J. (1981) Paedomorphism in Middle Cambrian xystridurine trilobites from northern Australia. *Alcheringa*, **5**: 209-224.

McNamara, K. J. (1982) Heterochrony and phylogenetic trends. *Paleobiology*, **8**: 130-

142.

McNamara, K. J. (1983) Progenesis in trilobites. *Special Papers in Palaeontology*, **30**: 59-68.

McNamara, K. J. (1986a) A guide to the nomenclature of heterochrony. *Journal of Paleontology*, **60**: 1-13.

McNamara, K. J. (1986b) The role of heterochrony in the evolution of Cambrian trilobites. *Biological Reviews*, **61**: 121-156.

McNamara, K. J. (1986c) Techniques of exuviation in Australian species of the Cambrian trilobite *Redlichia*. *Alcheringa*, **10**: 403-412.

McNamara, K. J. & Rudkin, D. M. (1984) Techniques of trilobite exuviation. *Lethaia*, **17**: 153-173.

Menzies, R. J.; George, R. Y. & Rowe, G. T. (1973) *Abyssal Environment and Ecology of the Worlds Oceans*. John Wiley & Sons, New York. 488 pp.

Miall, A. D. (1970) Continental marine transition in the Devonian of Prince of Wales Island, Northwest Territories, Canada. *Canadian Journal of Earth Sciences*, **7**: 125-144.

Milnes, A. R.; Compston, W. & Daily, B. (1977) Pre- and syn-tectonic emplacement of Early Palaeozoic granites in south-eastern South Australia. *Journal of the Geological Society of Australia*, **24**: 87-106.

Moore, P. S. (1979) Sedimentology of the Billy Creek Formation (Cambrian, Flinders Ranges) and it's equivalents on the north east coast of Kangaroo Island, South Australia. *University of Adelaide, PhD thesis (Unpublished)*.

Morris, A. W. (1975) Dissolved molybdenum and vanadium in the northeast Atlantic Ocean. *Deep-Sea Research*, **22**: 49-54.

Morse, J. W. (1974) Calculation of diffusive fluxes across the sediment-water interface. *Journal of Geophysical Research*. **79**: 5045-5048.

Morse. J. W. & Mackenzie, F. T. (1990) *Geochemistry of Carbonates*. Elsivier, Amstadam. 707 pp.

Morse, J. W.; Cornwell, J. C.; Arakaki, T.; Lin, S. & Huerta-Diaz, M. (1992). Iron sulfide and carbonate diagenesis in Baffin Bay, Texas. *Journal of Sedimentary Petrology*, **62**: 671-680.

Moulin, E.; Jordens, A. & Wollast, R. (1985) Influence of aerobic bacterial respiration on the early dissolution of carbonates in coastal sediments. *Progress in Belgian Oceanographic Research, Preceedings*. **1985**(March): 196-208.

Mucci, A.; Canvel, R. & Zhong, S. (1989) The solubility of calcite and aragonite in sulfate-free seawater and the seeded growth kinetics and composition of the precipitates at 25$^{0}$ C. *Chemical Geology*, **74**: 309-320.

Müller, K. J. (1979) Phosphaocopine ostracods with preserved appendages from the Upper Cambrian of Sweden. *Lethaia*, **12**: 1-27.

Müller, K. J. (1985) Exceptional preservation in calcareous nodules. Philisophical *Transactions of the Royal Society of London B*, **311**, 67-73.

Müller, K. J. & Hinz-Schallreuter, I. (1994) Palaeoscolecid worms from the Middle Cambrian of Australia. *Palaeontology*, **36**: 549-592.

Müller, K. J. & Walossek, D. (1985) A remarkable arthropod fauna from the Upper Cambrian "Orsten" of Sweden. *Transactions of the Royal Society of Edinburgh, Earth Sciences*, **76**: 161-172.

Murray, J. W.; Balistrieri, L. S. & Paul, B. (1984) The oxidation state of manganese in marine sediments and ferromanganese nodules. *Geochimica et Cosmochimica Acta*, **48**: 1237-1248.

Murray, J. W.; Emerson, S. & Jahnke, R. (1980) Carbonate saturation and the effect of pressure on the alkalinity of interstitial waters from the Guatemala Basin. *Geochimica et Cosmochimica Acta*, **44**: 963-972.

Murray, J. W; Spell, B. & Paul, B. (1983) The contrasting geochemistry of manganese and chromium in the eastern tropical Pacific Ocean. In: Water. C.S. Wong; E.

Boyle; K.W. Bruland & E.D. Goldburg (eds.), *Trace Metals in Sea*. 609-669. Plenum Press, New York.

Murray, J. W.; Jannasch, H. W.; Honjo, S.; Anderson, R. F.; Reesburgh, W. S.; Top, Z.; Friederich, G. E.; Codispoti, L. A. & Izdar, E. (1989) Unexpected changes in the oxic/anoxic interface in the Black Sea. *Nature*, **338**: 411-413.

Nathan, Y. & Sass, E. (1981) Stability relations of apatites and calcium carbonates. *Chemical Geology*, **34**: 103-111.

Nedin, C. (1992) The Palaeontology and Palaeoecology of the Lower Cambrian Emu Bay Shale, Kangaroo Island, South Australia. *The Paleontological Society Special Publication*, **6**: 221.

Nedin, C. (1994) The Emu Bay Shale: a Lower(?) Cambrian fossil Lagerstätte from Kangaroo Island, South Australia. *Australasian Palaeontological Convention '94, Abstracts & Programme*, p. 44.

Nedin, C. (1995) The Emu Bay Shale, a Lower Cambrian fossil Lagerstätte, Kangaroo Island, South Australia. *Association of Australiasian Palaeontologists, Memoir*, **18**: 31-40.

Newell, N. D. (1955) Depositional fabric in Permian reef limestones. *Journal of Geology*, **63**: 301-309.

Nilson, T. H. & McLaughlin, R. J. (1985) Comparison of tectonic framework and depositional pattern of the Hornmelen Strike-slip Basin of Norway and the Ridge and Little Sulphur Creek strike-slip Basins of California. *Society of Economic Paleontologists and Mineralogists, Special Publication*, **37**: 79-103.

Öpik, A. A. (1958) The Cambrian trilobite *Redlichia*: organisation and generic concept. *Bureau of Mineral Resources, Geology and Geophysics, Bulletin*, **42**: 1-50.

Öpik, A. A. (1975a) Templetonian and Ordian xystridurid trilobites of Australia. *Bureau of Mineral Resources, Geology and Geophysics, Bulletin*, **121**: 1-84.

Öpik, A. A. (1975b) Cymbric Vale fauna of New South Wales and Early Cambrian biostratigraphy. *Bureau of Mineral Resources, Geology and Geophysics,*

*Bulletin*, **159**: 1-78.

Orlowski, S. (1985) A trilobite with North American affinity in the Lower Cambrian of Poland. *Journal of Paleontology*, **59**: 975-978.

Oschmann, W. (1988) Kimmeridge Clay sedimentation-a new cyclic model. *Palaeogeography, Palaeoclimatology, Palaeoecology*. **65**: 217-251.

Oschmann, W. (1991) Anaerobic-poikiloaerobic-aerobic: a new facies zonation for modern and ancient neritic redox facies. In: G. Einsele, G.; Ricken, W. & Seilacher, A. (eds.), *Cycles and events in Stratigraphy*. 565-571. Springer-Verlag, Berlin.

Oschmann, W. (1993) Environmental oxygen fluctuations and the adaptive response of marine benthic organisms. *Journal of the Geological Society of London*, **150**: 187-191.

P'an Kiang (1957) On the discovery of Homopoda from South China. *Acta Palaeontologica Sinica*, **5**: 523-526.

Parrish, J. T. (1982) Upwelling and petroleum source beds, with reference to the paleozoic. *American Association of Petroleum Geologists, Bulletin*, **66**: 750-774.

Pederson, T. F. (1988) Late Pleistocene carbon enhancements in the Panama Basin, frequency and causes. *Chemical Geology*, **70**: 111.

Pederson, T. F. & Calvert, S. E. (1990) Anoxia vs. productivity: what controls the formation of organic-carbon-rich sediments and sedimentary rocks? *American Association of Petroleum Geologists, Bulletin*, **74**: 454-466.

Pederson, T. F. & Price, N. B. (1982) The geochemistry of manganese carbonate in Panama Basin sediments. *Geochimica et Cosmochimica Acta*, **46**: 59-68.

Perkins, C. & Walshe, J. L. (1993) Geochronology of the Mount Read Volcanics, Tasmania, Australia. *Economic Geology*, **88**: 1176-1197.

Perkins, R. D. & Tsentas, C. I. (1976) Microbal infestations of carbonate substrates

planted on the St. Croix shelf, West Indies. *Geological Society of America, Bulletin*, **87**: 1615-1628.

Peterson, C. H. & Andre, S. M. (1980) An experimental analysis of interspecific competiotion amongst marine filter-feeders in a soft-sediment environment. *Ecology*, **61**: 129-139.

Pilipchuk, M. F. & Volkov, I. I. (1974) Behavior of molybdenum in processes of sediment formation and diagenesis in the Black Sea. *American Association of Pertroleum Geologists, Memoir*, **20**: 542-553.

Pinna, G. (1985) Exceptional preservation in the Jurassic of Osteno. *Philosophical Transactions of the Royal Society of London*, **B311**: 171-180.

Piper, D. Z. (1988) The metal oxide fraction of pelagic sediments in the equatorial North Pacific Ocean: a source of metals in ferromanganese nodules. *Geochimica et Cosmochimica Acta*, **52**: 2127-2145.

Piper, D. Z. (1994) Seawater as the source of minor elements in black shales, phosphorites and other sedimentary rocks. *Chemical Geology*, **114**: 95-114.

Plint, A. G. & van de Poll, H. W. (1984) Structural and sedimentary history of the Quaco Head area, southern New Brunswick. *Canadian Journal of Earth Science*, **21**: 753-761.

Plotnick, R. E. (1986) Taphonomy of a modern shrimp: Implications for the arthropod fossil record. *Palaios*, **1**: 286-293.

Pocock, K. J. (1964) *Estaingia*, a new trilobite genus from the Lower Cambrian of South Australia. *Palaeontology*, **7**: 458-471.

Pocock, K. J. (1967) An abherrant group of trilobites from the Lower Cambrian of South Australia: systematics, functional morphology, segmentation and growth. *University of Adelaide, PhD. thesis (unpublished).*

Pocock, K. J. (1970) The Emuellidae, a new family of trilobites from the Lower Cambrian of South Australia. *Palaeontology*, **13**: 522-562.

Poulson, C. (1927) The Cambrian Ozarkian and Canadian faunas of northwest Greenland. Meddelelser om Grønland, 70: 233-343.

Presley, B. J. (1969) *Chemistry of interstitial water from marine sediments*. Ph.D. thesis, University of California, Los Angeles. 225p.

Prévôt, L. E. & Lucas, J. (1990) Phosphate. In: Briggs, D. E. G. & Crowther, P.R. (eds.), *Palaeobiology: A Synthesis*. 256-257. Blackwell Scietific, Cambridge.

Quan Yi & Bengtson, S. (1989) Palaeontology and biostratigraphyof the Early Cambrian Meisshucunian Stage in Yunnan province, South China. *Fossils and Strata*, **24**: 1-156,

de Raaf, J. F. M.; Boetsma, J. R. & van Gelder, A. (1977) Wave generated structures and sequences from a shallow marine succession. Lower Carboniferous, County Cork, Ireland. *Sedimentology*, **4**: 1-52.

Raiswell, R. & Berner, R. A. (1985) Pyrite formation in euxinic and semi-euxinic sediment. *American Journal of Science*. **285**: 710-724.

Ramsköld, L. & Hou Xianguang (1991) New Early Cambrian animal and onychophoran affinities of enegmatic metazoans. *Nature*, **351**: 225-228.

Rayment, R. A. (1971) *Introduction to Quantative Paleoecology*. Elsevier, Amsterdam. 226 pp.

Raymond, P. E. (1920) The appendages, anatomy, and relationships of trilobites. Memoirs of the Connecticut Academy of Arts and Sciences, 16: 1-97.

Reading, H. G. (1980) Characteristics and recognition of strike-slip fault systems. *Special Publication of the International Association of Sedimentologists*, **4**: 7-26.

Reis, O.M. (1888) Die Coelacanthinen, mit besanderer Berücksichtgung der Gattungen des weissen Jura Bayerns. *Palaeontographica*, **35**: 1-96.

Reis, O.M. (1893) Untersuchungen uber die Petrificirung der Muskulatur. *Archiv fur Mikroskopische Anatomie*, **41**: 492-584.

Resser, C.E. & Howell, B.F. (1938) Lower Cambrian Olenellus zone of the Appalachians. *Geological Society of America, Bulletin*, **49**: 195-248.

Revsbech, P. N. (1983) In situ measurements of oxygen profiles of sediments by use of oxygen microelectrodes In: Gnairer, E. & Forstner, H. (eds.), *Polarographic Oxygen Sensors*. 265-273. Springer-Verlag, Berlin.

Revsbech, P. N.; Jørgensen, B. B. & Blackburn, T. H. (1980) Oxygen in the sea bottom measured with a microelectrode. *Science*, **207**: 1355-1356.

Rhoads, D. C. & Morse, I. W. (1971) Evolutionary and ecologic significance of oxygen-deficient marine basins. *Lethaia*, **4**: 413-428.

Rhoads, D. C. & Pannella, G. (1970) The use of molluscan shell growth patterns in ecology and paleoecology. *Lethaia*, **3**: 143-161.

Rhoads, D. C. & Young, D. K. (1970) The influence of deposit feeding organisms on bottom-sediment stability and trophic structure. *Journal of Marine Research*, **28**: 150-178.

Richards, F. A. (1965) Anoxic basins and fjords. In: Riley, J. P. & Skirrow, G. (eds.), *Chemical Oceanography*. 611-646. Academic Press, New York.

Riggs, S. R. (1982) Phosphatic bacteria in the Neogene phosphorites of the Atlantic coastal plain-continental shelf system. *IGCP Project 156 "Phosphorites" Newsletter*, **11**: 34.

Robison, R. A. (1984) New occurrences of the unusual trilobite Naraoia from the Cambrian of Idaho and Utah. *University of Kansas, Paleontological Contributions*, **112**: 1-8.

Robison, R. A. (1991) Middle Cambrian biotic diversity: examples from four Utah Lagerstätten. In: Simonetta, A. M. & Conway Morris, S. (eds.), *The Early Evolution of Metazoa and the Significance of Problematic Taxa*. 57-74. Cambridge University Press, Cambridge.

Robison, R. A. & Richards, B. C. (1981) Larger bivalved arthropods from the Middle

Cambrian of Utah. *The University of Kansas, Paleontological Contributions*, **106**: 1-19.

Røe, S. L. & Steel, R. J. (1985) Sedimentation, sea-level rises and tectonics at the Triassic-Jurassic boundary (Statfjord Formation), Tampen Spur, Northern North Sea. *Journal of Petroleum Geology*, **8**: 163-186.

Rolfe, W. D. I. (1969) Phyllocardia. In: Moore, C. (ed.), *Treatise on Invertebrate Paleontology, Pt. R, Arthropoda*. R296-R331. The University of Kansas Press, Lawrence.

Runnegar, B. (1982) Oxygen requirements, biology and phylogenetic significance of the late Precambrian worm *Dickinsonia*, and the evolution of the burrowing habit. *Alcheringa*, **6**: 223-239.

Rust, B. R. (1978) Depositional models for braided alluvium. *Memoir of the Canadian Society of Petroleum Geologists*, **5**: 605-625.

Ruttenburg, K. C. & Berner, R. A. (1993) Authigenic apatite formation and burial in sediments from non-upwelling, continental margin environments. *Geochimica et Cosmochimica Acta*, **57**: 991-1007.

Sageman, B. B. (1989) The benthic boundary biofacies model: Harland Shale Member, Greehorn Formation (Cenomanian), Western Interior, North America. *Palaeogeography, Palaeoclimatology, Palaeoecology*, **74**: 87-110.

Sageman, B. B.; Wignall, P. B. & Kauffman, E.G. (1991) Biofacies models for oxygen-deficient facies in epicontinental seas: Tool for palaeoenvironmental analysis. In: Einsele, G.; Ricken, W. & Seilacher, A. (eds.), *Cycles and events in Stratigraphy*. 542-564. Springer-Verlag, Berlin.

Santschi, P. H.; Bower, P.; Nyffeler, U. P.; Azevedo, A. & Broecker, W. S. (1983) Estimates of the resistance to chemical transport posed by the deep-sea boundary layer. *Limnology and Oceanography*, **28**: 899-912.

Sarmiento, J. L.; Herbet, T. & Toggweiler, J. R. (1988) Mediterranean nutrient balance and episodes of anoxia. *Global Biochemical Cycles*, **2**: 427-444.

Savilov, A. I. (1959) Biological aspects of the bottom fauna groupings of the North Okotok Sea. *Transactions of the Institute of Oceanology*, **20**: 67-136.

Savrda, C. E. & Bottjer, D. J. (1987) The exaerobic zone, a new oxygen deficient marine biofacies. *Nature*. **327**: 54-56.

Savrda, C. E. & Bottjer, D. J. (1991) Oxygen-related biofacies in marine strata: an overview and update. *Geological Society of London, Special Publication*, **58**: 201-220.

Savrda, C. E.; Bottjer, D. J. & Gorsline, D. S. (1984) Development of a comprehensive oxygen-deficient marine bioface model: evidencefrom Santa Monica, San Padro and Santa Barbara Basins, California continental borderland. *American Association of Petroleum Geologists, Bulletin*, **68**: 1179-1192.

Scharpf, L. G. Jr. (1974) Transformations of naturally occurring organoposphorus compounds in the environment. In: Griffith, J. D.; Beeton, A.; Spencer, J. M. & Mitchel, D. T. (eds.), *Environmental Phosphorus Handbook*. 393-412. Wiley, New York.

Schlanger, S. O. & Jenkyns, H. C. (1976) Cretaceous oceanic anoxic events: causes and consequences. *Geologie en Mijnbouw*, **55**: 79-184.

Schopf, J. W.; Hays, J. M. & Walker, M. R. (1983) Evolution of Earth's earliest ecosystems: recent progress and unsolved problems. In: Schopf, J. W. (ed.), *The Earth's Earliest Biosphere: Its Origin and Evolution*. 361-384. Princeton University Press, Princeton.

Schultze, H-P. (1989) Three-dimensional muscle preservation in Jurassic fishes of Chile. *Revista Geologica de Chile*, **16**: 183-215.

Scotese, C. R. (1986) Phanerozoic reconstructions: a new look at the assembly of Asia. *University of Texas Institute for Geophysics, Technical Report*, **66**.

Seccombe, P. K.; Spry, P. G.; Both, R. A.; Jones, M. T. & Schiller, J. C. (1985) Base metal mineralization in the Kanmantoo Group, South Australia: a regional sulphur isotope study. *Economic Geology*, **88**: 1824-1841.

Seilacher, A. (1990) Taphonomy of Fossil-Lagerstätten. In: Briggs, D. E. G. & Crowther, P. R. (eds.), *Palaeobiology, a synthesis*. 266-270. Blackwell, Oxford.

Seilacher, A.; Reif, W-E. & Westphal, F. (1985) Sedimentological, ecological and temporal patterns of fossil Lagerstätten. *Philosophical Transactions of the Royal Society of London*, **B311**: 5-23.

Shaffer, G. (1986) Phosphate pumps and shuttles in the Black Sea. *Nature*, **321**: 515-517.

Shaw, A. B. (1957) Quantitative trilobite studies II. Measurement of the dorsal shell of non-agnostidean trilobites. *Journal of Paleontology*, **31**: 193-207.

Shaw, T. J.; Gieskes, J. M. & Jahnke, R. A. (1990) Early diagenesis in differing depositional environments: The response of transition metals in pore water. *Geochimica et Cosmochimica Acta*, **54**: 1233-1246.

Shimmield, G. B. & Price, N. B. (1986) The behavoir of molybdenum and manganese during early sediment diagenesis - offshore Baja California, Mexico. *Marine Chemistry*, **19**: 261-280.

Simpson, G. G. (1969) The first three billion years of community evolution. *Brookhaven Symposium in Biology*, **22**: 162-177.

de Sitter, L. U. (1964) *Structural Geology*. McGraw Hill, New York. 551 pp.

Smart, P. L.; Dawans, J. M. & Whitaker, F. (1988) Carbonate dissolution in a modern mixing zone. *Nature*, **335**: 811-813.

Smith, S. V. (1984) Phosphorus versus nitrogen limitation in the marine environment. *Limnology and Oceanography*, **29**: 1149-1160.

Smith, R. & Kamerling, P. (1969) Geological framework of the Great Australian Bight. *Journal of the Australian Petroleum Exploration Association*, **9**: 60-66.

Sprigg, R. C. (1952) Sedimentation in the Adelaide Geosyncline and the formation of the continental terrace. *Sir Douglas Mawson Anniversary Volume, University of*

*Adelaide*: 153-159.

Sprigg, R. C. (1955) The Point Marsden Cambian Beds, Kangaroo Island, South Australia. *Transactions of the Royal Society of South Australia*, **78**: 165-168.

Sprigg, R. C.; Campana, B. & King, D. (1954) Kingscote map sheet, Geological Atlas of South Australia 1:253,440 series. *Geological Survey of South Australia.*

Steel, R. J. & Gloppin, T. G. (1989) Late Caledonian (Devonian) basin formation, western Norway: signs of strike-slip tectonics during infilling. *Special Publication of the International Association of Sedimentologists*, **4**: 79-103.

Stoessell, R. K. (1992) Effects of sulfate reduction on $CaCO_3$ dissolution and precipitation in mixing-zone fluids. *Journal of Sedimentary Petrology*, **62**: 873-880.

Stuart, W. J. & Johnson, J. E. (1970) Final report on the geology of Kangaroo Island, O.E.L. 24, South Australia. *Beach Petroleum N.L.* (unpublished)

Stuart, W. J. & von Sanden, A. T. (1972) Palaeozoic history of the St. Vincent Gulf region, South Australia. *Australian Petroleum Exploration Association Journal*, **12**: 9-16.

Styles, F. L. (1985) Calcium carbonate solubility in marine sediments: evidence for equilibrium and non-equilibrium behavior. *Geochimica et Cosmochimica Acta*, **49**: 877-888.

Summerhayes, C. P. (1969) Marine Geology of the New Zealand subantarctic sea floor. *Memoir of the New Zealand Oceanographic Institute*, **50**: 1-92.

Sunagawa, I. (1981) Characteristics of crystal growth in nature as seen from the morphology of mineral crystals. *Bulletin Minéalogie*, **104**: 81-87.

Sunagawa, I. (1982) Morphology of crystals in relation to growth conditions. *Estudios Geológicos*, **38**: 127-134.

Tate, R. (1883) The botany of Kangaroo Island. *Transactions of the Royal Society of South Australia*, **6**: 116-176.

Taylor, S. R. & McLennan, S. M. (1985) *The Continental Crust: its composition and Evolution*. Blackwell, Oxford. 312 pp.

Thompson, B. P. (1969) Palaeozoic Era. In: Parkin, L. W. (ed.), *Handbook of South Australian Geology*. 97-108. Geological Survey of South Australial, Adelaide.

Thomson, J.; Higgs, N. C.; Croudace, I. W.; Colley, S. & Hydes, D. J. (1993) Redox zonation of elements at an oxic/post-oxic boundary in deep-sea sediments. *Geochimica et Cosmochimica Acta*, **57**: 579-595.

Thorson, G. (1966) Some factors influencing the recruitment of marine benthic communities. *Netherlands Journal of Sea Research*, **3**: 267-293.

Todd, J. F.; Elsinger, R. J. & Moore, W. S. (1988) The distribution of uranium and thorium isotopes in two anoxic fjords: Framvaren Fjord (Norway) and Saanich Inlet (British Columbia). *Marine Chemistry*, **23**: 393-415.

Trefry, J. H. & Presley, B. J. (1982) Manganese fluxes from Mississippi Delta sediments. *Geochimica et Cosmochimica Acta*, **46**: 1715-1726.

Turpaeva, E. P. (1959) Food interrelationships of dominant species in marine benthic biocoenoses. *Transactions of the Institute of Oceanology*. **20**: 137-148.

Urban, E. R. Jr. & Kirchman, D. L. (1992) Effect of kaolinite clay on the feeding activity of the eastern oyster *Crassostrea virginica* (Gmelin). *Journal of Experimental Marine Biology and Ecology*, **160**: 47-60

Valantine, J. W. (1973) *Evolutionary Paleoecology of the Marine Biosphere*. Prentice-Hall, New Jersey. 511 pp.

Vetter, R. D.; Powell, M. A. & Somero, G. N. (1991) Metazoan adaptions to hydrogen sulfide. In: Bryant, C. (ed.), *Metazoan life without oxygen*. 109-128. Chapman and Hall, London.

Vine, J. D. & Tourtelot, E. B. (1970) Geochemistry of black shale deposits - a summary. *Economic Geology*, **65**: 253-272.

Viohl, G. (1990) Solnhofen Lithographic Limestones. In: Briggs, D. E. G. & Crowther, P. R. (eds.), *Palaeobiology: A Synthesis*. 285-289. Blackwell Scientific, Cambridge.

Vogel, S. (1983) *Life in Moving Fluids*. Willard Grant Press, Boston. 352 pp.

Wade, A. (1915) The supposed oil-bearing areas of South Australia. *South Australia Geological Survey, Bulletin*, **4**: 1-54.

Walcott, C. D. (1912) Cambrian geology and palaeontology. II. Middle Cambrian Branchiopoda, Malacostraca, Trilobita and Merostomata. *Smithsonian Miscellaneous Collections*, **57**: 145-228.

Walossek, D.; Hinz-Schallreuter, I.; Shergold, J. H. & Müller, K. J. (1993) Three dimentional oopreservation of arthropod integument from the Middle Cambrian of Australia. *Lethaia*, **26**: 7-15.

Wanty, R. B. & Goldhaber, M. B. (1992) Thermodynamics and kinetics of reactions involving vanadium in natural systems: accumulation of vanadium in sedimentary rocks. *Geochimica et Cosmochimica Acta*, **56**: 1471-1483.

Watts, T. R. & Gausden, J. (1966) Stansbury West No. 1 Well - well completion report. Beach Petroleum N. L. *South Australia Mines Department Open File 656. (unpublished)*

Wedepohl, K. H. (1971) Environmental influences on the chemical composition of shales and clays. In: Ahrens, L. H.; Press, F.; Runcorn, S. K. & Urey, H. C. (eds.), *Physics and Chemistry of the Earth , Vol 8*. 305-334. Pergamon Press, Oxford.

Werner, E. E. & Gilliam, J. F. (1984) The ontogenetic niche and species interactions in size-structured populations. *Annual Review of Ecology and Systematics*, 15: 393-425.

Whiteaves, J. F. (1892) Description of a new genus and species of phyllocarid crustacean from the Middle Cambrian of Mount Stephen, British Columbia. *Canadian Records of Science*, **5**: 205-208.

Whitehouse, F. D. (1939) The Cambrian faunas of north-eastern Australia. Part 3, the polymerid trilobites. *Memoirs of the Queensland Museum*, **11**: 179-282.

Whittard, W. F. (1953) *Palaeoscolex piscatorum* gen. et sp. nov., a worm from the Tremadocian of Shropshire. *Quarterly Journal of the Geological Society of London*, **109**: 125-135.

Whittington, H. B. (1957) The ontogeny of trilobites. *Biological Reviews*, **32**: 407-440.

Whittington, H. B. (1971a) The Burgess Shale: history of research and preservation of fossils. *Proceedings of the North American Paleontological Convention*, **1**: 1170-1201.

Whittington H. B. (1971b) Redescription of *Marella splendens* (Trilobitoidia) from the Burgess Shale, Middle Cambrian, British Columbia. *Philosophical Transactions of the Royal Society of London*, **B290**: 409-443.

Whittington, H. B. (1977) The Middle Cambrian trilobite *Naraoia*, Burgess Shale, British Columbia. *Philosophical Transactions of the Royal Society of London*, **B290**: 409-443.

Whittington, H. B. (1980) The significance of the fauna of the Burgess Shale, Middle Cambrian, British Columbia. *Proceedings of the Geological Association*, **91**: 127-148.

Whittington, H. B. (1988) Hypostomes and ventral cephalic sutures in Cambrian trilobites. *Palaeontology*, **31**: 577-609.

Whittington, H. B. (1990) Articulation and exuviation in Cambrian trilobites. *Philosophical Transactions of the Royal Society of London*, **B329**: 27-46.

Whittington, H. B. & Briggs, D. E. G. (1985) The largest Cambrian animal *Anomalocaris*, Burgess Shale, British Columbia. *Philosophical Transactions of the Royal Society of London*, **B309**: 569-609.

Wignall, P. B. (1990a) Benthic palaeoecology of the Late Jurassic Kimmeridge Clay of England. *The Palaeontological Association, Special Papers in Palaeontology*, **43**: 1-74.

Wignall, P. B. (1990b) Observations on the evolution and classification of dysaerobic communities. *The Paleontological Society, Special Publication*, **5**; 99-111.

Wignall, P. B. (1993) Distinguishing between oxygen and substrate control in fossil benthic assemblages. *Journal of the Geological Society of London*, **150**: 193-196.

Wilde, P.; Chen Junyang; Stachowitsch, M. & Erdtmann B. D. (1990a) Anoxitrophy and its consequences in the Chengjiang fauna - Lower Cambrian of China: Analog in modern anoxic events in the Adriatic. *Geological Society of America, Abstract with Programs*, **28**: 196.

Wilde, P.; Quinby-Hunt, M. S. & Berry, W. B. N. (1990b) Vertical advection from oxic or onoxic water from the main pycnocline as a cause of rapid extinction or rapid radiations. In: Kaufman, E. G. & Walliser, O. H. (eds.), *Extinction Events in Earth History*. 85-98. Springer Verlag, Berlin.

Wilby, P.R. & Martill, D.M. (1992) Fossil fish stomachs: a microenvironment for exceptional preservation. *Historical Biology*, 6: 25-36.

Wyrtki, K. (1962) The oxygen minima in relation to ocean circulation. *Deep Sea Research*, **9**: 11-24.

Zeigler, A. M.; Scortese, C. R.; McKerrow, W. S. & Johnson, M. E. (1979) Paleozoic paleogeography. *Annual Review of Earth and Planetary Sciences*, **7**: 473-502.

Zhang Wentang & Hou Xianguang (1985) Preliminary notes on the occurrence of the unusual trilobite *Naraoia* in Asia. *Acta Palaeontologica Sinica*, **24**: 591-595. [In Chinese with English summery]

Zhang Wentang & Jell, P. A. (1987) *Cambrian trilobites of North China. Chinese trilobites housed in the Smithsonian Institute*. Scientific Press, Beijing. 459 pp.

Zhang Wentang; Lu Yanhou; Zhu Zhaoling; Qian Yi; Lin, H.; Zhou Zhiyi; Zhang Sangui & Yuan Jinliang (1980) Cambrian trilobite faunas of southwest China. *Acta Palaeontographica Sinica, Series B*, **16**: 1-497. [Chinese with English summary]

Zhao Yuan-long, Yuan Jin-liang, Huang You-zhuang; Mao jia-ren; Qian Yi; Zhang Zheng-hua & Gong Xian-ying (1994) Middle Cambrian Kaili Fauna in Taijiang, Guizhou. *Acta Palaeontologica Sinica*, **33**: 263-271.

Zhuravlev, A. Y. & Gravestock, D. I. (1994) Archaeocyaths from Yorke Peninsula, South Australia and archaeocyathan Early Cambrian zonation. *Alcheringa*, **18**: 1-55.

de Zwaan, A. (1991) Molluscs. In: Bryant, C. (ed.), *Metazoan life without oxygen*. 186-217. Chapman and Hall, London.

# APPENDIX 1

Sedimentary log of the Emu Bay Shale Lagerstätte at Big Gully, cliff section. Descriptions include dominant fossils visible in outcrop. For an analysis of fossil distribution throughout the Lagerstätte, see section 6.4 and Figs. 6.1 - 6.4.

C = Claystone

Sl = Siltstone

FS = Fine Sand

MS = Medium Sand

CS = Coarse Sand

G = Gravel

CG = Conglomerate

**Formation:** Emu Bay Shale

**Section:** Big Gully Cliff Section 0.0 - 0.5m

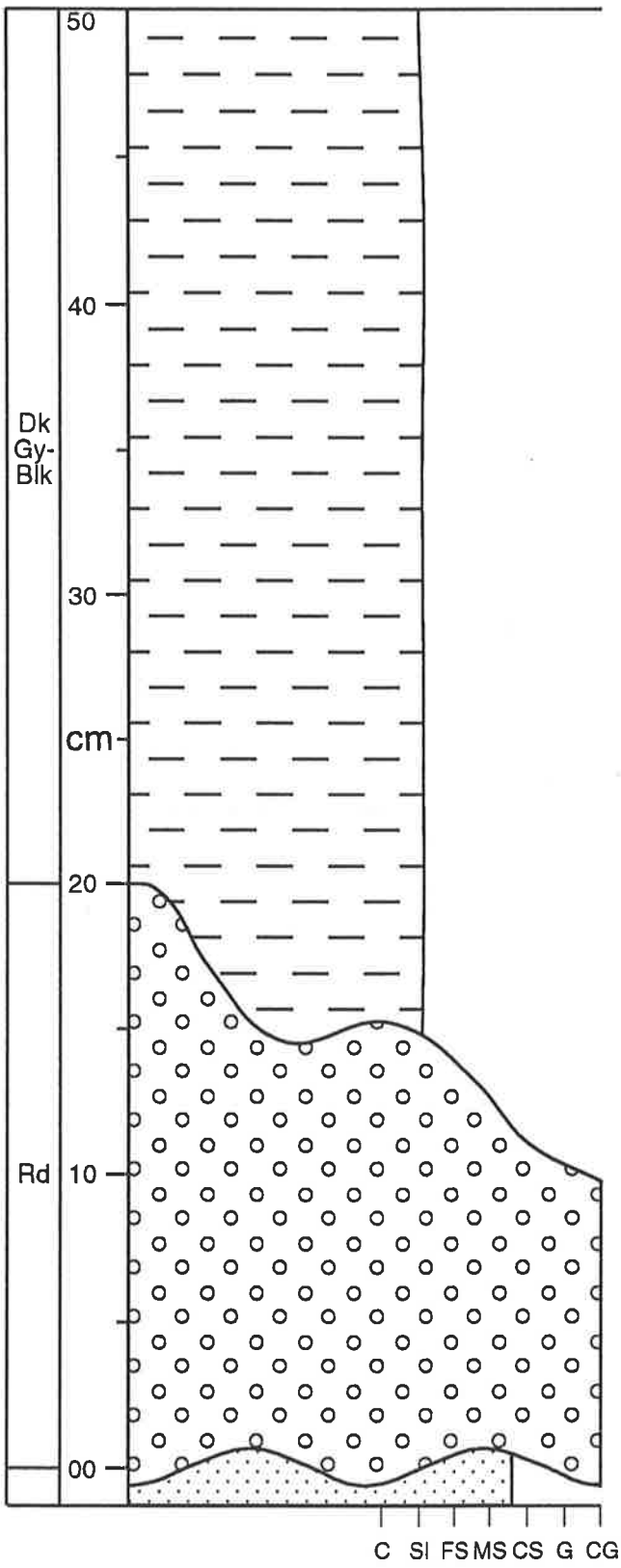


## Description

**Massive siltstone**: dark grey to commonly black, weathers green, sandy in part, micaceous, calcareous. No fossils apparent.

**Massive siltstone**: dark grey to black, weathers green, calcareous, very micaceous in part, occasionally sandy, grading to occasional to rare very fine to fine grained, sandstone stringers with rare basal granule layers. Rarely fossiliferous, fossils occuring - *Redlichia takooensis*.

**Conglomerate**: red, medium grained ferruginous sandstone matrix, clasts of lithified siltstone, granule-pebble sized clasts of micrite, quartzite and granitic gneiss, well cemented with ferruginous cement, calcarious in part, hard.

**Formation:** Emu Bay Shale

**Section:** Big Gully Cliff Section 0.5 - 1.0m

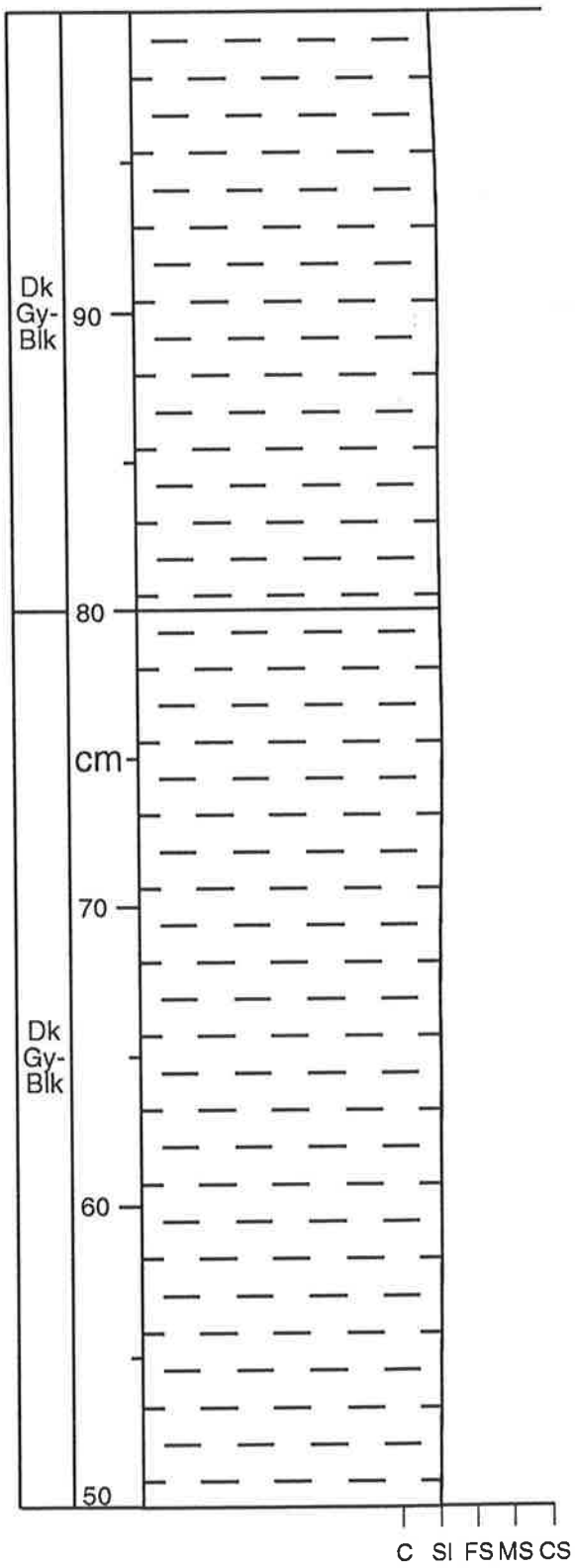


## Description

**Massive siltstone**: dark grey to commonly black, weathers green, rare orange stain, calcareous, micaceous, arenaceous in part. rarely fossiliferous, fossils present - *Redlichia takooensis* and *Isoxys communis*.

**Massive siltstone**: dark grey to black, weathers green, argillaceous in part, calcareous, commonly micaceous, rare very fine to fine grained sandstone stringers. Rarely fossiliferous, fossils occurring - *Redlichia takooensis*.

**Formation:** Emu Bay Shale

**Section:** Big Gully Cliff Section 1.0 - 1.5m

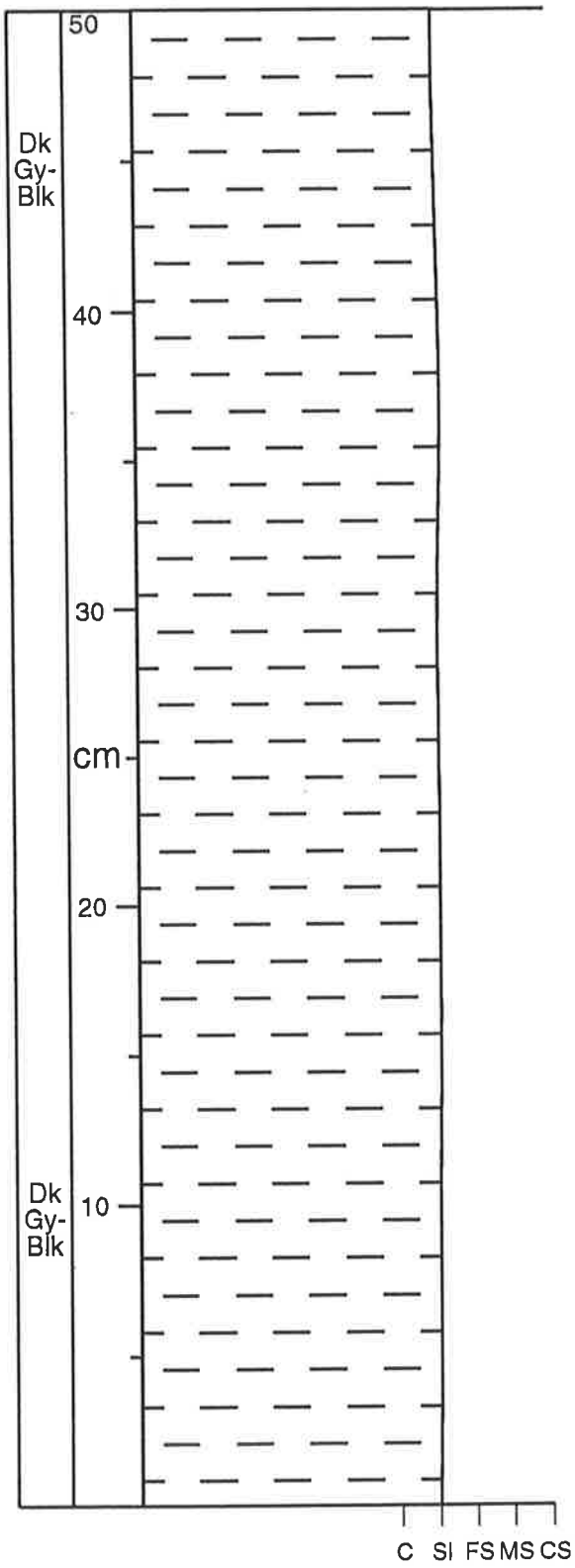


**Description**

**Massive siltstone**: dark grey to black, weathers green, micaceous, calcareous, laminated in part, arenaceous with rare very fine sandstone stringers. Rarely fossiliferous, fossils occurring - *Redlichia takooensis*.

**Formation:** Emu Bay Shale

**Section:** Big Gully Cliff Section 1.5 - 2.0m

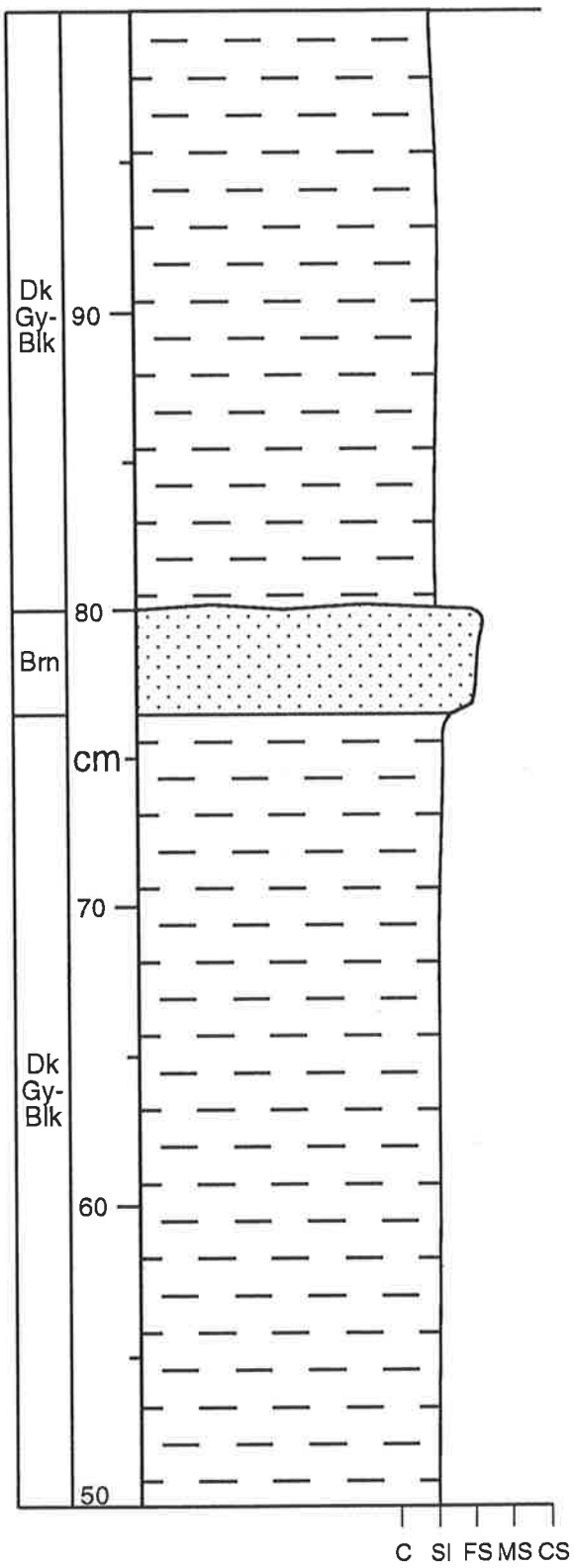


## Description

**Massive siltstone**: dark grey to black, weathers green, occasionally weathers black, calcareous, micaceous, arenaceous in part. Rarely fossiliferous, fossils occurring - *Redlichia takooensis*.

**Sandstone**: brown, fine grained, moderately sorted, commonly argillaceous, grading to siltstone, commonly micaceous, slightly calcareous, sub-round grains, interlaminated with siltstone at the base, undulose to rippled top. Non fossiliferous.

**Massive siltstone**: dark grey to black, weathers green, occasionally weathers to a black friable condition, calcareous, micaceous, arenaceous, in part grading to very fine to fine grained sandstone stringers. No fossils apparent.

**Formation:** Emu Bay Shale

**Section:** Big Gully Cliff Section 2.0 - 2.5m

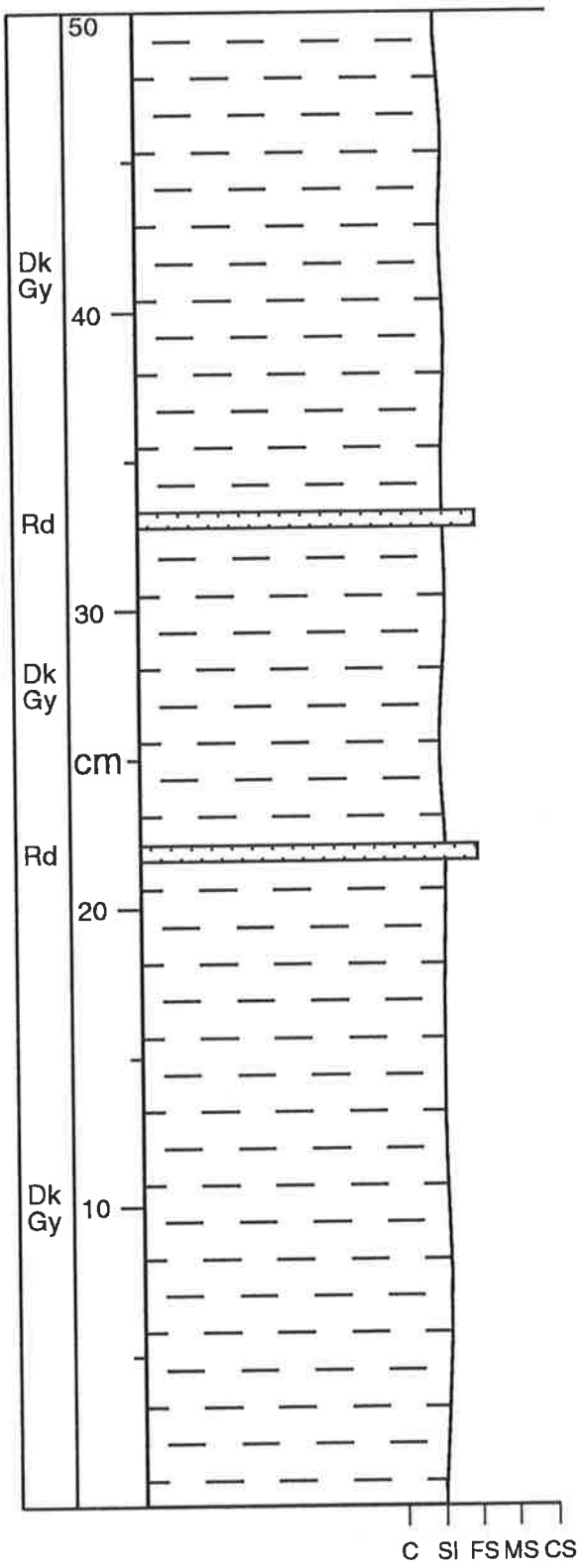


## Description

**Massive siltstone**: dark grey, weathers reddish-brown, commonly micaceous, calcareous, arenaceous in part, rare silty to very fine grained sandstone, ferruginous laminations. Fossils occurring - *Redlichia takooensis*, *Husaspis bilobata*, *Myoscolex ateles*, *Isoxys communis*.

**Sandstone**; red, fine grained, moderate sorting, argillaceous, common ferrruginous cement and stain, micaceous, calcareous in part. Non fossiliferous.

**Massive siltstone**: dark grey, weathers reddish-brown, micaceous, calcareous, commonly arenaceous with interlaminations of brown very fine sandstone. Fossils occurring - *Redlichia takooensis*, *Husaspis bilobata.*

**Sandstone**; red, fine grained, moderate sorting, argillaceous, common ferrruginous cement and stain, micaceous, calcareous in part. Non fossiliferous.

**Massive siltstone**: dark grey, weathers reddish-brown, commonly micaceous, calcareous, arenaceous rarely grading to very fine sandstone stringers. Rarely fossiliferous, fossils occurring, *Redlichia takooensis*, *Hsuaspis bilobata*, *Isoxys communis*.

**Formation:** Emu Bay Shale

**Section:** Big Gully Cliff Section 2.5 - 3.0m

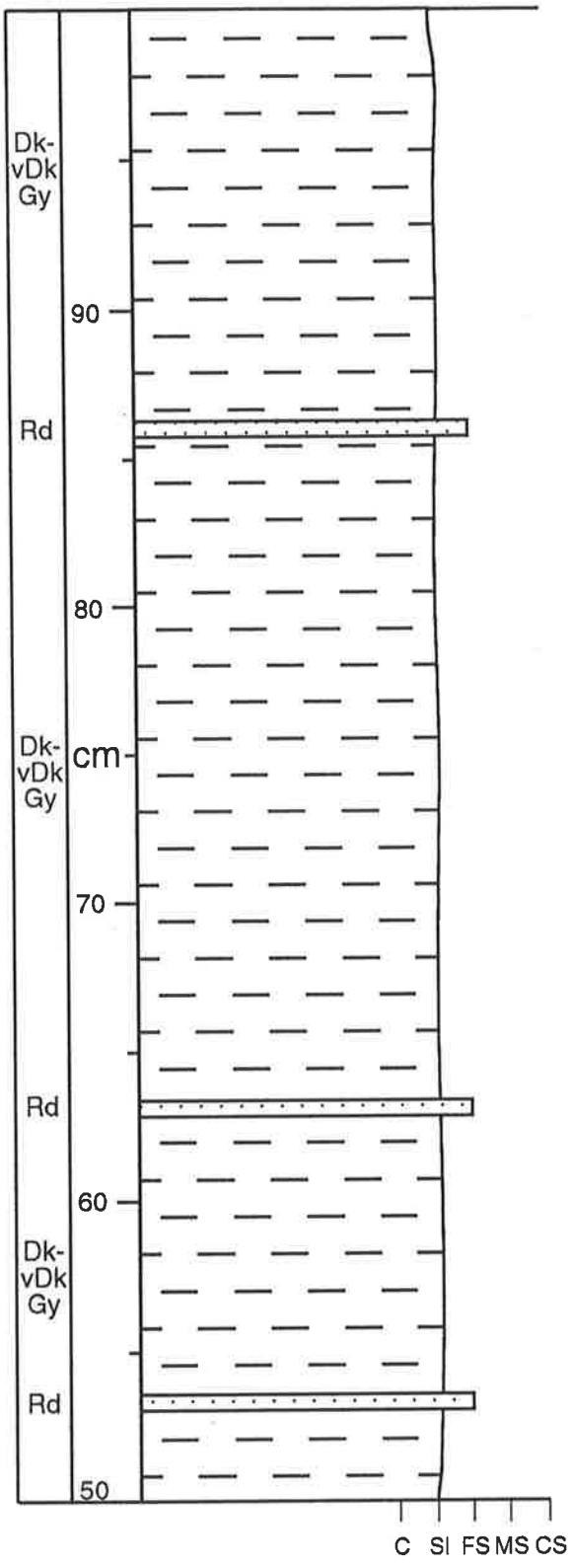


## Description

**Massive siltstone**: Dark grey to black in part, micaceous, calcareous, argillaceous, arenaceous in part. Fossils occurring - *Myoscolex ateles*, *Redlichia takooensis*.

**Sandstone**: red, fine grained, moderately sorted, ferruginous cement in part, calcareous. Non fossiliferous.

**Massive siltstone**: Dark grey to very dark grey in part, micaceous, calcareous, argillaceous, arenaceous in part. Fossils occurring - *Myoscolex ateles*.

**Sandstone**: red, fine grained, moderately sorted, ferruginous cement in part, calcareous. Non fossiliferous.

**Sandstone**: red, fine grained, moderately sorted, ferruginous cement in part, calcareous. Non fossiliferous.

**Formation:** Emu Bay Shale

**Section:** Big Gully Cliff Section 3.0 - 3.5m

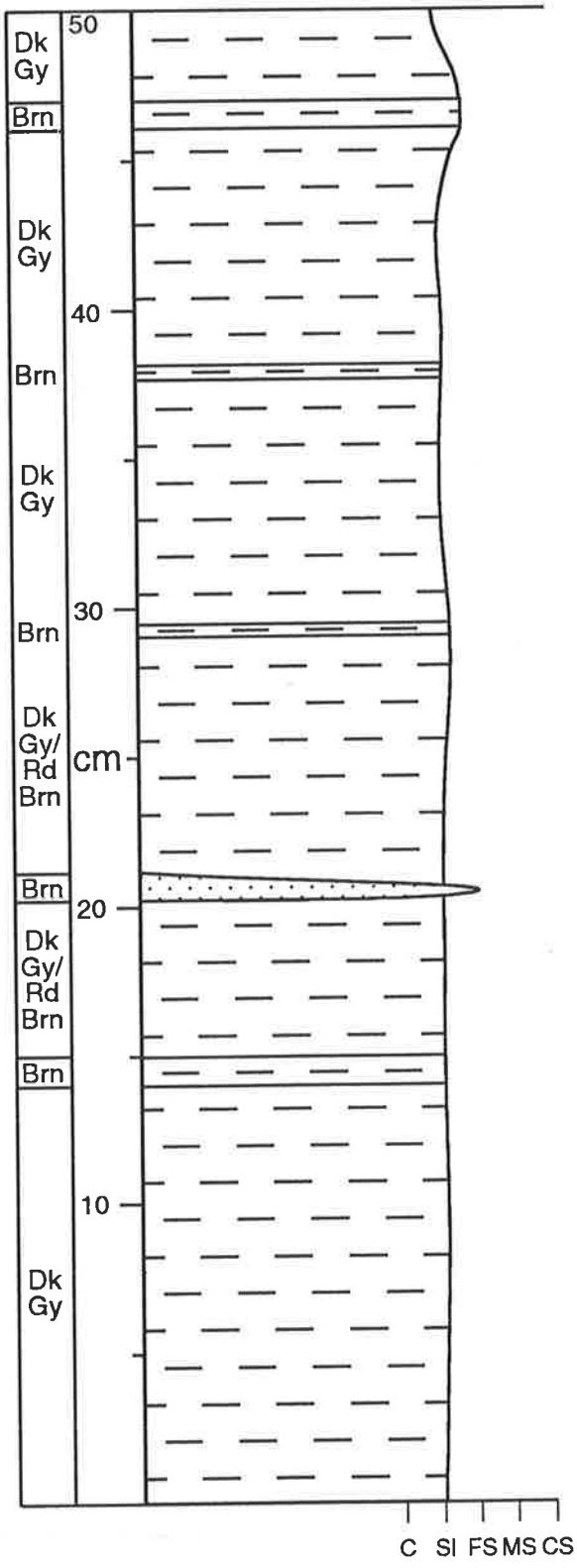


## Description

**Siltstone**: interlaminated brown to red brown, calcareous, micaceous, arenaceous grading to very fine sandstone stringers which thicken up to 1 cm, but generally less than 2 mm, laminations show sharp bases. Fossils occurring - *Myoscolex ateles*, *Isoxys communis*, *Redlichia takooensis*.

**Sandstone**: brown, fine grained, calcareous in part, micaceous, argillaceous, pinches out to the south. Non fossiliferous

**Siltstone**: brown to red brown, calcareous, micaceous, laminated arenaceous rarely grading to very fine sandstone stringers, laminations show sharp bases. Fossils occurring - *Myoscolex ateles*, *Isoxys communis*.

**Formation:** Emu Bay Shale

**Section:** Big Gully Cliff Section 3.5 - 4.0m

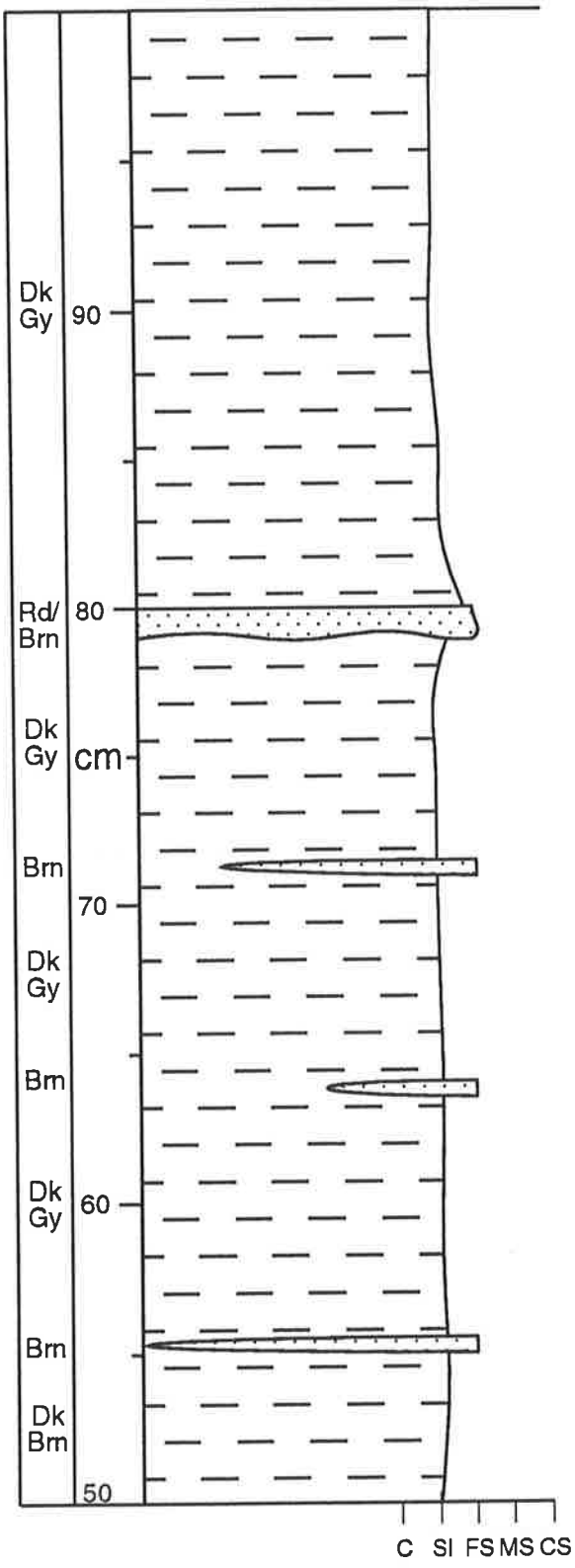


## Description

**Massive siltstone**: Dark grey, micaceous, calcareous, arenaceous grading to very fine sandstone in part. Fossils occurring - *Myoscolex ateles*, *Redlichia takooensis*, *Hsuaspis bilobata*.

**Sandstone**: brown, abundant argillaceous matrix, grading to siltstone in part, rarely feldspathic, micaceous, calcareous in part, bottom undulose but sharp, top gradational into brown siltstone. Non fossiliferous.

**Siltstone**: Dark brown, micaceous, calcareous, arenaceous grading to very fine sandstone laminations in part. Fossils occurring - *Myoscolex ateles*.

**Sandstone**: brown, abundant argillaceous matrix, grading to siltstone in part, rarely feldspathic, micaceous, calcareous in part. Non fossiliferous.

**Formation:** Emu Bay Shale

**Section:** Big Gully Cliff Section 4.0 - 4.5m

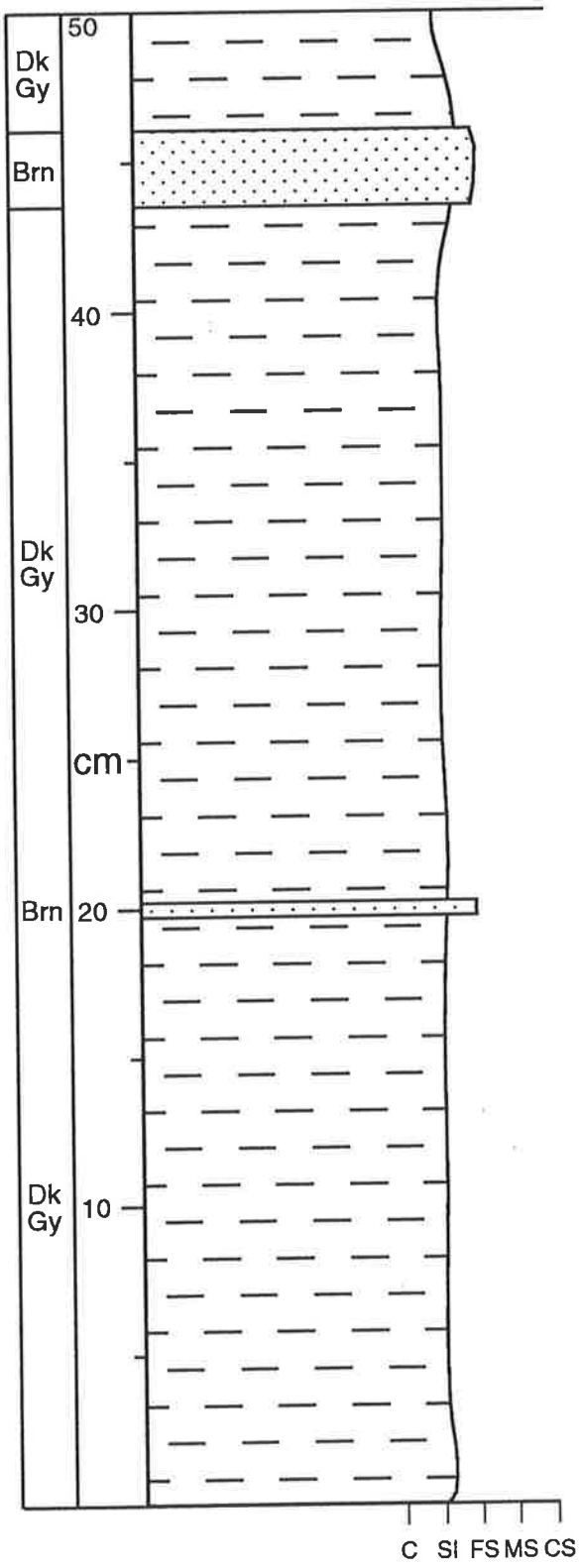


## Description

**Sandstone**: brown to dark brown, very fine grained, abundant argillaceous matrix, calcareous in part, micaceous in part. Non fossiliferous.

**Massive siltstone**: dark grey, calcareous, micaceous, arenaceous in part with rare very fine sandstone stringers. Fossils occurring - *Hsuaspis bilobata, Isoxys communis, Myoscolex ateles.*

**Sandstone**: brown, very fine grained, argillaceous, calcareous in part, micaceous in part. Non fossiliferous.

**Massive siltstone**: dark grey, calcareous, micaceous, arenaceous in part with rare very fine sandstone stringers. Fossils occurring - *Redlichia takooensis, Isoxys communis.*

**Formation:** Emu Bay Shale

**Section:** Big Gully Cliff Section 4.5 - 5.0m

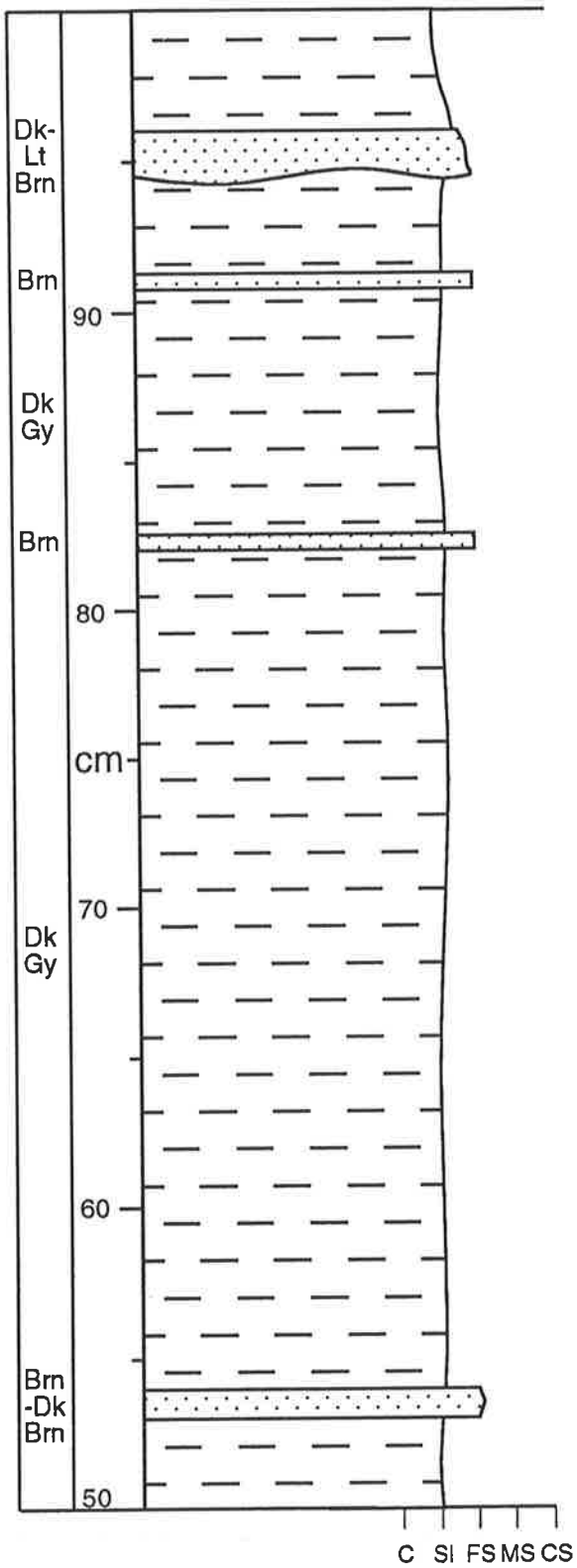


## Description

**Sandstone**: brown to dark brown, very fine grained, common argillaceous matrix, micaceous in part, calcareous in part, bottom undulose but sharp, top gradational to brown siltstone. Non fossiliferous.

**Siltstone**: dark grey and brown interlaminated siltstones, calcareous, occasionally micaceous, arenaceous grading to brown, very fine grained sandstone in part. Fossils occurring - *Myoscolex ateles*, *Hsuaspis bilobata*.

**Massive siltstone**: dark grey, calcareous with common calcite covered joint surfaces in lower part, occassionally micaceous, arenaceous in part. Fossils occurring - *Myoscolex ateles*, *Redlichia takooensis*, *Hsuaspis bilobata*, *Isoxys communis*.

**Sandstone**: brown to dark brown, very fine grained, common argillaceous matrix, micaceous in part, calcareous in part. Non fossiliferous.

**Formation:** Emu Bay Shale

**Section:** Big Gully Cliff Section 5.0 - 5.5m

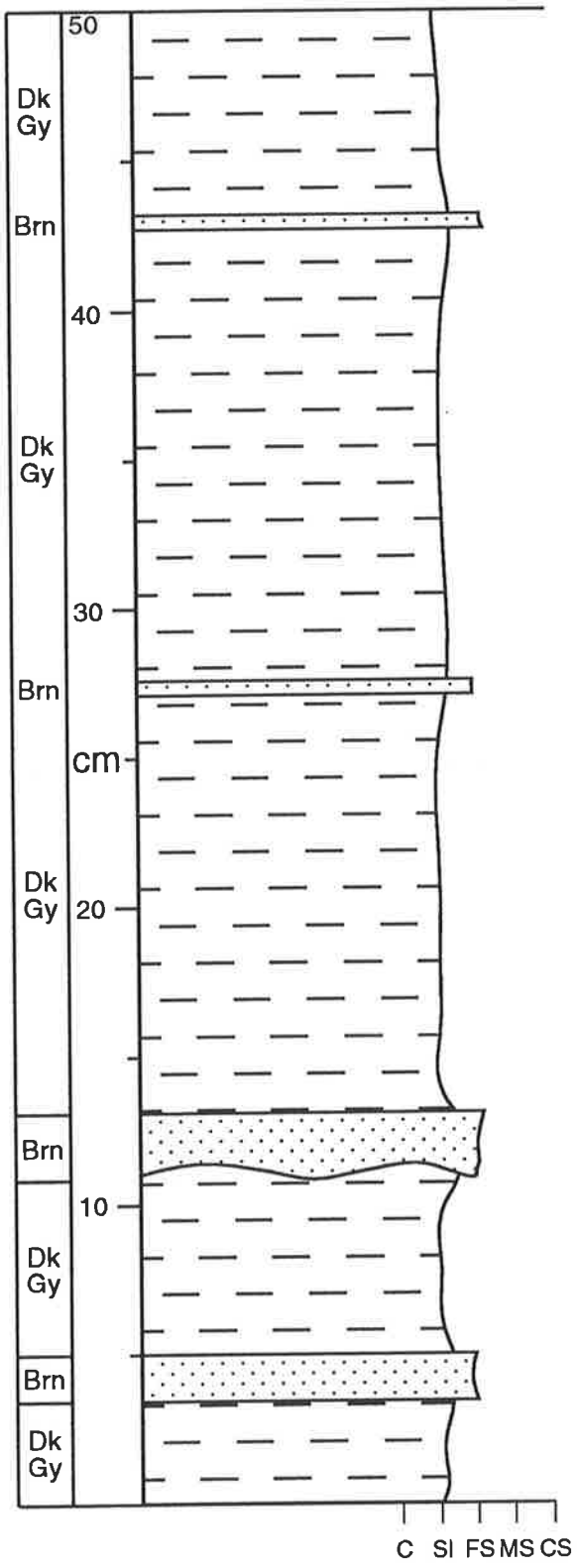


## Description

**Siltstone**: dark grey to occasionally brown, grading to very fine sandstone in part, rarely micaceous, calcareous, flat laminated. Fossils occurring - *Redlichia takooensis*, *Hsuaspis bilobata*, *Myoscolex ateles*.

**Sandstone**: brown, very fine grained, abundant argillaceous matrix, micaceous in part, calcareous, base undulose but sharp, top gradational to brown to grey siltstone. non fossiliferous.

**Sandstone**: brown, very fine grained, abundant argillaceous matrix, micaceous in part, calcareous. non fossiliferous.

**Formation:** Emu Bay Shale

**Section:** Big Gully Cliff Section 5.5 - 6.0m

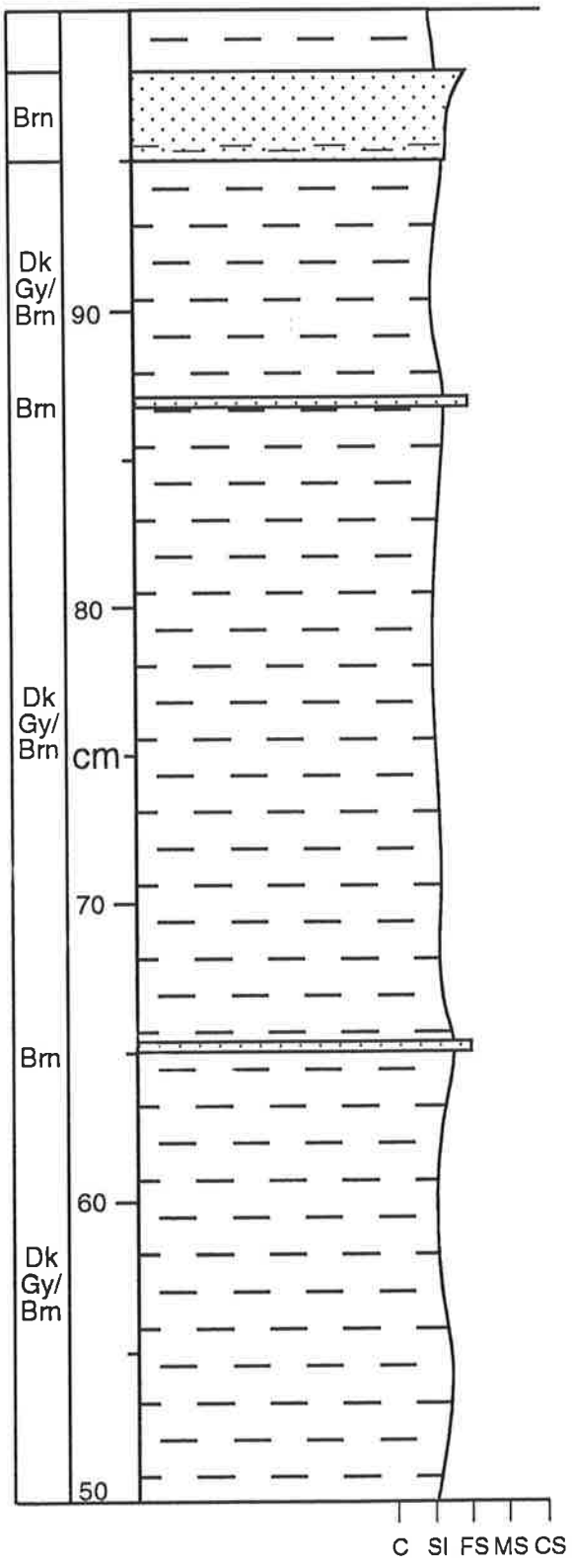


## Description

**Sandstone**: brown, very fine grained, abundant argillaceous matrix grading from siltstone at base, micaceous, calcareous in part. Non fossiliferous.

**Massive siltstone**: dark grey to brown, arenaceous grading to very fine sandstone in part, micaceous in part, feldspathic, calcareous. Fossils occurring - *Redlichia takooensis.*

**Siltstone**: dark grey to brown, grading to very fine sandstone in part, micaceous, calcareous, flat laminated. Fossils occurring - *Hsuaspis bilobata.*

**Formation:** Emu Bay Shale

**Section:** Big Gully Cliff Section 6.0 - 6.5m

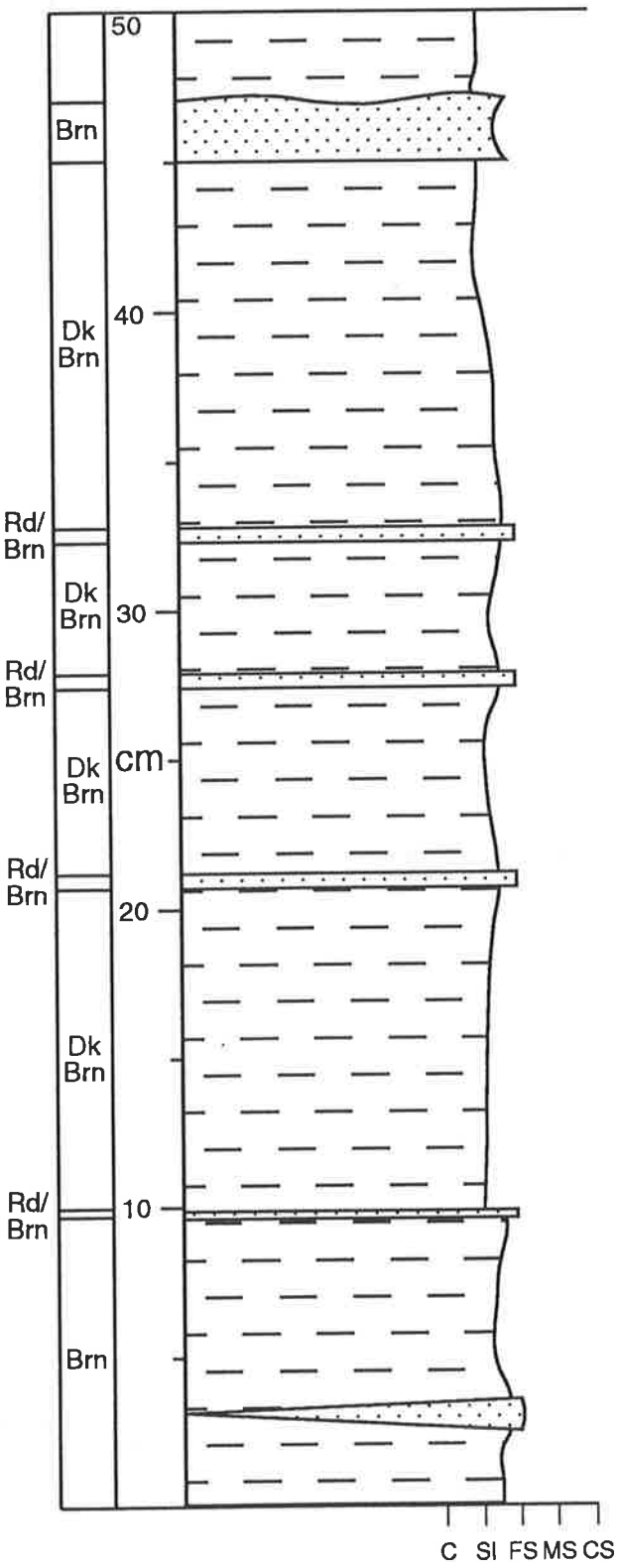


## Description

**Sandstone**: brown, very fine to fine grained, feldspathic, arkosic, abundant argillaceous matrix, calcareous, rarely micaceous, base sharp but top reworked. Non fossiliferous.

**Massive siltstone**: dark brown, arenaceous in part, calcareous, micaceous in part. Fossils occurring - *Redlichia takooensis*, *Husaspis bilobata*.

**Sandstone**: red-brown, very fine grained, argillaceous in part, calcareous, rarely micaceous, ferruginous. Non fossiliferous.

**Massive siltstone**: dark brown, arenaceous in part, calcareous, micaceous in part. Fossils occurring - *Redlichia takooensis*, *Husaspis bilobata*.

**Sandstone**: red-brown, very fine grained, argillaceous in part, calcareous, rarely micaceous, ferruginous. Non fossiliferous.

**Formation:** Emu Bay Shale

**Section:** Big Gully Cliff Section 6.5 - 7.0m

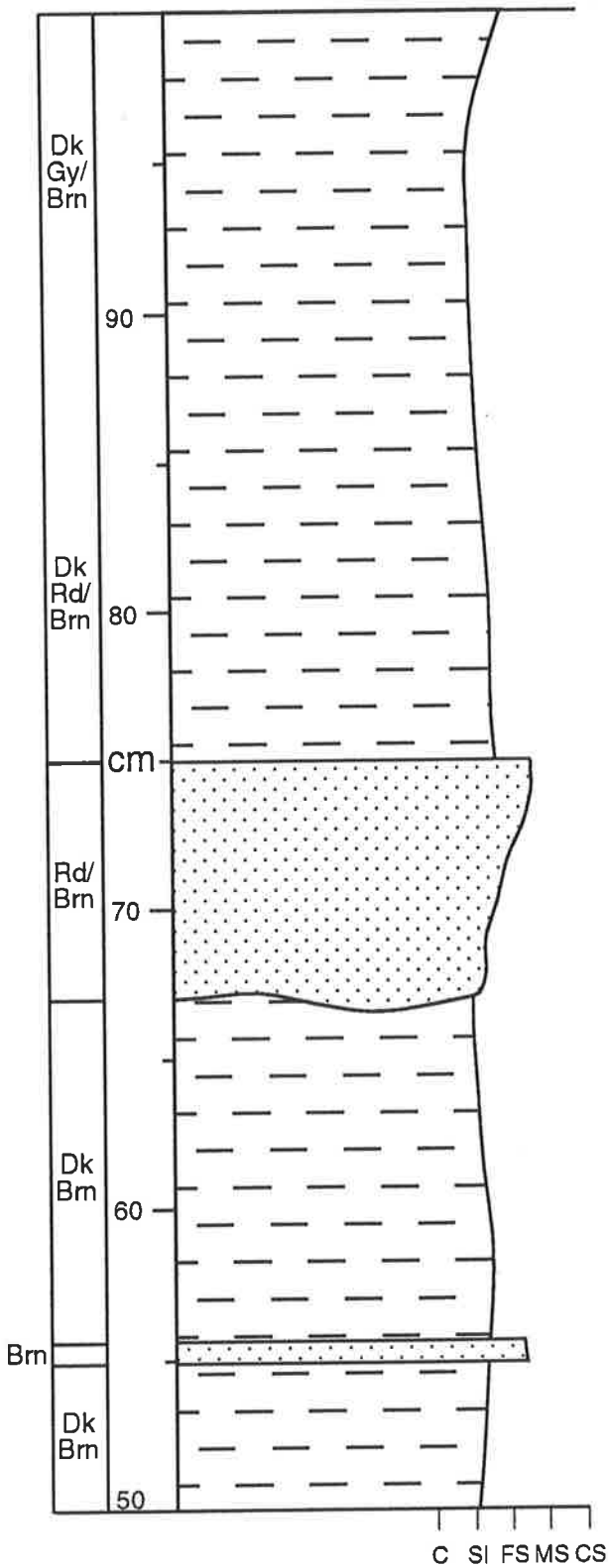


## Description

**Massive siltstone**: dark grey to dark brown, arenaceous in part occassionally grading into very fine grained arkosic sandstone laminations, micaceous, calcareous. Fossils occurring - *Hsuaspis bilobata*, *Myoscolex ateles*.

**Sandstone**: Red-brown, very fine to fine grained, feldspathic, arkosic, moderately sorted, micaceous, calcareous, common argillaceous matrix grading to interlaminated dark brown siltstone in part, base undulose, top sharp. Non fossiliferous.

**Massive siltstone**: dark brown, arenaceous occasionally grading to very fine sandstone stringers, micaceous, calcareous. Fossils occurring - *Hsuaspis bilobata*, *Isoxys communis*.

**Formation:** Emu Bay Shale

**Section:** Big Gully Cliff Section 7.0 - 7.5m

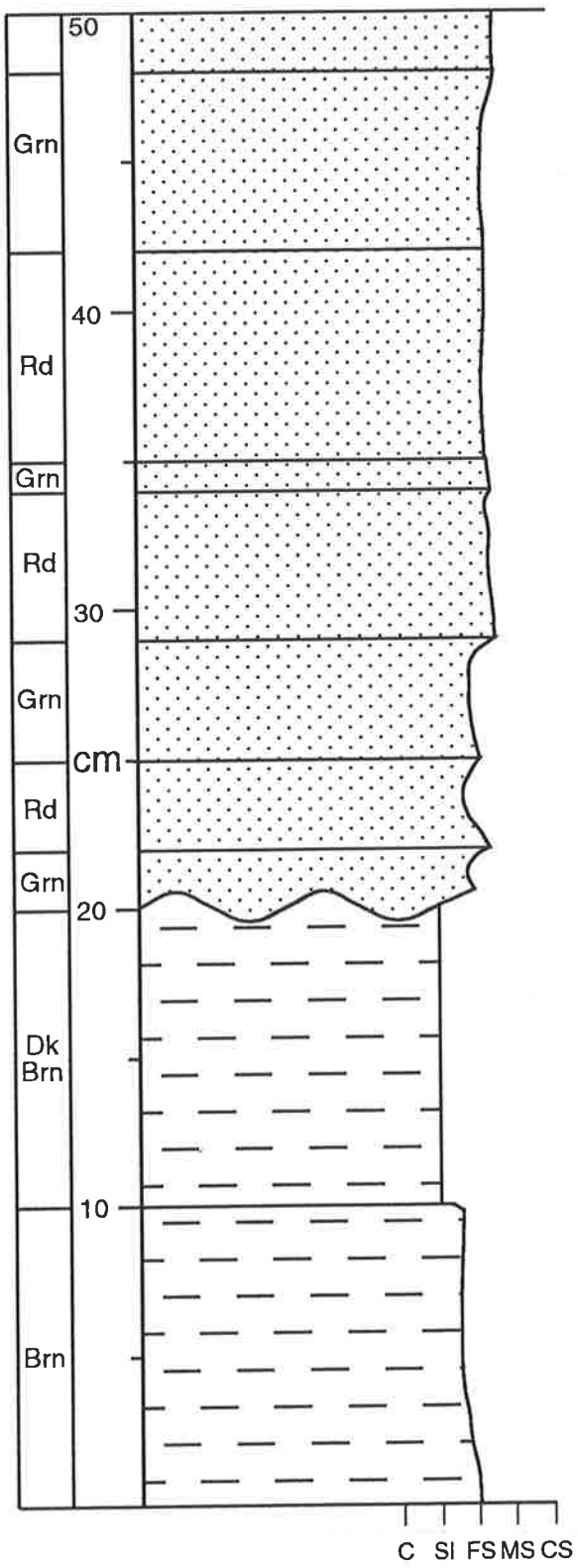


## Description

**Sandstone**: red, very fine to occasionally fine grained, abundant argillaceous matrix grading to coarse siltstone in part, calcareous, ferrugenous staining. Non fossiliferous.

**Sandstone**: green, very fine grained, abundant argillaceous matrix commonly grading to siltstone, calcareous, rarely micaceous. Non fossiliferous.

**Siltstone**: dark brown to brown, dominantly arenaceous grading to buff, very fine grained sandstone sepecially near the base, micaceous, calcareous with calcite veins near the top. Fossils occurring - *Redlichia takooensis*.

**Formation:** Emu Bay Shale

**Section:** Big Gully Cliff Section 7.5 - 8.0m

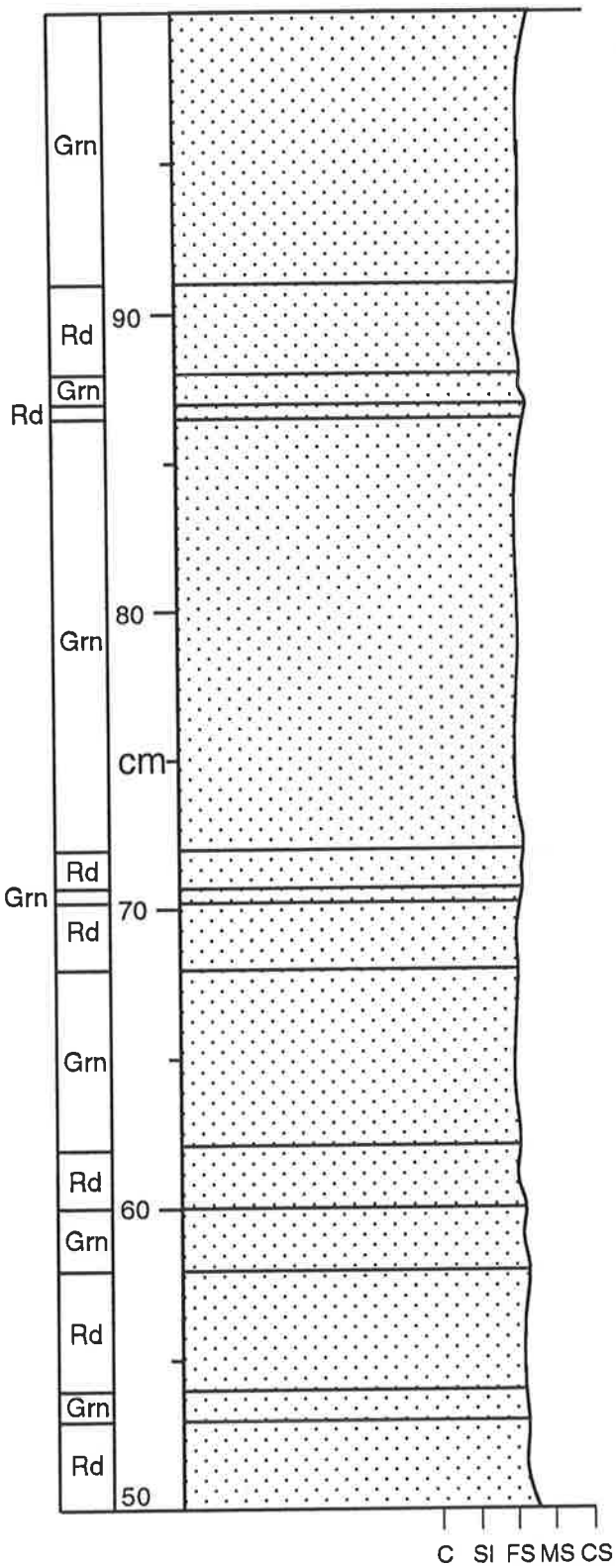


## Description

**Sandstone**: red, very fine to occasionally fine grained, abundant argillaceous matrix grading to coarse siltstone in part, calcareous, ferrugenous staining. Non fossiliferous.

**Sandstone**: green, very fine grained, abundant argillaceous matrix commonly grading to siltstone, calcareous, rarely micaceous. Non fossiliferous.

# APPENDIX 2

Numbers of fossils occurring at specific levels in the Emu Bay Shale Lagerstätte at Big Gully.

Counts taken from the wave-cut platform, along strike at at various intervals above the base of the unit. Part and counterpart, where found, counted as 1

| Metres | Redlichia | Hsuaspis | Isoxys | Myoscolex | Palaeoscolex | Anomalocaris | Naraoia | Xandarella |
|---|---|---|---|---|---|---|---|---|
| 7.1 | 5 | 2 | 0 | 0 | 0 | 0 | 0 | 0 |
| 6.8 | 100 | 187 | 54 | 7 | 1 | 4 | 0 | 0 |
| 6.5 | 27 | 8 | 2 | 6 | 38 | 9 | 0 | 0 |
| 6.44 | 0 | 0 | 9 | 1 | 0 | 0 | 0 | 0 |
| 6.35 | 1 | 0 | 124 | 98 | 28 | 0 | 0 | 0 |
| 6.25 | 15 | 12 | 9 | 5 | 0 | 1 | 0 | 0 |
| 6.11 | 14 | 9 | 0 | 2 | 0 | 4 | 2 | 0 |
| 5.9 | 116 | 153 | 83 | 32 | 35 | 4 | 0 | 1 |
| 5.68 | 125 | 62 | 3 | 2 | 3 | 1 | 2 | 0 |
| 5.6 | 1 | 35 | 4 | 6 | 33 | 4 | 0 | 1 |
| 5.5 | 29 | 21 | 0 | 1 | 12 | 3 | 0 | 0 |
| 5.16 | 20 | 78 | 12 | 9 | 78 | 1 | 1 | 1 |
| 4.93 | 15 | 4 | 1 | 2 | 0 | 0 | 0 | 0 |
| 4.81 | 0 | 0 | 2 | 3 | 0 | 0 | 0 | 0 |
| 4.72 | 2 | 0 | 32 | 83 | 28 | 0 | 0 | 0 |
| 4.65 | 29 | 41 | 0 | 0 | 9 | 2 | 0 | 0 |
| 4.35 | 58 | 29 | 2 | 0 | 8 | 0 | 0 | 0 |
| 4.1 | 20 | 7 | 3 | 1 | 10 | 0 | 0 | 0 |
| 4.05 | 16 | 33 | 0 | 0 | 3 | 1 | 0 | 0 |
| 3.79 | 0 | 0 | 5 | 4 | 0 | 0 | 0 | 0 |
| 3.7 | 1 | 0 | 12 | 25 | 52 | 0 | 0 | 0 |
| 3.62 | 12 | 9 | 0 | 0 | 12 | 0 | 0 | 0 |
| 3.55 | 29 | 31 | 0 | 4 | 12 | 2 | 0 | 0 |
| 3.05 | 12 | 19 | 0 | 1 | 0 | 0 | 0 | 0 |

| Metres | Redlichia | Hsuaspis | Isoxys | Myoscolex | Palaeoscolex | Anomalocaris | Naraoia | Xandarella |
|---|---|---|---|---|---|---|---|---|
| 3.0 | 29 | 18 | 6 | 2 | 15 | 1 | 0 | 0 |
| 2.95 | 54 | 36 | 10 | 4 | 31 | 3 | 0 | 0 |
| 2.5 | 14 | 24 | 0 | 1 | 10 | 0 | 0 | 0 |
| 2.4 | 2 | 1 | 2 | 0 | 9 | 0 | 0 | 0 |
| 2.0 | 0 | 0 | 0 | 0 | 0 | 0 | 0 | 0 |
| 1.5 | 2 | 0 | 0 | 1 | 0 | 0 | 0 | 0 |
| 1.0 | 1 | 1 | 0 | 0 | 0 | 0 | 0 | 0 |
| 0.5 | 1 | 0 | 0 | 0 | 0 | 0 | 0 | 0 |

# APPENDIX 3

Measurements on *Hsuaspis bilobata*. Measurements after Shaw (1957).

A1: Total cranidial length.

A2: Occipital intramarginal cephalic length.

A3: Pre-occipital cranidial length.

A4: Pre-occipital intramarginal cranidial length.

B: Total glabellar length.

B1: Occipital glabellar length.

C1: Palpebral chord length.

D: Occipital mid-palpebral distance.

D1: Pre-occipital mid-palpebral distance.

E: Sagittal width of the occipital lobe.

F1: Sagittal width of cephalic frontal area.

H: Sagittal width of the pre-glabellar field.

I1: Palpebral cephalic width.

I2: Occipital cephalic width.

J: Palpebral cranidial width.

J1: Posterior cranidial width.

J2: Maximum width of the frontal area.

K: Transverse occipital length.

K1: Palpebral glabellar width.

K2: Maximum glabellar width.

KD: Posterior occipital ring to anterior of palpebral lobe.

KD1: Posterior of glabellar to anterior palpebral lobe.

1046- specimen numbers held at the University of Adelaide.

CPC- specimen numbers from Cymbric Vale, New South Wales (Öpik 1975b).

Numbers ending in "E" indicate specimens from Emu Bay.

F16441 is the holotype of *Hsuaspis bilobata* held at the South Australian Museum.

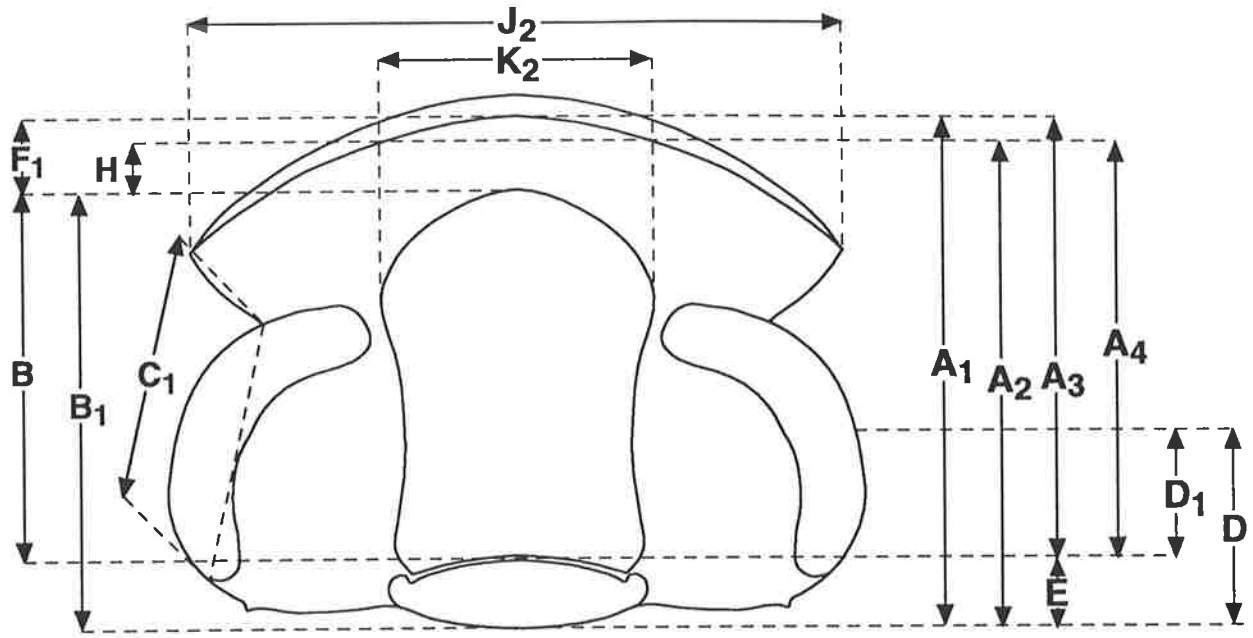
J2
K2
F1
H
B
B1
C1
A1
A2
A3
A4
D1
D
E

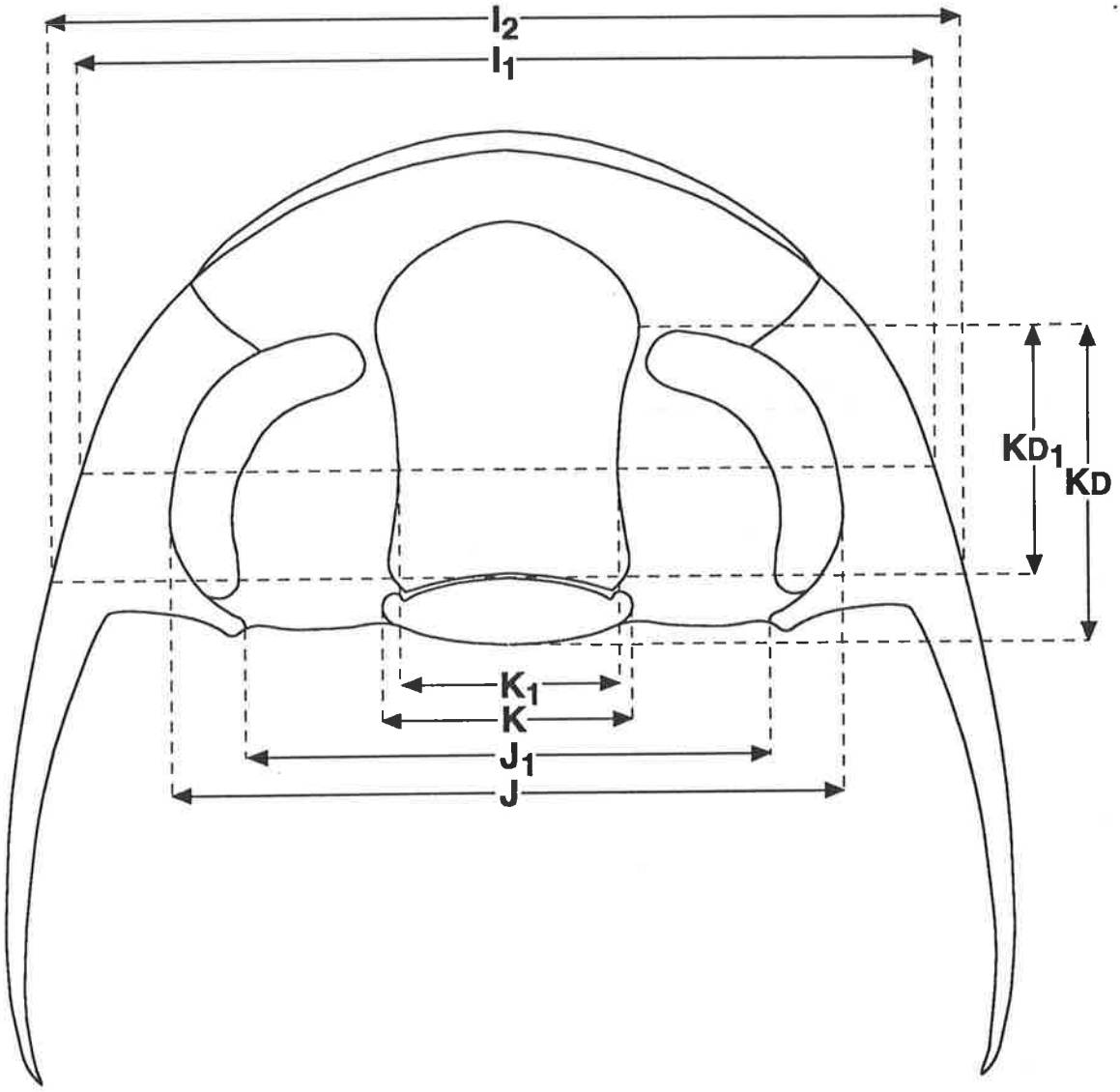
I2
I1
KD1
KD
K1
K
J1
J

| Sample | A1 | A2 | A3 | A4 | B | B1 | C1 | D | D1 | E | F1 | H |
|---|---|---|---|---|---|---|---|---|---|---|---|---|
| 1046-547a | 2.40 | 2.29 | 1.91 | 1.74 | 1.46 | 1.95 | 0.88 | 0.98 | 0.49 | 0.49 | 0.45 | 0.34 |
| -590b | 2.15 | 2.05 | 1.73 | 1.58 | 1.33 | 1.75 | 0.80 | 0.80 | 0.38 | 0.43 | 0.40 | 0.30 |
| -543a | 1.98 | 1.89 | 1.61 | 1.50 | 1.27 | 1.63 | 0.68 | 0.78 | 0.40 | 0.38 | 0.28 | 0.26 |
| AY1 | 1.98 | 1.82 | 1.72 | 1.57 | 1.25 | 1.57 | 0.60 | 0.58 | 0.33 | 0.25 | 0.41 | 0.25 |
| -702 | 1.34 | 1.26 | 1.13 | 1.04 | 0.92 | 1.14 | 0.34 | 0.50 | 0.28 | 0.22 | 0.22 | 0.14 |
| -701 | 1.30 | 1.19 | 1.09 | 0.98 | 0.85 | 1.06 | 0.33 | 0.46 | 0.25 | 0.21 | 0.24 | 0.13 |
| -700 | 0.78 | 0.70 | 0.68 | 0.60 | 0.56 | 0.66 | 0.24 | 0.22 | 0.12 | 0.10 | 0.14 | 0.04 |
| -770 | - | - | - | - | - | - | 0.75 | 0.89 | 0.49 | 0.40 | - | - |
| -261 | 6.00 | 5.75 | 5.00 | 4.75 | 4.10 | 5.10 | 2.05 | 1.90 | 0.90 | 1.00 | 0.90 | 0.60 |
| -258b | 4.60 | 4.20 | 3.75 | 3.35 | 2.80 | 3.65 | 1.80 | 1.45 | 0.60 | 0.85 | 1.20 | 0.55 |
| -336 | 8.50 | 6.80 | 7.20 | 5.50 | 5.10 | 6.40 | 2.30 | 2.40 | 1.10 | 1.30 | 2.10 | 0.40 |
| -258a | 7.30 | 6.80 | 6.10 | 5.60 | 4.80 | 6.00 | 2.00 | 1.80 | 0.60 | 1.20 | 1.70 | 0.80 |
| -A336 | 10.90 | 10.20 | 9.30 | 8.60 | 7.80 | 8.40 | 2.90 | 3.10 | 1.50 | 1.60 | 2.50 | 0.80 |
| -263 | 7.30 | 7.00 | 6.40 | 6.10 | 4.50 | 5.40 | 2.00 | 1.50 | 0.60 | 0.90 | 1.90 | 1.00 |
| -649a | 5.50 | 5.20 | 4.40 | 4.10 | 3.40 | 4.50 | - | - | - | 1.10 | 1.00 | 0.70 |
| -649a | 3.30 | 3.00 | 2.50 | 2.20 | 1.70 | 2.50 | - | - | - | 0.80 | 0.60 | 0.50 |
| -649a | 7.10 | 6.40 | 5.70 | 5.00 | 4.50 | 5.90 | - | - | - | 1.40 | 1.20 | 0.50 |
| -649a | 4.00 | 3.75 | 3.00 | 2.75 | 2.00 | 3.00 | - | - | - | 1.00 | 0.80 | 0.55 |
| -649b | 3.45 | 3.15 | 2.80 | 2.50 | 2.00 | 2.65 | - | - | - | 0.65 | 0.80 | 0.50 |
| -649b | 3.10 | 2.80 | 2.60 | 2.30 | 1.90 | 2.40 | - | - | - | 0.50 | 0.70 | 0.40 |
| -560E | 4.00 | 3.60 | 3.35 | 2.95 | 2.45 | 3.00 | 1.60 | 0.45 | 1.10 | 0.65 | 0.95 | 0.50 |
| -560E | 7.20 | 6.40 | 6.10 | 5.30 | 4.60 | 5.70 | 2.50 | 0.90 | 2.00 | 1.10 | 1.50 | 0.70 |
| -560E | 7.30 | 6.30 | 6.20 | 5.20 | 4.50 | 5.60 | 2.40 | 1.20 | 2.30 | 1.10 | 1.70 | 0.70 |
| -560E | 8.80 | 8.10 | 7.60 | 6.90 | 5.80 | 7.00 | 2.50 | 1.70 | 2.90 | 1.20 | 1.80 | 1.10 |

| Sample | I1 | I2 | J | J1 | J2 | K | K1 | K2 | KD | KD1 | I2 as %A1 | J-K1 |
|---|---|---|---|---|---|---|---|---|---|---|---|---|
| 1046-547a | 3.70 | 4.13 | 3.1 | 2.45 | 2.85 | 1.15 | 0.98 | 0.95 | 1.58 | 1.09 | 1.72 | 2.13 |
| -590b | 3.33 | 3.73 | 2.84 | 2.20 | 2.65 | 0.98 | 0.88 | 0.90 | 1.36 | 0.99 | 1.73 | 1.96 |
| -543a | 3.10 | 3.36 | 2.65 | 2.05 | 2.63 | 0.90 | 0.75 | 0.80 | 1.34 | 0.96 | 1.70 | 1.90 |
| AY1 | 3.12 | 3.30 | 2.66 | 2.00 | 2.50 | 0.88 | 0.78 | 0.80 | 1.18 | 0.93 | 1.67 | 1.88 |
| -702 | - | - | 2 | 1.36 | 1.56 | 0.40 | 0.37 | 0.51 | 0.90 | 0.68 | - | 1.25 |
| -701 | 2.23 | 2.40 | 1.95 | 1.36 | 1.60 | 0.45 | 0.39 | 0.49 | 0.83 | 0.65 | 1.85 | 1.13 |
| -700 | 1.30 | 1.75 | 1.3 | 0.80 | 1.06 | 0.18 | 0.15 | 0.28 | 0.56 | 0.42 | 1.92 | 0.62 |
| -770 | 3.75 | 3.95 | 2.98 | 2.35 | 2.67 | 1.00 | 0.92 | 0.93 | - | - | - | 2.06 |
| -261 | 9.35 | 9.80 | 7 | 5.80 | - | 2.25 | 2.40 | 2.70 | 3.90 | 2.90 | 1.63 | 4.60 |
| -258b | 7.15 | 7.55 | 5.3 | 4.20 | 5.00 | 1.90 | 1.30 | 2.00 | 2.85 | 1.95 | 1.64 | 4.00 |
| -336 | 12.90 | 13.40 | 9.2 | 7.40 | 9.40 | 3.40 | 3.10 | 3.40 | 4.80 | 3.50 | 1.58 | 6.10 |
| -258a | 11.50 | 12.00 | 8.2 | 7.00 | 8.60 | 2.80 | 2.70 | 3.00 | 4.70 | 3.50 | 1.64 | 5.50 |
| -A336 | 16.00 | 17.80 | 12 | 10.00 | 12.40 | 4.40 | 4.30 | 4.20 | 5.90 | 5.30 | 1.63 | 7.70 |
| -263 | 11.20 | 12.00 | 8.2 | 6.50 | 8.20 | 2.60 | 2.70 | 3.00 | 3.90 | 3.00 | 1.64 | 5.50 |
| -649a | - | - | - | - | - | - | - | 2.50 | - | - | - | - |
| -649a | - | - | - | - | - | - | - | 1.30 | - | - | - | - |
| -649a | - | - | - | - | - | - | - | 2.50 | - | - | - | - |
| -649a | - | - | - | - | - | - | - | 1.50 | - | - | - | - |
| -649b | - | - | - | - | - | - | - | 1.30 | - | - | - | - |
| -649b | - | - | - | - | - | - | - | 1.10 | - | - | - | - |
| -560E | - | - | 4.8 | 4.00 | 5.20 | 2.00 | 1.80 | 1.80 | 2.32 | 1.77 | - | 2.80 |
| -560E | - | - | 7.8 | 6.00 | 8.40 | 3.20 | 3.00 | 3.30 | 4.00 | 2.90 | - | 4.80 |
| -560E | - | - | 7.8 | 6.00 | 8.69 | 3.20 | 3.00 | 3.30 | 4.20 | 3.10 | - | 4.80 |
| -560E | - | - | 9.2 | 6.40 | 9.00 | 3.70 | 3.30 | 3.50 | 5.00 | 3.80 | - | 5.30 |

| Sample | H as %A1 | J1-K | J1-K/2 | J1-K/2 as% A1 | J/A1 | Preoc Glab | Preoc Glab/A1 | K2/A1 | Eye Lobe | Eye Lobe/A1 |
|---|---|---|---|---|---|---|---|---|---|---|
| 1046-547a | 0.14 | 1.30 | 0.65 | 0.27 | 1.29 | 0.37 | 0.15 | 0.4 | 0.72 | 0.30 |
| -590b | 0.14 | 1.22 | 0.61 | 0.28 | 1.32 | 0.34 | 0.158 | 0.42 | - | - |
| -543a | 0.13 | 1.15 | 0.57 | 0.29 | 1.34 | 0.31 | 0.16 | 0.4 | 0.68 | 0.34 |
| AY1 | 0.13 | 1.12 | 0.56 | 0.28 | 1.34 | 0.32 | 0.162 | 0.4 | 0.67 | 0.34 |
| -702 | 0.10 | 0.96 | 0.48 | 0.34 | 1.49 | 0.24 | 0.18 | 0.38 | 0.54 | 0.40 |
| -701 | 0.10 | 0.91 | 0.45 | 0.35 | 1.5 | 0.23 | 0.182 | 0.38 | 0.48 | 0.37 |
| -700 | 0.05 | 0.49 | 0.25 | 0.41 | 1.66 | 0.15 | 0.192 | 0.36 | 0.35 | 0.45 |
| -770 | - | 1.35 | 0.68 | - | - | - | - | - | - | - |
| -261 | 0.10 | 3.55 | 1.77 | 0.30 | 1.17 | 1.20 | 0.2 | 0.45 | 1.40 | 0.23 |
| -258b | 0.12 | 2.30 | 1.15 | 0.25 | 1.15 | 0.85 | 0.18 | 0.43 | 1.20 | 0.26 |
| -336 | 0.05 | 4.00 | 2.00 | 0.24 | 1.08 | 1.60 | 0.19 | 0.4 | 2.00 | 0.24 |
| -258a | 0.11 | 4.20 | 2.10 | 0.29 | 1.12 | 1.30 | 0.18 | 0.41 | - | - |
| -A336 | 0.07 | 5.60 | 2.80 | 0.26 | 1.1 | 2.50 | 0.23 | 0.39 | - | - |
| -263 | 0.12 | 3.90 | 1.95 | 0.27 | 1.12 | 1.50 | 0.21 | 0.41 | - | - |
| -649a | 0.13 | | - | - | - | - | - | 0.45 | - | - |
| -649a | 0.15 | | - | - | - | - | - | 0.39 | 0.80 | 0.24 |
| -649a | 0.07 | | - | - | - | - | - | 0.35 | 1.80 | 0.25 |
| -649a | 0.14 | | - | - | - | - | - | 0.38 | 1.10 | 0.28 |
| -649b | 0.14 | | - | - | - | - | - | 0.38 | - | - |
| -649b | 0.13 | | - | - | - | - | - | 0.35 | 0.76 | 0.25 |
| -560E | 0.15 | 2.40 | 1.20 | 0.30 | 1.2 | 0.68 | 0.17 | 0.45 | 1.10 | 0.28 |
| -560E | 0.10 | 2.80 | 1.40 | 0.19 | 1.08 | 1.70 | 0.24 | 0.46 | 1.80 | 0.25 |
| -560E | 0.10 | 2.80 | 1.40 | 0.19 | 1.07 | 1.40 | 0.19 | 0.45 | - | - |
| -560E | 0.12 | 2.70 | 1.35 | 0.15 | 1.04 | 2.00 | 0.23 | 0.4 | | |

| Sample | A1 | A2 | A3 | A4 | B | B1 | C1 | D | D1 | E | F1 | H |
|---|---|---|---|---|---|---|---|---|---|---|---|---|
| -267E | 9.20 | 8.60 | 7.70 | 7.10 | 6.00 | 7.50 | 3.00 | 2.00 | 3.50 | 1.50 | 1.70 | 1.10 |
| -267E | 9.00 | 8.50 | 7.30 | 6.80 | 6.00 | 7.70 | 2.80 | 1.50 | 3.20 | 1.70 | 1.30 | 0.80 |
| -270aE | 10.00 | 9.00 | 8.30 | 7.30 | 6.10 | 7.80 | 3.20 | 1.70 | 3.40 | 1.70 | 2.20 | 1.20 |
| -278bE | 11.00 | 10.00 | 9.10 | 8.10 | 6.80 | 8.70 | 3.20 | 2.00 | 3.90 | 1.90 | 2.30 | 1.30 |
| -278bE | 10.20 | 9.30 | 8.70 | 7.80 | 6.70 | 8.20 | 3.10 | 1.80 | 3.30 | 1.50 | 2.50 | 1.10 |
| -268E | 10.50 | 9.80 | 8.80 | 8.10 | 7.10 | 8.60 | 3.30 | 1.30 | 3.00 | 1.70 | 2.10 | 1.50 |
| -370a | 10.60 | 9.70 | 8.90 | 8.00 | 7.00 | 8.70 | 3.40 | 1.40 | 3.10 | 1.70 | 1.90 | 1.00 |
| -578 | 5.70 | 5.10 | 4.70 | 4.10 | 3.70 | 4.70 | 1.80 | 1.10 | 2.10 | 1.00 | 1.00 | 0.40 |
| -578 | 9.20 | 8.60 | 7.70 | 7.10 | 5.80 | 7.30 | 3.10 | 1.30 | 2.80 | 1.50 | 1.90 | 0.70 |
| -578 | 4.40 | 4.10 | 3.30 | 3.00 | 2.60 | 3.70 | 1.60 | 0.60 | 1.70 | 1.10 | 0.70 | 0.40 |
| -578 | 3.70 | 3.20 | 3.20 | 2.70 | 2.25 | 2.75 | 1.20 | 0.70 | 1.20 | 0.50 | 0.80 | 0.45 |
| -532a | 9.20 | 8.50 | 7.80 | 7.10 | 5.90 | 7.30 | 2.60 | 1.60 | 3.00 | 1.40 | 1.90 | 1.20 |
| -372 | 7.70 | 6.90 | 6.50 | 5.70 | 5.00 | 6.20 | 2.50 | 0.90 | 2.10 | 1.20 | 1.50 | 0.80 |
| CPC 13152 | 16.00 | 14.70 | 13.50 | 12.20 | 11.20 | 13.70 | 5.00 | 2.50 | 5.00 | 2.50 | 2.30 | 1.00 |
| CPC 13153 | 12.00 | 10.08 | 10.00 | 8.80 | 8.00 | 10.00 | 3.90 | 1.60 | 3.60 | 2.00 | 2.00 | 0.80 |
| CPC 13155 | 8.30 | 7.58 | 7.05 | 6.33 | 5.60 | 6.75 | 2.60 | 1.01 | 2.30 | 1.25 | 1.55 | 0.83 |
| CPC 13156 | 10.10 | 9.33 | 8.60 | 7.83 | 7.00 | 8.50 | 3.66 | 1.10 | 2.60 | 1.50 | 1.60 | 0.83 |
| F16441 | 5.82 | 5.18 | 4.91 | 4.27 | 3.64 | 4.55 | 1.82 | 2.91 | 3.82 | 0.91 | 1.27 | 0.63 |

| Sample | I1 | I2 | J | J1 | J2 | K | K1 | K2 | KD | KD1 | I2 as %A1 | J-K1 |
|---|---|---|---|---|---|---|---|---|---|---|---|---|
| -267E | - | - | 10.2 | 7.40 | 10.00 | 4.00 | 3.50 | 3.80 | 5.40 | 3.90 | - | 6.70 |
| -267E | - | - | 10.6 | 7.60 | 11.00 | 4.70 | 3.40 | 3.60 | 5.50 | 3.80 | - | 7.20 |
| -270aE | - | - | 10.8 | 7.20 | 11.40 | 3.80 | 3.50 | 3.90 | 5.40 | 3.70 | - | 7.30 |
| -278bE | - | - | 11.2 | 8.80 | 12.70 | 4.10 | 4.10 | 4.30 | 6.60 | 4.70 | - | 7.10 |
| -278bE | - | - | 10.5 | 8.60 | 11.00 | 3.90 | 3.70 | 4.00 | 6.00 | 4.50 | - | 6.80 |
| -268E | - | - | 11.8 | 8.60 | 12.50 | 3.90 | 3.80 | 4.10 | 6.40 | 4.90 | - | 8.00 |
| -370a | 15.80 | 17.00 | 12 | 9.70 | - | 4.00 | 4.20 | 4.20 | 6.50 | 4.80 | 1.60 | 7.80 |
| -578 | 8.70 | 9.40 | 6.4 | 5.80 | 7.20 | 2.40 | 2.50 | 2.50 | 3.50 | 2.50 | 1.65 | 3.90 |
| -578 | 14.10 | 15.70 | 11 | 9.00 | 11.00 | 3.60 | 3.80 | 4.00 | 5.60 | 4.10 | 1.71 | 7.20 |
| -578 | 6.80 | 7.20 | 5 | 4.40 | 5.40 | 1.40 | 1.30 | 1.50 | 2.80 | 1.70 | 1.63 | 3.70 |
| -578 | 5.40 | 6.20 | 4.4 | 3.60 | 4.80 | 1.30 | 1.50 | 1.50 | 2.20 | 1.70 | 1.68 | 2.90 |
| -532a | 14.70 | 15.60 | 10.9 | 8.80 | 11.20 | 4.00 | 4.30 | 4.50 | 5.60 | 4.20 | 1.70 | 6.60 |
| -372 | - | - | 8.8 | 7.80 | 9.00 | 3.10 | 3.00 | 3.20 | 4.60 | 3.40 | - | 5.80 |
| CPC 13152 | - | - | 19.3 | 17.00 | 23.00 | 7.67 | 7.33 | 8.33 | 9.17 | 6.53 | - | - |
| CPC 13153 | - | - | 14.1 | 12.00 | 14.20 | 5.00 | 5.00 | 5.70 | 7.00 | 5.00 | - | 9.10 |
| CPC 13155 | - | - | 9.03 | 8.20 | 8.00 | 3.20 | 3.00 | 3.67 | 4.83 | 3.58 | - | 6.03 |
| CPC 13156 | - | - | 11.2 | 9.30 | 10.30 | 4.30 | 4.17 | 4.67 | 6.10 | 4.60 | - | 7.13 |
| F16441 | 8.91 | 9.64 | 6.91 | 5.54 | 6.91 | 2.55 | 2.55 | 2.73 | 3.52 | 2.61 | 1.66 | 4.36 |

| Sample | H as %A1 | J1-K | J1-K/2 | J1-K/2 as% A1 | J/A1 | Preoc Glab | Preoc Glab/A1 | K2/A1 | Eye Lobe | Eye Lobe/A1 |
|---|---|---|---|---|---|---|---|---|---|---|
| -267E | 0.12 | 3.40 | 1.70 | 0.18 | 1.11 | 2.10 | 0.23 | 0.41 | 2.20 | 0.24 |
| -267E | 0.09 | 2.90 | 1.45 | 0.16 | 1.18 | 2.20 | 0.24 | 0.4 | 2.20 | 0.24 |
| -270aE | 0.12 | 3.40 | 1.70 | 0.17 | 1.08 | 2.40 | 0.24 | 0.39 | 2.50 | 0.25 |
| -278bE | 0.12 | 4.70 | 2.35 | 0.21 | 1.02 | 2.10 | 0.19 | 0.39 | - | - |
| -278bE | 0.11 | 4.70 | 2.35 | 0.23 | 1.03 | 2.20 | 0.22 | 0.39 | - | - |
| -268E | 0.11 | 4.70 | 2.35 | 0.22 | 1.12 | 2.20 | 0.21 | 0.39 | 2.60 | 0.25 |
| -370a | 0.09 | 5.70 | 2.85 | 0.27 | 1.13 | 2.20 | 0.21 | 0.4 | - | - |
| -578 | 0.07 | 3.40 | 1.70 | 0.29 | 1.19 | 1.20 | 0.21 | 0.44 | - | - |
| -578 | 0.08 | 5.40 | 2.70 | 0.29 | 1.2 | 1.70 | 0.18 | 0.43 | 2.40 | 0.26 |
| -578 | 0.09 | 3.00 | 1.50 | 0.34 | 1.14 | 1.10 | 0.2 | 0.34 | - | - |
| -578 | 0.14 | 2.30 | 1.15 | 0.31 | 1.19 | 0.55 | 0.15 | 0.41 | 0.90 | 0.24 |
| -532a | 0.13 | 4.80 | 2.40 | 0.26 | 1.18 | 1.70 | 0.18 | 0.49 | - | - |
| -372 | 0.10 | 4.70 | 2.35 | 0.31 | 1.14 | 1.60 | 0.21 | 0.42 | 1.90 | 0.25 |
| CPC 13152 | 0.06 | 9.33 | 4.67 | 0.29 | 1.21 | 4.67 | 0.29 | 0.52 | 4.00 | 0.25 |
| CPC 13153 | 0.07 | 7.00 | 3.50 | 0.29 | 1.18 | 3.00 | 0.25 | 0.48 | 3.40 | 0.28 |
| CPC 13155 | 0.10 | 5.00 | 2.50 | 0.30 | 1.09 | 2.02 | 0.24 | 0.44 | 1.80 | 0.22 |
| CPC 13156 | 0.08 | 5.00 | 2.50 | 0.25 | 1.11 | 2.40 | 0.24 | 0.46 | - | - |
| F16441 | 0.11 | 2.90 | 1.45 | 0.25 | 1.19 | 1.03 | 0.18 | 0.44 | 1.45 | 0.25 |

# APPENDIX 4

Geochemical analysis of the Emu Bay Shale Lagerstätte.

Analyses carried out on a Philips PW 1480 X-Ray Fluorescence Spectrometer, calibrated using a number of international standards.

Major elements were analysed using fused glass discs and a Sc tube.

Trace elements were analysed using pressed discs and a Rh or W tube.

Samples prefixed "R" from the Emu Bay Shale Lagerstätte at Big Gully.
Samples prefixed "EB" from the Emu Bay Shale, Emu Bay.

"Deep Sea", "California" and "Black Sea" measurements taken from Brumsack (1980, 1986, 1989)

| Sample | Metres | $SiO_2$% | $Al_2O_3$% | $Fe_2O_3$% | $MnO_2$ | $MgO_2$% | CaO% | $Na_2O$% | $K_2O$% | $TiO_2$% | $P_2O_5$% | $SO_3$% |
|---|---|---|---|---|---|---|---|---|---|---|---|---|
| RS42 | 7.10 | 52.96 | 14.91 | 6.37 | 0.08 | 3.89 | 5.20 | 1.49 | 5.21 | 0.57 | 0.34 | 0.03 |
| RS47 | 6.80 | 51.72 | 13.73 | 6.51 | 0.06 | 3.82 | 6.55 | 1.42 | 4.49 | 0.64 | 0.35 | 0.04 |
| RS14 | 6.50 | 54.36 | 14.74 | 5.93 | 0.07 | 4.03 | 4.77 | 1.39 | 4.92 | 0.63 | 0.41 | 0.02 |
| RS17 | 6.35 | 46.38 | 12.71 | 7.24 | 0.09 | 4.50 | 9.11 | 1.12 | 4.41 | 0.61 | 0.36 | 0.03 |
| RS49 | 6.25 | 52.15 | 14.67 | 6.02 | 0.05 | 3.99 | 5.81 | 1.31 | 4.98 | 0.63 | 0.58 | 0.05 |
| R640 | 6.11 | 50.55 | 13.54 | 6.30 | 0.06 | 4.49 | 7.39 | 1.26 | 4.67 | 0.61 | 0.32 | 0.03 |
| RS48 | 5.90 | 51.87 | 13.83 | 6.20 | 0.06 | 3.74 | 6.73 | 1.43 | 4.50 | 0.63 | 0.48 | 0.05 |
| R553 | 5.68 | 50.88 | 13.53 | 7.32 | 0.06 | 4.14 | 6.88 | 1.29 | 4.64 | 0.61 | 0.45 | 0.03 |
| R573 | 5.50 | 50.21 | 13.79 | 5.88 | 0.07 | 3.39 | 8.89 | 1.39 | 4.54 | 0.59 | 0.46 | 0.03 |
| RS16 | 5.16 | 51.62 | 14.52 | 6.68 | 0.05 | 3.56 | 6.31 | 1.49 | 5.02 | 0.56 | 1.26 | 0.04 |
| RS15 | 4.93 | 52.90 | 15.14 | 6.78 | 0.06 | 3.76 | 4.76 | 1.47 | 5.20 | 0.59 | 0.23 | 0.01 |
| R507 | 4.81 | 46.93 | 12.78 | 6.90 | 0.11 | 4.64 | 9.47 | 1.07 | 4.50 | 0.58 | 0.28 | 0.03 |
| R522 | 4.65 | 53.48 | 15.26 | 6.51 | 0.06 | 3.75 | 5.07 | 1.46 | 5.31 | 0.58 | 0.38 | 0.03 |
| RS43 | 4.35 | 52.14 | 14.42 | 6.79 | 0.06 | 3.91 | 5.70 | 1.41 | 5.06 | 0.59 | 0.41 | 0.04 |
| RS45 | 4.10 | 52.14 | 14.14 | 6.60 | 0.06 | 3.68 | 6.47 | 1.45 | 4.63 | 0.62 | 0.48 | 0.04 |
| RS14 | 3.79 | 54.36 | 14.74 | 5.93 | 0.07 | 4.03 | 4.77 | 1.39 | 4.92 | 0.63 | 0.41 | 0.02 |
| RS46 | 3.62 | 52.17 | 14.16 | 6.54 | 0.06 | 3.68 | 6.48 | 1.44 | 4.62 | 0.62 | 0.51 | 0.05 |
| RS50 | 3.55 | 50.32 | 14.06 | 6.80 | 0.06 | 4.17 | 6.54 | 1.27 | 4.81 | 0.61 | 0.34 | 0.04 |
| RS41 | 3.00 | 50.33 | 13.55 | 6.23 | 0.07 | 4.46 | 7.34 | 1.25 | 4.68 | 0.61 | 0.32 | 0.04 |
| RS40 | 2.50 | 48.42 | 13.20 | 6.41 | 0.08 | 3.53 | 9.49 | 1.40 | 4.35 | 0.58 | 0.42 | 0.03 |
| RS47 | 2.00 | 51.72 | 13.73 | 6.51 | 0.06 | 3.82 | 6.55 | 1.42 | 4.49 | 0.64 | 0.35 | 0.04 |
| RS44 | 1.50 | 49.83 | 13.69 | 5.87 | 0.07 | 3.41 | 8.89 | 1.40 | 4.54 | 0.59 | 0.46 | 0.04 |
| R514 | 1.00 | 50.97 | 12.68 | 5.88 | 0.08 | 4.07 | 7.48 | 1.40 | 4.26 | 0.59 | 0.45 | 0.04 |
| RS13 | 0.50 | 50.66 | 13.94 | 6.75 | 0.08 | 4.27 | 6.85 | 1.29 | 4.57 | 0.62 | 0.34 | 0.02 |

| Sample | Metres | Y | Sr | Rb | Nb | Zr | Th | Pb | U | Ga | Cu | Zn |
|---|---|---|---|---|---|---|---|---|---|---|---|---|
| RS42 | 7.10 | 23.60 | 105.40 | 195.10 | 12.20 | 109.50 | 12.20 | 43.60 | 3.90 | 21.60 | 53.00 | 71.00 |
| RS47 | 6.80 | 26.90 | 116.60 | 173.10 | 12.80 | 133.70 | 12.80 | 32.80 | 4.60 | 20.30 | 60.00 | 61.00 |
| RS14 | 6.50 | 25.40 | 135.50 | 168.30 | 13.30 | 117.40 | 14.00 | 47.40 | 3.40 | 21.90 | 59.00 | 81.00 |
| RS17 | 6.35 | 27.10 | 106.50 | 174.60 | 13.50 | 120.10 | 16.70 | 46.10 | 3.50 | 23.10 | 31.00 | 62.00 |
| RS49 | 6.25 | 31.40 | 108.40 | 198.70 | 13.00 | 113.10 | 13.00 | 26.80 | 4.50 | 21.50 | 50.00 | 61.00 |
| R640 | 6.11 | 26.50 | 104.40 | 182.40 | 14.30 | 122.90 | 16.00 | 25.70 | 2.70 | 23.40 | 38.00 | 61.00 |
| RS48 | 5.90 | 28.60 | 121.70 | 175.70 | 12.80 | 133.50 | 12.80 | 34.20 | 3.30 | 20.10 | 62.00 | 62.00 |
| R553 | 5.68 | 25.80 | 104.70 | 180.40 | 13.50 | 133.30 | 14.70 | 48.30 | 5.50 | 22.40 | 41.00 | 61.00 |
| R573 | 5.50 | 25.80 | 136.70 | 178.90 | 13.20 | 115.70 | 16.00 | 26.60 | 2.90 | 24.60 | 41.00 | 146.00 |
| RS16 | 5.16 | 24.50 | 103.80 | 195.20 | 13.20 | 108.60 | 16.00 | 45.10 | 3.70 | 25.40 | 59.00 | 70.00 |
| RS15 | 4.93 | 23.50 | 95.90 | 203.10 | 12.60 | 110.80 | 18.00 | 34.10 | 1.90 | 25.30 | 61.00 | 65.00 |
| R507 | 4.81 | 24.50 | 105.50 | 181.30 | 13.60 | 130.30 | 15.90 | 44.30 | 3.40 | 22.80 | 31.00 | 89.00 |
| R522 | 4.65 | 24.60 | 104.90 | 203.60 | 12.60 | 110.90 | 16.00 | 38.10 | 3.50 | 25.40 | 51.00 | 123.00 |
| RS43 | 4.35 | 23.70 | 105.50 | 195.00 | 12.40 | 117.30 | 12.40 | 42.20 | 4.70 | 19.70 | 43.00 | 99.00 |
| RS45 | 4.10 | 29.50 | 123.10 | 178.70 | 12.80 | 123.40 | 12.80 | 39.10 | 2.80 | 19.80 | 66.00 | 70.00 |
| RS14 | 3.79 | 25.40 | 135.50 | 168.30 | 13.30 | 117.40 | 14.00 | 47.40 | 3.40 | 21.90 | 59.00 | 81.00 |
| RS46 | 3.62 | 29.90 | 122.80 | 180.60 | 13.10 | 125.80 | 13.10 | 34.40 | 4.10 | 21.10 | 64.00 | 69.00 |
| RS50 | 3.55 | 23.50 | 103.20 | 191.50 | 12.70 | 115.40 | 12.70 | 36.10 | 4.30 | 18.90 | 52.00 | 65.00 |
| RS41 | 3.00 | 25.20 | 103.40 | 182.20 | 12.60 | 123.20 | 12.60 | 27.40 | 4.60 | 18.50 | 31.00 | 63.00 |
| RS40 | 2.50 | 22.90 | 136.50 | 168.70 | 11.70 | 116.60 | 13.40 | 43.60 | 5.00 | 19.10 | 49.00 | 81.00 |
| RS47 | 2.00 | 26.90 | 116.60 | 173.10 | 12.80 | 133.70 | 12.80 | 32.80 | 4.60 | 20.30 | 60.00 | 61.00 |
| RS44 | 1.50 | 23.70 | 133.30 | 172.90 | 12.00 | 114.10 | 12.00 | 53.30 | 3.60 | 18.70 | 37.00 | 141.00 |
| R514 | 1.00 | 29.50 | 103.90 | 152.40 | 13.30 | 163.10 | 16.50 | 498.40 | 3.40 | 25.20 | 70.00 | 2162.00 |
| RS13 | 0.50 | 26.50 | 86.00 | 181.60 | 14.80 | 143.50 | 15.70 | 524.80 | 3.20 | 25.90 | 37.00 | 2651.00 |

| Sample | Metres | Ni | Ba | Sc | V | Co | Ce | Nd | La | Cr | Mo | nMo |
|---|---|---|---|---|---|---|---|---|---|---|---|---|
| RS42 | 7.10 | 47.00 | 469.00 | 13.50 | 111.30 | 17.70 | 70.00 | 32.00 | 37.00 | 90.00 | 1.00 | 1.00 |
| RS47 | 6.80 | 43.00 | 437.00 | 14.10 | 107.30 | 9.00 | 63.00 | 30.00 | 33.00 | 88.00 | 1.10 | 1.10 |
| RS14 | 6.50 | 46.00 | 397.00 | 13.00 | 90.70 | 12.80 | 61.00 | 26.00 | 31.00 | 75.00 | 2.10 | 2.10 |
| RS17 | 6.35 | 37.00 | 380.00 | 14.90 | 94.10 | 16.00 | 69.00 | 37.00 | 37.00 | 76.00 | 1.30 | 1.30 |
| RS49 | 6.25 | 44.00 | 451.00 | 15.00 | 110.50 | 10.80 | 82.00 | 41.00 | 40.00 | 88.00 | 1.60 | 1.60 |
| R640 | 6.11 | 42.00 | 420.00 | 14.50 | 99.60 | 9.80 | 70.00 | 30.00 | 35.00 | 86.00 | 0.70 | 0.70 |
| RS48 | 5.90 | 41.00 | 444.00 | 14.40 | 108.00 | 11.10 | 73.00 | 34.00 | 36.00 | 89.00 | 1.80 | 1.80 |
| R553 | 5.68 | 40.00 | 429.00 | 14.10 | 109.10 | 8.30 | 74.00 | 32.00 | 33.00 | 84.00 | 2.10 | 2.10 |
| R573 | 5.50 | 43.00 | 433.00 | 14.90 | 102.60 | 9.60 | 62.00 | 31.00 | 33.00 | 85.00 | 1.50 | 1.50 |
| RS16 | 5.16 | 48.00 | 478.00 | 14.10 | 113.30 | 18.30 | 67.00 | 33.00 | 34.00 | 89.00 | 1.70 | 1.70 |
| RS15 | 4.93 | 48.00 | 467.00 | 13.80 | 113.20 | 13.50 | 60.00 | 28.00 | 31.00 | 90.00 | 0.60 | 0.60 |
| R507 | 4.81 | 45.00 | 388.00 | 14.10 | 95.10 | 14.00 | 65.00 | 30.00 | 33.00 | 79.00 | 2.00 | 2.00 |
| R522 | 4.65 | 50.00 | 480.00 | 15.60 | 114.10 | 11.40 | 64.00 | 29.00 | 32.00 | 91.00 | 1.20 | 1.20 |
| RS43 | 4.35 | 46.00 | 452.00 | 13.50 | 111.00 | 10.80 | 63.00 | 32.00 | 32.00 | 89.00 | 1.30 | 1.30 |
| RS45 | 4.10 | 46.00 | 443.00 | 14.30 | 108.10 | 11.10 | 73.00 | 35.00 | 35.00 | 93.00 | 1.30 | 1.30 |
| RS14 | 3.79 | 46.00 | 397.00 | 13.00 | 90.70 | 12.80 | 61.00 | 26.00 | 31.00 | 75.00 | 2.10 | 2.10 |
| RS46 | 3.62 | 43.00 | 446.00 | 13.30 | 109.70 | 10.10 | 70.00 | 35.00 | 35.00 | 96.00 | 1.40 | 1.40 |
| RS50 | 3.55 | 42.00 | 422.00 | 14.00 | 106.00 | 15.00 | 69.00 | 31.00 | 33.00 | 86.00 | 1.00 | 1.00 |
| RS41 | 3.00 | 42.00 | 418.00 | 13.20 | 99.10 | 10.20 | 65.00 | 31.00 | 35.00 | 92.00 | 1.30 | 1.30 |
| RS40 | 2.50 | 46.00 | 420.00 | 13.90 | 97.50 | 14.60 | 65.00 | 30.00 | 33.00 | 83.00 | 1.30 | 1.30 |
| RS47 | 2.00 | 43.00 | 437.00 | 14.10 | 107.30 | 9.00 | 63.00 | 30.00 | 33.00 | 88.00 | 1.10 | 1.10 |
| RS44 | 1.50 | 40.00 | 433.00 | 14.40 | 104.20 | 9.30 | 65.00 | 32.00 | 31.00 | 88.00 | 1.60 | 1.60 |
| R514 | 1.00 | 42.00 | 465.00 | 13.80 | 102.20 | 12.80 | 71.00 | 32.00 | 40.00 | 78.00 | 2.70 | 2.70 |
| RS13 | 0.50 | 41.00 | 472.00 | 14.90 | 104.90 | 10.80 | 68.00 | 31.00 | 37.00 | 91.00 | 2.60 | 2.60 |

| Sample | Metres | nMn | $nP_2O_5$ | nU | nCu | nNi | nBa | nV | nCr | nZn | nPb |
|---|---|---|---|---|---|---|---|---|---|---|---|
| RS42 | 7.10 | 0.89 | 2.00 | 1.34 | 1.88 | 1.27 | 1.05 | 1.23 | 0.98 | 0.84 | 2.18 |
| RS47 | 6.80 | 0.67 | 2.06 | 1.59 | 2.12 | 1.17 | 0.98 | 1.18 | 0.96 | 0.72 | 1.64 |
| RS14 | 6.50 | 0.78 | 2.41 | 1.17 | 2.09 | 1.25 | 0.89 | 1.00 | 0.81 | 0.95 | 2.37 |
| RS17 | 6.35 | 1.00 | 2.12 | 1.21 | 1.10 | 1.00 | 0.85 | 1.04 | 0.83 | 0.73 | 2.31 |
| RS49 | 6.25 | 0.56 | 3.41 | 1.55 | 1.77 | 1.19 | 1.01 | 1.22 | 0.96 | 0.72 | 1.34 |
| R640 | 6.11 | 0.67 | 1.88 | 0.93 | 1.34 | 1.14 | 0.94 | 1.10 | 0.93 | 0.72 | 1.28 |
| RS48 | 5.90 | 0.67 | 2.82 | 1.14 | 2.19 | 1.11 | 0.99 | 1.19 | 0.97 | 0.73 | 1.71 |
| R553 | 5.68 | 0.67 | 2.65 | 1.90 | 1.45 | 1.08 | 0.96 | 1.20 | 0.91 | 0.72 | 2.41 |
| R573 | 5.50 | 0.78 | 2.71 | 1.00 | 1.45 | 1.17 | 0.97 | 1.13 | 0.92 | 1.72 | 1.33 |
| RS16 | 5.16 | 0.56 | 7.41 | 1.28 | 2.09 | 1.30 | 1.07 | 1.25 | 0.97 | 0.82 | 2.26 |
| RS15 | 4.93 | 0.67 | 1.35 | 0.66 | 2.16 | 1.30 | 1.04 | 1.25 | 0.98 | 0.76 | 1.71 |
| R507 | 4.81 | 1.22 | 1.65 | 1.17 | 1.10 | 1.22 | 0.87 | 1.05 | 0.86 | 1.05 | 2.21 |
| R522 | 4.65 | 0.67 | 2.24 | 1.21 | 1.80 | 1.36 | 1.07 | 1.26 | 0.99 | 1.45 | 1.91 |
| RS43 | 4.35 | 0.67 | 2.41 | 1.62 | 1.52 | 1.25 | 1.01 | 1.23 | 0.97 | 1.16 | 2.11 |
| RS45 | 4.10 | 0.67 | 2.82 | 0.97 | 2.34 | 1.25 | 0.99 | 1.19 | 1.01 | 0.82 | 1.96 |
| RS14 | 3.79 | 0.78 | 2.41 | 1.17 | 2.09 | 1.25 | 0.89 | 1.00 | 0.81 | 0.95 | 2.37 |
| RS46 | 3.62 | 0.67 | 3.00 | 1.41 | 2.26 | 1.17 | 1.00 | 1.21 | 1.04 | 0.81 | 1.72 |
| RS50 | 3.55 | 0.67 | 2.00 | 1.48 | 1.84 | 1.14 | 0.94 | 1.17 | 0.93 | 0.76 | 1.81 |
| RS41 | 3.00 | 0.78 | 1.88 | 1.59 | 1.10 | 1.14 | 0.93 | 1.09 | 1.00 | 0.74 | 1.37 |
| RS40 | 2.50 | 0.89 | 2.47 | 1.72 | 1.73 | 1.25 | 0.94 | 1.08 | 0.90 | 0.95 | 2.18 |
| RS47 | 2.00 | 0.67 | 2.06 | 1.59 | 2.12 | 1.17 | 0.98 | 1.18 | 0.96 | 0.72 | 1.64 |
| RS44 | 1.50 | 0.78 | 2.71 | 1.24 | 1.31 | 1.08 | 0.97 | 1.15 | 0.96 | 1.66 | 2.66 |
| R514 | 1.00 | 0.88 | 2.65 | 1.17 | 2.48 | 1.14 | 1.04 | 1.13 | 0.85 | 25.44 | 24.92 |
| RS13 | 0.50 | 0.88 | 2.00 | 1.24 | 1.31 | 1.11 | 1.05 | 1.16 | 0.99 | 31.19 | 26.24 |

| Sample | Mo | Mn | $P_2O_5$ | nMo | nMn | $nP_2O_5$ |
|---|---|---|---|---|---|---|
| EB-004 | 1.9 | 1500 | 1900 | 1.9 | 1.67 | 1.12 |
| EB-012 | 2.3 | 1950 | 2100 | 2.3 | 2.17 | 1.24 |
| EB-014 | 2.3 | 1900 | 2000 | 2.3 | 2.11 | 1.18 |
| Deep Sea | 45.0 | 12150 | - | 45.0 | 13.9 | - |
| California | 12.61 | 198 | - | 12.61 | 0.22 | - |
| Black Sea | 45.0 | 882 | - | 45.0 | 0.98 | - |